

**MODELLING OF RECOMBINANT *ESCHERICHIA COLI*
FERMENTATIONS AT MEDIUM AND HIGH CELL
DENSITY PRODUCING BOVINE SOMATOTROPIN**

A thesis submitted to the University of London
for the degree of
DOCTOR OF PHILOSOPHY

by

Andrew Richard Cockshott C.Eng. M.Sc.

Department of Chemical and Biochemical Engineering
University College London
Torrington Place
London WC1E 7JE

October 1993

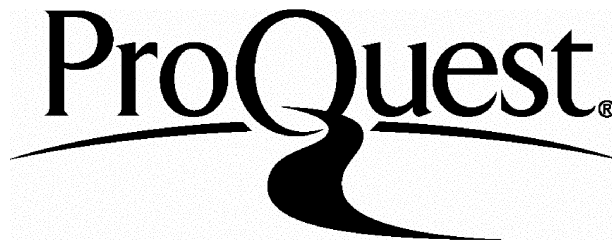
ProQuest Number: 10017740

All rights reserved

INFORMATION TO ALL USERS

The quality of this reproduction is dependent upon the quality of the copy submitted.

In the unlikely event that the author did not send a complete manuscript and there are missing pages, these will be noted. Also, if material had to be removed, a note will indicate the deletion.



ProQuest 10017740

Published by ProQuest LLC(2016). Copyright of the Dissertation is held by the Author.

All rights reserved.

This work is protected against unauthorized copying under Title 17, United States Code.
Microform Edition © ProQuest LLC.

ProQuest LLC
789 East Eisenhower Parkway
P.O. Box 1346
Ann Arbor, MI 48106-1346

To Margie and my parents
for all their love and support....

and to my children, Iain (4 years) and Jenny (3 years),
for getting me out of bed so early in the morning.

ACKNOWLEDGEMENTS

I am grateful to all the seventy or so people who gave me technical help during the course of this project. In particular I would like to thank the following groups and individuals:

At Dista Products Ltd. (Speke, Liverpool):

Dr W. Cook's group for assistance with the creation of the working cell bank and teaching me various microbiological techniques. Mrs B. Morris' group for help with some of the chemical assays and Dr W. McKinley's group, especially Mr. P. Whyment, for invaluable assistance with the HPLC.

At Eli Lilly and Company (Indianapolis, Indiana, U.S.A.):

Drs M. Foglesong and A. Russell for setting up and supporting this project and to the staff of departments KY408 and 409 who gave advice on fermentation and modelling. Also to Dr. C. Hershberger and his group for cloning the host/vector used throughout this work.

At University College London:

I am indebted to the excellent technical support from the engineering and electronics workshops and in particular to Mr. B. Doyle. For their help in many discussions I would also like to thank Prof. M. D. Lilly and Dr. J. Ward.

I would also like to acknowledge the help of my three supervisors who have done so much to make the last three years both productive and enjoyable:

Dr W. Muth (Eli Lilly) and Dr. W. Cook (Dista) who never begrudged (at least openly!) taking time out from their extremely busy schedules to discuss work with me. Their experience and knowledge was a tremendous help. Even more important was their wisdom to let me learn by my own mistakes and to pursue my own ideas.

Finally I would like to thank Dr I. D. L. Bogle (U.C.L.) for his technical support on modelling, his guidance and his encouragement.

Financial support for this project was given by the Science and Engineering Research Council, U.K. and Eli Lilly and Company, Indianapolis, Indiana, U.S.A.

ABSTRACT

The aim of this thesis was to determine the effect of glucose feeding and time of induction on the productivity of a recombinant *E. coli* fermentation. The process chosen is currently the most common industrial recombinant fermentation process (i.e. temperature induced *E. coli* producing high yields of heterologous protein and using a complex feed) for which there is a scarcity of information in the literature.

Two different induction times were considered: A "medium" cell density process induced at 4.5 g DCW/L which used air sparging and a "high" cell density process induced at 9.0 g DCW/L which used oxygen enriched sparging to support the higher cell densities. All experiments were performed in a 7L fermenter using a host/vector in which the bovine somatotropin (B.S.T.) gene was controlled via the cI857 temperature sensitive repressor.

Results showed that there was an optimal glucose feedrate to maximise the B.S.T. titre or yield above which acetate inhibition occurred and below which the cells were starved of glucose. It was also shown that inducing at twice the cell density did not affect the specific rate of acetate production and led to the same or higher specific B.S.T. production rate. Thus the high cell density fermentation had a faster rate of B.S.T. production (since it had more cells) but also reached inhibitory concentrations of acetate sooner. As a result the final B.S.T. titre was lower in the high cell density process.

As an aid to understanding and comparing the processes an unstructured mathematical model of the fermentation was developed. The model predicted the glucose, biomass, acetate and B.S.T. concentration throughout a fermentation given inoculum conditions and the profiles for glucose feeding and temperature. Uniquely the model predicts the production and inhibitory effect of acetate including the increased production of acetate due to peptone feeding.

It was shown how the model could accurately predict the effects of glucose feeding but was unable to predict the effects of time of induction. However examples are shown of how the existing model could be used for process development. Significantly the model is simpler than existing mathematical models for recombinant *E.coli* fermentation and is therefore more likely to be useful in an industrial context.

TABLE OF CONTENTS

	Page
ACKNOWLEDGEMENT	3
ABSTRACT	4
TABLE OF CONTENTS	5
LIST OF FIGURES	9
LIST OF TABLES	13
1. INTRODUCTION	
1.1 Summary	14
1.2 Introduction	14
1.3 Project goals	17
1.4 Literature review of recombinant <i>E. coli</i> fermentation	18
1.4.1 General comments	18
1.4.2 Overview of <i>E. coli</i> metabolism	19
1.4.3 Effects of glucose feeding	21
1.4.3.1 Effect of high glucose concentration on growth	23
1.4.3.2 Effect of low glucose concentration on growth	23
1.4.3.3 Effect of low glucose concentration on production	24
1.4.3.4 Production of acetate	26
1.4.3.5 Inhibition of growth by acetate	28
1.4.3.6 Inhibition of recombinant protein production by acetate	29
1.4.4 Effects of peptone feeding	30
1.4.5 Effects of temperature	30
1.4.5.1 Effect on growth	31
1.4.5.2 Effect on recombinant protein production	31
1.4.5.3 Effect on cell maintenance requirements	33
1.4.6 Effect of growth on recombinant protein production	34
1.4.7 Effect of recombinant protein production on growth	34
1.4.8 Other effects	36
1.4.8.1 Ammonia	36
1.4.8.2 Dissolved oxygen and carbon dioxide	36

Table of contents

1.4.8.3	Medium osmolarity	36
1.4.9	High cell density fermentation	37
1.4.9.1	Definition of high cell density	37
1.4.9.2	Potential benefits	37
1.4.9.3	Actual benefits	38
1.4.9.4	Effect of induction time on productivity	39
1.5	Literature review of mathematical modelling	40
1.5.1	Potential benefits	40
1.5.2	Actual benefits	42
1.5.3	Types of mathematical model	42
1.5.4	Recombinant <i>E. coli</i> models	44
1.5.4.1	Structured models	44
1.5.4.2	Unstructured models	46
1.6	Conclusions from literature reviews	48
1.7	Project plan	49
2.	MATERIALS AND METHODS	50
2.1	Summary	50
2.2	Microorganism	50
2.3	Equipment	50
2.3.1	Fermenter	50
2.3.2	HPLC	54
2.4	Methods	54
2.4.1	Preparation of the working cell bank	54
2.4.2	Fermentation media	57
2.4.2.1	Starting media	57
2.4.2.2	Media feed	60
2.4.3	Preparation of the fermenter	61
2.4.4	Fermentation	62
2.5	Assays	65
2.5.1	Biomass	65
2.5.2	Glucose	65
2.5.3	Acetate	65
2.5.4	HPLC	65
3.	RESULTS AND DISCUSSION	
3.1	Summary	68

Table of contents

3.2	Introduction	68
3.2.1	Experimental strategy	68
3.2.2	Format of results section	69
3.3	Reproducibility and Accuracy	75
3.4	Growth-only fermentations	77
3.4.1	Effect of different media	77
3.4.2	Effect of peptone feeding	84
3.4.3	Conclusions from growth-only fermentations	89
3.5	Medium cell density fermentations	90
3.5.1	Effect of different media	90
3.6	High cell density fermentations	99
3.6.1	Effect of different media	99
3.6.2	Effect of glucose feeding	108
3.6.3	Effect of glucose starvation	115
3.7	Comparison of medium and high cell density fermentations	123
3.8	Conclusions	131
4.	MODELLING	132
4.1	Summary	132
4.2	Introduction	132
4.3	The B.S.T. model	133
4.4	Parameter estimation	138
4.4.1	Biomass Production	139
4.4.1.1	Maximum specific growth rate at 30°C	139
4.4.1.2	Effect of temperature on specific growth rate	142
4.4.1.3	Effect of low glucose concentration on growth	142
4.4.1.4	Inhibition of growth by acetate	143
4.4.1.5	Inhibition of growth by B.S.T. production	143
4.4.2	B.S.T. production	144
4.4.2.1	Maximum specific B.S.T. production rate	144
4.4.2.2	Inhibition of B.S.T. production by acetate	147
4.4.2.3	Effect of temperature on B.S.T. production	149
4.4.2.4	Effect of low glucose concentration on production	151
4.4.3	Acetate production	151
4.4.3.1	Maximum specific acetate production rate	152
4.4.3.2	Effect of growth on acetate production	152
4.4.4	Glucose consumption	154

Table of contents

4.4.4.1	Maintenance coefficient	154
4.4.4.2	Yield of biomass on glucose	155
4.4.4.3	Yield of B.S.T.and acetate on glucose	155
4.4.5	Volume balance equation	157
4.4.6	Fitting the model to a high cell density fermentation	160
4.4.7	Summary of parameter estimation and sensitivity analysis	160
4.5	How to run the model	165
4.6	Comparison of model predictions and experimental results	166
4.6.1	Effect of glucose feeding on high cell density fermentations	166
4.6.2	Medium cell density fermentation	176
4.7	Examples of using the model	179
4.7.1	Predicting the effects of process variations	179
4.7.2	Interpreting ammonia consumption profiles	181
4.7.3	Determining the constant glucose feedrate to optimise yield.	183
4.8	Discussion and conclusions	186
5. CONCLUSIONS		188
APPENDIX A:	Measurement of dry cell weight	190
APPENDIX B:	Biomass error analysis	199
APPENDIX C:	Calculation of specific growth rate	201
APPENDIX D	Supplementary process plots	204
NOMENCLATURE		220
BIBLIOGRAPHY		223

LIST OF FIGURES

1.1	Effect of constant glucose feedrate on the specific yield of MAE-hGH	22
1.2	Effect of low glucose concentration on specific growth rate	25
1.3	Effect of temperature on specific growth rate	32
2.1	Fermenter geometry	52
2.2	Equipment for oxygen enriched sparging	53
2.3	Preparation of the working cell bank	55
3.1	Overview of experiments and model development	70
3.2	Effect of different media on growth	
3.2a	Biomass concentration and total biomass produced	80
3.2b	% CO ₂ in fermenter exit gas and ammonium hydroxide feedrate	81
3.2c	Phosphate and acetate concentrations	82
3.2d	Glucose feedrate and glucose concentration	83
3.3	Effect of peptone feeding on growth	
3.3a	Biomass concentration and total biomass produced	86
3.3b	%CO ₂ in fermenter exit gas and ammonium hydroxide feedrate	87
3.3c	Glucose and acetate concentrations	88
3.4	Effect of different media on medium cell density fermentations	
3.4a	Glucose feedrate and temperature profiles	93
3.4b	Biomass concentration and total biomass produced	94
3.4c	Glucose and phosphate concentrations	95
3.4d	Acetate concentration and total acetate produced	96
3.4e	B.S.T. and total B.S.T. produced	97
3.4f	%CO ₂ in fermenter exit gas and ammonium hydroxide feedrate	98
3.5	Effect of different media on high cell density fermentations	
3.5a	Glucose feedrate and temperature profiles	102
3.5b	Biomass concentration and total biomass produced	103
3.5c	Glucose and acetate concentrations	104
3.5d	Acetate concentration and total acetate produced	105
3.5e	B.S.T. and total B.S.T. produced	106
3.5f	%CO ₂ in fermenter exit gas and ammonium hydroxide feedrate	107

3.6	Effect of glucose feeding on high cell density fermentations	
3.6a	Glucose feedrate and temperature profiles	110
3.6b	Biomass concentration and total biomass produced	111
3.6c	Glucose and acetate concentrations	112
3.6d	B.S.T. and total B.S.T. produced	113
3.6e	%CO ₂ in fermenter exit gas and ammonium hydroxide feedrate	114
3.7	Effect of glucose starvation on high cell density fermentations	
3.7a	Glucose feedrate and temperature profiles	117
3.7b	Biomass concentration and total biomass produced	118
3.7c	Glucose concentrations	119
3.7d	Acetate concentration and total acetate produced	120
3.7e	B.S.T. and total B.S.T. produced	121
3.7f	%CO ₂ in fermenter exit gas and ammonium hydroxide feedrate	122
3.8	Comparison of medium and high cell density fermentations	
3.8a	Glucose feedrate and temperature profiles	125
3.8b	Biomass concentration and total biomass produced	126
3.8c	Glucose and phosphate concentrations	127
3.8d	Acetate concentration and total acetate produced	128
3.8e	B.S.T. and total B.S.T. produced	129
3.8f	%CO ₂ in fermenter exit gas and ammonium hydroxide feedrate	130
4.1	Observed specific growth rate calculated from a logarithmic plot of total carbon dioxide produced vs. time.	140
4.2	Observed specific growth rate calculated from a logarithmic plot of total biomass in fermenter vs. time.	141
4.3a	A comparison of specific B.S.T. production rate for one medium and two high cell density fermentations	145
4.3b	A comparison of glucose and acetate concentrations for one medium and two high cell density fermentations	146
4.4	Effect of acetate concentration on specific B.S.T. production rate	148
4.5	Effect of temperature on specific B.S.T. production rate	150
4.6	A comparison of specific acetate production rate for one medium and two high cell density fermentations	153
4.7	Calculation of yield coefficient for biomass	156
4.8	Correlation between total biomass produced and total ammonium hydroxide fed.	159

Comparison of model predictions and Expt. 8:	
4.9	Glucose, B.S.T., acetate and biomass 161
4.10	Ammonium hydroxide feedrate 162
4.11	Glucose feedrates for Expts. 8, 11 and 12 169
Comparison between model predictions and Expt. 11:	
4.12	Glucose, B.S.T., acetate and biomass 170
4.13	Ammonium hydroxide feedrate 171
4.14	Volume 172
Comparison between model predictions and Expt. 12:	
4.15	Glucose, B.S.T., acetate and biomass 173
4.16	Ammonium hydroxide feedrate 174
4.17	Effect of glucose feeding on B.S.T. production for Expts. 8,11 and 12 175
4.18	Comparison between model predictions and Expt. 7 177
4.19	Comparison between "corrected" model predictions and Expt. 7 178
4.20	Plot of model prediction for Expt. 11 of ammonium hydroxide feedrate and the amount of that feedrate due to biomass and acetate production. 182
4.21	Effect of constant glucose feedrate on specific product yield 184
4.22	Effect of constant glucose feedrate on biomass and B.S.T. concn. 185
A1.1	Correlation between rinsed and non-rinsed DCW for different media 195
A1.2	Expanded portion of Fig. A1.1 196
Comparison of exponential growth on media A and B:	
A1.3	%CO ₂ in fermenter exit gas and total glucose used 197
A1.4	Total biomass produced 198
B1.1	Absolute and relative biomass error vs. biomass 200
C1.1	Examples of different ways of calculating specific growth rate 203
D3.2	Effect of different media on growth
D3.2a	Estimated broth volume and pH 205
D3.2b	Oxygen flowrate and dissolved oxygen concentration 206
D3.3	Effect of peptone feeding on growth
D3.3a	Estimated broth volume and pH 207
D3.3b	Oxygen flowrate and dissolved oxygen concentration 208
D3.3c	Respiratory quotient 209

List of figures

D3.4	Effect of different media on medium cell density fermentations	
D3.4a	Estimated broth volume and pH	210
D3.4b	Dissolved oxygen concentration and respiratory quotient	211
D3.5	Effect of different media on high cell density fermentations	
D3.5a	Estimated broth volume and pH	212
D3.5b	Oxygen flowrate and dissolved oxygen concentration	213
D3.6	Effect of glucose feedrate on high cell density fermentations	
D3.6a	Estimated broth volume and pH	214
D3.6b	Oxygen flowrate and dissolved oxygen concentration	215
D3.7	Effect of glucose starvation on high cell density fermentations	
D3.7a	Estimated broth volume and pH	216
D3.7b	Oxygen flowrate and dissolved oxygen concentration	217
D3.8	Comparison of medium and high cell density fermentations	
D3.8a	Estimated broth volume and pH	218
D3.8b	Oxygen flowrate and dissolved oxygen concentration	219

LIST OF TABLES

2.1	Phenotype selection plates used when making the working cell bank	56
2.2	Fermentation chemicals and their suppliers	58
2.3	Composition of the four different media used in this thesis	59
2.4	Growth conditions in medium and high cell density fermentations	62
2.5	Peptone feedrates and concentrations	63
2.6	Composition of sulphitolysis reagent	66
2.7	Composition of the H.P.L.C. mobile phase	67
3.1	Summary of experiments	71
3.2	Reproducibility of assays	76
3.3	Effect of different media on the extent of exponential growth	78
4.1	Summary of parameter estimation	163
4.2	Summary of sensitivity analysis	164
4.3	Predictions of the effects of process variations on final B.S.T. yield and titre	179
A1.1	Wavelengths chosen for measurement of optical density in <i>E. coli</i> fermentations	191
A1.2	Cell pellet rinsing methods used for direct determination of dry cell weight by centrifugation for <i>E. coli</i> fermentations	192

1 INTRODUCTION

1.1 Summary

In this chapter the state of our current knowledge about recombinant *Escherichia coli* fermentations is discussed and related to the project goals and plan. The chapter starts with an introduction as to why recombinant *E. coli* fermentations are important and where our current knowledge is most lacking. This leads naturally on to explaining the choice of the host/vector and fed-batch fermentation process to be studied in this thesis and to a statement of the project goals.

The next section is a review of previous experimental work with *E. coli* fermentations and describes the effects of the most important variables (e.g. glucose feeding and temperature) on growth and recombinant protein production. Where possible these relationships are described mathematically so that later in the thesis they can be incorporated into a mathematical model. This is followed by a review of mathematical models of recombinant *E. coli* fermentations which shows that there are no existing models which can be used to describe the process studied in this thesis and proposes the basic form of a new model. The chapter ends by stating the project plan.

1.2 Introduction

The recent ability to genetically manipulate (or "engineer") micro-organisms *in vitro* so that they can produce foreign proteins in high yields and purity has had the biggest impact on the pharmaceutical industry since the discovery of antibiotics in the 1940's. Many companies throughout the world, both large pharmaceutical companies and small biotechnology ones, are now scaling up processes using such recombinant organisms to make a wide variety of products. These include tumour viruses, human and animal growth hormones, neuro-active peptides, blood clotting factors, insulin, interferons, immunoglobins and other human serum proteins (De Boer and Shepard, 1983; Georgiou, 1988).

Such processes involve a fermentation stage where recombinant cells are grown and protein produced, and downstream stages where the product is purified. A major commercial concern is to optimise the conditions in the fermenter so that a high yield of product is obtained. However as recently reported (Galindo *et al.*, 1990) there are still few publications concerning recombinant fermentations. The literature that is available, discussed in detail below, is often based on recombinant processes with much lower productivities than the current industrial norms or uses the expression of homologous proteins and is thus of limited use. One objective of this work is to help fill this gap in the literature by investigating a recombinant fermentation producing a high yield of a heterologous protein.

Recombinant microorganisms usually consist of a host organism and a plasmid (the vector) into which has been inserted a gene for the foreign protein of interest. There is a wide range of bacterial and animal cell hosts but the most common by far is the Gram negative bacterium *Escherichia coli*. A wide variety of plasmids have been used with *E. coli* in an attempt to increase foreign gene expression. These differ in the construction of the plasmid and in particular the promoter/operator sequence that precedes the foreign gene and controls its expression. The common feature of these promoter systems is that they must provide a mechanism for switching gene expression off and on so that growth and product expression can be separated. (If gene expression occurs during growth then growth is slower and product yield is less. (Bentley *et al.*, 1990)).

The preferred industrial promoter system used at present is the combination of either of the phage lambda promoters (pL or pR) controlled by the temperature sensitive lambda cI857 repressor. At 30°C cI857 represses gene expression but when the temperature is raised to some temperature greater than 37°C and less than 45°C cI857 changes conformation and no longer binds to the DNA and gene expression occurs. Such a system is an improvement on the earlier promoters (e.g. *lacUV5*, *trp*, *tac*) which either needed to be induced or repressed with expensive chemicals or were "leaky" in that expression could not be completely switched off (Georgiou, 1988). Another advantage of using lambda pL or pR promoters is that they are up to ten times stronger than the older ones (De Boer and Shepard, 1983).

This variety in the host/vector systems used in recombinant fermentations is reflected in the literature which makes it difficult to use previous research when trying to optimise a particular process using a given host/vector system. For example literature on chemical

induction may not be particularly useful when considering how to optimise a temperature induction. To compound the problem a variety of processes are described including continuous, batch and fed-batch with and without complex feeds (e.g. peptone). Thus another objective of this work is to add to the literature on the currently preferred industrial process - i.e a fed-batch process using a complex peptone feed and which uses a host/vector containing the temperature sensitive lambda pL/cI857 promoter/repressor system.

Another way to obtain more product from a given fermenter is to increase the cell density. Typical industrial recombinant *E. coli* fermentations use air sparging and reach cell densities of between 10 and 20 g DCW/L. However by using oxygen enriched sparging cell densities up to 100 g DCW/L have been reported in the literature for recombinant *E. coli* (Yee and Blanch, 1993). Unfortunately much of this work has concentrated on the techniques used to achieve these cell densities rather than their effect on productivity. Thus another objective of this work is to develop a high cell density process (using oxygen enriched sparging) for the model host/vector system and to examine what effect this has on productivity.

Finally for any given host/vector system the process can be optimised to give the maximum productivity by altering the environmental conditions (e.g. glucose concentration, temperature, pH, etc.) within the fermenter. Determining the correct profiles for these variables has traditionally been a process of conducting a whole series of experimental fermentations and adjusting one environmental variable at a time whilst keeping the others constant. For example several experimental fermentations might be run side-by-side with slightly different glucose feedrate values. The experiment would then be repeated using the feedrate that gave the best yield but with, say, temperature varied between the fermentations.

However mathematical models of the process offer the potential of shortening this process by allowing "experiments" to be performed on a computer in a fraction of the time and at much less expense. This approach appears more promising as computer power decreases in price and the modelling techniques improve. Unfortunately, though, despite the large number of models that have been developed few have been used to optimise industrial fermentations (Royce, 1993). This has mainly been due to the fact that the models have been difficult to understand and use. Also there are no models in the literature that are directly applicable to the fermentation that is used in this project. In particular there are no models for recombinant *E. coli* fermentations which consider the

production of acetate and its inhibitory effect on growth and recombinant production. Thus another aim of this work is to develop a mathematical model of the fermentation studied in this thesis and to show how this can be used to improve the understanding and productivity of this process.

The main objectives of this work are now summarised.

1.3 Project goals.

In view of the above comments the choice of process to study and the project goals can now be stated:

Choice of process

It was decided to study the most preferred industrial recombinant fermentation process - i.e. a fed-batch fermentation with a complex peptone feed and which uses a recombinant *E. coli* host/vector (RV308/pHKY531), containing the temperature sensitive pL/cI857 promoter/repressor system, and producing high yields of a heterologous protein (met-asp-bovine somatotropin). [Note: throughout this project the term "B.S.T." will be used as shorthand notation for "met-asp-bovine somatotropin"].

Project goals

1. To develop a mathematical model of the "medium" (using air sparging and induced at 4.5 g DCW/L) and "high" (using oxygen sparging and induced at 9 g DCW/L) cell density fermentations and to use them to improve the yield and understanding of these processes.
2. To compare the two types of process in terms of specific B.S.T. production rate and final concentration of B.S.T.

The plan for achieving these goals is outlined in Sec. 1.7 after first reviewing in detail the literature on recombinant *E. coli* fermentations and the mathematical modelling of such fermentations.

1.4 Literature review of recombinant *E. coli* fermentations.

1.4.1 General comments

The purpose of this review of the literature on recombinant *E. coli* fermentations is to determine how the most important variables (i.e. glucose feedrate, peptone feedrate and temperature) affect the specific rate of production of biomass, product and acetate. The first two terms are required because the final recombinant yield depends on both the number of cells in the reactor and the rate at which they are producing. The specific rate of acetate production is also important because acetate can inhibit growth and product formation (Luli and Strohl, 1990; Jensen and Carlsen, 1990). Where possible these effects will be expressed mathematically so that they can be incorporated into a mathematical model of the process.

Other variables (e.g. dissolved oxygen concentration) also have a large effect on product yield but are not investigated in this work and are therefore only mentioned briefly at the end of the literature review.

Thus the following literature review is split into sections each of which examines the effect of a single variable (e.g. glucose feed) on the specific rate of production of either acetate, production or biomass. This approach should make it easier to understand the overall fermentation and it also makes it easier to relate the literature results to the development of a mathematical model.

Unfortunately many of the experiments reviewed do not separate out the various effects in this way and so the same paper may be mentioned in different sections. Another problem, alluded to in the introduction, is that conclusions drawn from fermentations with one *E. coli* host/vector may not be applicable to another host/vector. For example Luli and Strohl (1990) showed that different strains of *E. coli* produced acetate at different rates and that some strains could assimilate acetate whilst others could not.

However the major problem by far in understanding and modelling *E. coli* fermentations is the complexity of the cell itself and in particular its metabolism. To give some idea of this complexity (and also to provide a framework for discussing some of the variables such as glucose feedrate) the next section gives an overview of *E. coli* metabolism.

1.4.2 Overview of *E. Coli* Metabolism

Glucose is the normal carbon and energy source used in *E. coli* fermentations. Each molecule of glucose is broken down (catabolised) by the cell into two molecules of pyruvate in a series of enzyme catalysed reactions known as the Embden-Meyerhof pathway. This process gives a yield of energy in the form of two molecules of adenosine tri-phosphate (ATP) and reducing power in the form of two molecules of nicotinamide adenine dinucleotide in its phosphorylated form (NADPH₂). The fate of the pyruvate then depends on whether oxygen is available.

Under anaerobic conditions (oxygen starvation) *E. coli* converts pyruvate into a mixture of acids (e.g. acetic, lactic, succinic, etc.). These steps do not produce any more energy and use up all the reducing power generated in the Embden-Meyerhof pathway. Thus the net energy yield from the anaerobic breakdown of one molecule of glucose is two molecules of ATP.

Under aerobic conditions pyruvate is converted via the tricarboxylic acid (or TCA) cycle and the respiratory chain into carbon dioxide and water. The net yield from these steps (once all the reducing power generated has been converted to ATP) is a further 34 molecules of ATP. Thus the net energy yield from the aerobic breakdown of glucose is 36 molecules of ATP - i.e. 18 times more than that obtained under anaerobic conditions. Thus it is extremely important to keep the cells adequately supplied with oxygen.

Almost all the energy derived from the breakdown of glucose is used in the biosynthesis of large molecules such as DNA, RNA, phospholipids and proteins. Protein synthesis is by far the most important of these consuming 88% of the total energy for biosynthesis (Bailey and Ollis, 1986a). The building blocks for these large molecules are created from the intermediary metabolites. For example some of the carbon molecules from glucose are channelled from the Embden-Meyerhof pathway into phospholipid production. This diversion of metabolites into biosynthesis reduces the flux through the T.C.A. cycle and the respiratory chain and hence reduces the energy yield.

Elements not present in glucose have to be obtained from other substrates. Nitrogen, for example, can be obtained from ammonia (fed during many fermentations to control the pH) or from amino acids. Obviously it takes less energy to make proteins from larger

building blocks like amino acids which is why they are often fed to *E. coli* fermentations during the production phase (often in the form of hydrolysed protein which is cheaper than pure amino acids).

E. coli has evolved to be extremely efficient at utilising substrates - often under conditions where the concentrations of those substrates change dramatically over time and where they may be present in very low concentrations. One way to achieve this efficiency is to have many reaction steps (as is the case in the above pathways) which are each near equilibrium. Another way is to have tight control of all the pathways so that energy is not wasted in producing molecules which are not needed.

Such control of metabolic pathways is often accomplished by inhibition of the first enzyme of a pathway by the end product of that pathway. For example many amino acids inhibit the first step in their biosynthesis. Thus if a sufficient amount of that amino acid is available the pathway making it will temporarily shut down until the level drops again. Another example is the inhibition of the first step of the Embden-Meyerhof pathway by ATP. Thus if the concentration of ATP in the cell is high (i.e. energy is already available) it will slow down the catabolism of glucose. However there are a variety of other control mechanisms (Stryer, 1981).

This very brief review of *E. coli* metabolism should at least give some indication of the complexity of *E. coli* metabolism. A typical production fermenter may consist of 10^{18} cells. Each of these cells will continuously alter the concentration and activity of over a thousand enzymes in response to environmental changes it detects. Furthermore the history of the cells (i.e. what happened to them prior to inoculating the fermenter) will affect how they respond to environmental changes. This enormous complexity is the very essence of why optimising a fermentation is so much more difficult than optimising a purely chemical process.

Also, although there is a great deal about the above pathways and control mechanisms that is understood there is also a lot, especially when dealing with recombinant *E. coli*, which remains unknown. For example it is not understood how the cell responds to the metabolic demands placed on it when, during induction, it leaves a state of balanced growth and starts recombinant protein expression. Nor is it clear what physiological changes occur during this period which allow the cell to respond to such a redirection of energy and precursors (MacDonald and Neway, 1990; George *et al.*, 1992).

1.4.3 Effects of glucose feeding

As explained above glucose is used by *E. coli* both as an energy source and for biosynthesis. There are several effects of glucose on an *E. coli* fermentation. These are summarised here before discussing them in more detail in the following sections.

- If the concentration of glucose becomes too high it will inhibit growth. Therefore it is often not possible to batch in sufficient glucose at the start of the run to last for the entire fermentation - hence it is necessary to feed glucose.
- If the glucose concentration becomes too low (e.g. by feeding glucose at too slow a rate) then the specific growth rate and the specific production rate may be reduced.
- However if glucose is fed at too high a rate then acetate will be produced and this will inhibit growth and product formation.

To summarise: It is necessary to feed glucose since batching in a sufficient amount at the start of the fermentation would give rise to inhibitory concentrations of glucose. However if glucose is fed at too fast a rate acetate will be produced which will inhibit growth and product formation whilst if it is fed at too slow a rate the same result will occur because of a lack of glucose as carbon and energy source. Thus it is reasonable to assume that there is an optimum glucose feedrate which maximises final product yield.

This has been proved by Jensen and Carlsen (1990) in a experiment where they fed glucose at different rates to fed-batch recombinant *E. coli* fermentations producing MAE-hGH under the control of a strong constitutive promoter. Their results are shown in Fig. 1.1 where it can be seen that there was indeed an optimum glucose feedrate to obtain the best specific yield of recombinant product. This result will be considered again in the chapter on modelling.

(Before reviewing the literature on the above effects in detail it should be added that there is another possible effect of glucose. This is known as "catabolite repression" where fast growth in the presence of excess glucose represses production. This is discussed in Sec. 1.4.6 under the heading "the effect of growth on recombinant protein production").

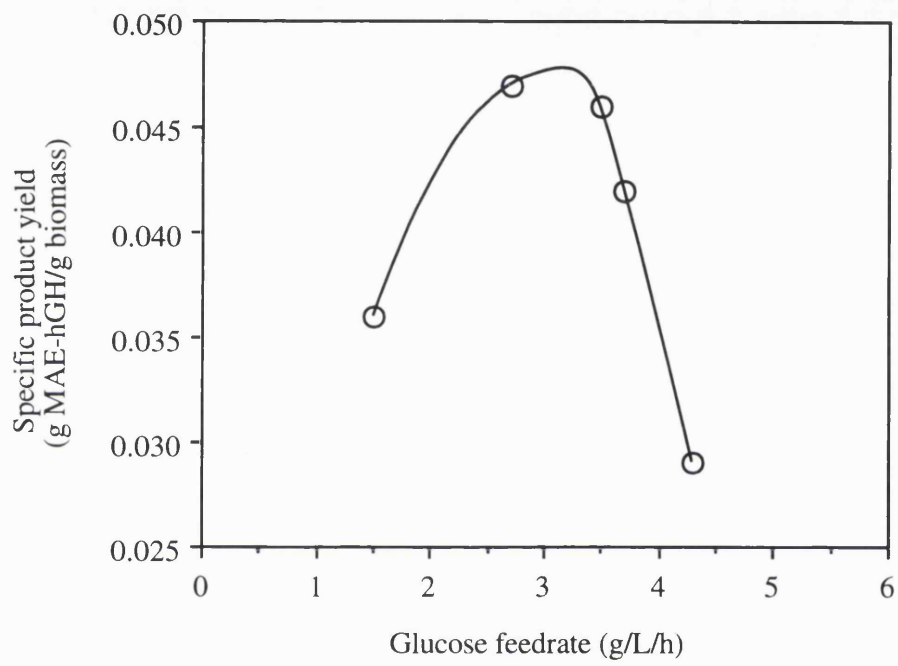


Figure 1.1: Effect of constant glucose feedrate on specific yield of MAE-hGH in a fed-batch *E. coli* fermentation (Jensen and Carlsen, 1990)

1.4.3.1 Effect of high glucose concentration on growth

Matsui *et al.* (1989) found that glucose concentrations in the range 20-50 g/L inhibited growth but that no inhibition was detected at concentrations below 20 g/L. Probably this is a strain dependent effect since, for example, Shiloach *et al.* (1991) found that 40 g/L of glucose was not growth inhibitory.

In practice to avoid any growth inhibition most recombinant *E. coli* fermentations start with glucose concentrations below this value (e.g. 12.5 g/L as used in this project) and, since this is normally insufficient for the whole fermentation, start to feed glucose before it becomes exhausted.

1.4.3.2 Effect of low glucose concentration on growth

If the glucose concentration drops too low (e.g. by feeding glucose at too slow a rate) the specific growth rate will decrease. The relationship between glucose concentration and specific growth rate was first determined by Monod (1942) :

$$\mu = \mu_{\max} \left(\frac{S}{S + K_1} \right) \quad (1.1)$$

where $K_1 = 0.004$ g glucose/L. This is plotted in Fig. 1.2 from which it can be seen that the glucose concentration must be kept above about 40 mg/L to prevent glucose limitation of growth (Robbins and Taylor, 1989)

Alternative equations for specific growth rate include the following (Roels and Kossen, 1978):

Blackman:

$$\mu = \begin{cases} \mu_{\max} & \text{when } S > \mu_{\max} B' \\ \frac{S}{B'} & \text{when } S \leq \mu_{\max} B' \end{cases} \quad (1.2)$$

Tiessier:
$$\mu = \mu_{\max} \left(1 - \exp\left(-\frac{S}{K}\right) \right) \quad (1.3)$$

Moser:
$$\mu = \mu_{\max} \left(\frac{S^d}{S^d + K} \right) \quad (1.4)$$

All these equations, including the Monod one, are empirical and are not derived theoretically (the Monod equation can be derived theoretically if the growth rate is controlled by a single, slow, enzyme catalysed reaction but as Monod himself pointed out this is not normally the case). Thus there is nothing sacrosanct about any of the above equations; they all happen to give reasonable approximations as to how the specific growth rate varies as the level of glucose becomes limiting. In general there is little to choose between them and the Monod equation is normally used (Roels and Kossen, 1978).

1.4.3.3 Effect of low glucose concentration on recombinant protein production

In contrast to the effect of low glucose concentration on growth its effect on recombinant protein production is less well understood. The Jensen and Carlsen (1990) fed-batch result, discussed in Sec. 1.4.3 and shown in Fig. 1.1, proved that if the glucose feedrate during production was too low then specific yield of recombinant product was reduced. They suggested that this was due to insufficient glucose being provided to supply energy for cell maintenance and peptide synthesis.

It would be logical to propose a relationship between the specific production rate and the glucose concentration in the same form as Monod equation for growth (i.e. Eqn. 1.1):

$$r_P = r_{P,\max} \left(\frac{S}{S + K_2} \right) \quad (1.5)$$

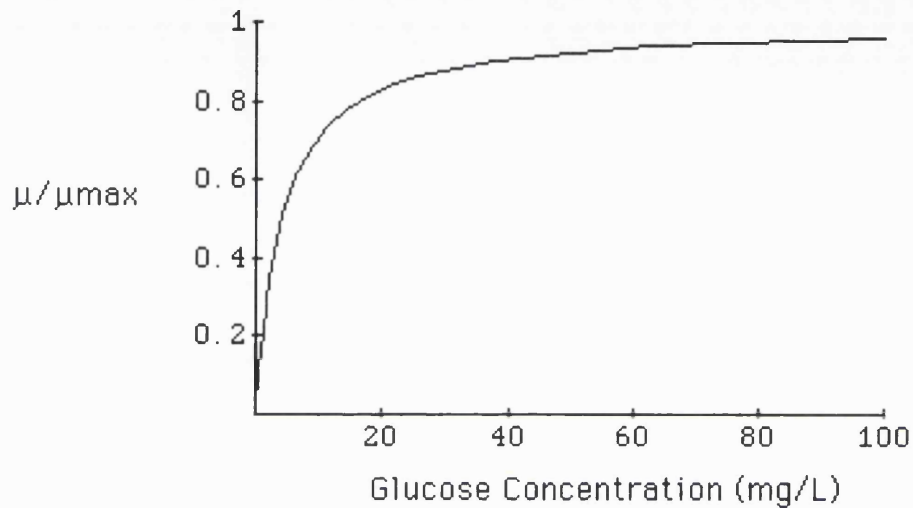


Figure 1.2: The effect of low glucose concentration on specific growth rate (Monod, 1942).

Notes:

1. The term μ/μ_{\max} measures the variation between the actual specific growth rate (μ) from maximum specific growth rate (μ_{\max}).
2. For glucose concentration above approximately 40 mg/L μ/μ_{\max} is close to one - i.e. the actual specific growth rate will be nearly equal to the maximum specific growth rate.

Jensen and Carlsen (1990) found that in continuous culture there was no detectable reduction in the specific production rate of a recombinant protein (MAE-hGH) down to glucose concentrations of 0.01 g/L (the lowest value at which they did the experiment). If it is assumed that they would have detected a reduction in the specific production rate of 10% this sets an upper limit for K_2 in Eqn. 1.5 for their system given by :

$$r_{P,\max} \left(\frac{0.01}{0.01 + K_2} \right) \geq 0.9 r_{P,\max}$$

which simplifies to: $K_2 \leq 0.001 \text{ g / L}$ (1.6)

If this value is compared with $K_1 = 0.004 \text{ g/L}$ in the equivalent expression for growth kinetics (Eqn. 1.1) it can be seen that this implies that low glucose concentrations effect growth more than recombinant protein production. For example if the glucose concentration is 0.001 g/L then Eqns. 1.1 and 1.5 give values for specific growth and production rates which are, respectively, one fifth and one half of their maximum values. One way of thinking about this is to consider a competition between growth and product formation for the limited glucose supply.

In summary Eqns. 1.1 and 1.5 can be used to describe the effect of low glucose concentration on growth and product formation. The relationship for growth has been observed directly whereas for product formation it is inferred from the fed batch result of Jensen and Carlsen (1990). It should be stressed that both expressions do not imply any particular mechanism at work. (Note: for convenience the terms "glucose limited" and "glucose starved" are used in the rest of this thesis to mean glucose concentrations that are sufficiently low to affect, respectively, growth and product formation).

1.4.3.4 Production of acetate

When *E. coli* is grown aerobically in continuous culture acetic acid is produced if either the glucose concentration or the growth rate exceeds certain critical values. (Doelle *et al.*, 1982). Jensen and Carlsen (1990) showed in continuous culture that a recombinant strain producing MEA-hGH only started to excrete acetate when the specific growth rate

exceeded 0.4 1/h. The specific rate of acetate production increased linearly with the specific growth rate as it was increased above this critical level.

Bajpai (1987) obtained the same result with non-recombinant *E. coli* and proposed the following correlation :

$$r_A = \begin{cases} 0 & \text{when } \mu < \mu_{crit} \\ k(\mu - \mu_{crit}) & \text{when } \mu \geq \mu_{crit} \end{cases} \quad (1.7)$$

where the constants μ_{crit} and k had values of 0.51 1/h and 0.81 g acetate/g DCW respectively. The correlation was also found to fit other experimental results provided different values of μ_{crit} and k were used - i.e. these values are strain dependent (Han *et al.* (1992)). For example best fits were obtained using values of 0.145 1/h and 1.6 g acetate/g DCW for the data of Fieschko and Ritch (1986) and 0.2 1/h and 0.645 g acetate/g DCW for the data of Reiling *et al.* (1985). Both experiments used chemostat cultured *E. coli*.

Majewski and Domach (1990) showed that Eqn. 1.7 could be derived theoretically based on the assumption that there was a limiting enzyme activity of one of the TCA cycle enzymes. However since there are at least four alternative mechanisms proposed for the effect of acetate production (Luli and Strohl, 1990) it is probably wiser simply to take Eqn. 1.7 as a purely empirical expression which has no mechanistic foundation.

Strategies for reducing acetate production in fed-batch fermentations have generally been based on feeding glucose at a rate that keeps glucose limiting and reduces the growth rate below the critical value for acetate production. The following have all been successfully used to determine the glucose feedrate:

- Pre-determined constant feed profile (Jensen and Carlsen, 1990)
- A simple model of the fermentation (Allen and Luli, 1987)
- Dissolved oxygen concentration (Mori *et al.*, 1979)
- pH (Robbins and Taylor, 1989)
- Acetate monitoring (Shimuzu *et al.*, 1988)

Finally it should also be made clear that acetate can also be consumed by *E. coli* although this is strain dependent (Luli and Strohl, 1990).

1.4.3.5 Inhibition of growth by acetate

The effects of acetate on growth have generally been investigated by adding various concentrations of sodium acetate to exponentially growing batch cultures. Most studies indicate that acetate concentrations in the range 5-10 g/L have a noticeable inhibitory effect on growth, whilst concentrations in the range 10-20 g/L cause growth to cease (Pan *et al.*, 1987; Konstantinov *et al.*, 1990; Luli and Strohl, 1990; Yee and Blanch, 1993).

Unfortunately the inhibitory effects of acetate on growth may be complicated by the production of other metabolites. For example Landwall and Holme (1977) showed that growth inhibition was caused by the accumulation of acetate (10 g/L), lactate (1.3 g/L), succinate (1.3 g/L), propionate (0.5 g/L), and isobutyrate (0.3 g/L). Addition of any of these acids on their own at the above concentrations did not affect growth.

Two investigators have attempted to quantify the effect of acetate on growth. Koh *et al.* (1992), using shake-flasks, found that the following equation described their results:

$$\frac{\mu}{\mu_{\max}} = \frac{1}{1 + k_A A} \quad (1.8)$$

They found that the value of k_A ranged from 0.12 to 0.37 L/g acetate depending on the strain and medium. Inhibition was most noticeable for recombinant strains and for growth in defined rather than complex media. They also stated that "an alternative linear model for acetate inhibition, based on fed-batch data, $\mu = k'A\mu_{\max}$, has been proposed by Luli and Strohl (1990)". Clearly this is in error since the equation predicts that acetate is a promoter of growth! In fact the Luli and Strohl data was also based on shake-flask experiments and the acetate inhibition relationship was logarithmic. Yet another correlation can be obtained from the data of Pan *et al.* (1987) which shows a simple linear correlation between the inhibition of specific growth rate and acetate concentration.

In conclusion there appears to be good evidence for the inhibitory effect of acetate on growth but there is no obvious choice of an expression to quantify it.

Finally it should be added that the mechanism of growth inhibition by acetate is thought, at least in part, to be due to the protonated form being able to cross the cell membrane and act as a decoupler of the proton motive force (Luli and Strohl, 1990). The effect of acetate inhibition is therefore more pronounced at lower pH where the equilibrium is shifted towards the protonated form of acetate. However in this project the pH was kept constant in all fermentations so this extra complication did not arise.

1.4.3.6 Inhibition of recombinant protein production by acetate

Jensen and Carlsen (1990) added different concentrations of sodium acetate to glucose limited chemostat cultures of *E. coli* producing a recombinant product (MAE-hGH). They found that at 2.4 g acetate/L growth was unaffected but the specific production rate decreased by about 38%. At 6.1 g acetate/L both growth and specific production rate were reduced. This suggests that the inhibitory effect of acetate is more pronounced on production than it is on growth.

The following fed-batch experiments have also implicated acetate as an inhibitor of recombinant production. However these results are not as straightforward since they all allowed acetate to accumulate in the medium during the experiment rather than injecting it to give a known concentration at a specific time.

Calcott *et al.* (1988) found that overfeeding glucose caused accumulation of 12-16 g acetate/L and a reduction of recombinant (B.S.T.) expression of 50%. Strandberg and Enfors (1991a) found that in batch cultures acetate concentrations rapidly increased to about 5 g/L after induction and this was proposed as the reason that production stopped at the same time. This was supported by a fed-batch experiment in which, by feeding glucose at a low rate, acetate concentration was kept at near zero and production continued to much higher levels.

1.4.4 Effects of peptone feeding.

Peptone (an enzymatic digest of casein) is often added to industrial recombinant fermentations to improve yields (George *et al.*, 1992). Typically it is a 50/50 mixture of bound and free amino acids and the latter can be readily assimilated into the product protein thus saving the cell from expending energy to make these amino acids itself.

A number of authors have noted that adding peptone increases product yields. For example Nancib *et al.* (1991) increased the yield of glyceraldehyde-3-phosphate dehydrogenase by adding peptone and yeast extract and Mizutani *et al.* (1986) achieved higher yields of recombinant product by feeding amino acids. Ramirez and Bentley (1993) have also shown that feeding strategies that consider the primary amino acid composition of the product protein can lead to improved product yields. Another advantage of peptone feeding is that it may reduce proteolytic degradation of a product protein (Tsai *et al.*, 1987). Unfortunately it may also have any or all of the following, poorly understood, effects on the fermentation:

- Adding peptone can increase the rate of acetate production. For example in a complex medium *E. coli* K12D1 produces acetate at a lower growth rate than in minimal medium (Meyer *et al.*, 1984). Furthermore the specific acetate production rate was twice as high in the former case.
- Overfeeding peptone can cause high concentrations of amino acids which can inhibit the synthesis of specific metabolites for growth and product formation (Rinas *et al.*, 1989).
- Adding peptone may cause an increase in growth rate and increase in the yield of cells on glucose. However Koh *et al.* (1992) found that this effect was dependent on the host/vector used. Two recombinant host/vectors were grown in shake flasks on minimal medium with and without additional peptone. For one host/vector there was no effect whilst the other grew twice as fast in the presence of peptone.

To summarise: Peptone feeding was used in the process studied in this thesis because it is typically used in current industrial recombinant fermentations. However it complicates understanding of the process since it has poorly defined effects on growth and product formation.

1.4.5 Effects of temperature

1.4.5.1 Effect of temperature on growth

The effect of temperature on the growth of non-recombinant *E. coli* is shown in Fig. 1.3. (Bailey and Ollis, 1986b). At low temperatures the growth rate increases with temperature in an Arrhenius manner. However at some temperature (about 45°C) there is a rapid decline in the growth rate. A similar response between enzyme activity and temperature is well known and has led to the suggestion that as the temperature rises the cell growth rate increases due to the increase in enzyme activity but at some temperature the most thermally sensitive enzyme will denature and the cell will die.

For a recombinant cell containing a temperature sensitive promoter the situation is more complex. The lambda pL/cI857 system is considered repressed below 37°C. However while there is a fairly sharp cut off point there is still some small amount of gene expression at temperatures less than 37°C (Chen *et al.*, 1992). Any gene expression will cause a metabolic burden on the cell and hence a reduction in the growth rate (Da Silva and Bailey, 1986). Thus as the temperature is increased from 30 to 37°C we would expect at first to see an Arrhenius increase in the growth rate which slows down as we approach 37°C and gene expression starts to occur. In practice if the temperature is kept low enough (say 30°C) to prevent significant gene expression the effect of temperature during the growth phase on final yield of product will be negligible (although if the temperature is too low a longer growth phase will be required leading to a reduction in productivity).

1.4.5.2 Effect on temperature on recombinant protein production

Park and Ryu (1990) studied the effect of temperature on the specific production rate of a recombinant protein (*trpA*) under the control of the pL/cI857 promoter/repressor system. They used a two stage continuous reactor system and found that the specific production rate of *trpA* increased approximately linearly with temperature up to about 41°C. They

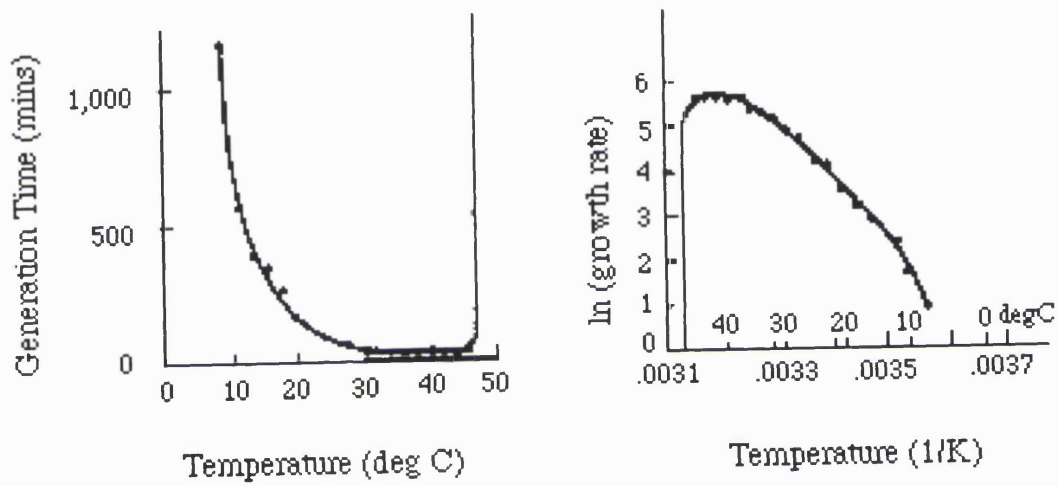


Figure 1.3: Effect of temperature on specific growth rate (Bailey and Ollis, 1986b).

Reproduced by permission of McGraw-Hill Ltd., Maidenhead, England.

proposed that this was due to a decrease in repressor activity. Above 41°C the specific production rate fell drastically which they proposed was due to increased protease activity. Assumptions had to be made about the number of non-plasmid harbouring cells but their results makes sense and we can conclude that during the production phase there is some temperature which will maximise productivity.

Unfortunately there is no experimental work on the lambda pL/cI857 promoter/repressor system which defines the effect of different temperatures on gene expression in a batch or fed-batch system nor anything on the effect of the rate of temperature increase during induction. There is a great deal of recent literature on the effect of temperature on host/vector systems where the copy number is temperature sensitive and on systems where the plasmid is unstable. However neither of these areas are relevant to the model system studied in this work.

A rapid rise in temperature (e.g. from 30 to 38°C as in this project) can also lead to the production of heat shock proteins which have been implicated in increased rates of proteolysis (Niedhart and VanBogelen, 1987). However in this project the recombinant product (B.S.T.) forms inclusion bodies within the cell and this probably protects the protein from degradation (Cheng *et al.*, 1981).

1.4.5.3 Effect of temperature on maintenance energy

The *E. coli* cell requires energy for certain specific maintenance functions such as turnover of cell materials and osmotic work to maintain concentration gradients (Pirt, 1975). This maintenance term, expressed as g glucose/g cells/h, has been correlated to temperature for a range of bacteria by the expression (Esener *et al.*, 1983):

$$m_r = C \exp\left(-\frac{\Delta H}{RT}\right) \quad (1.9)$$

The best available estimate for ΔH for *E. coli* grown on glucose was found to be 83.7 kJ/mol (Esener *et al.*, 1983).

1.4.6 Effect of growth on recombinant protein production

In some fermentations growth on excess glucose can cause repression of product formation - an effect known as catabolite repression (Pirt, 1975). However Jensen and Carlsen (1990) studied the production of MAE-hGH in continuous culture and found that the specific production rate of MAE-hGH was not affected by the specific growth rate (range 0.1 to 1.0 1/h) or by the glucose concentration (range 0.01 to 1.0 g/L). They concluded that the production of MAE-hGH was not catabolite repressed and confirmed this by showing that MAE-hGH yield was not affected by the addition of indole acetic acid, a c-AMP analogue that eliminates catabolite repression.

Of course growth will have an indirect effect on specific production rate since it will affect the concentration of glucose and acetate which (as described in Sec. 1.4.3) will affect the specific production rate of recombinant protein.

1.4.7 Effect of recombinant protein production on growth

MacDonald and Neway (1990) studied the effect of induction of recombinant (IL-2) gene expression on growth. They did this at different cell densities in fed-batch culture using a temperature shift from 30 to 37°C. They found that exponential growth ceased within half an hour of the start of IL-2 expression. Glucose concentration was kept at 8 +/- 1 g/L and acetate concentration was only 1 g/L at the time exponential growth stopped. Therefore glucose limitation or acetate inhibition were unlikely to have caused the rapid decrease in growth rate. Furthermore they showed that when the host organism without plasmid or containing the same plasmid but without the IL-2 gene was subjected to the same temperature shift growth increased as expected. Therefore they concluded that growth slowed as a direct result of the induction of IL-2 expression and not in response solely to temperature shift.

It is important to stress that since in these experiments the glucose was in excess this effect is not due to the effect of low glucose concentrations on growth but is instead a direct effect of production on growth. The actual mechanism of this effect is not clear

although, for example, Da Silva and Bailey (1986) have shown theoretically that foreign protein expression imposes a large metabolic burden on the cell.

One of the simplest ways this result could be expressed mathematically is as follows:

$$\mu = \mu_{\max} \left(1 - \frac{r_P}{r_{P,1}} \right) \quad (1.10)$$

where the value of $r_{P,1}$ would have to be determined experimentally. Once again it should be emphasised that this is simply a best guess at a mathematical expression which is consistent with the results and does not imply any mechanism for the effect.

Finally Bentley *et al.* (1990) also found experimentally that the growth rate of recombinant *E. coli* was reduced by the expression rate of foreign protein. However their results were complicated by the fact that two proteins were expressed: chloramphenicol-acetyl-transferase (CAT) and β -lactamase, the former induced and the latter constitutively. They found a linear decrease in specific growth rate with increasing protein content. It is unclear why they did not express their results in the form of Eqn. 1.10 since verbally this is how they were described. It is also unclear why the specific product concentration should be important since it is not the same thing as the specific production rate and it was not suggested that the product was toxic to the cell. In view of these concerns it was decided to still use Eqn. 1.10 to describe the effect of production on growth.

1.4.8 Other effects

1.4.8.1 pH/Ammonia

Ammonia is normally used to control the pH of recombinant fermentations at a constant value. Consequently during the fermentation the concentration of ammonia in the fermenter increases, particularly when acetate production is high. Concentrations of ammonia of 170 mM can inhibit growth (Thompson *et al.*, 1985).

1.4.8.2 Dissolved oxygen and carbon dioxide

Low concentrations of dissolved oxygen can lead to anaerobic fermentation and the production of acetate. Normally this is avoided by providing enough oxygen and agitation to maintain dissolved oxygen concentrations at or above 20 percent of air saturation.

Partial pressures of carbon dioxide above 0.3 atm are also to be avoided since they can also lead to an increase in acetate production (Pan *et al.*, 1987).

1.4.8.3 Medium osmolarity

High salt concentrations in the medium can reduce growth rates and yield of recombinant protein and are therefore to be avoided (Jensen and Carlsen, 1990). Generally this is done by careful feeding of nutrients.

1.4.9 High cell density fermentation.

1.4.9.1 Definition of high cell density.

In this project the terms "medium" and "high" cell density fermentation are used simply as a convenient way of describing the two types of fermentation process studied. "Medium" refers to the air sparged process induced at a cell density of about 4.5 g DCW/L. This is typical of current industrial practice (Strandberg *et al.*, 1991c). "High" cell density refers to the process induced at about 9.0 g DCW/L which uses oxygen enriched sparging.

In the literature the term high cell density has generally referred to achieving cell densities at the end of the fermentation which are considered high by the standard of the time. This means that the term has meant different things to different authors at different times (e.g. >6 g DCW/L by Whitney *et al.* (1989); >10 g DCW/L by Shiloach *et al.* (1991); >20 g DCW/L by Yee and Blanch (1992)).

Therefore in the following sections the term "high cell density" has generally been avoided and for each fermentation discussed the cell density is stated explicitly.

1.4.9.2 Potential benefits.

Knorre *et al.* (1990) have listed the potential benefits of obtaining higher cell densities than are achieved in present day industrial recombinant fermentations:

- Reduced fermenter size.
- Higher volumetric productivity.
- Facilitated recovery.
- Reduced volume in downstream processing.
- Reduced medium sterilisation requirements.
- Reduced waste and recycle stream.
- Reduced operating and manufacturing costs.

All these benefits are, of course, dependent on achieving higher final titres. Theoretically we can estimate the potential titres that could be achieved (Calcott *et al.*, 1988):

The maximum theoretical cell density for *E. coli* is about 160-200 g DCW/L (Markl *et al.*, 1993). If it is assumed that expression levels of 30% of total cell protein as cloned product can be achieved (i.e. similar to present values) and that the cell mass is about 60% protein then the final product titre that could be achieved is:

$$160 \times 0.30 \times 0.60 = 29 \text{ g/L}$$

Realistically titres of 20 g/L might be a more reasonable target (Calcott *et al.*, 1988). Thus there is a potential for at least a fourfold improvement over current industrial titres (e.g. 1-5 g recombinant product/L).

1.4.9.3 Actual benefits.

In practice cell densities for non-recombinant *E. coli* have been obtained that are close to the theoretical limit discussed above. The highest value achieved to date was by Lee *et al.* (1989) who used a membrane cell recycle reactor to remove inhibitory metabolites and reach cell densities of 145 g DCW/L. The record for the more normal fed-batch reactor is 125 g DCW/L (Mori *et al.*, 1979).

For fed-batch *E. coli* cultures producing a recombinant product the highest cell densities are somewhat less than these values. For example the highest cell density achieved so far for recombinant *E. coli* is 92-100 g DCW/L by Yee and Blanch (1993). However this run only produced 45 mg/L of product (a rat anionic trypsin) possibly because of its toxicity.

The highest final concentration of recombinant product reported so far for *E. coli* is 19.2 g/L of SpA- β galactosidase (Strandberg and Enfors, 1991a). The corresponding cell density was 77.0 g DCW/L thus the recombinant product constituted about 41% of total cell protein.

Clearly therefore the actual benefits of high cell density culture can be close to the theoretical values discussed in the previous section.

1.4.9.4 The effect of time of induction on recombinant protein production.

The preceding section showed that high titres of recombinant product are possible in high cell density culture. The key question, though, is whether there is a corresponding increase in product with increasing biomass - in other words does the specific yield stay constant at higher cell densities. Since these high cell densities are only achieved (in induced systems) by delaying induction this amounts to asking what is the effect of induction timing on specific biomass and foreign protein production and hence specific yield. Unfortunately there is very little information available in the literature to answer this question. Most of the work at higher cell densities has concentrated on ways of achieving these cell densities rather than investigating the effect on recombinant production.

Yee and Blanch (1993) found that IPTG induction at approximately 7.5 g DCW/L gave a final specific product yield of rat anionic trypsin of 0.9 g/g whereas induction at 75 g DCW/L gave 0.6 g/g (the corresponding total yields being 13 mg/L and 56 mg/L due to greater biomass in the late induced run). However it is not possible to draw firm conclusions from this since the late induced run may have been glucose starved whereas the early induced run was not. MacDonald and Neway (1990) also induced at different cell densities and found lower specific yields of product (IL-2) with later induction times. However acetate concentrations reached high levels (15 g/L) in some of the runs making it difficult to separate out the possible inhibitory effect of acetate from the effect of induction time itself.

George *et al.* (1992) showed that induction (using IPTG) at 1.1 g DCW/L gave a specific yield of TGF α -PE40 of 160 U/mg whilst induction at 4.7 g DCW/L gave 110 U/mg. However their data is more useful than that given above since the acetate profiles were similar for both runs (maximum 3.5 g acetate/L). Furthermore their data was used to calculate the specific production rate of TGF α -PE40 in the two fermentations (although this is not done in their paper). It was virtually identical (38 and 40 U/mg protein/h) in both runs suggesting that the cell density at induction does not affect the specific production rate.

In conclusion it appears that the specific recombinant production rate is probably not affected by the timing of induction and that differences in final specific yields are therefore related to other factors such as acetate inhibition or biomass production.

1.5 Literature review of mathematical modelling

The above literature review has focussed on what is known about recombinant *E. coli* fermentations. In the following sections the literature on the mathematical modelling of such fermentations is reviewed. The aim is to see how such models could be of benefit and whether there are any models which are appropriate for the process considered in this thesis.

The first section considers the potential benefits of mathematical modelling followed by a section on the actual benefits gained to date for recombinant *E. coli* fermentations. This is followed by a detailed discussion of the current models available for such fermentations.

1.5.1 Potential benefits of mathematical modelling

The following is a list of potential benefits of modelling fermentations starting with those that are easiest to achieve:

- Increased understanding of the process.
The rigorous quantitative nature of mathematical modelling and the requirement of proposing and testing mechanisms to account for the fermentation results leads, by its nature, to an increased understanding of the process. The important point, very seldom mentioned in the literature, is that this benefit can accrue even if the final model itself is unsuccessful. For example the structured model of Nielsen *et al.* (1989) was unsuccessful at predicting accurately the results of "runaway" plasmid replication (i.e. a dramatic increase in plasmid copy number during induction) but nevertheless improved the understanding of the process substantially (Nielsen and Villadsen, 1992).
- Process development.
A successful fermentation model can be used to perform "experiments" on a computer at a fraction of the cost and time of real fermentations thereby saving time and money. For example Asenjo *et al.* (1986) used a mathematical model for process development

of a simultaneous saccharification and fermentation process for the direct bioconversion of insoluble cellulose.

- Process optimisation.

A more ambitious goal is to use the model "in reverse" to determine, for example, the glucose feeding profile that would be required to optimise the final product titre. Cheruy and Durand (1979) used this approach to optimise the yield of an erythromycin fermentation by changing the pH and temperature profiles.

- Model-based control.

Finally models could be used on-line to control the process.

The aim of the model developed in this project is to increase the understanding of the process and to improve yield. Clearly such a model could also be used to reduce the need for experimentation. However it should be clear from the discussion of *E. coli* metabolism at the start of the literature review that any model will have to be a gross simplification compared with the complex reality of the fermentation. Therefore it is unlikely that mathematical models could ever entirely replace the need for experimentation. Indeed this may not be a desirable goal anyway. The history of industrial fermentation development is liberally sprinkled with examples of major process improvements that occurred due to experiments that went wrong! As in so much of science and engineering serendipity has played a major role.

Perhaps the real benefit of mathematical modelling can be that it frees the experimenter from routine interpolative experiments (which could be done on a computer) and allows him or her to try more innovative and extrapolative experiments which are more likely to lead to major breakthroughs.

1.5.2 Actual benefits of mathematical modelling

For recombinant *E. coli* fermentations the actual benefits of mathematical modelling have, so far, been small. Several models have been proposed that increase the understanding of the process (e.g. Bentley and Kompala, 1989; Nielson *et al.* 1989). However few models of recombinant *E. coli* fermentations have been used for process development, optimisation or model-based control and in general the recombinant *E. coli* fermentation models developed to date have had little industrial application (Zabriskie and Arcuri, 1986; Royce, 1993). There are several reasons for this:

- Most of the models have come from the academic community where the emphasis has been on model synthesis.
- Many of the models are complex, difficult to understand and contain many parameters which are strain dependent. Consequently companies are unwilling to invest time in the development and identification of such models especially if the model parameters need to be re-estimated every time a new strain is developed.
- Finally the models are often specific to certain host/vectors and process factors (e.g. plasmid stability and variable copy number) yet fail to include more universal physiological effects such as acetate production and inhibition.

Clearly there is a need for simpler recombinant fermentation models which are based on common host/vectors and which incorporate acetate production and inhibition. The basic form of such a model is outlined in Sec. 1.5.4.2 after first reviewing the types of mathematical model available and previous attempts at modelling recombinant *E. coli* fermentations.

1.5.3 Types of mathematical model.

Mathematical models can be categorised according to whether they are segregated or non-segregated and whether they are structured or unstructured.

A segregated model considers the cells in a fermenter as a heterologous population where different cells may have different properties (e.g. inclusion body size). This approach leads to complicated mathematics in the model (e.g. with population distributions) and longer computational times in solving the model equations. Thus there are very few segregated fermentation models. However there are times when such models are necessary. For example if it is necessary to take into account cells with different plasmid copy numbers (Seo and Bailey, 1985) or if a size distribution of inclusion bodies has to be determined (Bogle *et al.*, 1991). All the recombinant models described in the rest of this chapter are, however, unsegregated and therefore assume that the fermenter can be described in terms of an "average" cell.

Structured models, as their name implies, impose some internal structure on the cell - normally this consists of separate internal "compartments" or "pools" containing, for instance, DNA and proteins. Unstructured models are less realistic in that they treat the cell as a "black box" as far as physiology is concerned.

Most of the published models of recombinant *E. coli* are structured. The main reason for this is that it is logical to think of recombinant cells in terms of compartments of host and foreign (i.e. plasmid) DNA. Also the first recombinant models often concentrated on factors such as runaway plasmid replication which are most conveniently handled by structured models.

Before considering structured and unstructured models for recombinant *E. coli* in more detail another type of model should be mentioned. Artificial Neural Network (ANN) models consist of a number of simple interconnected nonlinear processing units (neurons) having adjustable connection strengths (weights). The network is "trained" by adjusting the connection weights until a set of inputs produces the desired set of outputs (Rivera and Karim, 1992). Inputs could, for example, be temperature, glucose and peptone feedrates, and the outputs biomass, glucose and product concentrations.

The ANN approach, still in its infancy, is potentially a rapid way of developing fermentation models for process development (Di Massimo-Peel *et al.*, 1992). However ANN models generally require many fermentation data sets for "training" and are less suited to interpretation and extrapolation beyond the data sets they are trained with (Glassey *et al.*, 1992). Since a major aim of this thesis was to improve the understanding of the fermentation process studied, by developing a model which has some physical meaning, it was decided not to use an ANN approach.

1.5.4 Recombinant *E. coli* models

1.5.4.1 Structured models

The classic example of a structured model is the two component model of Williams (1967). In fact this was developed for a non-recombinant fermentation but is the basis of many subsequent attempts at modelling recombinant fermentations

The cell is assumed to consist of two components: the synthetic (RNA) portion R and the genetic (DNA plus protein) portion D. It is assumed that:

- i). R is produced from an external nutrient A.
- ii) The D component is fed from the R component
- iii) Doubling of the D component leads to cell division
- iv) The total biomass (M) is the sum of D and R

From this and a few simple kinetic assumptions the following equations can be derived:

$$\frac{dA}{dt} = -k_1AM \quad (1.10a)$$

$$\frac{dR}{dt} = k_1AM - k_2RD \quad (1.10b)$$

$$\frac{dD}{dt} = -k_2RD \quad (1.10c)$$

$$\frac{dM}{dt} = k_1AM \quad (1.10d)$$

The solution to these model equations describes many of the experimentally observed features of batch growth including the lag and stationary phases and the change of cell size and composition with changes in the specific growth rate. The disadvantage of this and other structured models is that it is difficult to determine the model parameters. Nevertheless this example shows that by considering some very simple cell structure we can account for features of the fermentation such as the lag phase that can not be easily accounted for by unstructured models.

Models of recombinant *E. coli* fermentations have been based on the same ideas but have used more compartments. For example, Bentley and Kompala (1989) developed an eight compartment model which includes all the major cell components (e.g. amino acids, nucleotides etc.). The model could correctly predict the effect of protein synthesis and induced "runaway" replication on the growth rate. However it was very complex. A simplified version was therefore developed by Nielsen *et al.* (1989) which had four compartments (Plasmid and host DNA and foreign and host protein). Again the model predictions of reduced growth rate on induction were confirmed by experiment but even this simpler version of the model had about 25 parameters.

A general problem with the above recombinant models is that they have focused on specific issues such as "runaway" plasmid replication. However such systems are seldom used for industrial recombinant protein production. Other recombinant *E. coli* models have also focused on features which are of limited industrial importance. For example: the *lac* promoter system in conjunction with runaway plasmid replication (Lee and Bailey, 1984) and the *tac* promoter, runaway plasmid replication and culture instability (Tonga *et al.*, 1993).

Furthermore virtually none of the recombinant *E. coli* structured models in the literature include terms to predict the production of acetate or its inhibitory effects on growth and production. One exception is the model of Strudsholm *et al.* (1992) which was developed from the Nielsen *et al.* (1989) model but included a term for acetate production and assimilation (the model had about 23 parameters). However this model was developed to take account of diauxic growth during batch production (i.e. growth on acetate after glucose had been exhausted). The model could not be used to predict the effect of glucose feedrate on acetate production.

Finally it might seem reasonable that the above structured models, even if they are not appropriate for this project, might be simplified to their equivalent unstructured model or at least that some of the kinetic terms might be used. In practice it is extremely difficult to relate the terms in a structured model (e.g. rate of production of host plasmid) to terms in the unstructured model (e.g. rate of production of biomass) and therefore it is normally better to start from scratch with the unstructured model (Nielsen, private communication, 1993).

1.5.4.2 Unstructured models

There have only been a few published unstructured recombinant *E. coli* models none of which are useful for this project. For example the model of Lee *et al.* (1985) describes product formation in an unstable recombinant population and the model of Mizutani *et al.* (1987) describes the effect of runaway plasmid replication.

Therefore the approach that has been taken in this project is to start from scratch and develop a new unstructured model of the process. The basic form of such an unstructured model to describe growth, product formation and glucose consumption has been described by, for example, Pirt (1975):

$$\frac{dX}{dt} = \mu X - \frac{X}{V} Q \quad (1.11a)$$

$$\frac{dP}{dt} = r_p X - \frac{P}{V} Q \quad (1.11b)$$

$$\frac{dS}{dt} = \frac{Q_{gluc} c_{gluc}}{V} - \frac{\mu X}{Y_{SX}} - \frac{r_p X}{Y_{SP}} - mX - \frac{S}{V} Q \quad (1.11c)$$

$$\frac{dV}{dt} = Q - Q_{samp} \quad (1.11d)$$

Where:

$$Q = Q_{gluc} + Q_{pept} + Q_{amm} - Q_{evap} \quad (1.12)$$

$$\mu = \mu_{max} f(S, A, r_p) \quad (1.13)$$

$$r_p = r_{p,max} f(S, A) \quad (1.14)$$

Each of these equations can be explained as follows

Biomass production (Eqn. 1.11a)

The rate of change of biomass concentration is equal to the specific growth rate times the biomass concentration (i.e. growth is autocatalytic). The term $\frac{X}{V} Q$ takes account of the change in biomass due to volume changes and sampling.

Recombinant production (Eqn. 1.11b)

This is equivalent to the biomass production equation except that product concentration appears in place of biomass concentration.

Glucose consumption (Eqn. 1.11c)

There are five terms on the right hand side of this equation. The terms $\frac{Q_{gluc}c_{gluc}}{V}$ and $\frac{S}{V}Q$ take account of the change in concentration due to glucose feeding and volume changes.

The terms $\frac{\mu X}{Y_{SX}}$ and $\frac{r_P X}{Y_{SP}}$ relate the amount of biomass and product produced to the amount of glucose consumed by means of the yield coefficients. The maintenance term "mX" reflects the widely observed effect (e.g. Heijnen and Roels, 1981) that some glucose is used to support maintenance functions within the cell.

The volume balance (Eqn. 1.11d) completes the model. However before it can be used to model the fermentation studied in this thesis further modifications need to be made to it. First an equation for acetate production needs to be included. Second the kinetic equations (i.e. 1.13 and 1.14) need to be defined. These changes are made in Chapter 4 by using the information from the literature review (Sec. 1.4) and the experimental results (Secs. 3.4 - 3.7).

There is one major drawback of unstructured models such as this that has not yet been discussed. That is they assume that the cellular composition remains constant. During exponential growth this is probably true (Esener *et al.*, 1983) but it is unlikely to be true when environmental conditions are changing rapidly such as during the induction period.

Finally for completeness the model of Sonnleitner and Kappeli (1986) should be mentioned. This is probably the most accepted yeast model (Nielsen and Villadsen, 1992) and is based on the assumption of a limited respiratory capacity. Thus if the flux of glucose into the yeast cell exceeds a certain value it is channelled into ethanol production. The model is mentioned because there is an obvious analogy with acetate production in *E. coli* which occurs due to overfeeding glucose. However the model was rejected for this thesis since the problem considered here is more complicated (e.g. with peptone feeding and temperature changes) and also because the mechanism for acetate production may not

be the same as that for yeast (i.e. respiratory limitation). However the model will be mentioned again in Chapter 4.

1.6 Conclusions from literature reviews

From the literature review of recombinant *E. coli* it is clear that the most important variables affecting productivity of the process are: glucose feeding, temperature and peptone feeding. Where possible it was shown how mathematical expressions could be obtained relating these variables to the specific production rate and the specific growth rate so that they could later be incorporated into a model of the process.

In the review of the modelling of recombinant *E. coli* fermentations it was shown that there are no existing models that could be used for the process used in this thesis project because none of them took acetate into account. It was therefore decided to develop a new model from scratch. An unstructured model was chosen since these are generally easier to understand. It was shown how the basic form of such an unstructured model could be obtained from the literature.

1.7 Project plan.

In order to achieve the project goals stated in Sec. 1.3, and in the light of the literature review, the following project plan was decided upon:

- Perform several "medium" cell density fermentations (induced at 4.5 g DCW/L and using air sparging) which differ only in their glucose feed profiles. The results from these runs would be used to develop a model of the process (i.e. the first project goal). This model would then be used to determine the best glucose feed profile to optimise the yield of B.S.T.
- Perform several "high" cell density fermentations (induced at 9.0 g DCW/L and using oxygen sparging) which differ only in their glucose feed profiles. Use these results and the model to determine the best glucose feed profile to optimise the yield of B.S.T.
- Compare the two optimised processes in terms of final titres, net production rate and specific production rate of B.S.T. (i.e. the second project goal)
- In order to make the model identification easier it was decided to:
 - a) Use a simple glucose feedrate profile (i.e. no closed-loop control)
 - b) Choose the feedrate so that in both the medium and high cell density runs the glucose became limiting at least two hours after induction. This meant each run would have a period of recombinant production which was not glucose limited making it easier to compare runs.

2 MATERIALS AND METHODS

2.1 Summary

This chapter lists the materials and methods used during the thesis.

2.2 Microorganism

The host/vector used throughout this project was RV308/pHKY531 which was constructed and cloned by Eli Lilly and Company (Indianapolis, Indiana, U.S.A).

The host (RV308) is a derivative of *E. coli* K-12 which is thiamine deficient. The vector is a *rop*⁻ plasmid which expresses met-asp-bovine somatotropin. It also contains genes for tetracycline resistance and the cI857 temperature sensitive repressor which controls B.S.T. expression. It was constructed by inserting the B.S.T. gene from pCZR115 (Schoner *et al.*, 1984) into pHKY309 which was derived from pHKY292. The parental plasmid for construction of pHKY292 was equivalent to pL110/K2 (Wilhelm *et al.*, 1990).

2.3 Equipment

2.3.1 Fermenter

A 7L glass fermenter (model i2000, LH fermentation Ltd., Maidenhead, Berks., U.K.) was used for all fermentations. Broth volumes varied between 3L and 6L. A standard mixing configuration was used: three equally spaced six bladed Rushton disc turbines and four tank baffles (Fig. 2.1)

pH was measured using a 10-465-3184 combined electrode and DO₂ with a 322756702 polarographic probe (Ingold, Urdorf, Switzerland).

Two 5 Kg load cells (Defiant Weighing, Kent, U.K.) were used to continuously measure the ammonium hydroxide and glucose feeds which were fed from 1L and 2L calibrated glass cylinders. The ammonium hydroxide solution was fed automatically to control the pH at 7.0. Glucose was fed using a model 101U 0-32 rpm Watson-Marlow pump (Falmouth, U.K.).

Peptone was fed at room temperature from a 2L flask continuously mixed with a magnetic stirrer. At critical times (i.e. before and after batching and at the end of the fermentation) the peptone flask was removed from the stirrer plate and placed briefly on a load cell so that accurate peptone feedrates could be determined. Two Watson-Marlow (Falmouth, U.K.) 101U pumps were used to feed peptone: A 0-32 rpm one for the batched peptone and a 0-2 rpm one for the continuous feed.

An LH i3000 instrumentation unit provided local display of pH, DO₂, agitation speed, inlet gas flowrate, broth temperature and both load cells. Every three minutes a record of these parameter values was sent to a data logging computer Bio-I (BCS Ltd., Maidenhead, Kent, U.K.). This system provided facilities for both real-time and historical data trending.

The inlet and exit gases from the fermenter were pumped to a MM 8-80 mass spectrometer (VG Gas Analysis, Winsford, U.K.) where they were analysed for percent nitrogen, oxygen, carbon dioxide and argon. This analysis was performed every 2-3 minutes and sent automatically to the Bio-I computer.

The inlet gas mixing system is shown in Fig. 2.2. Total gas flowrate into the fermenter was measured by a HI-TEC F100 thermal mass flowmeter (Bronkhorst High Tech B.V., Ruurlo, Netherlands) and controlled by an automatic control valve using a setpoint entered at the fermenter instrument panel. If required, oxygen could be bled into the inlet air prior to this control valve. The oxygen flowrate was controlled manually by a needle valve and displayed locally at the oxygen mass flowmeter. The oxygen supply came from a gas cylinder (B.O.C., London) and was regulated to 1.2 bar g - i.e. slightly above the plant air supply (1.1 bar g). Before entering the fermenter the inlet gas passed through a 0.22 micron sterilising filter.

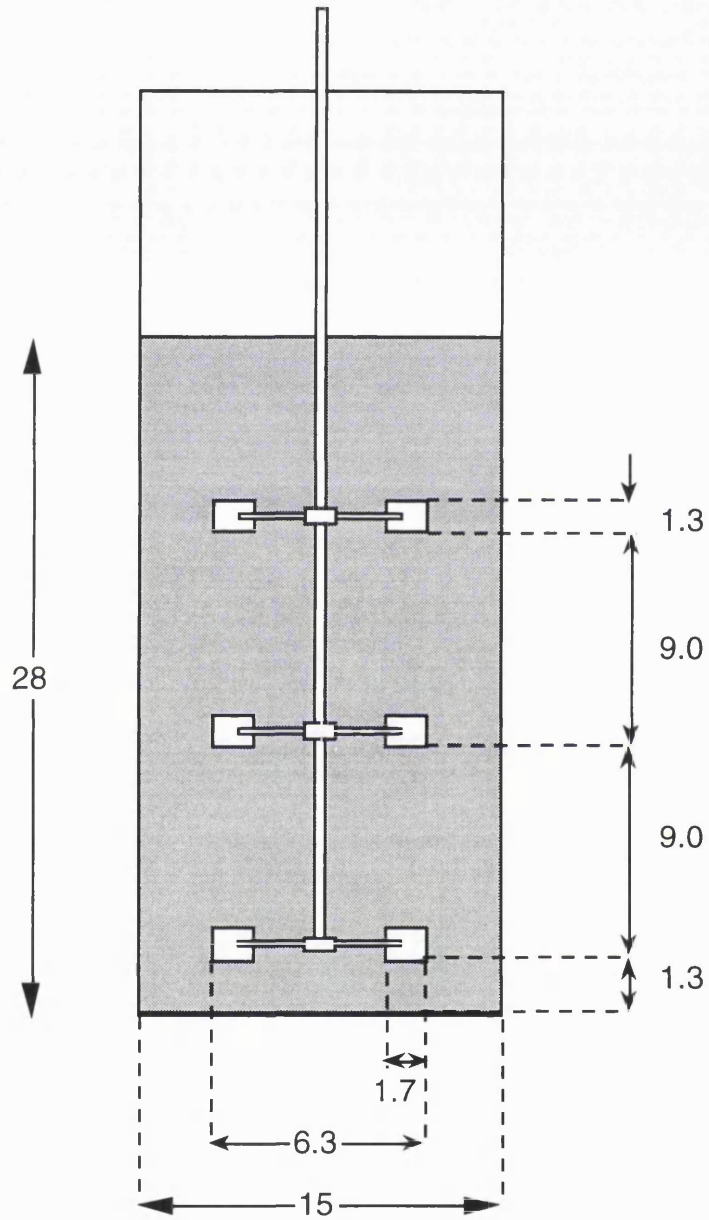


Figure 2.1: Fermenter geometry (all dimensions in cm)

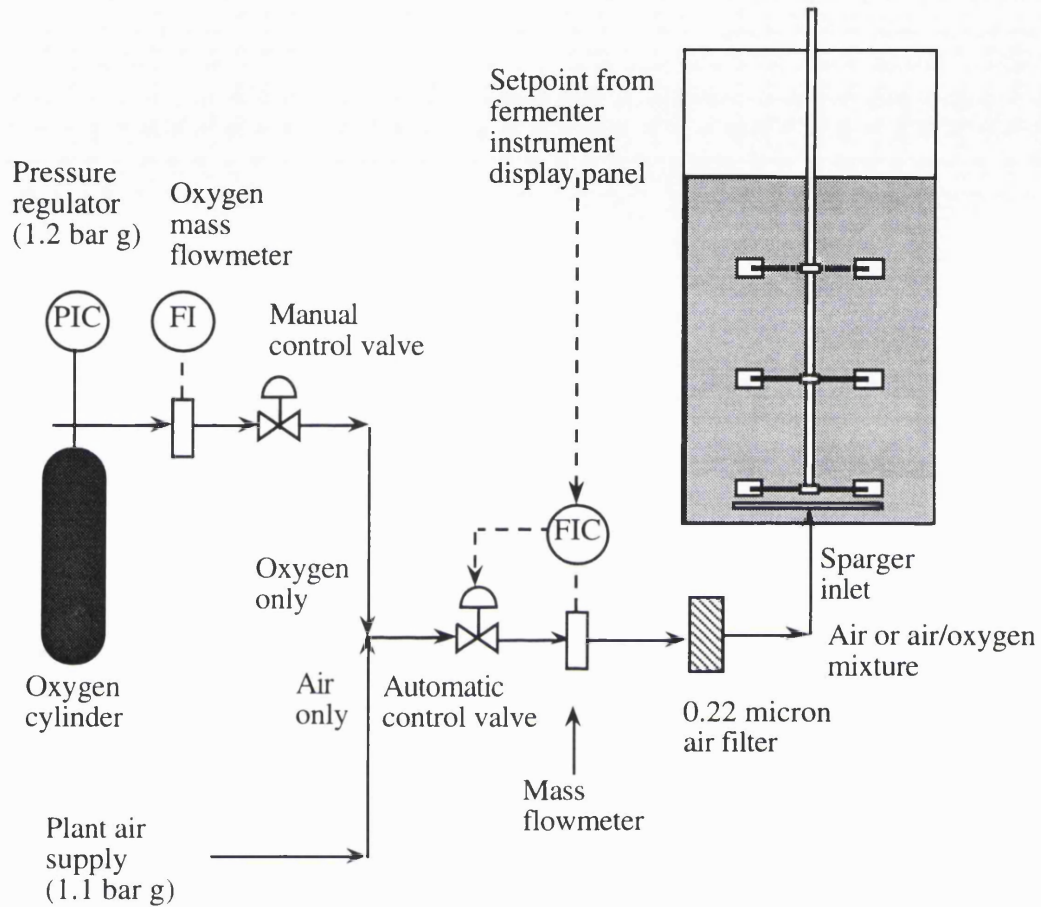


Figure 2.2: Equipment for oxygen enriched sparging

Notation: FI = flow indicator
 FIC = flow indicator and controller
 PIC = pressure indicator and controller.

2.3.2 High Performance Liquid Chromatography (HPLC)

B.S.T. was assayed using an HPLC system obtained from Millipore (U.K.) Ltd., Waters Chromatography Division (Watford, U.K.). This comprised the following:

Waters model 510 HPLC pump.

Waters intelligent sample processor (WISP) model 712 for automatic sample injection.

Waters temperature control module (TCM).

NEC Powermate SX Plus computer (2/42 MB).

Waters Baseline 810 chromatography software

NEC Pinwriter P60 printer

The HPLC column was obtained from HiChrom Ltd., (Reading, Berks., U.K.) contained Nucleosil 300-5 C4 packing and was 25 cm long with 4.6 mm internal diameter.

2.4 Methods

2.4.1 Preparation of the working cell bank

After cloning the host/vector Eli Lilly and Company created a master cell bank of 100+ frozen straws in Indianapolis, U.S.A. and a sub-master cell bank of some 50 frozen straws at Dista Products Ltd., Liverpool, U.K. At the start of this project a working cell bank of 77 frozen bio/freeze vials was created from the latter. This was then transferred to University College London and provided a convenient source of starting material for all the fermentations. The procedure for creating the working cell bank is described below and shown in Fig. 2.2 (all steps after removing the frozen straw were done aseptically):

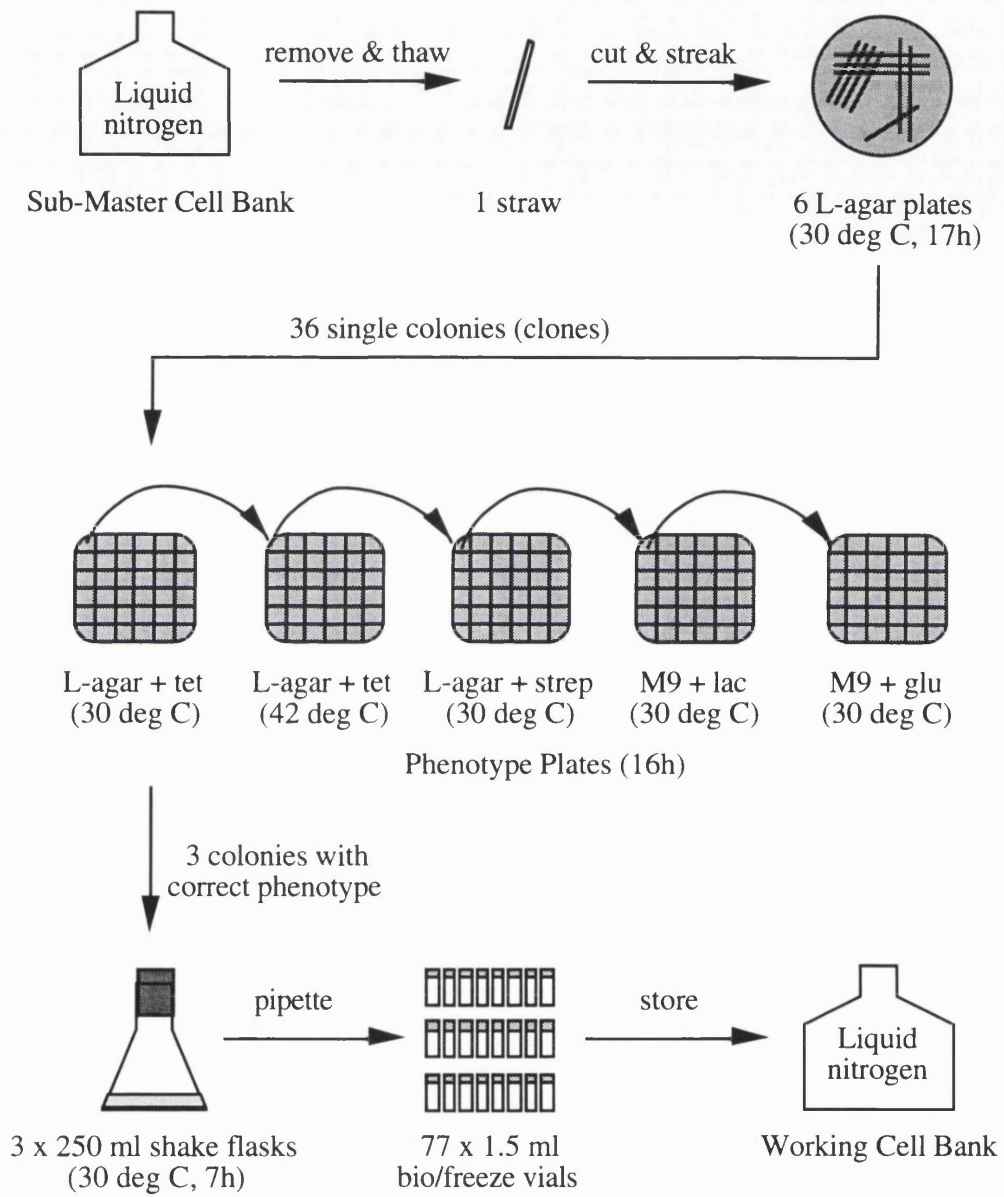


Figure 2.3: Preparation of the working cell bank.

A single frozen straw containing RV308/pHKY531 was removed from the sub-master cell bank, thawed at 25°C, cut open and the contents streaked on to 6 L-agar plates. After incubation at 30°C for 17 hours six colonies were taken from each plate and spotted onto the phenotype selection plates shown in Table 2.1.

Table 2.1

Phenotype selection plates used when making working cell bank.

Plate Number	Medium	Incubation temp. (°C)	Correct growth response
1	L-agar + 5 µg tet./ml	30	good
2	L-agar + 5 µg tet./ml	42	poor
3	L-agar + 25 µg strep./ml	30	good
4	M9 + lactose	30	none
5	M9 + glucose	30	good

The purpose of this step was to ensure that colonies of the correct phenotype were selected prior to growing them up to provide enough material for making the working cell bank. Colonies of the correct phenotype will show the growth responses indicated in the above table. The reasons for this are explained as follows:

- Plate 1: RV308/pHKY531 will grow well on plate 1 since the plasmid confers tetracycline resistance on the cell.
- Plate 2: RV308/pHKY531 will exhibit reduced growth since the higher incubation temperature (42°C) will induce B.S.T. expression (see Sec. 1.4.5) at the expense of growth.
- Plate 3: RV308/pHKY531 will grow well on plate 3 since the host *E. coli* strain gives it resistance to streptomycin.
- Plate 4: RV308/pHKY531 is unable to metabolise lactose and will therefore not grow on plate 4 which consists of minimal media (M9) and lactose.
- Plate 5: However when glucose is used instead of lactose growth is normal.

Thus after incubation for sixteen hours three individual colonies were selected that exhibited the correct phenotype. Each of these colonies was transferred by sterile loop into a 250 ml shake flask containing 50 ml L-broth.

The three shake flasks were incubated for 7 hours at 30°C, 250 rpm on a 1 inch throw shaker. At the end of this period 1.5 ml aliquots of the broth were transferred into 2 ml bio/freeze vials. Each individual shake flask provided enough broth for a separate sub-clone lot consisting of 20 to 30 ampoules. Thus three separate lots of sub-clones (a total of 77 bio/freeze vials) were stored in the vapour phase of liquid nitrogen and this working cell bank was then transferred to University College, London. The same sub-clone was used in all but two of the fermentations in this thesis.

2.4.2 Fermentation media

2.4.2.1 Starting media.

A list of the chemicals used for fermentation and their suppliers is given in Table 2.2. Four different media were used during this work (see Table 2.3). The differences between them are summarised below. (Note: All media had the same concentrations of tetracycline hydrochloride and batched glucose).

Medium O: This was the original medium used.

Medium A: As medium O but with twice the amount of potassium phosphate and sodium phosphate. The citric acid concentration was also doubled to help chelate the stronger medium.

Medium B: As medium O but twice the concentration of everything.

Medium C: As medium O but two and a half times everything except citric acid (4x) and sodium phosphate dibasic (6x). This medium also had extra trace elements.

Table 2.2

Fermentation chemicals (all GPR grade) and their suppliers

Chemical	Supplier
Citric acid	BDH Ltd., Poole, U.K.
$(\text{NH}_2)_2\text{Fe}(\text{SO}_4).6\text{H}_2\text{O}$	FSA Lab Supplies, Loughborough, U.K.
$\text{ZnSO}_4.7\text{H}_2\text{O}$	BDH Ltd., Poole, U.K.
$\text{CuSO}_4.5\text{H}_2\text{O}$	BDH Ltd., Poole, U.K.
$\text{MnSO}_4.\text{H}_2\text{O}$	BDH Ltd., Poole, U.K.
$\text{CoCl}_2.6\text{H}_2\text{O}$	BDH Ltd., Poole, U.K.
$\text{NaMoO}_4.2\text{H}_2\text{O}$	BDH Ltd., Poole, U.K.
$\text{Na}_2\text{B}_4\text{O}_7$	BDH Ltd., Poole, U.K.
KH_2PO_4	FSA Lab Supplies, Loughborough, U.K.
NH_4Cl	FSA Lab Supplies, Loughborough, U.K.
Na_2HPO_4	FSA Lab Supplies, Loughborough, U.K.
K_2SO_4	BDH Ltd., Poole, U.K.
$\text{CaCl}_2.2\text{H}_2\text{O}$	BDH Ltd., Poole, U.K.
$\text{MgSO}_4.7\text{H}_2\text{O}$	BDH Ltd., Poole, U.K.
Thiamine hydrochloride	BDH Ltd., Poole, U.K.
Tetracycline hydrochloride	Merck, Darmstadt, Germany
Glucose monohydrate	BDH Ltd., Poole, U.K.

Table 2.3

Composition of the four different media used in this thesis (all in g/L).

	O	A	B	C
Citric acid	.33	.66	.66	1.32
(NH ₂) ₂ Fe(SO ₄).6H ₂ O	.60	.60	1.20	1.50
ZnSO ₄ .7H ₂ O	.0032	.0032	.0064	0.0080
CuSO ₄ .5H ₂ O	.00033	.00033	.00066	.00083
MnSO ₄ .H ₂ O	.00057	.00057	.00114	.00143
CoCl ₂ .6H ₂ O				.0015
NaMoO ₄ .2H ₂ O				.0015
Na ₂ B ₄ O ₇				.00039
KH ₂ PO ₄	1.98	3.96	3.96	4.93
NH ₄ Cl	1.32	1.32	2.65	3.30
Na ₂ HPO ₄	1.05	2.10	2.10	6.61
K ₂ SO ₄	6.62	6.62	13.23	16.54
CaCl ₂ .2H ₂ O	0.33	0.33	0.66	0.83
MgSO ₄ .7H ₂ O	0.66	0.66	1.32	1.65
Thiamine hydrochloride	.0066	.0066	.0132	.0165
Tetracycline hydrochloride	.0020	.0020	.0020	.0020
Glucose (batch)	12.5	12.5	12.5	12.5

2.4.2.2 Media feed

Some of the high cell density fermentations used medium B+. This consisted of medium B plus an extra mineral feed during the fermentation. This extra feed was made up of the following solutions:

Solution A 2.16 g $\text{CaCl}_2 \cdot 2\text{H}_2\text{O}$ in 60 ml DI water.

Solution B 4.30 g $\text{MgSO}_4 \cdot 7\text{H}_2\text{O}$ in 60 ml DI water.

Solution C 8.5 g KH_2PO_4 + 11.4 g Na_2HPO_4 in 150 ml DI water.

Solution D 2.16 g Citric Acid + 2 mls of trace element solution in 50 ml DI water.
(the trace element solution contained 10.3 g/L $\text{CoCl}_2 \cdot 6\text{H}_2\text{O}$
+ 1.07 g/L $\text{NaMoO}_4 \cdot 2\text{H}_2\text{O}$ + 0.185 g/L $\text{Na}_2\text{B}_4\text{O}_7$).

All the solutions were autoclaved at 121°C for 20 minutes. Solution A and B were kept separate and neither was pH adjusted (their respective post-autoclave pHs being 6.1 and 7.7). Solutions C and D were mixed after autoclaving and pH adjusted to 7.0 using 20M ammonium hydroxide.

Solutions A and B were fed to the fermenter as 6 x 10 ml sterile injections at hourly intervals between 8 and 13 hours. The mixed C and D sterile solution was pumped into the fermenter at 36 ml/h between 8 and 13 hours.

Using the above protocol the total amount of CaCl_2 , MgSO_4 , PO_4 , Co, Mo, B and citric acid fed was equal to the amount of these components in the original batched medium B.

2.4.3 Preparation of the fermenter

Prior to each fermentation the temperature, inlet gas flow meter and (if used) the oxygen flowmeter were calibrated against external standards. The oxygen flowmeter was calibrated using oxygen. The inlet gas flowmeter was calibrated using air which, since it was a mass flowmeter, will cause a slight error when oxygen is added to the inlet gas mixture. The worst error will occur when the inlet gas contains the most oxygen which in this thesis was 50%. In this worst case the volumetric flow will be 4% in error. In most of the runs the error will be much less than this and, of course, there will be no error when air-only sparging was used.

Peptone powder (Sheffield Products, N.Y., U.S.A.) was dissolved in hot D.I. water at a concentration of either 100 g peptone/L or 176 g peptone/L (see next section). D-glucose monohydrate (BDH Ltd., Poole, U.K.) was dissolved in hot D.I. water and used at a concentration of 500 g glucose/L in all fermentations. Both feeds were sterilised at 121°C for 30 minutes and after cooling connected to the (sterilised) fermenter.

All the chemicals in the fermenter medium except tetracycline and thiamine were dissolved in D.I. water, transferred to the fermenter then made up to a pre-sterilisation volume of 3.5 L. The fermenter was sterilised at 121°C and 1 bar abs. for 30 minutes at 600 rpm. Typical post-sterilisation volume was 3.25 L.

After sterilisation and when the medium had cooled down tetracycline hydrochloride and thiamine hydrochloride solution were added through a sterile 21 gauge needle and 0.2 µm acrodisc (Gelman Science). Enough glucose solution was pumped into the fermenter (approximately 85 ml) to give the required starting concentration (12.5 g glucose/L).

The pH probe was calibrated by taking a sample and checking with an independently calibrated pH probe. pH was then adjusted to 7.0 by feeding either 4M or 8M ammonium hydroxide solution (FSA Lab Supplies, Loughborough, U.K.). The DO₂ probe was calibrated so that at 30°C and 800 r.p.m. with 3.25 SLPM air sparging the probe read 100% and with nitrogen sparging read 0%.

2.4.4 Fermentation

Each medium or high cell density fermentation consisted of a growth period at 30°C followed by a production phase when the temperature was raised to start B.S.T. gene expression. All experiments had the same growth conditions.

Every fermentation was inoculated using 1 ml of thawed cells from a single bio/freeze vial taken from the working cell bank. The advantage of using such a small inoculum was that the entire growth phase took place in the fermenter and was therefore closely monitored and controlled. The alternative of growing a larger inoculum in a (less well controlled) shake flask would have led to more process variability. A summary of growth conditions is given in Table 2.4.

Table 2.4

Growth conditions in medium and high cell density fermentations.

Parameter	Setpoint	Unit	Comments
pH	7.0	-log[H ⁺]	Ammonium hydroxide (no acid)
Temperature	30.0	°C	
Back Pressure	0.0	bar gauge	

Initially the agitation was set at 800 rpm but was increased to 1500 rpm (maximum) when the DO₂ reached about 30% (normally a few hours before the growth period ended).

Growth was allowed to continue until the concentration of CO₂ in the exit gas reached 1.8% (medium cell density fermentations) or 3.6% (high cell density fermentations) at which point the production phase was started by increasing the temperature. Typically the growth phase for the medium cell density fermentations lasted about 19 hours but varied by +/- 1 hour probably due to variation in inoculum size (the high cell density fermentations had approximately an extra hour of growth before being induced). To make it easier to compare fermentations all run times were standardised on the time that the concentration of the %CO₂ in the exit gas reached 1.8%. This time was set at 5.75 hours

so that the fermentations in this report could be compared with a comparable industrial fermentation. Using this convention inoculation was typically at -13 hours.

For induction the temperature profile was raised from 30°C to 38°C over 48 minutes. Since it was not possible to automatically ramp the temperature this was achieved by manually increasing the temperature setpoint by 1°C every 6 minutes. One hour after reaching 38°C the temperature setpoint was raised to 39.5°C and stayed there for the rest of the fermentation.

Glucose feeding was started in all fermentations at about 6.05 hours and was fed at room temperature at a concentration of 500 g glucose/L. The feedrate was varied between some runs to see the effect on productivity.

Peptone feeding was started when the temperature reached 37°C for both medium and high cell density fermentations. It always consisted of a "batched" amount fed quickly in the first 12 minutes followed by a much slower continuous feed until the end of the run. Two different feedrates and concentrations were used - defined as low or high in the following table:

Table 2.5

Peptone feedrates and concentrations.

	Concentration (g peptone/ L solution)	"Batched" g peptone (ml solution)	Slow feedrate g peptone/h (ml solution/h)	Typical total fed = "batched" + slow feed (g peptone)
Low	100	42 (420)	7 (70)	42 + 42 = 84
High	176	39 (220)	20 (114)	39 + 120 = 159

The figure for total peptone fed is based on a typical six hours of feeding before the fermentation is terminated. It can be seen that in the high feedrate regime about twice as much peptone is fed in total although about the same amount is "batched" in.

In all fermentations the dissolved oxygen concentration was kept above 20% air saturation. For medium cell density fermentations this was achieved with a constant air sparge of 3.25 SLPM. For high cell density fermentations the air sparge was enriched with pure oxygen (see Sec. 2.3.1 and Fig. 2.2). The oxygen was always required just after induction started in these high cell density runs.

Typically fermentations were terminated eight hours after the production phase started. Small amounts of a sterilised silicone based antifoam were fed manually to the reactor to reduce foaming. Normally this would consist of a total of 2ml of antifoam during the production phase.

Samples were taken every hour for four hours before the production phase started and thereafter every half hour. Each 17 ml sample was preceded by a 17 ml waste sample to clear the sample line of stagnant broth. Samples were analysed for biomass, glucose, acetate, and B.S.T.

The growth-only fermentations had the same conditions as the induced runs but with the temperature kept at 30°C for the whole run. Oxygen enriched sparging was used. Glucose was fed at sufficient rate to keep it from becoming limiting or inhibitory (i.e. 1-40 g/L). Peptone was either not fed at all or fed at the high feedrate shown in Table 2.5.

2.5 Assays

2.5.1 Biomass

Immediately after sampling 1 ml of broth was pipetted into each of four 1 ml Eppendorf tubes and centrifuged at 5000 rpm for 10 minutes. The supernatant was poured into glass vials and frozen for acetate and glucose analysis. The remaining pellets were dried overnight at 105°C, cooled in a desiccator and weighed. This gave the dry cell weight of unrinsed cells which was converted to a rinsed dry cell weight value by use of the calibration curves described in Appendix A. Biomass was determined by subtracting the B.S.T. titre from the rinsed dry cell weight (since B.S.T. is retained within the cells).

2.5.2 Glucose

Glucose was analysed using hexokinase diagnostic kit F115-A from Sigma Chemical Company (Poole, Dorset, U.K.)

2.5.3 Acetate

Acetate was measured using an enzyme kit, catalogue number 148261, from Boehringer Mannheim (Mannheim, Germany).

2.5.4 HPLC

B.S.T. was assayed using an HPLC method that was modified from that used by Riggin and co-workers (Riggin *et al.*, 1987). Immediately after sampling 3 mls of broth were

pipetted into each of two 50 ml centrifuge tubes to which 3 mls of methanol were then added to kill the recombinant cells. The killed broth samples were stored at -18°C in the freezer until the end of the fermentation.

The samples were then removed, shaken, and centrifuged at 3000 rpm for 10 minutes. The supernatant was discarded and 30 mls of a sulphitolysis reagent added to each sample. Details of the reagents used are given in Table 2.6.

Table 2.6

Composition of sulphitolysis reagent (made up in deionised water).

Chemical (all AnalR grade)	Concentration (g/L)	Supplier
Sodium lauryl sulphate	20.0	FSA Lab Supplies,Loughborough, U.K.
Tris(hydroxy)methylamine	6.06	FSA Lab Supplies,Loughborough, U.K.
Sodium sulphite anhyd.	12.0	FSA Lab Supplies,Loughborough, U.K.
Potassium tetrathionate	3.04	BDH Ltd., Poole, U.K.
EDTA disodium salt	0.37	FSA Lab Supplies,Loughborough, U.K.

Thirty mls of this sulphitolysis reagent was also added to 10 mg of B.S.T. reference standard in a vial supplied by Eli Lilly and Company (Indianapolis, Indiana, U.S.A.).

All samples were stirred with small magnetic stirrer bars for at least 12 hours to allow for derivitisation to s-sulphonates. At least 2 ml of each sample were then filtered into an HPLC vial through a 0.2 µm nylon filter. Up to 60 vials were loaded on to the automatic sample injector and the chromatography conditions set up as follows:

Isocratic pump rate	0.5 mls/h
Sample injection volume	20.0 µL
Sample injection time	40 mins
U.V. detector	214 nm (1V F.S.D.)
Column temperature	60 °C

The composition of the mobile phase is given in Table 2.7.

Table 2.7

Composition of the HPLC mobile phase (made up in D.I. water).

Chemical (all AnalR grade)	Concentration (g/L)	Supplier
Ammonium dihydrogen orthophosphate	2.9	FSA Lab Supplies,Loughborough, U.K.
Diammonium hydrogen orthophosphate	1.42	FSA Lab Supplies,Loughborough, U.K.
Sodium lauryl sulphate	10.0	FSA Lab Supplies,Loughborough, U.K.
Propan-1-ol	28 % v/v	BDH Ltd., Poole, U.K.

The BST s-sulphonate peak eluted at approximately 24 minutes and the reference standard at 18 minutes. The ratio of the peak areas (integrated using the Waters Baseline 810 software) gave the B.S.T. concentration in the sample.

3 RESULTS AND DISCUSSION

3.1 Summary

In this chapter the results of twelve fermentations are discussed qualitatively. Growth-only fermentations were performed to develop a medium and to show the effect of peptone feeding on acetate production. Medium and high cell density fermentations were then conducted using this new medium and were shown to be inhibited by acetate. It was shown how reduced glucose feeding led to less acetate and higher titres but that if glucose feeding was reduced too much then glucose starvation occurred and the B.S.T. production rate was decreased.

A comparison between the medium and high cell density fermentations showed that the latter produced B.S.T. at a faster rate because it had more cells at the time of induction. However it also produced acetate at a faster rate and reached inhibitory levels of acetate after a shorter period of production. Therefore the final B.S.T. titre in the high cell density process was less.

In the Chapter 4 a mathematical model is developed to describe these fermentations in a more quantitative and rigorous manner.

3.2 Introduction

3.2.1 Experimental strategy

The project goals and plan have been stated in Secs. 1.3 and 1.7. The original experimental strategy to achieve them was to perform several medium and high cell density fermentations and then to compare the most productive examples of each process. It was assumed that the medium would not be limiting and that acetate could be kept below inhibitory values by controlling the glucose feedrate. Thus it was anticipated that the productivity of the fermentation would only be limited by the maximum specific

activity (i.e. the maximum amount of B.S.T. each cell could contain). Thus the mathematical model of the process, which would be developed concurrently with the experiments, would include a term for the maximum specific activity.

In practice two problems arose:

1. Medium limitation did occur with the original medium - therefore a more concentrated medium had to be developed and tested.
2. It proved impossible to keep acetate concentrations below inhibitory values with the manual glucose feedrate control available.

Thus the most productive medium and high cell density fermentations done were both limited by acetate inhibition before they could reach the maximum specific activity. Therefore the final model that was developed is not as fundamental as hoped since it does not include a term for maximum specific activity.

3.2.2 Format of results section.

The following sections of Chapter 3 describe the results of twelve fermentations. An overview of these experiments is given in Fig. 3.1 and they are described in more detail in Table 3.1. The left hand side of Fig. 3.1 shows the experimental work (discussed below) whilst the right hand side (discussed in Chapter 4) shows the interaction between the experiments and the model development.

In Fig.3.1 it can be seen that the first experiments were medium cell density fermentations using medium O. These were found to be phosphate limited soon after induction. (One of these experiments is described in Sec. 3.5 where it fits in more conveniently with the other medium cell density fermentation). It was also discovered that acetate production increased dramatically when the peptone feed started. However the situation was complicated by other events that were also occurring at this time (e.g. temperature rise, B.S.T. production etc.).

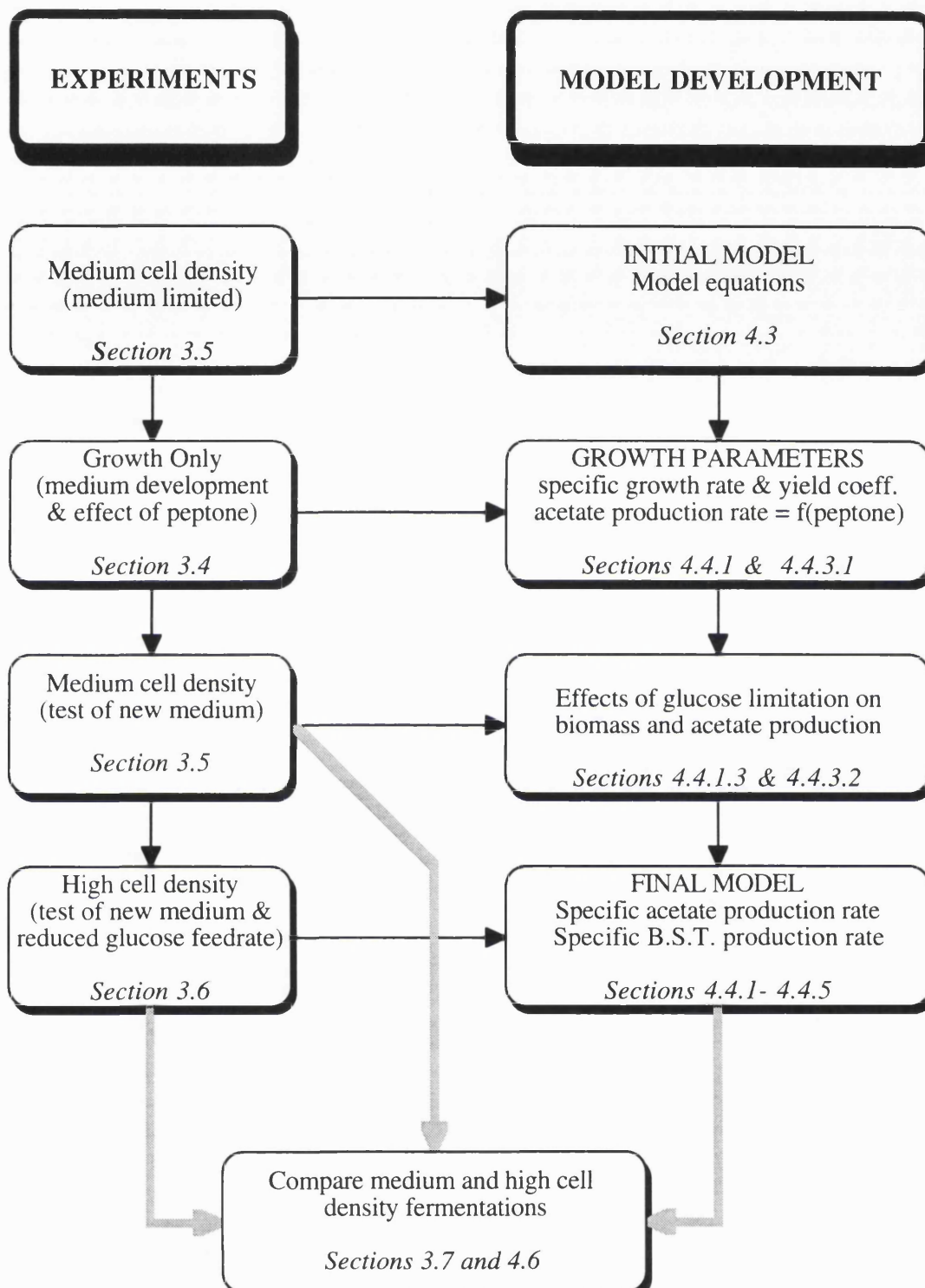


Figure 3.1: Overview of experiments and model development.

Table 3.1

Summary of experiments.

(Note: MCD = medium cell density; HCD = high cell density. See Secs. 2.4.2.1 and 2.4.2.2 for description of media. See Sec. 2.4.4 for definition of peptone feedrates).

Sec.	Title	Expt. No.	Medium	Peptone Feedrate
3.4.1	Effect of media on growth	1	A	none
		2	B	none
		3	C	none
		4	C	none
3.4.2	Effect of peptone feed on growth	2	B	none
		5	B	high
3.5	Effect of medium on MCD fermentations (Benchmark MCD fermentation)	6	O	low
		7	B	high
3.6.1	Effect of medium on HCD fermentations (Benchmark HCD fermentation)	8	B	high
		9	B+	high
3.6.2	Effect of glucose feeding on HCD fermntns.	9	B+	high
		10	B+	high
3.6.3	Effect of glucose starvation on HCD fermntns.	10	B+	high
		11	B+	high
		12	B+	high
3.7	Comparison of MCD and HCD benchmark fermentations	7	B	high
		8	B	high

To develop a new medium for the induced fermentations and to get a better understanding of the effect of peptone feeding a series of growth-only experiments were conducted (Sec. 3.4).

Once a new medium was developed it was tested by repeating one of the original medium cell density runs using the new medium. These experiments are described in Sec. 3.5. The final experiments were all at high cell density and are described in Sec. 3.6. The first was another test of the new medium and this was followed by ones in which the glucose feedrate was reduced to try to limit acetate production and increase productivity.

For each set of experiments there is some text followed by several plots. The text always has the same layout: Objectives of the experiment, brief description of the method, main conclusions, conclusions about glucose feeding and then further observations. The main conclusions relate to the objectives of the experiment. The conclusions about glucose feeding relate to the effect of glucose feeding on the rate of production of biomass, acetate and B.S.T (this part is absent for the growth-only runs since all of them had excess glucose and were not therefore affected by glucose feedrates). The further observations relate to anything else which was observed which doesn't fit into the other categories. At the end of this chapter all the conclusions and observations are summarised and these are then used in Chapter 4 to develop the mathematical model.

The various plots which are shown are listed below. To keep the number of plots in the main results section down to a manageable level some of the less important plots - i.e. estimated broth volume, pH, oxygen flowrate, dissolved oxygen concentration and respiratory quotient - have been placed in Appendix D. (The labelling of these plots follows a similar convention to that used in the main text - e.g. the supplementary plots to Figs. 3.8a-f are labelled D3.8a-d).

1. Assay data: biomass, glucose, acetate, B.S.T. and phosphate.

These are shown for every fermentation (except for phosphate assays which were only done on a few runs). Unfortunately the assay data have to be measured as concentrations (e.g. the concentration of glucose in the tank is measured not the total amount). Thus an estimate of the broth volume is needed to compare the assay data.

2. Estimated broth volume

The broth volume is shown in Appendix D for every fermentation and was calculated by working backwards from the final degassed broth volume and allowing for evaporation,

sampling and feeds of glucose, peptone and ammonia. (For simplicity the sampling rate was assumed constant and hence the volume plots are not saw-toothed as they should be). Typically broth volume decreases during growth due to sampling, increases rapidly due to the batched peptone feed, and thereafter increases less rapidly due to peptone and glucose feeding. Run to run variations are due to different feeding strategies and/or different post sterilisation volumes.

3. Total biomass produced, total acetate produced and total B.S.T. produced.

These were plotted for most of the fermentations and were calculated by multiplying the estimated broth volume by the relevant assay and allowing for amounts removed due to sampling. The reason for including these plots is that there were large volume changes during each run and also because it is the totalised values which were examined when comparing rates of production.

4. Exit gas % CO₂.

The exit gas % CO₂ plot is shown for all fermentations since it gives an accurate and continuous indication of the total metabolic activity in the fermenter. It is therefore a good way of comparing fermentations. Since the inlet gas flowrate and the inlet gas % CO₂ are constant the exit gas % CO₂ is proportional to the % CO₂ production rate (mol CO₂ / h). However it has not been converted to the more usual volumetric carbon dioxide production rate (mol CO₂ / L / h) since this would involve dividing by the estimated broth volume which is not measured directly and varies within and between runs. Strictly speaking in runs with oxygen enriched sparging the exit gas % CO₂ was not proportional to the volumetric carbon dioxide production rate since the inlet gas % CO₂ was reduced (e.g. from 0.04% to 0.02%). However this effect was negligible compared with the high values of exit gas % CO₂ at the times when oxygen enriched sparging was used (i.e. 10 - 25%). More importantly, as explained in Sec. 2.4.3, runs with oxygen enriched sparging actually had up to a 4% lower inlet gas volumetric flowrate. Consequently they will have up to 4% higher exit gas CO₂ concentrations. However at the oxygen flowrates used in most of the high cell density runs this error was less than 2% and was neglected.

5. Ammonium hydroxide feedrate.

This is shown for all fermentations since it gives another frequent and volume independent measure of what is happening in the fermenter. Because ammonium hydroxide is used to neutralise any acetic acid produced (the pH was kept constant at 7.0) it is also useful for comparing runs with different acetate production rates. It was calculated, after the run was completed, as an average of three successive flowrate

measurements. Each flowrate measurement was calculated every three minutes from the change in load cell measurements. An average over more readings would have given a smoother plot but would not have been so accurate at pinpointing times when the ammonium hydroxide feedrate rate dropped to zero. The feedrate was converted to units of ml of 8M ammonium hydroxide solution per hour for all runs.

6. Dissolved oxygen, temperature, pH, glucose feedrate and oxygen feedrate.

Dissolved oxygen is plotted for all runs (principally to show that it was not limiting) and the others parameters for selected fermentations. The pH, oxygen flowrate and dissolved oxygen plots are shown in Appendix D.

7. Respiratory quotient (RQ).

The respiratory quotient (the ratio of the carbon dioxide production rate divided by the oxygen consumption rate) is a useful metabolic indicator. However RQ values were meaningless after oxygen enriched sparging started since an accurate measurement of oxygen flowrate was not sent to the Bio-I computer. Therefore RQ plots are only shown (in Appendix D) for the few fermentations where metabolically interesting events occurred before oxygen enriched sparging was started.

Five final points need to be made:

1. All time scales are relative to reaching an exit gas carbon dioxide concentration of 1.8% at 5.75 hours (Sec. 2.4.4). Thus approximately the first 13 hours of growth are not shown.
2. All peptone feeding profiles were identical unless otherwise stated.
3. "Biomass" refers to rinsed dry cell weight minus B.S.T. titre (Sec. 2.5.1).
4. For clarity assay points have been joined up by straight lines. However this does not mean that the concentration really did vary linearly between the two points. This is important to remember when interpreting the glucose concentration plots.
5. The glucose assay points often appear to be zero. In fact there probably is still a very low concentration of glucose in the tank at this stage but it is less than that which can be detected by the assay (i.e. less than 0.02 g glucose/L).

3.3 Reproducibility and accuracy

Great care was taken to ensure that run-to-run variability was minimised. The major sources of such variability are due to variations in the inoculum and raw materials (especially complex ones), poor fermenter control and poor assay reproducibility. All these sources of variability were reduced as follows:

1. Inoculum variability:

- i) All inocula came from the same sub-clone (the two exceptions are stated).
- ii) The seed stage took place in the well controlled fermenter rather than in a poorly controlled shake flask.

2. Raw material variability:

- i) All critical chemicals (especially peptone) came from the same batch throughout the thesis.
- ii) Peptone solution was always autoclaved for exactly the same length of time.

3. Fermenter control:

- i) All critical instruments were calibrated prior to each run (Sec. 2.4.3).
- ii) The same fermenter (and internal configuration) was used for all fermentations.

4. Assays were done in duplicate or quadruplicate and where possible checked against external standards (Sec. 2.5). Table 3.2 shows the reproducibility of the various assays used and how they were calculated.

As a result of the above efforts the fermentations were found to be extremely reproducible (e.g. compare the growth period on any of the plots in Secs. 3.5 and 3.6). The most clear example of this reproducibility is the case of the two high cell density fermentations which differed only in that one had an extra mineral feed. These fermentations are described in Sec. 3.6.1 where error bars are also shown on the relevant plots.

Finally it is possible to get consistent errors such that results can be reproducible but inaccurate. This was minimised by calibration against external standards as described above. For biomass measurement there was no external standard and the accuracy of this measurement is discussed in detail in Appendix A.

Table 3.2

Reproducibility of assays (see notes below).

Measurement	Typical values	Reproducibility
Glucose	0 - 40 g/L	+/- 2%
Acetate	0 - 30 g/L	+/- 2%
B.S.T.	0 - 5 g/L	+/- 3%
Biomass (see note 4 below)	0 - 5 g/L 5 - 50 g/L	+/- 0.5 g/L +/- 3%

Notes:

1. Reproducibility is expressed either as a percentage of the measured value or as an absolute error (the latter was used if the error was found to be independent of the value of the parameter measured).
2. For glucose and acetate assays the reproducibility was calculated by averaging the variation between repeat assays for fifty samples and then dividing this by two (i.e. to get a +/- deviation rather than an error range).
3. For B.S.T. the variation between assays (taken on a duplicate sample) measured at Dista Products and U.C.L. using the same method but different equipment, operators and sulphitolysis reagent was taken. This was averaged over twelve samples and then divided by two to get the reproducibility.
4. For biomass the range between the highest and lowest of the four repeat assays for each sample were noted, averaged over sixty samples and divided by two. Unlike the above assays the error was found to be independent of the measured value for low biomass values (less than 5 g/L) - see Appendix B. The accuracy of the biomass measurement is discussed in Appendix A.

3.4 Growth-only fermentations

3.4.1 Effect of different media on growth (Expts. 1-4).

Objective:

To determine which medium should be used for the induced fermentations. This was necessary since it had been discovered in one of the first induced fermentations that the original medium became phosphate limited soon after induction. (This experiment is described in Sec. 3.5 where it fits in more conveniently with the other medium cell density experiment).

Method:

Three different media were tested to see which would support the most exponential growth without an adverse effect on specific growth rate. The three media used (A, B and C) were based on the original medium (medium O) but were more concentrated - they are described in Sec. 2.4.2.1 and summarised below. (Note: All media had the same concentration of tetracycline hydrochloride and batched glucose).

Medium O: This was the original medium used.

Medium A: As medium O but with twice the amount of potassium phosphate and sodium phosphate. The citric acid concentration was also doubled to help chelate the stronger medium.

Medium B: As medium O but twice the concentration of everything.

Medium C: As medium O but two and a half times everything except citric acid (4x) and sodium phosphate dibasic (6x). This medium also had extra trace elements.

All the experiments were conducted at 30°C without peptone feeding (note: the experiment with medium C was repeated twice to confirm the slower growth found and so that different media supplements could be added to see which component was growth limiting).

Glucose was fed to keep the glucose concentration in the range 1-30 g/L during exponential growth (Fig. 3.2d) so that it did not become inhibitory or limiting. For the same reason the oxygen flowrate was adjusted to keep the dissolved oxygen concentration above 20 percent of air saturation (Fig. D3.2b). The total air plus oxygen flowrate entering the reactor was kept constant at 3.25 SLPM. Ammonium hydroxide (8M) was fed to keep the pH at 7.0 (Figs. 3.2b and D3.2a).

Conclusions:

Medium B was chosen for all induced fermentations since it supported the most exponential growth without an adverse effect on the specific growth rate. Fig. 3.2a shows the biomass concentration and the total biomass produced (the estimated broth volume is shown in Fig.D3.2a). The % CO₂ in the exit gas (Fig.3.2b) was used to determine the time at which exponential growth stopped. The corresponding biomass and total biomass was then read off Fig. 3.2a and the information summarised below:

Table 3.3

Effect of different media on the extent of exponential growth.

Medium	Time (t) when expntl. growth stops (h)	Total biomass at time t (g)	Biomass at time t (g/L)	Comments
A	8.9	60	19	
B	10.2	95	28	
C	14.0	140	38	slower growth

Further observations:

1. From the limited number of phosphate assays taken (Fig. 3.2c) it was concluded that medium B was probably phosphate limited since there was no phosphate left at the time exponential growth stopped. There is a slight complication here since at approximately the same time the ammonium hydroxide consumption rate fell to zero (Fig. 3.2b) indicating that the glucose (Fig. 3.2d) may have become limiting. However it is not clear if this preceded or followed the phosphate limitation. In any event it is clear from Fig. 3.2c that the phosphate would have been depleted at about this time - thus Table 3.3 remains valid.

Also in this experiment the air flow was doubled at 10.48 hours (causing a sharp drop in exit gas % CO₂ as seen in Fig. 3.2b) and extra trace elements added at 12.27 hours. Neither of these events affected growth indicating that the fermentation was not limited either by trace elements in the medium, oxygen supply or concentration of carbon dioxide.

2. Media A and C had higher concentrations of phosphate relative to the other components than was the case with medium B. Therefore, as expected, they had excess phosphate at the time they stopped growing (Fig. 3.2c). In the case of medium A it is not known which medium component limited growth. However in the case of medium C (Expt. 3) extra magnesium sulphate and thiamine hydrochloride (in each case approximately half the batched amount dissolved in 20 mls sterile D.I. water) were injected separately between 14.27 and 14.45 hours. This caused a dramatic resumption of growth (Figs. 3.2a and b). In Expt. 4 with medium C only the magnesium sulphate was added (at 14.35 hours) and no effect on growth was detected. It was concluded that thiamine was probably the limiting nutrient in medium C.

3. From Figs 3.2b it can also be concluded that growth is not inhibited by carbon dioxide concentrations up to 20%.

4. Finally it should be mentioned that by testing more media it would obviously be possible to obtain one that would support higher growth without any adverse effects on growth rate. However in the limited time available it was decided to use medium B which was adequate though not optimal.

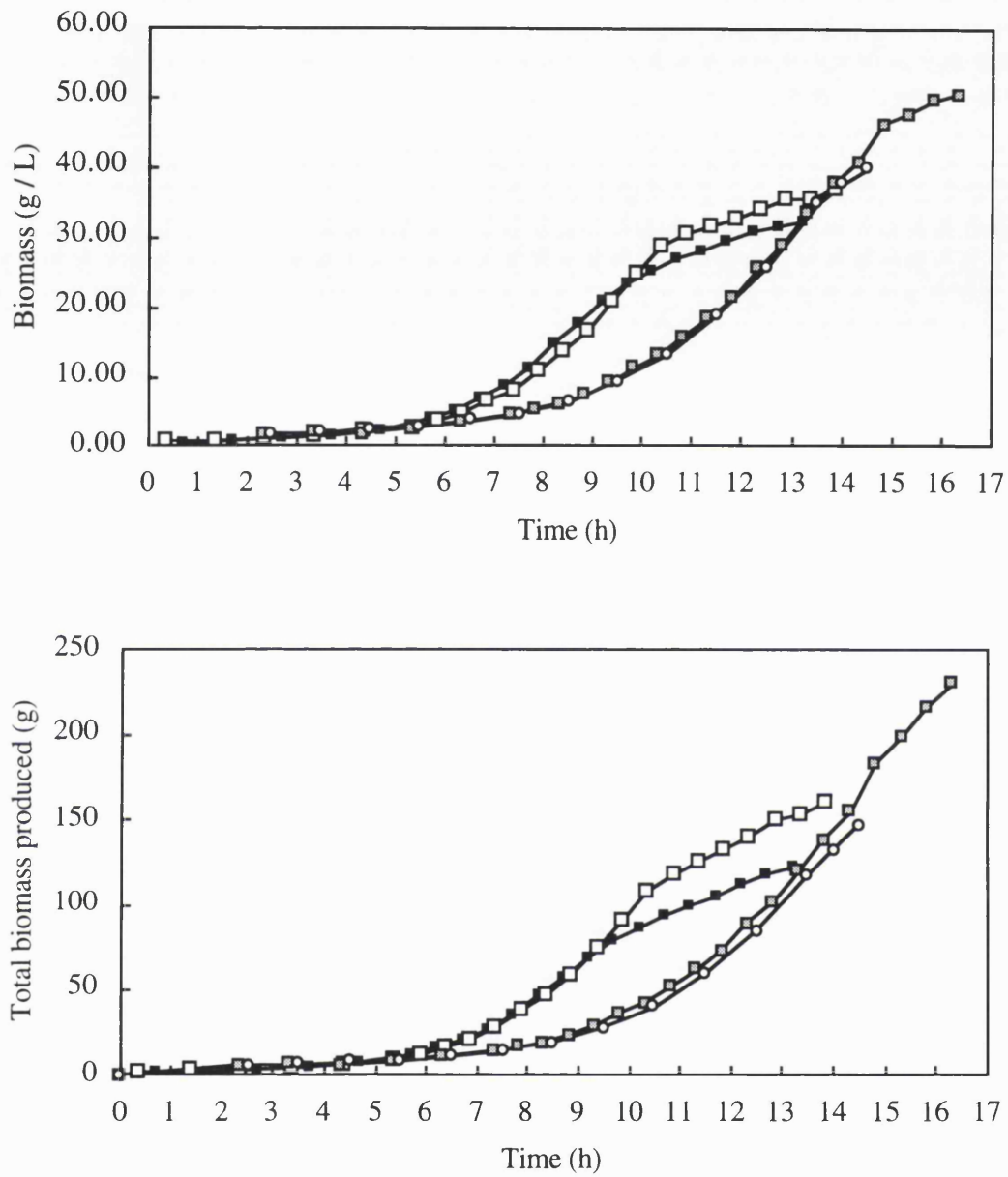


Figure 3.2a: Effect of different media on growth.
Biomass and total biomass produced.

- Medium A (Expt. 1)
- Medium B (Expt. 2)
- ▣ Medium C (Expt. 3)
- Medium C (Expt. 4)

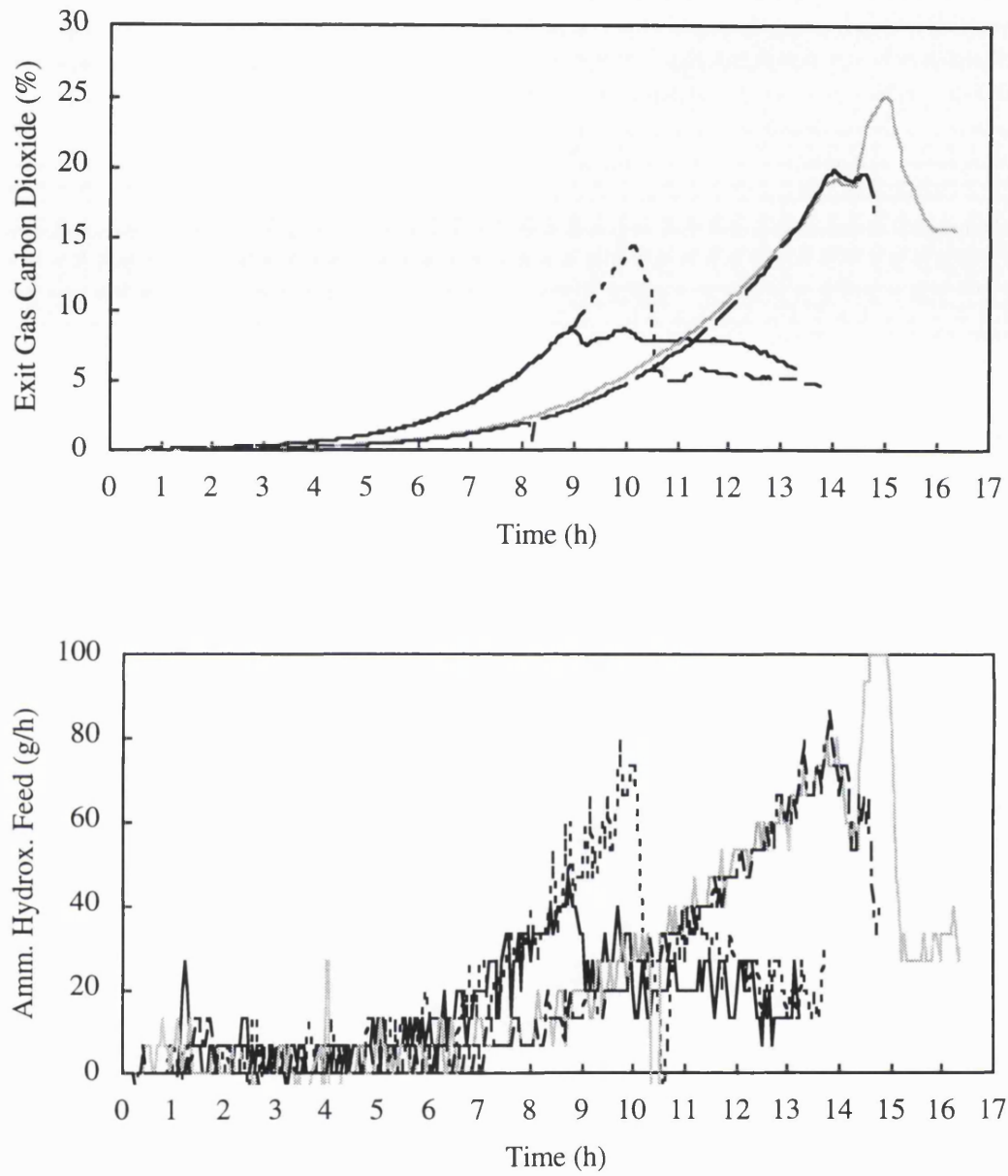


Figure 3.2b: Effect of different media on growth.
 % CO₂ in fermenter exit gas and ammonium hydroxide feedrate.

- Medium A (Expt. 1)
- - - Medium B (Expt. 2)
- Medium C (Expt. 3)
- - - Medium C (Expt. 4)

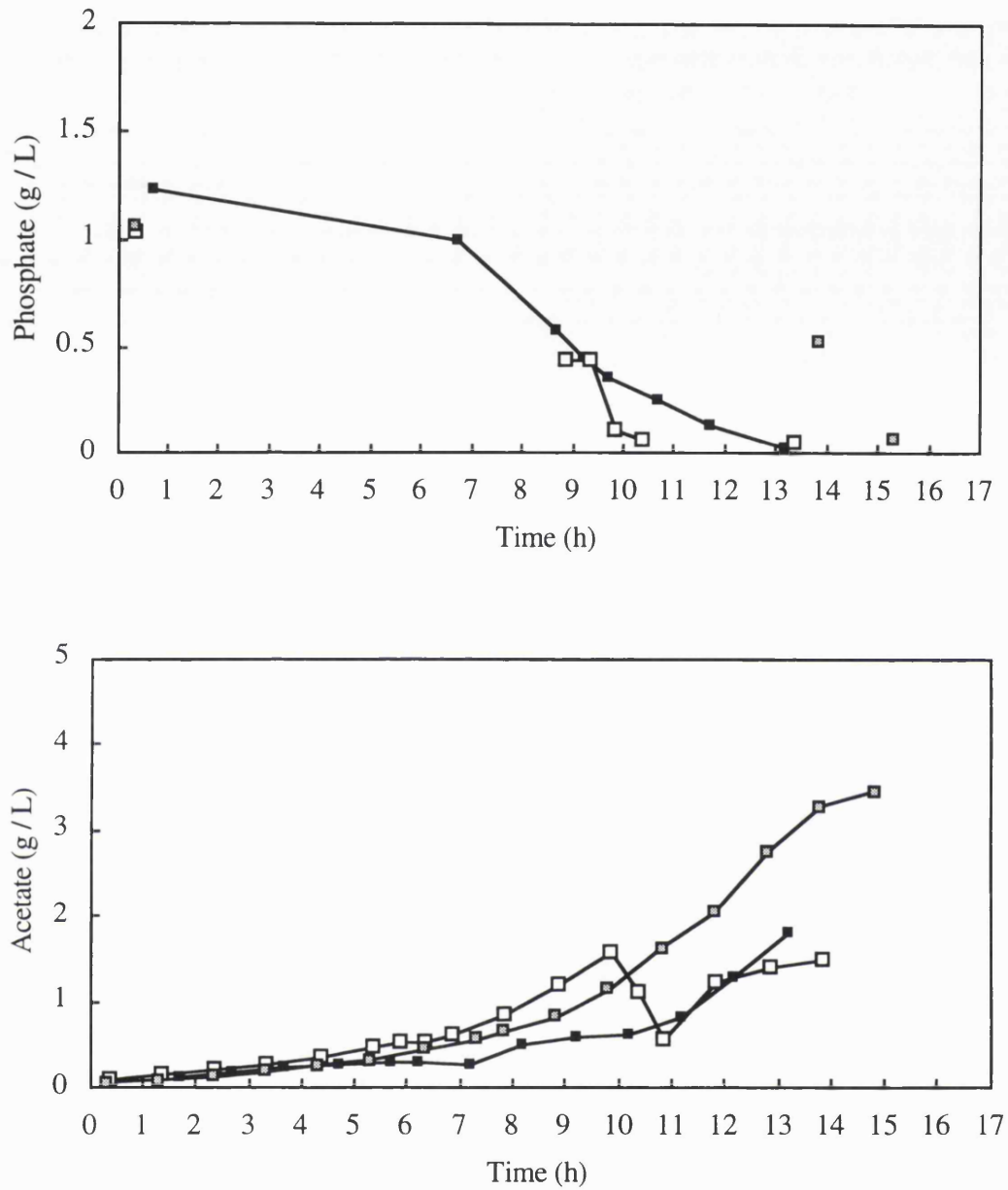


Figure 3.2c: Effect of different media on growth.
Phosphate and acetate concentrations.

- Medium A (Expt. 1)
- Medium B (Expt. 2)
- ▣ Medium C (Expt. 3)
- Medium C (Expt. 4). [assay data not available]

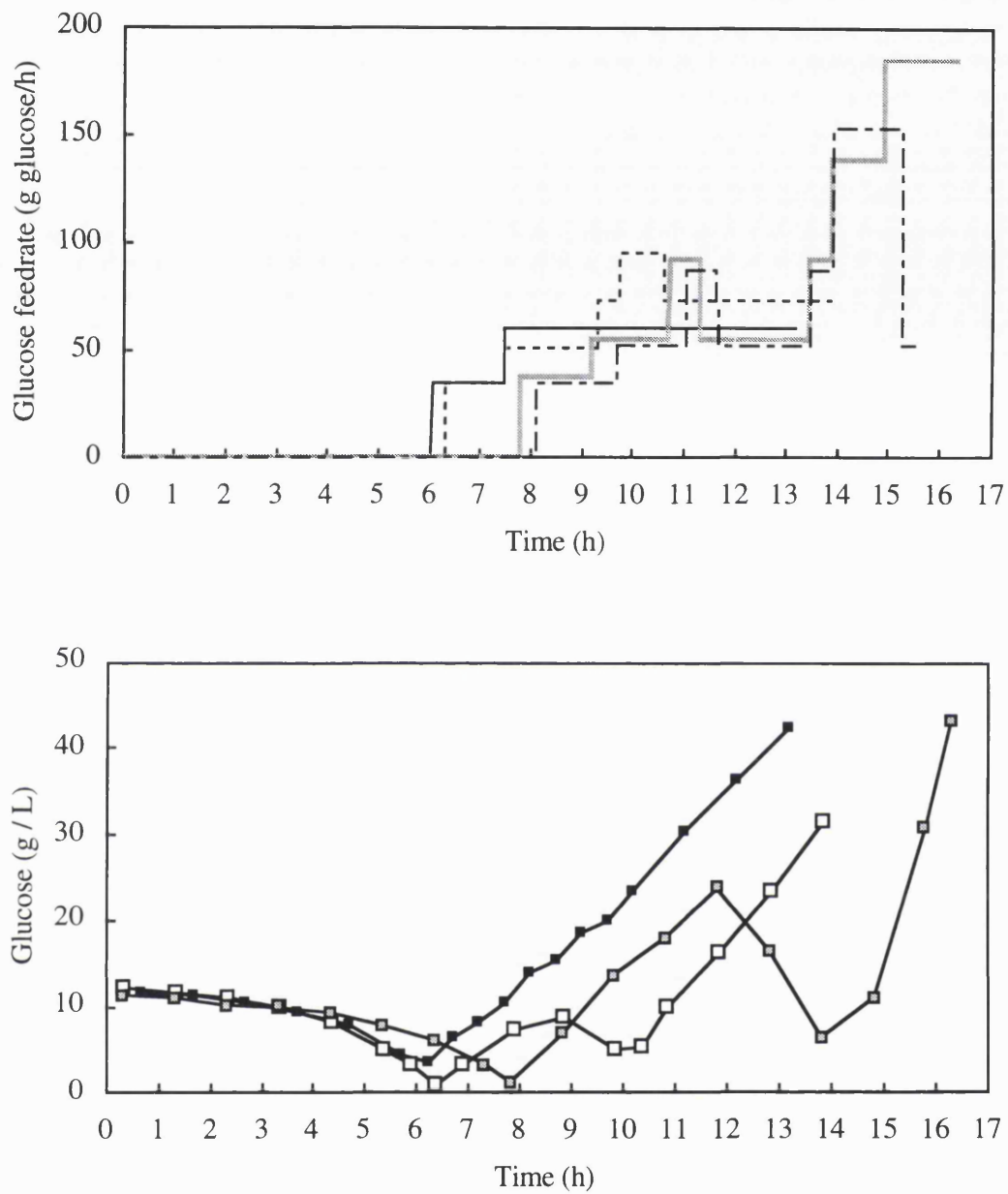


Figure 3.2d: Effect of different media on growth.

Glucose feedrate and glucose concentration.

- and ■ Medium A (Expt. 1)
- and □ Medium B (Expt. 2)
- and ▣ Medium C (Expt. 3)
- Medium C (Expt. 4). [assay data not available].

3.4.2 Effect of peptone feeding on growth (Expts. 2 and 5).

Objective:

To determine the effect of peptone feeding on growth and acetate production. This was necessary since it had been discovered in the first induced fermentations with medium O (described in Sec. 3.5) that acetate production increased at the same time that peptone feeding started. However a relationship between the two could not be proven since a number of other events were happening at the same time which might have been causing increased acetate production (e.g. temperature increasing or start of B.S.T. production).

Method:

Expt. 1 is the growth-only fermentation without peptone feeding described Sec. 3.4.1. This was compared with Expt. 5 which differed only in that it had a peptone feed which started at 5.77 h. The feedrate was the "high" one as defined in Table 2.5.(Sec. 2.4.4) - i.e. between 5.77 and 5.97 hours 39g of peptone were fed to the fermenter (220 ml solution) and thereafter was fed at 20 g peptone/h (114 mls solution/h). The extra peptone feed causes the volume profiles to differ between the two fermentations (Fig D3.3a). This has to be remembered when interpreting assay data which is expressed as a concentration (e.g. g biomass/L).

Both experiments were conducted at 30°C with glucose feeding to keep the glucose concentrations in the range 1-40 g/L (Fig. 3.3c) and oxygen flowrates to keep the dissolved oxygen above 20% (Fig. D3.3b).

Conclusion:

The addition of peptone leads to a sharp increase in acetate production (Fig.3.3c). This same effect was noted by Meyer *et al.* (1984) also using an *E. coli* K-12 derivative strain. One possible explanation of this is that peptone supplies free amino acids which are used in the TCA cycle causing less glucose to be used. If the same amount of glucose is taken up by the cells then the surplus will be excreted as acetate.

Further Observations:

1. The effect on growth is difficult to determine mainly due to errors introduced by the rinsing correlations (Appendix A). However it appears from the total biomass plot (Fig 3.3a) that peptone addition may increase the growth rate slightly. The exit gas % CO₂ plot at first shows a slight dip when the peptone feed starts (Fig. 3.3b). This is probably due the physical effect of adding 220 mls of liquid which absorbs some of the carbon

dioxide before it reaches equilibrium. After the dip the run with peptone has a higher exit gas % CO₂ but this doesn't confirm faster growth either since the extra carbon dioxide might just be due to carbon dioxide co-produced with the extra acetate.

2. The physical effect of adding peptone solution is also the probable cause of the drop in respiratory quotient that is observed at this time (Fig. D3.3c). Prior to this the respiratory quotient is in the range 1.00 to 1.05 as we would expect for growth on glucose. (After the oxygen feed starts the values for respiratory quotient become meaningless - see Sec. 3.2.2).

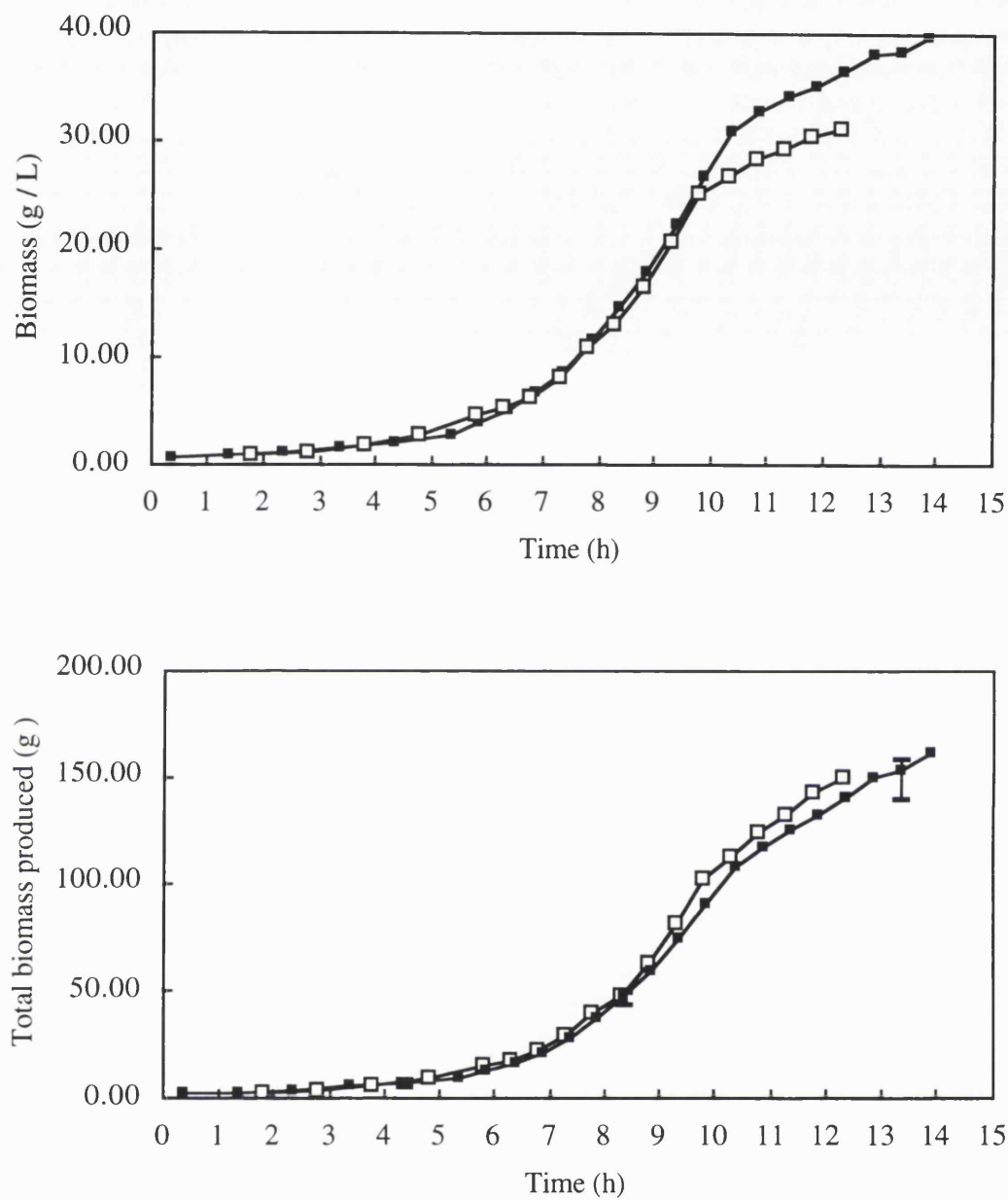


Figure 3.3a: Effect of peptone feeding on growth.

Biomass and total biomass produced.

(Error bars shown for Expt. 2 at 4.27, 8.27 and 13.27h)

- No peptone feed (Expt. 2).
- Peptone feed started at 5.77 h (Expt. 5).

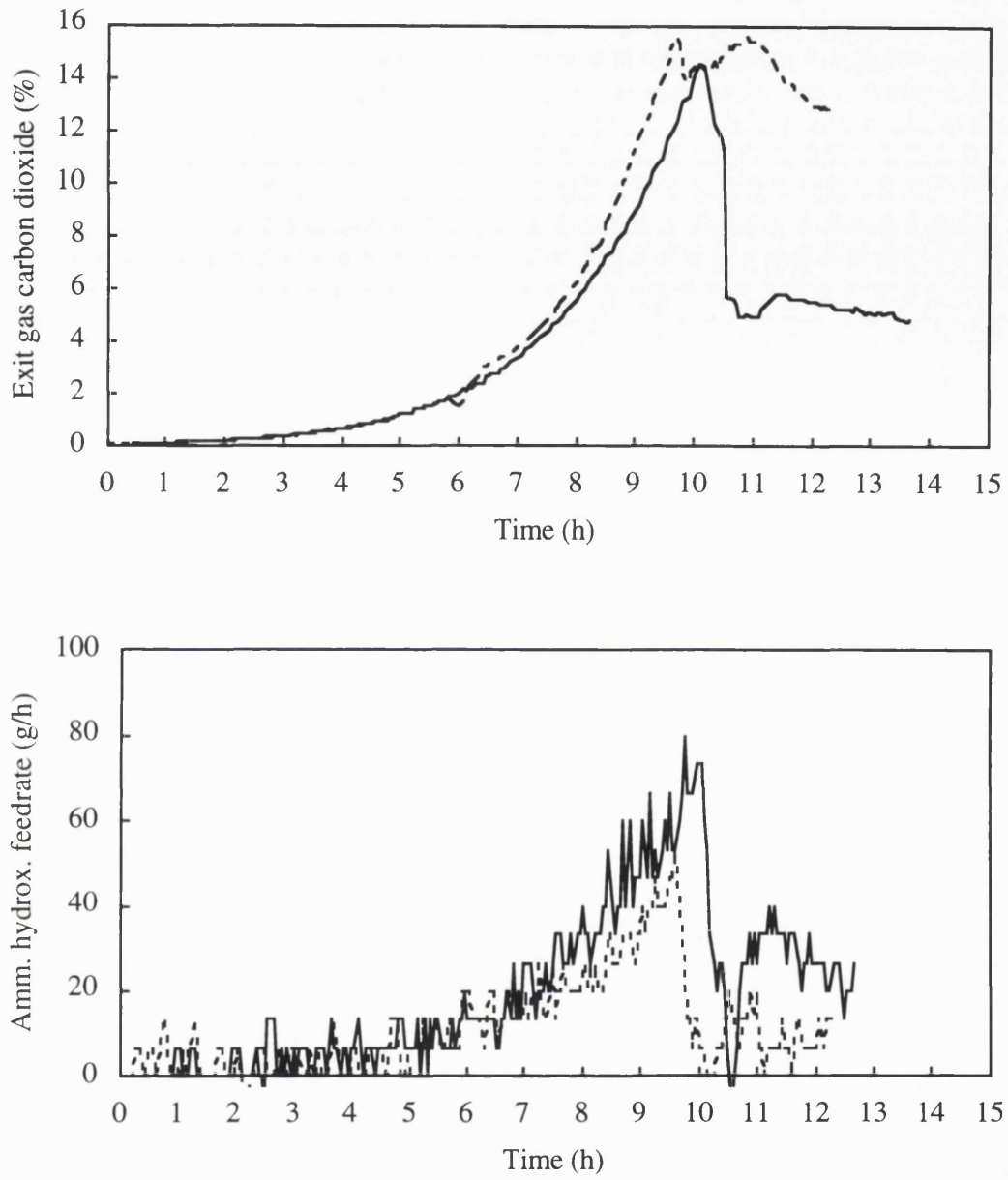


Figure 3.3b: Effect of peptone feeding on growth.
 % CO₂ in fermenter exit gas and ammonium hydroxide feedrate.

— No peptone feed (Expt. 2)
 - - - Peptone feed started at 5.77 h (Expt. 5).

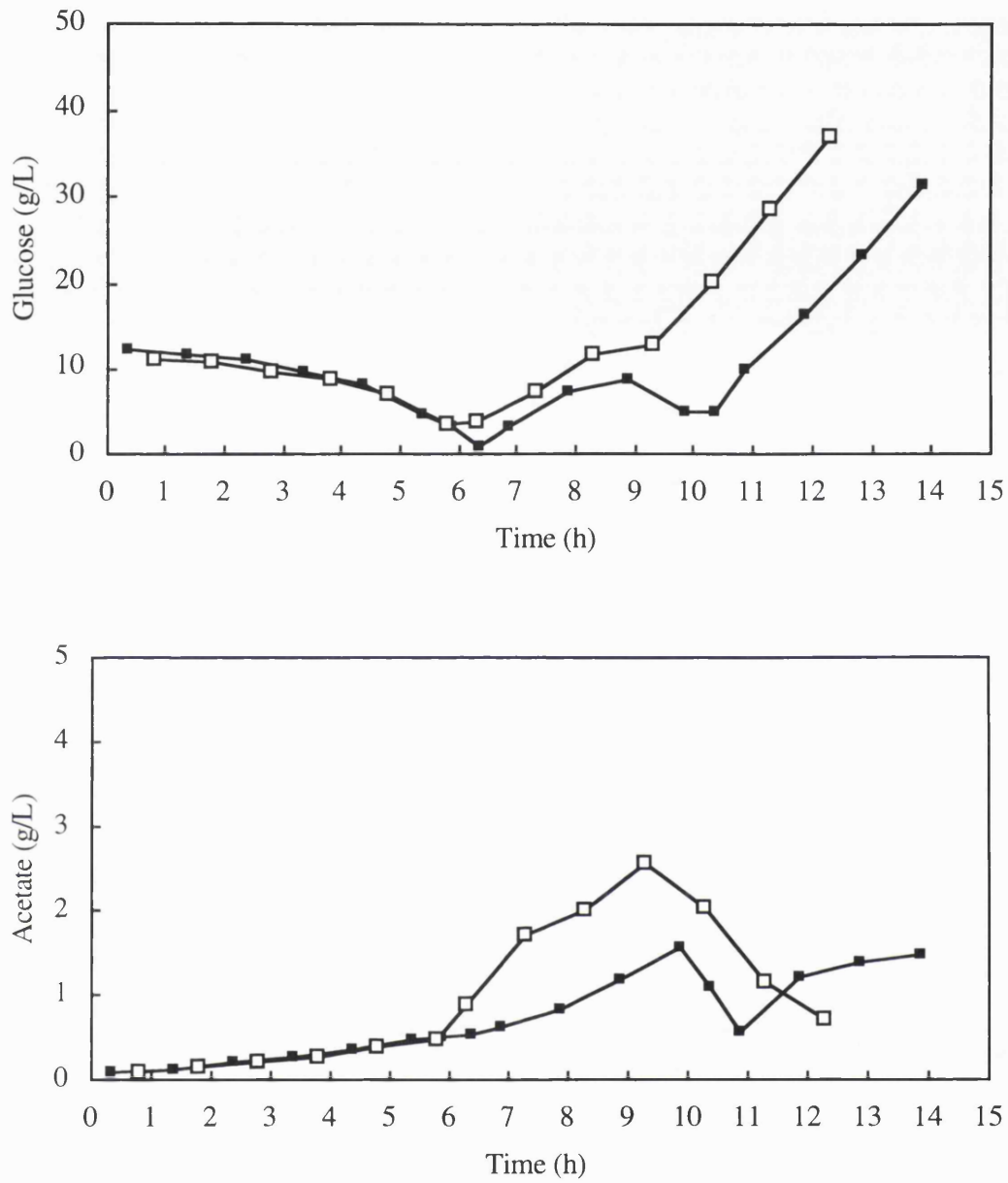


Figure 3.3c: Effect of peptone feeding on growth.
Glucose and acetate concentrations.

- No peptone feed (Expt. 2).
- Peptone feed started at 5.77 h (Expt. 5).

3.4.3 Conclusions from growth experiments (Expts 1-5).

1. Medium B should be used for all induced fermentations.
2. Peptone feeding causes initial acetate production to increase sharply.
3. Peptone feeding may increase growth rate slightly but this was not confirmed. The literature is unable to help much either since, for example, Koh *et al.*, (1992) found the effect of peptone on two recombinant host/vectors was different - in one case it increased growth whilst in the other case it had no effect.

3.5 Medium cell density fermentations - effect of different media (Expts. 6 and 7).

Objectives:

1. Determine the effect of phosphate limitation on medium cell density fermentations
2. Prove that it did not occur when medium B was used.
3. Obtain data that could be compared with high cell density fermentations.

Method:

Expt. 6 is one of the original medium cell density fermentations which used medium O (completed before the growth-only experiments were done). Expt. 7 is the same experiment using medium B (performed after the decision had been made to use medium B for all induced runs).

The only other difference between the two fermentations apart from media composition was the peptone feeding. Expt. 6 used the low peptone feeding rate and Expt 7 used the high peptone feeding rate as defined in Table 2.5 (Sec. 2.4.4). In both runs the peptone feeding started at 6.52h. Temperature induction was triggered by the exit gas carbon dioxide reaching 1.8% (Figs. 3.4a and 3.4f). Glucose was fed so that it became limiting after production started (Fig.3.4c) and the dissolved oxygen concentration was kept above 20% (Fig D3.4b) by a constant air sparge.

Conclusions:

1. Phosphate limitation causes a decrease in the B.S.T. production rate. The fermentation that used medium O became depleted of phosphate at about 9 hours (Fig. 3.4c) and thereafter had a lower rate of B.S.T. production (Fig. 3.4e).
2. Phosphate limitation does not occur with medium B (Fig 3.4c). As a consequence B.S.T. production continues at a constant rate until about 11 hours. At this time either something else is depleted or production is inhibited by a metabolite. The former is possible but unlikely since from growth-only experiments phosphate was found to be the limiting component of medium B for growth. It is more likely that the acetate concentration of about 8 g/L had become inhibitory at this point. This conclusion also agrees with the results of Jensen and Carlsen (1990) which showed that acetate concentration of 6 g/L could have an inhibitory effect on recombinant production (Sec. 1.4.3.6)

3. Finally data was obtained that could be compared with high cell density fermentations.

Conclusions about glucose feeding:

Glucose becomes limiting at about 8h in both runs (Fig. 3.4c). The effect on both fermentations is large as can be seen by the sharp decreases in exit gas % CO₂ and ammonium hydroxide feedrate (Fig. 3.4f) and the sharp increase in the respiratory quotient suggesting that some of the peptone is being metabolised (Fig. D3.4b). The effect on biomass, acetate and B.S.T. production was as follows:

1. Biomass production appears to decrease at the time glucose becomes limiting (Figs. 3.4b). However there are several other possible explanations for this:

- a). The temperature has just reached 39.5°C (this may slow growth).
- b). B.S.T. production is slowing growth down.
- c). Some component of the medium has become limiting.
- d). Some component of the peptone feed has become limiting.
- e). Some component of the peptone feed is inhibiting growth at this point.

Explanations (c), (d) and (e) can be eliminated since biomass production slows down in both runs at 8h but the peptone feeding rate and medium concentration was twice as high in Expt. 7. Explanation (b) is also unlikely since B.S.T. production began at 6.52 hours and although this appears to have slowed the rate of growth at that time there is no reason for it to be having a sudden affect at 8h. Therefore it can be concluded that biomass production at 8h either slows because of glucose limitation and/or the temperature rise. (Temperature was eliminated as the cause in the next set of experiments).

2. Acetate production decreased slightly after glucose limitation (Fig. 3.4d). The most likely explanation is that less glucose is being taken up by the cells even though the demand for glucose for energy is the same and therefore less acetate overflow is occurring. Interestingly in Expt. 6 the rate of acetate production increases again at 9h when B.S.T. and biomass production decline due to phosphate limitation - i.e. the lower demand for glucose means that more can overflow as acetate.

Further observations:

1. Both runs should have been identical up to approximately 9 hours when the phosphate runs out in the medium O fermentation. This is true with the exception that between 6.8

and 7.5 hours the exit gas % CO₂ (Fig. 3.4f), total B.S.T. (Fig. 3.4e) and total biomass (Fig. 3.4b) are slightly less for the medium B fermentation. The reason for this is uncertain.

2. The drop in respiratory quotient at about 6.6 h is probably due to the physical effect of peptone solution absorbing some of the carbon dioxide. The same effect was previously noted in the growth experiments with and without peptone feeding (Sec. 3.4.2).

3. The acetate production rate increases dramatically in both runs at about 6.5 hours. Exactly the same effect - a rapid increase in acetate production at induction - was noted (but not explained) by Strandberg and Enfors (1991b). The effect could be due to any of the events which were happening at this time:

- a) Temperature increase
- b) Start of B.S.T. production.
- c) Relatively low dissolved oxygen levels.
- d) Start of peptone feeding.

The growth-only experiments with and without peptone (Sec. 3.4.2 and 3.4.3) clearly indicate that (d) is the most likely since in those experiments the same phenomenon was found but events (a), (b) and (c) did not occur. This also explains the Strandberg and Enfors result because they state that at induction casamino acids were added to the fermenter.

4. Finally from Fig. 3.4c it can be seen that the phosphate consumption rate is much less after the glucose becomes limiting which is probably due to the lower growth after this time.

5. At the end of this and all induced runs the broth samples were examined and all cells were found to contain inclusion bodies (it varied between one, two and occasionally three per cell). This strongly suggests that there is no plasmid instability with this host vector - i.e. no plasmid free cells.

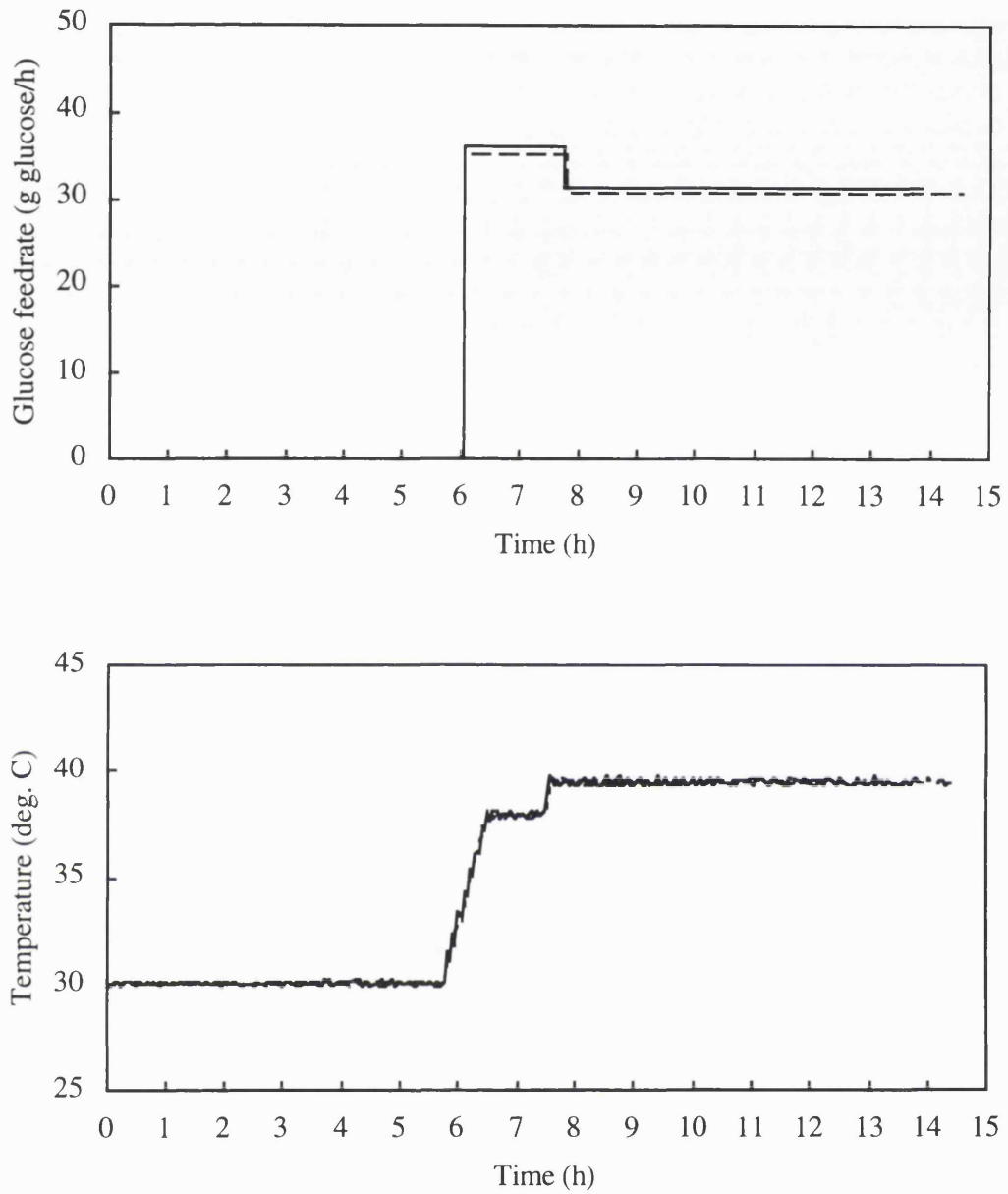


Figure 3.4a: Effect of different media on medium cell density fermentations.
Glucose feedrate and temperature profiles.

— Medium O (Expt. 6).
 ---- Medium B (Expt. 7)

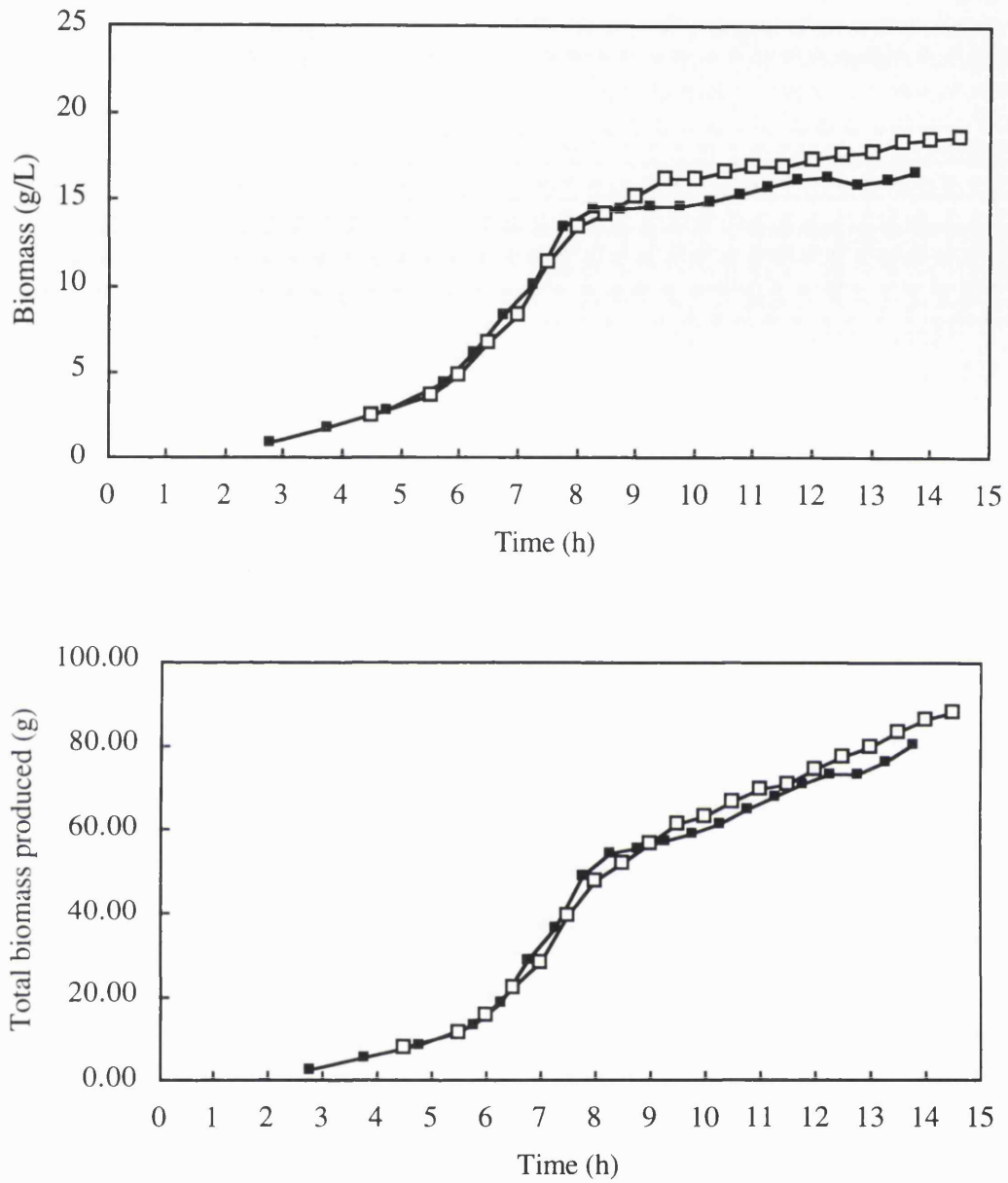


Figure 3.4b: Effect of different media on medium cell density fermentations.
Biomass and total biomass.

- Medium O (Expt. 6).
- Medium B (Expt. 7).

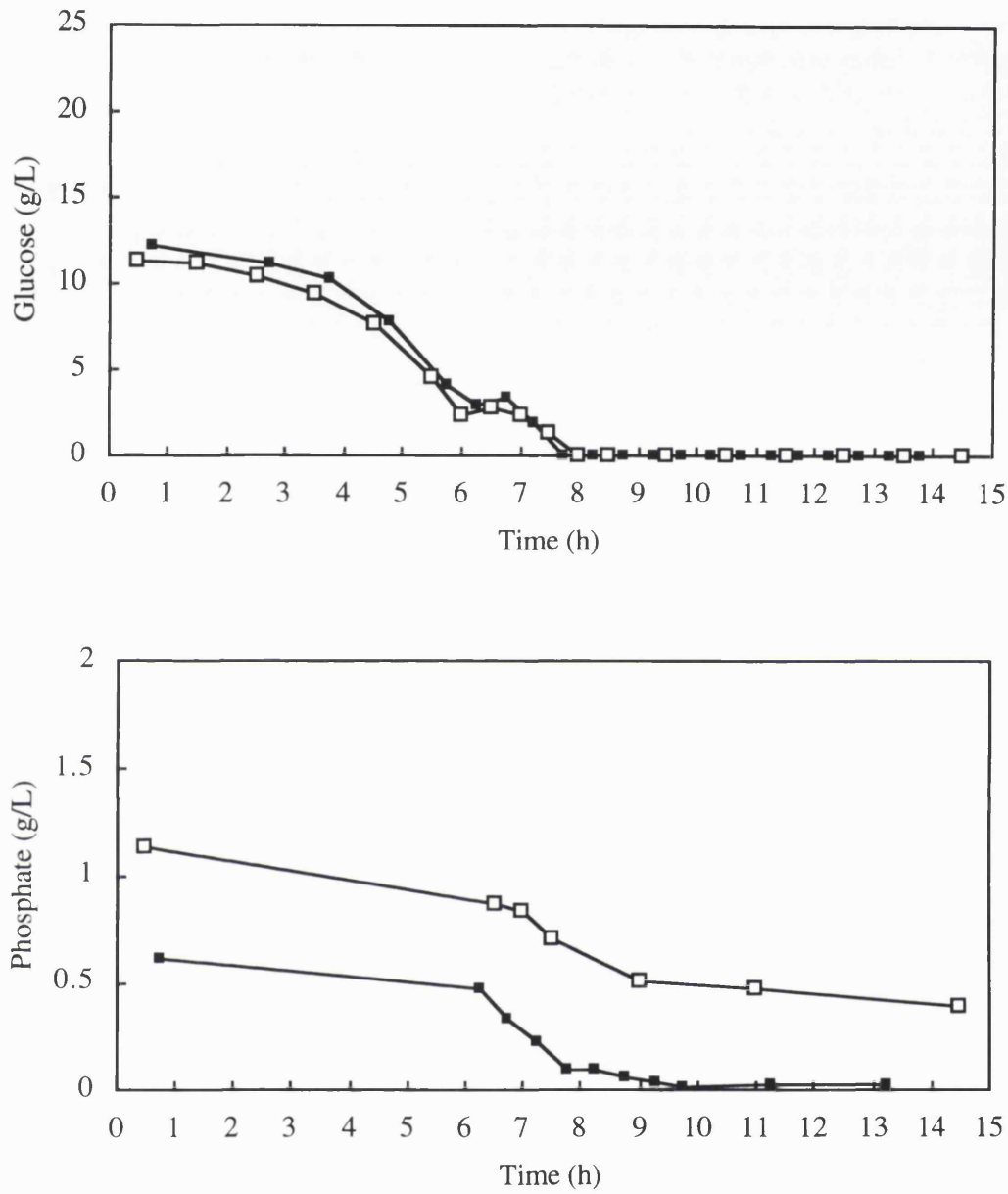


Figure 3.4c: Effect of different media on medium cell density fermentations. Glucose and phosphate concentrations.

- Medium O (Expt. 6).
- Medium B (Expt. 7).

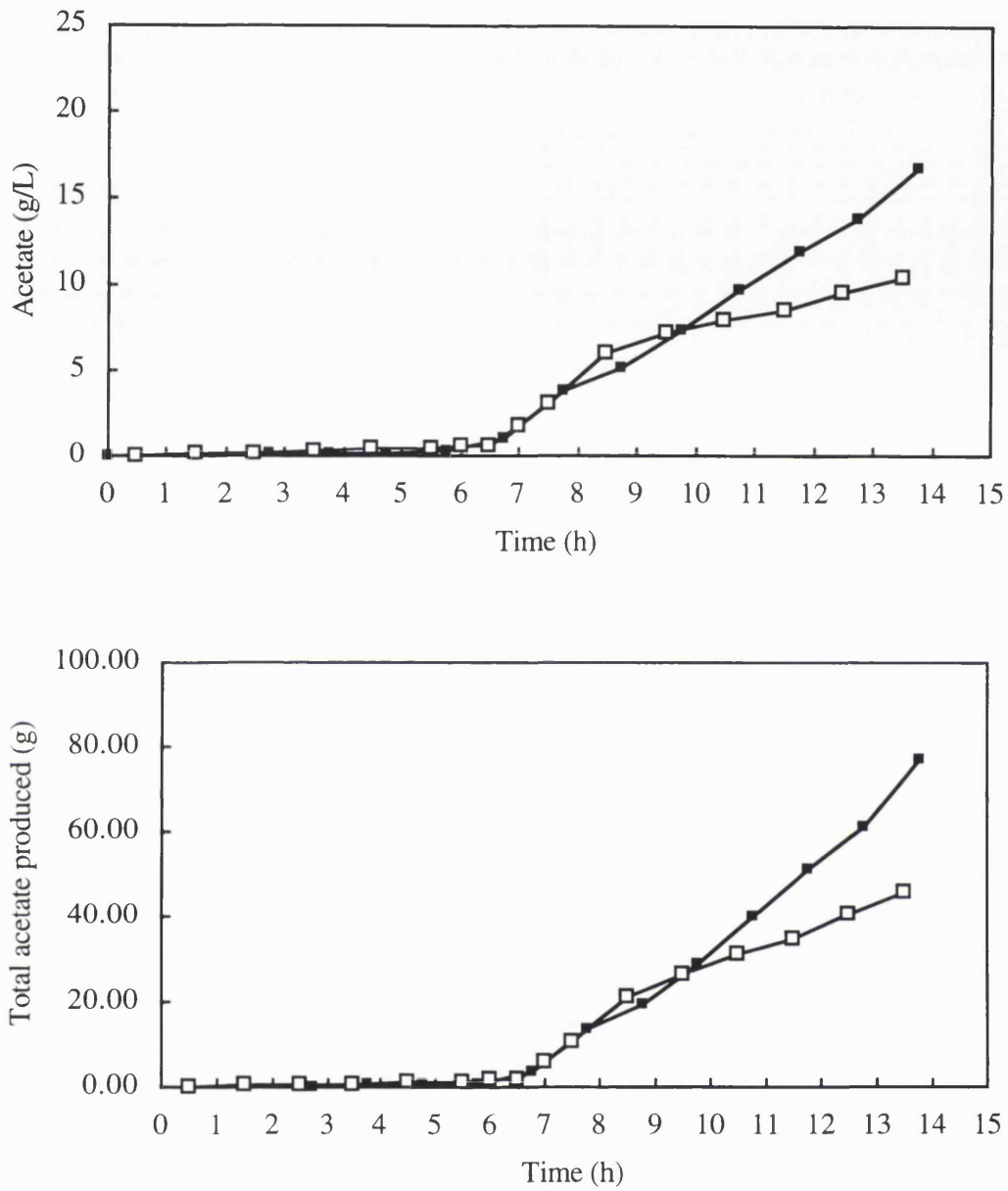


Figure 3.4d: Effect of different media on medium cell density fermentations. Acetate concentration and total acetate produced.

- Medium O (Expt. 6).
- Medium B (Expt. 7).

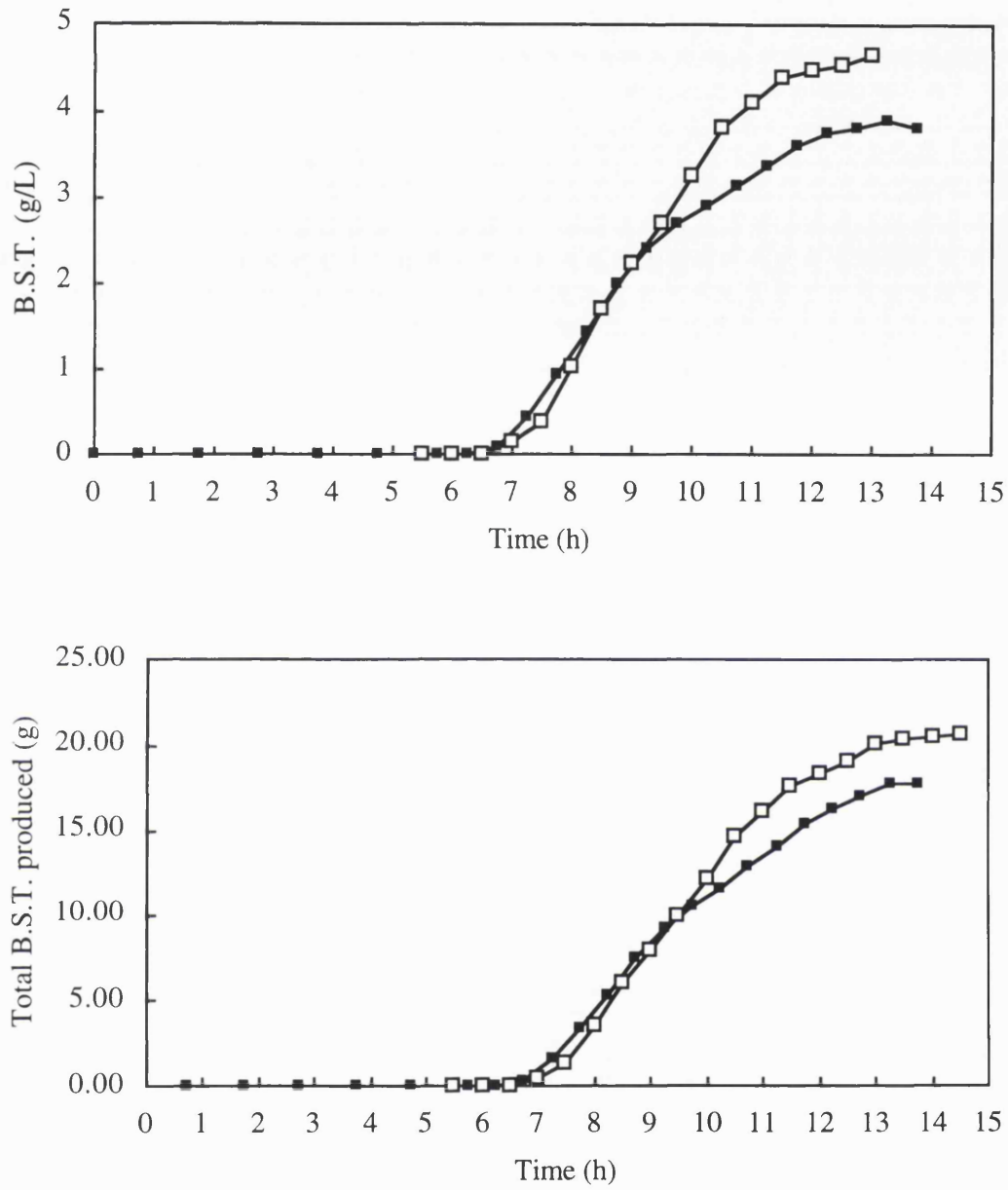


Figure 3.4e: Effect of different media on medium cell density fermentations. B.S.T. concentration and total B.S.T. produced.

- Medium O (Expt. 6).
- Medium B (Expt. 7).

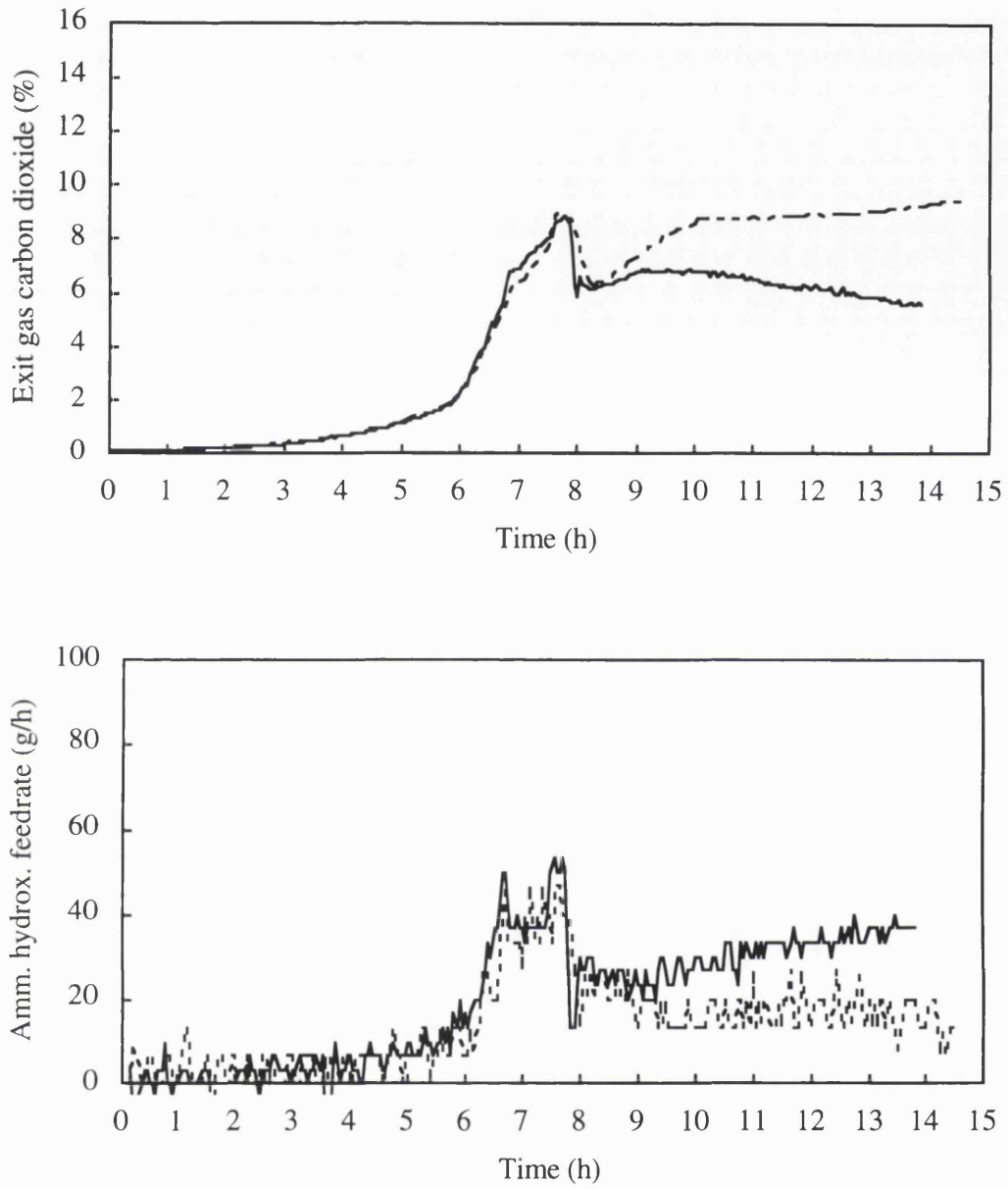


Figure 3.4f: Effect of different media on medium cell density fermentations. % CO₂ in fermenter exit gas and ammonium hydroxide feedrate.

— Medium O (Expt. 6).
 - - - Medium B (Expt. 7)

3.6 High cell density fermentations.

3.6.1 Effect of different media on high cell density fermentations (Expts. 8 and 9).

Objectives:

1. To prove that medium B was not limiting in the high cell density fermentations. (It was important to check this since the higher cell densities in these runs would use up more of the medium).
2. Obtain data so that the medium and high cell density fermentations could be compared.

Method:

The two fermentations shown here were identical except that one (designated medium B+) had extra mineral feeds between 8 and 13 hours. The total amount of CaCl₂, MgSO₄, PO₄, Co, Mo, B and citric acid fed to this run equaled the amount of these components in the original batched medium B (see Sec. 2.4.2.2).

The temperature profile was identical for both runs and induction was triggered by the exit gas % CO₂ reaching 3.6% (Figs. 3.5a and f). The glucose feedrates should have been identical but actually slightly more was fed to the B+ run (Fig. 3.5a). Oxygen enriched sparging was used to keep the dissolved oxygen above 20% (Fig D3.5b). The same high peptone feedrate (Sec. 2.4.4) was used in both runs.

Conclusions:

1. The extra mineral feed made no difference to either the total biomass or B.S.T. produced (Figs. 3.5b and e). It was concluded that the fermentations were not limited by CaCl₂, MgSO₄, PO₄, Co, Mo, B or citric acid. It is possible that one of the other medium components was limiting but this was considered unlikely given that phosphate was the limiting component of medium B during growth (Sec. 3.4.1). As with the previous medium cell density fermentation (Sec. 3.5) it was thought more likely that acetate inhibition was the cause of B.S.T. production decreasing since at this point the acetate concentration was about 8 to 12 g/L which is typical of inhibitory levels quoted in the literature (Jensen and Carlsen, 1989). It is also the same as that found in the medium cell density fermentation at the time B.S.T. production ceased (Sec. 3.5).

2. The data obtained from this experiment was used to compare the medium and high cell density fermentation processes. (Sec. 3.8).

Conclusions about glucose feeding:

The glucose became limited at 9.5h and 10h for Expts. 8 and 9 respectively (Fig. 3.5c). This was expected since Expt. 8 has a lower glucose feedrate (Fig. 3.5a). The % CO₂ and ammonium hydroxide plots (Fig. 3.5f) do not show such a sharp drop as was the case with the medium cell density fermentations described in Sec. 3.5. It was concluded that the glucose limitation was less severe in these runs due to the higher glucose feedrates. The effects on the various production rates were:

1. Biomass (Fig. 3.5b) and B.S.T. production (Fig. 3.5e) did not appear to be affected by glucose limitation. As suggested above this may be due to the higher glucose feedrates in these runs. (Also the temperature rise to 39.5°C, which occurs in both runs, does not dramatically affect growth and can be eliminated as the cause of the growth reduction seen in the medium cell density experiments - see Sec. 3.5).

2. Acetate production (Fig. 3.5d) was, by contrast, reduced slightly after glucose limitation in Expt. 8. In Expt. 9 no such reduction in acetate production occurs presumably due to the higher glucose feedrate in this run. (This is confirmed by the lower ammonium hydroxide consumption rate in Expt. 8 after 9.5h - Fig. 3.5f).

Further observations:

1. Error bars (as calculated in Sec. 3.3) are shown on the biomass and B.S.T. plots (Figs. 3.5b and e) indicating the good reproducibility between fermentations.

2. As expected from previous results the acetate production rate (Fig 3.5d) increases sharply when peptone feeding starts at 7.8 hours.

3. The exit gas % CO₂ plot (Fig. 3.5f) is identical for both runs up to 8 hours when the medium B+ fermentation has a slightly lower value. The only difference between the two runs at this time is the start of the extra mineral feed in the B+ fermentation. This extra solution is probably absorbing some of the CO₂ - the same physical effect that was observed in the growth experiments with and without peptone feeding (Sec. 3.4.2).

4. The total B.S.T. produced (Fig. 3.5e) stays constant at the end of the run indicating that there is negligible degradation of the B.S.T (as expected since inclusion bodies tend

to protect recombinant proteins from proteolytic degradation - Strandberg and Enfors 1991b). However the concentration of B.S.T. decreases due to increasing broth volume.

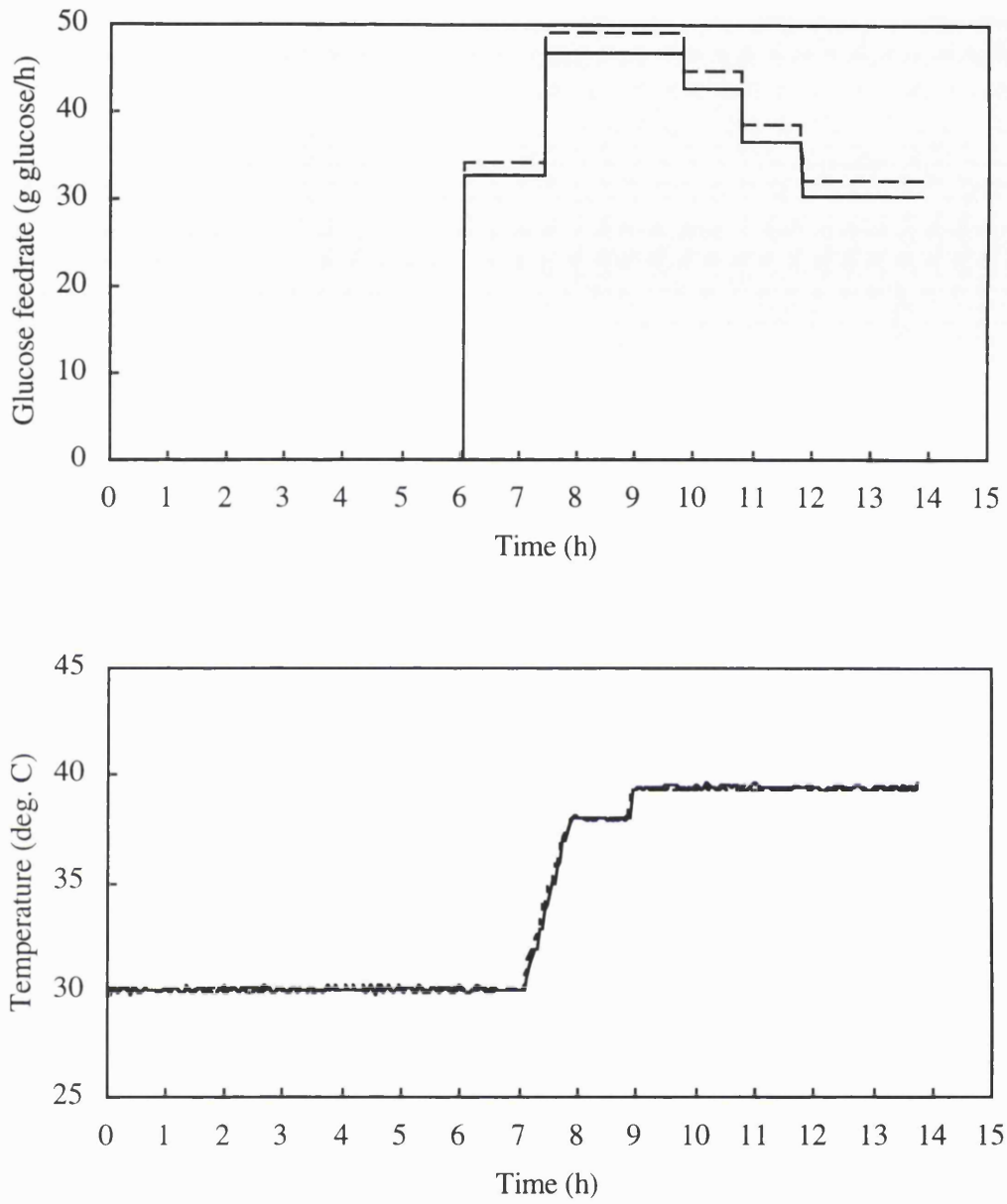


Figure 3.5a: Effect of different media on high cell density fermentations.
Glucose feedrate and temperature profiles.

— Medium B (Expt. 8).
 ---- Medium B+ (Expt. 9).

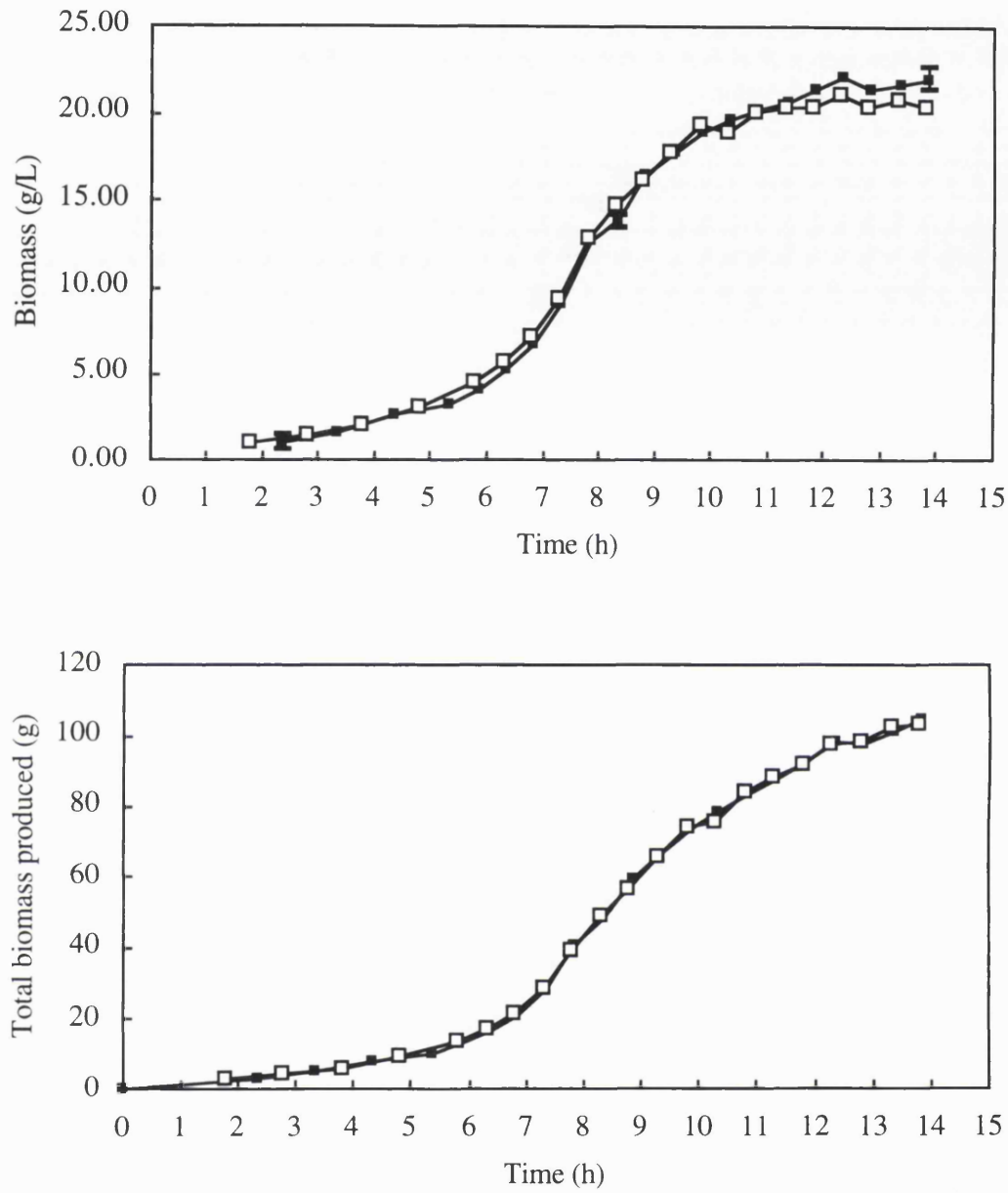


Figure 3.5b: Effect of different media on high cell density fermentations.

Biomass concentration and total biomass produced.
 (Error bars shown at 2.3, 8.3 and 13.7h for Expt. 8).

- Medium B (Expt. 8).
- Medium B+ (Expt. 9).

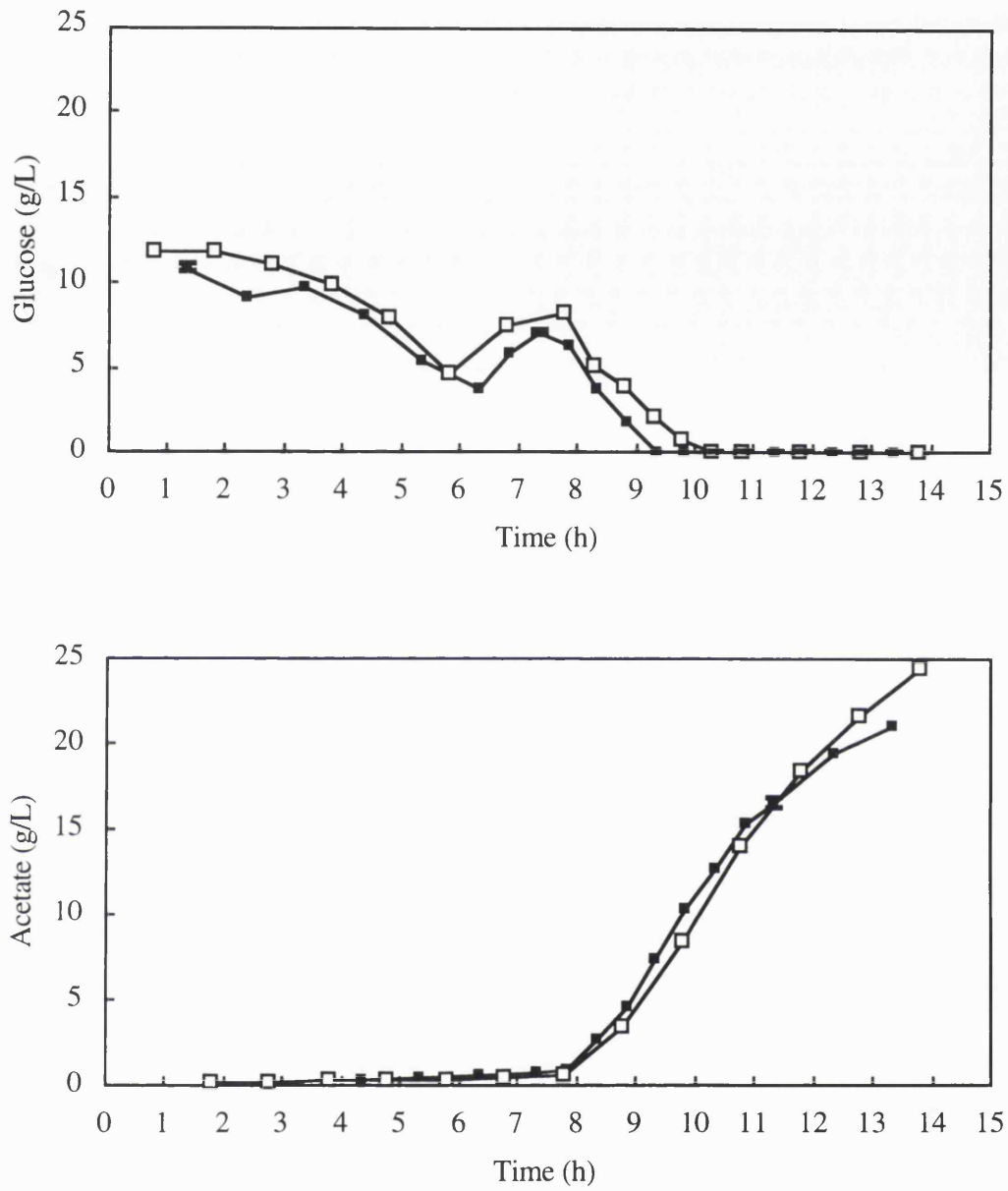


Figure 3.5c: Effect of different media on high cell density fermentations.

Glucose and acetate concentrations.

(Error bars shown at 1.3, 7.3 and 11.3h for Expt. 8).

- Medium B (Expt. 8).
- Medium B+ (Expt. 9).

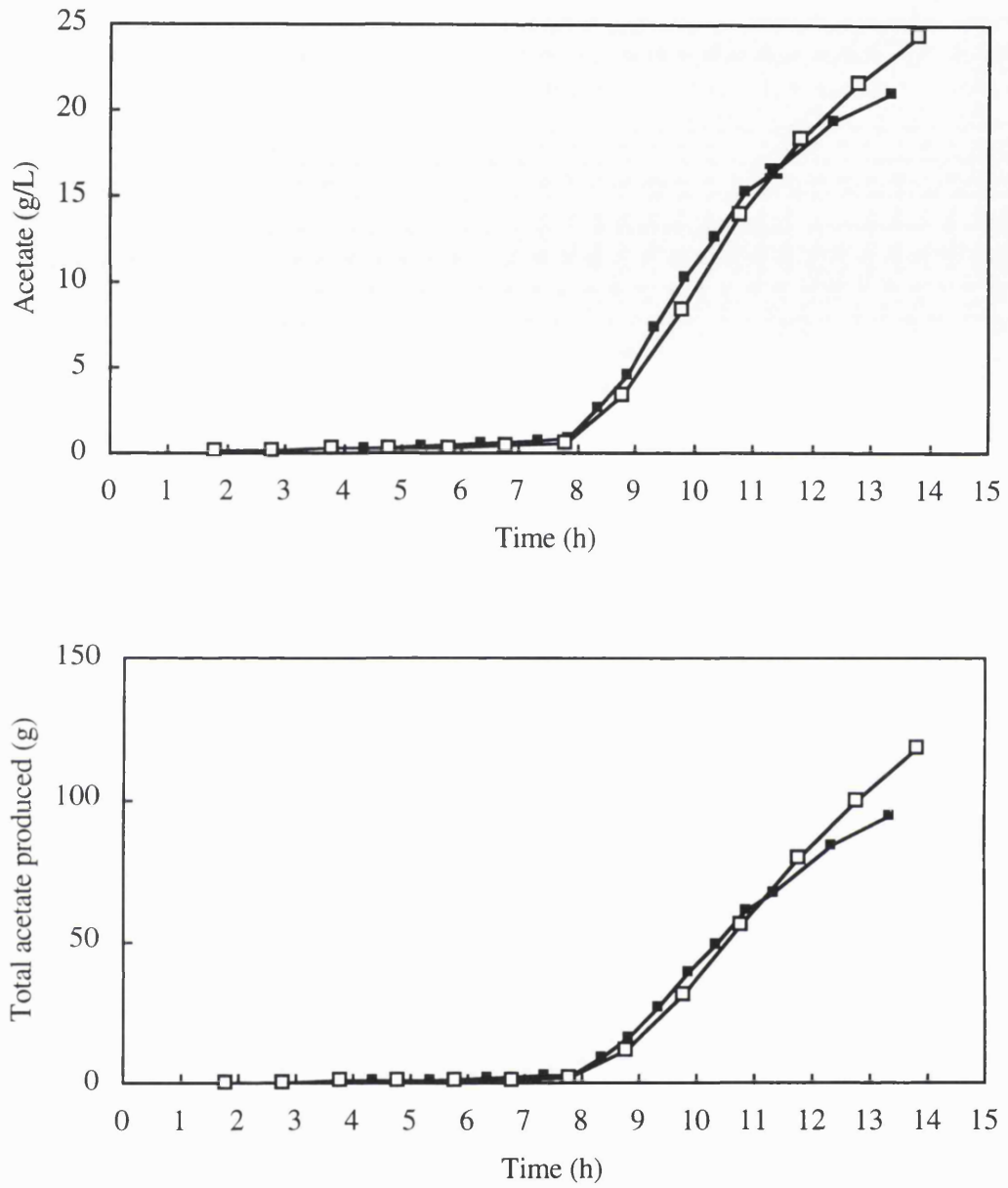


Figure 3.5d: Effect of different media on high cell density fermentations. Acetate concentration and total acetate produced.

- Medium B (Expt. 8).
- Medium B+ (Expt. 9).

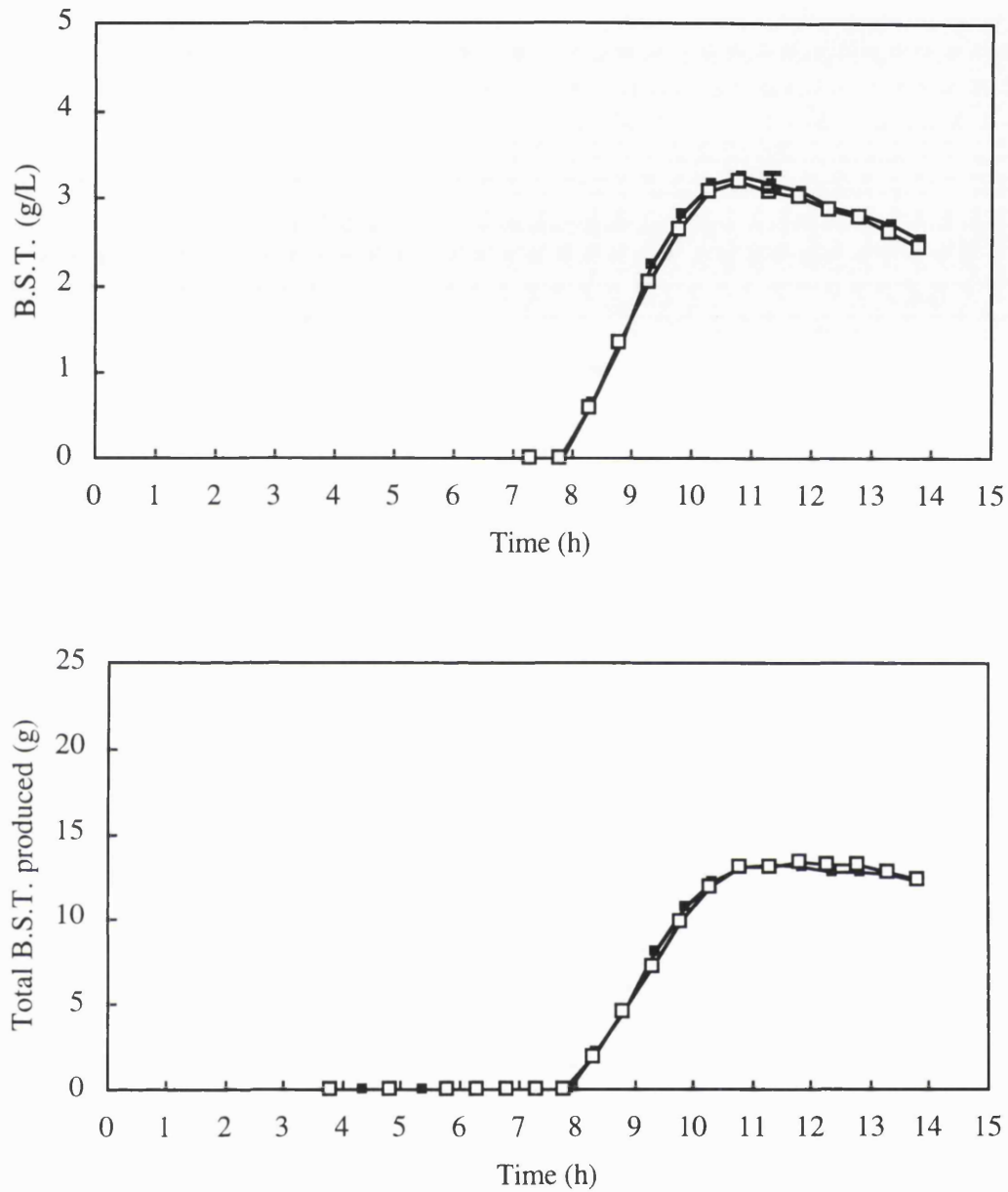


Figure 3.5e: Effect of different media on high cell density fermentations. B.S.T. concentration and total B.S.T. produced. (Error bar shown at 11.3h for Expt. 8).

- Medium B (Expt. 8).
- Medium B+ (Expt. 9).

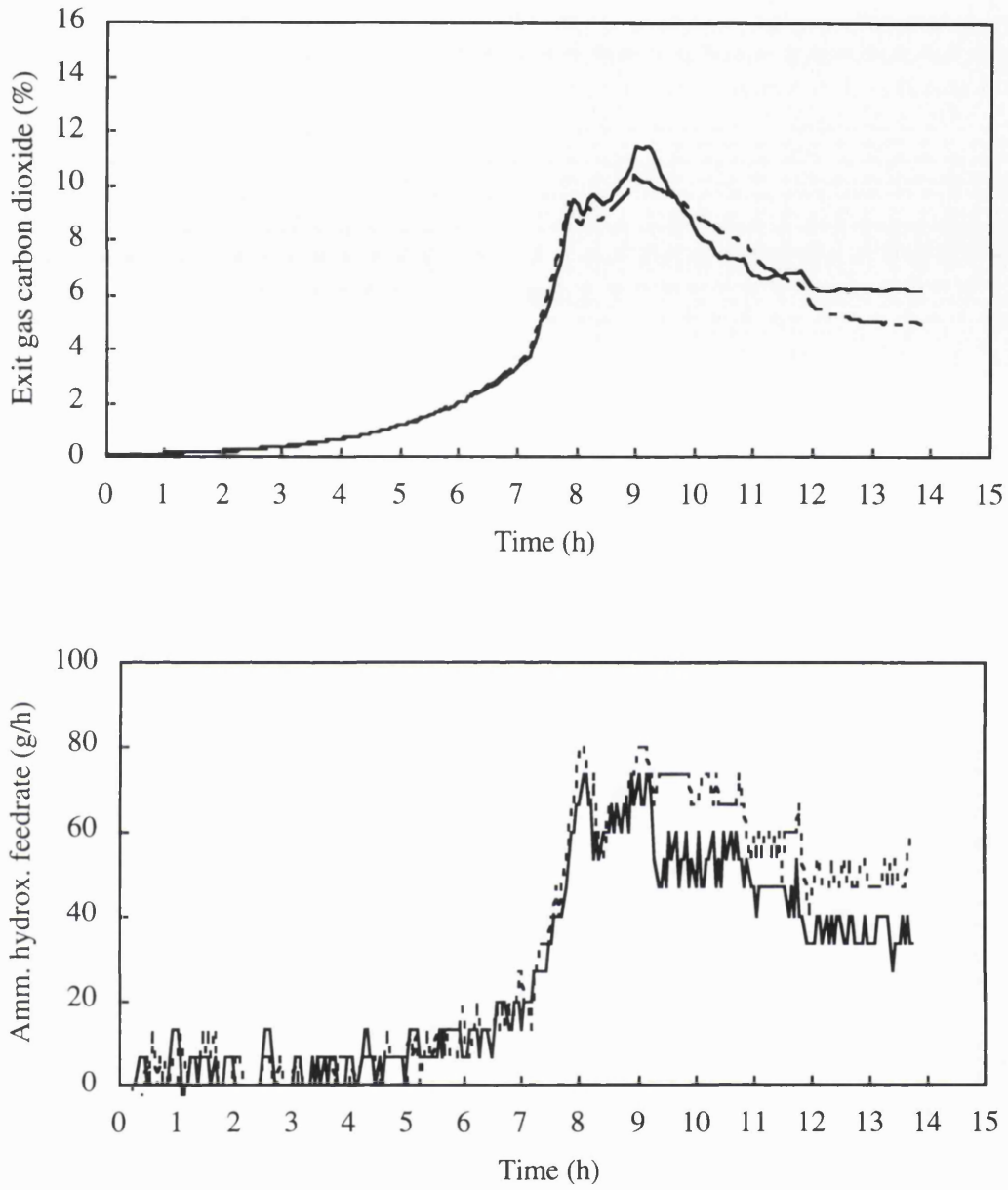


Figure 3.5f: Effect of different media on high cell density fermentations.
% CO₂ in fermenter exit gas and ammonium hydroxide feedrate.

— Medium B (Expt. 8).
---- Medium B+ (Expt. 9).

3.6.2 Effect of glucose feeding on high cell density fermentations (Expts. 9 and 10).

Objective:

Determine if reduced glucose feeding leads to lower acetate concentrations and hence more B.S.T. This was important since in the previous high cell density fermentations (Expts. 8 and 9. Sec. 3.6.1) it was concluded that the productivity was limited by acetate inhibition.

Method:

Both experiments used medium B+. Expt. 9 (labelled "control") was described in the previous section. Expt. 10 (labelled "low glucose feed") had a lower glucose feedrate as shown in Fig. 3.6a. - all other fermentation conditions were identical.

Conclusion:

Lower glucose feeding led to lower acetate concentrations and more B.S.T. (Figs. 3.6c and d). This suggests that acetate inhibition is indeed limiting the productivity of these fermentations.

Conclusions about glucose feeding:

In the low glucose feed run the glucose became limiting at 9h with a sharp drop in exit gas % CO₂ and ammonium hydroxide consumption (Figs. 3.6c and e) indicating a more severe glucose limitation than in the control run. The effects were:

1. Biomass (Fig. 3.6b) and B.S.T.(Fig. 3.6d) production did not appear to be affected by glucose limitation.
2. Acetate production was reduced in both runs after glucose limitation but the reduction was much greater in the run with low glucose feeding (Fig. 3.6c).

These results show that by reducing the glucose feeding acetate production can be reduced substantially without affecting either biomass or B.S.T. production. It can also be seen that the acetate production rate (between 9 and 10h) is the same in both runs even though one is glucose limited. This suggests that in the case of Expt. 10 the cells are excreting acetate at the maximum rate. However since no glucose is accumulating in the broth they must still be consuming all the glucose they are being fed. It is concluded that they are excreting the extra glucose in the form of other metabolites. The production of

other metabolites such as pyruvate has been noted in the literature (e.g. George *et al.*, 1992). Furthermore if such metabolites are produced they could contribute to the inhibitory effect of acetate (e.g. Landwall and Holme, 1977).

Further observations:

1. It is interesting to note that with the same mineral feeding (i.e. medium B+) and peptone feeding the physical effects of unsaturated solutions affecting the exit gas % CO₂ should be the same in both runs. As a result the exit gas % CO₂ plots (Fig. 3.6e) are identical up to the time the glucose becomes limiting (8.8h). Once again this indicates the excellent reproducibility of the fermentations.

2. Acetate concentrations of about 10 g/L appear to be slightly inhibitory to B.S.T. production. This is the acetate concentration in both runs at about 10 hours when the B.S.T. production rate starts to decline.

3. Acetate concentrations in the range of 12 - 15 g/L are very inhibitory to B.S.T. production. After 10 hours the acetate production rate in the low glucose feed run does start to decrease relative to the control fermentation (Fig. 3.6c). Thereafter the lower glucose feed run does have lower acetate concentrations and consequently produces slightly more B.S.T. Both runs stop producing B.S.T. when the acetate concentrations reach about 12-15 g/L. Again this is in general agreement with the literature results (e.g. Calcott *et al.* (1988) who showed that acetate concentrations of 12-16 g/L reduced the production rate of B.S.T. in their fermentations by 50%).

4. Biomass production does not appear to stop even when acetate concentrations are as high as 25 g/L (Figs. 3.6b and c).

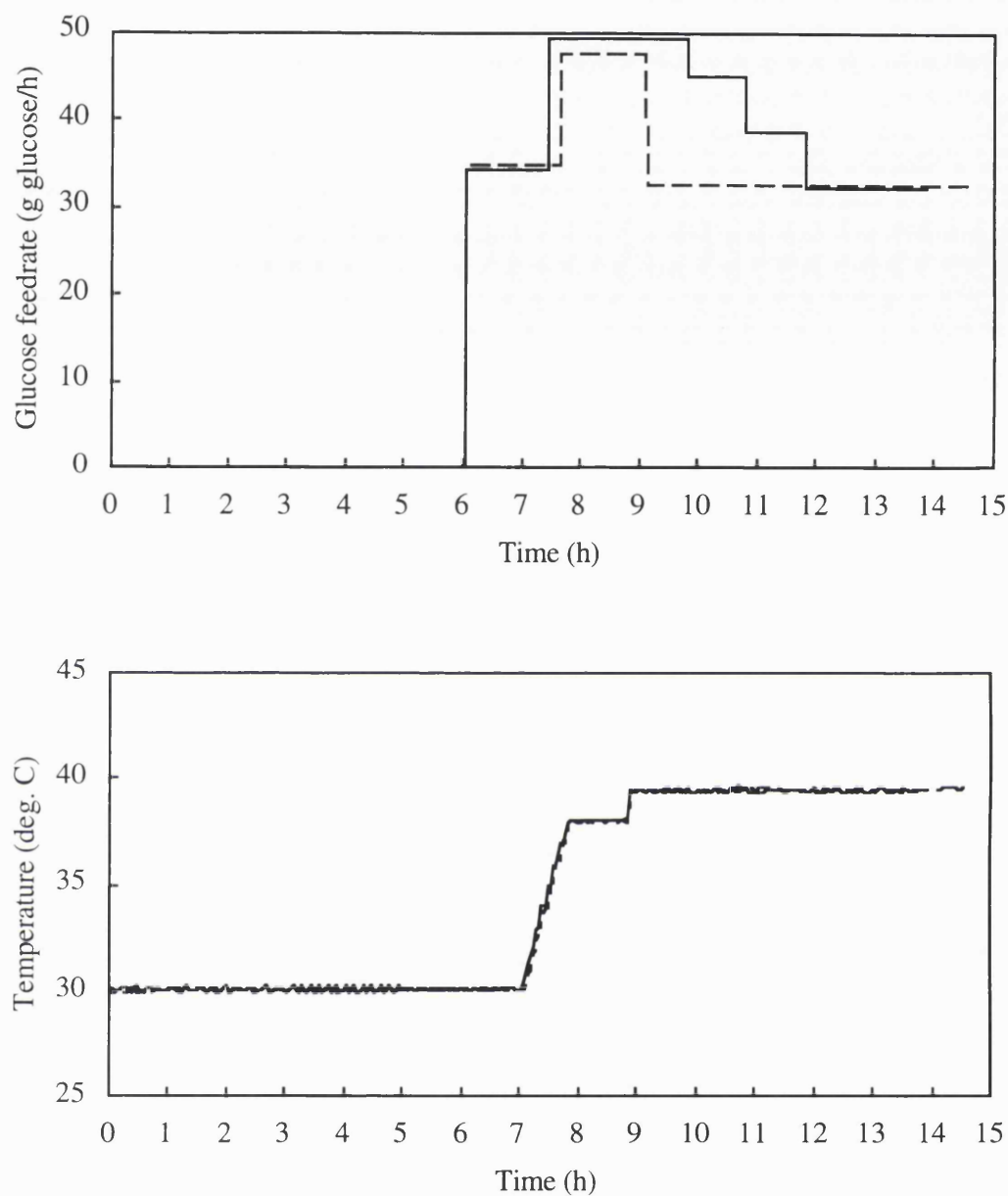


Figure 3.6a: Effect of glucose feeding on high cell density fermentations.
Glucose feedrate and temperature profiles.

— Control (Expt. 9).
---- Low glucose feedrate (Expt. 10).

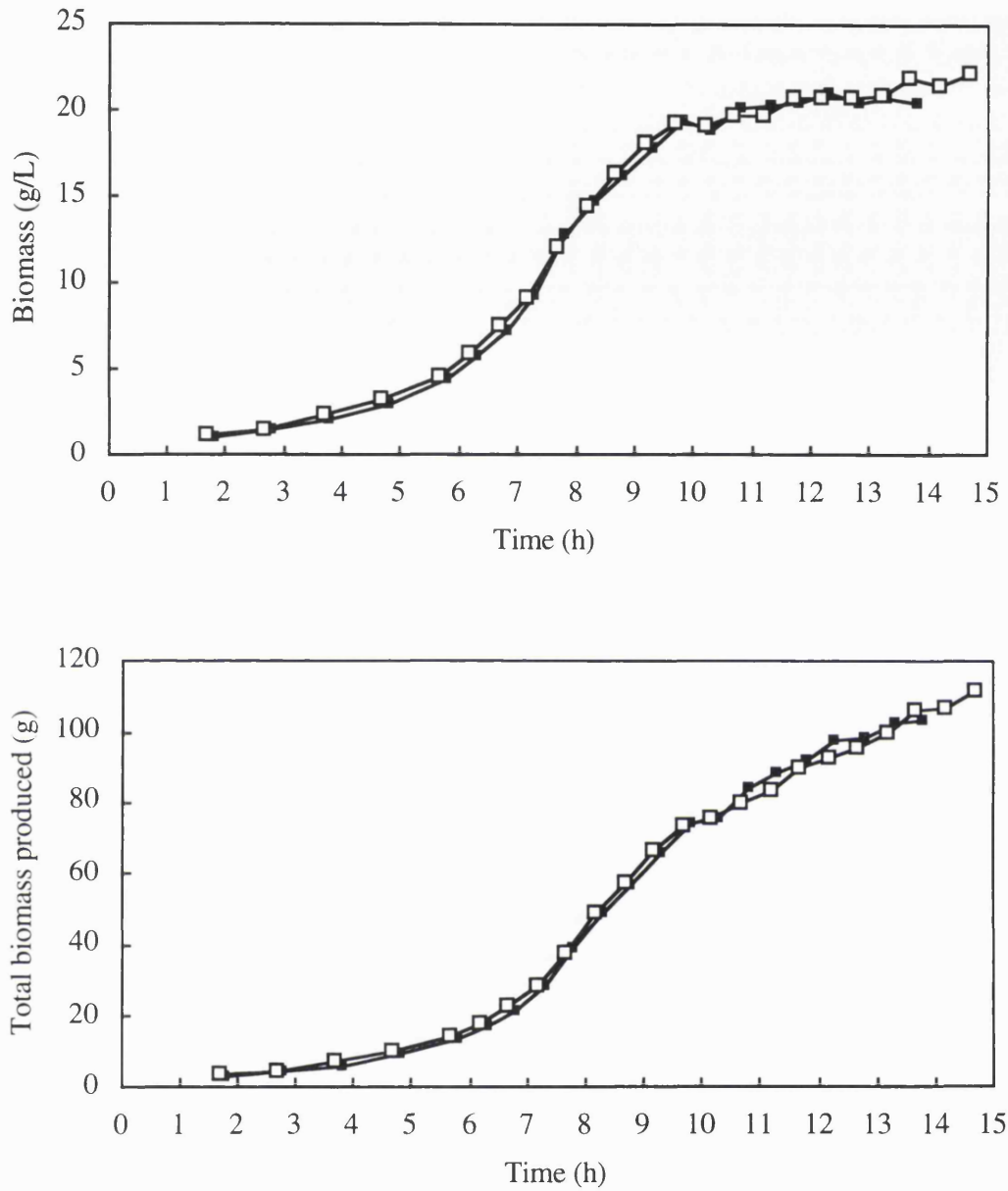


Figure 3.6b: Effect of glucose feeding on high cell density fermentations. Biomass concentration and total biomass produced.

- Control (Expt. 9).
- Low glucose feedrate (Expt. 10).

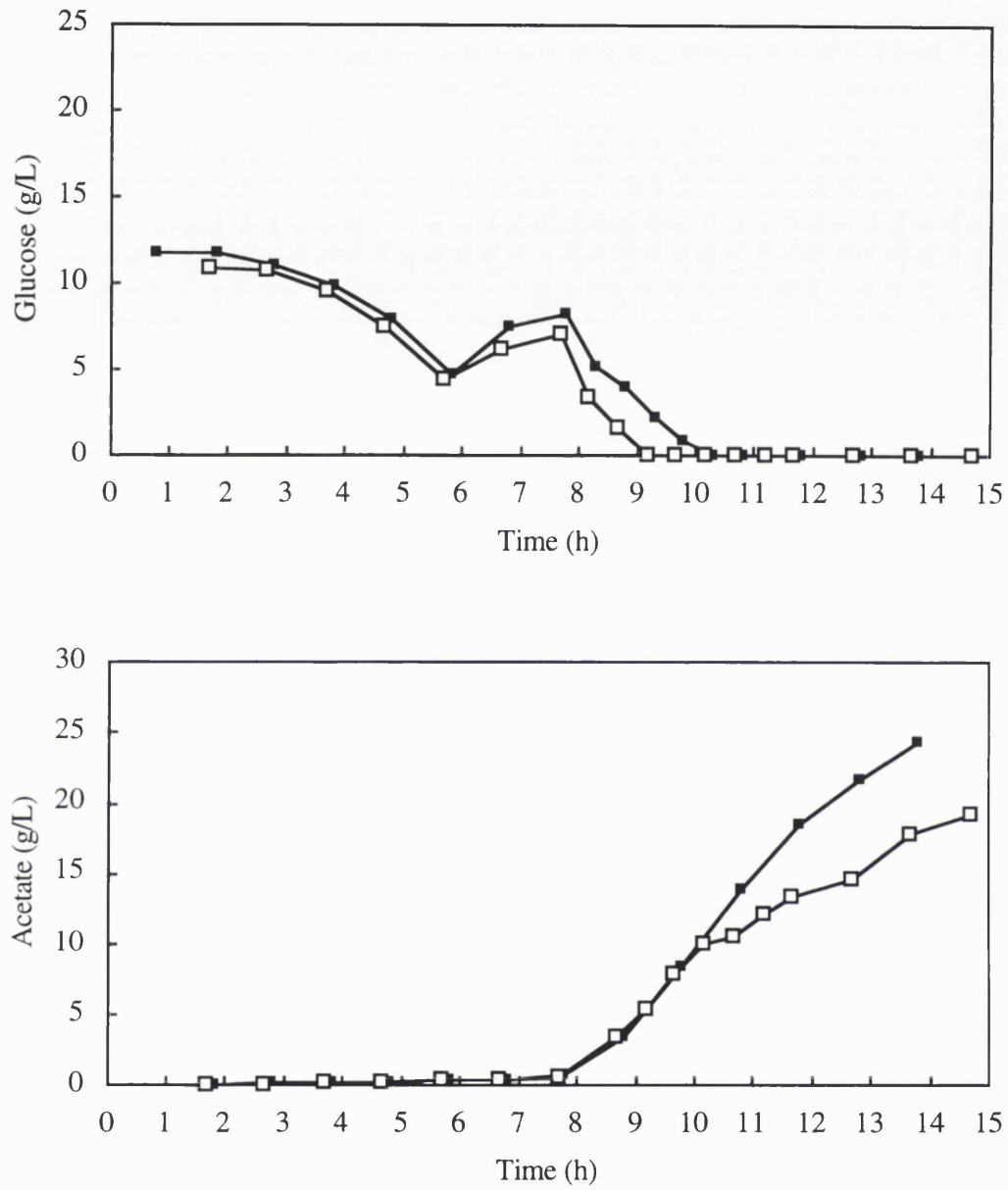


Figure 3.6c: Effect of glucose feeding on high cell density fermentations.
Glucose and acetate concentrations.

- Control (Expt. 9).
- Low glucose feedrate (Expt. 10).

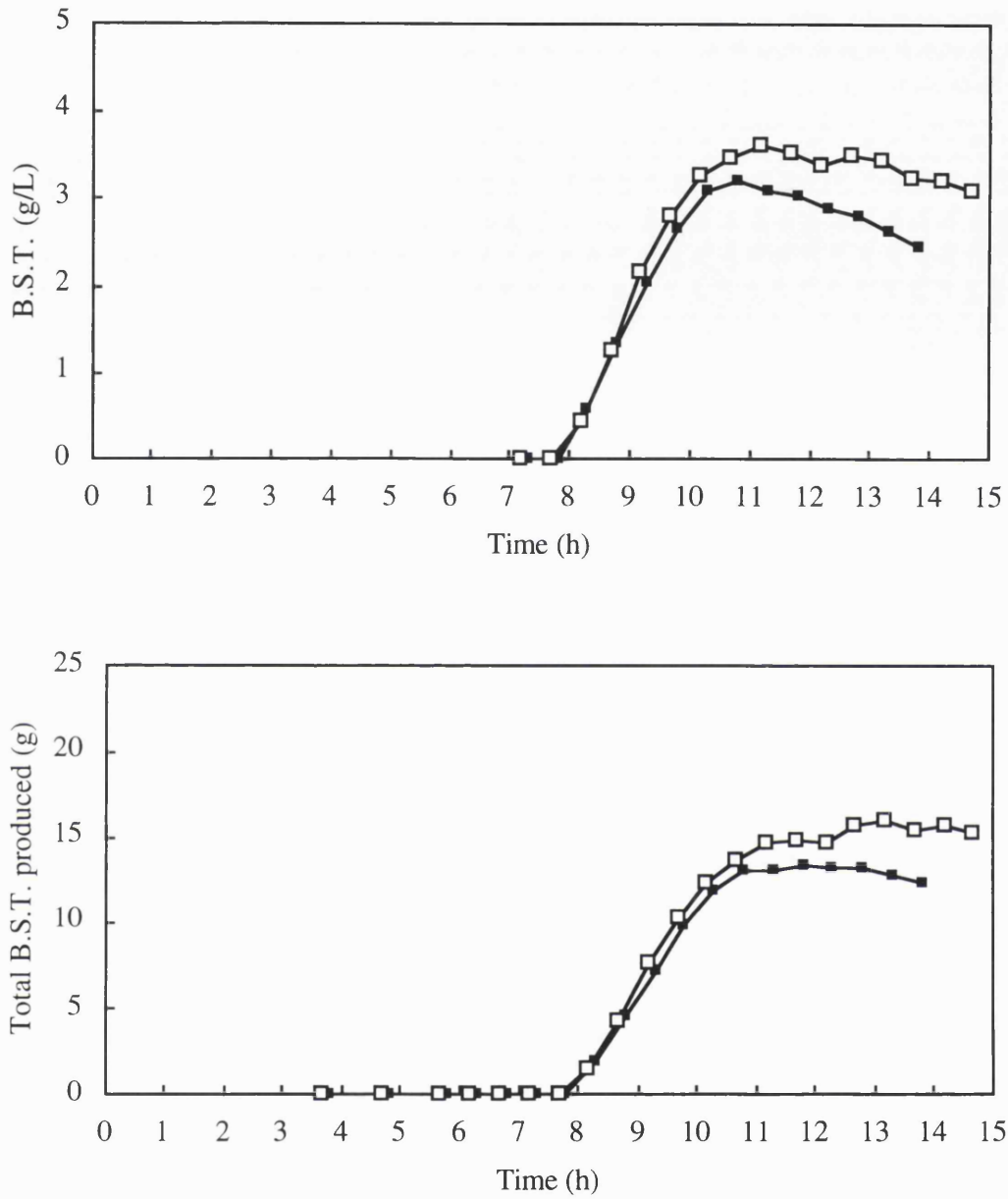


Figure 3.6d: Effect of glucose feeding on high cell density fermentations. B.S.T. concentration and total B.S.T. produced.

- Control (Expt. 9).
- Low glucose feedrate (Expt. 10).

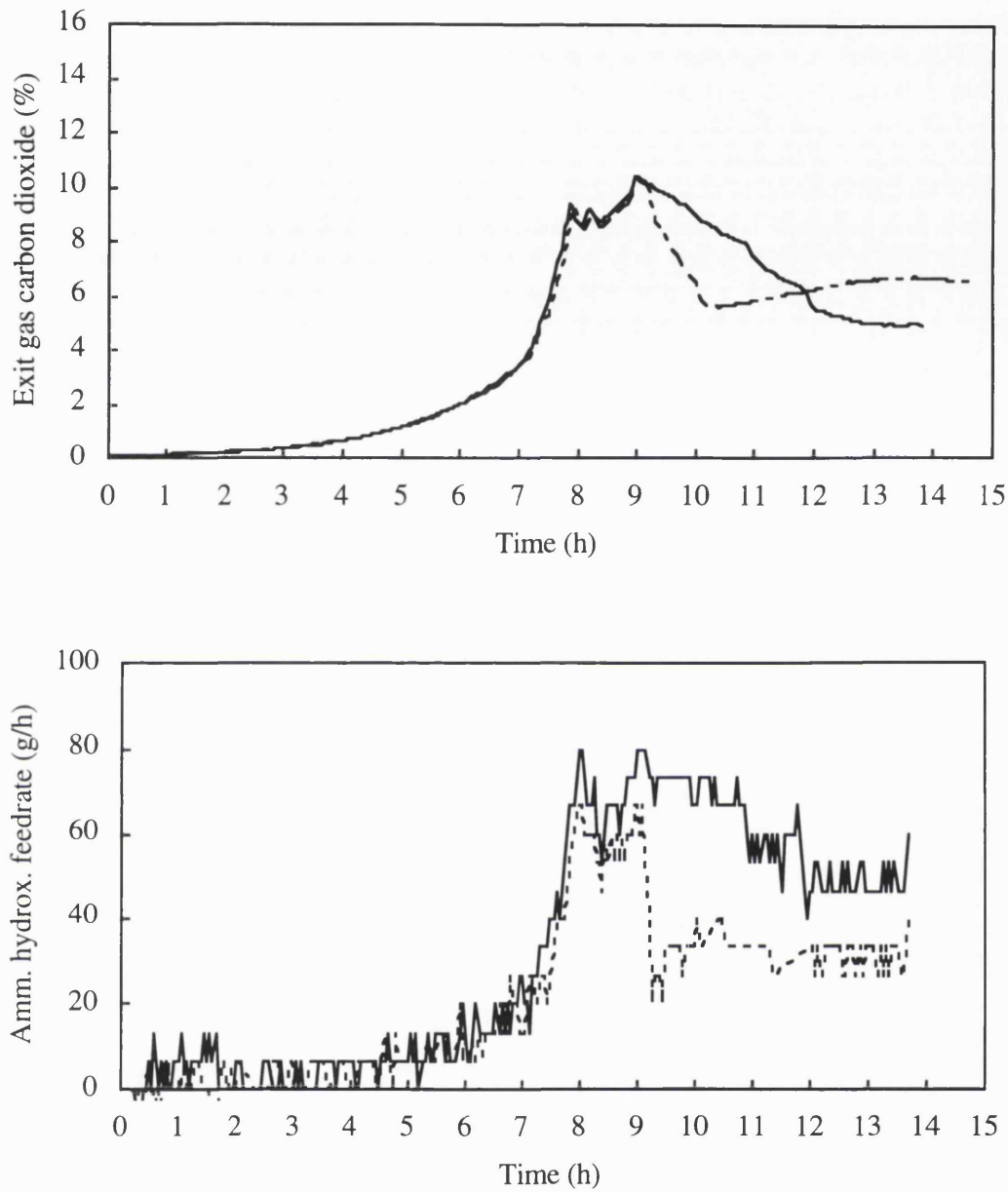


Figure 3.6e: Effect of glucose feedrate on high cell density fermentations. % CO₂ in fermenter exit gas and ammonium hydroxide feedrate.

— Control (Expt. 9).
 ---- Low glucose feedrate (Expt. 10).

3.6.3 Effect of glucose starvation on high cell density fermentations (Expts. 10-12).

Objective:

To see if further reductions in glucose feeding could cause even lower acetate production levels and hence higher B.S.T. titres.

Method:

Expt. 10 (described in the previous section) was repeated with even lower glucose feedrates (Fig. 3.7a). All other fermentation conditions were kept the same. Expts. 11 and 12 used a different sub-clone from the rest of the experiments in this thesis.

Conclusions:

Very low glucose feedrates (relative to those discussed above) do reduce acetate production still further and therefore lead to longer periods of B.S.T. production. However they also cause glucose starvation such that the rate of B.S.T. production is reduced directly due to lack of glucose.

The overall effect in these runs was that the lower the glucose feedrate the higher the final B.S.T. titre but the longer it took to reach it. The reason for this is discussed in Sec. 4.6.1 where this result is predicted quantitatively by the model.

Conclusions about glucose feeding:

The glucose becomes limiting at 8.7, 8.8 and 9.1h in Expts. 12, 11 and 10 respectively (Fig. 3.7c). However the glucose feedrates for Expts. 11 and 12 are much reduced (Fig. 3.7a) and therefore the glucose limitation is more severe as indicated by the very sharp drops in exit gas % CO₂ and ammonium hydroxide feedrate (Fig. 3.7f).

Consequently after glucose limitation the rates of acetate, biomass and B.S.T. are all reduced in Expts. 11 and 12 (Figs. 3.7b, d and e). Furthermore, as would be expected, the rate of production is most affected in the run with the lowest glucose feeding. (In fact in the lowest glucose feed run acetate is no longer being produced).

Thus, in contrast to previous runs, the glucose feeding has been reduced to such an extent that B.S.T. production is reduced. Thus Expts. 11 and 12 are glucose starved in that there is insufficient glucose to support the energy demand for B.S.T. synthesis.

Further observations:

1. Acetate concentrations of about 8-10 g/L (i.e. at the time the three acetate plots diverge) are slightly inhibitory to B.S.T. production as observed by the slight decline in B.S.T. production rate that is already occurring at this point (Figs. 3.7d and e).
2. Acetate concentrations in the range 12-15 g/L appear to stop B.S.T. production completely. In Expts. 10 and 11 B.S.T. production stopped (Fig. 3.7e) when the acetate concentrations were 12-13 g/L and 12-15 g/L respectively (Fig. 3.7d). In Expt. 12 acetate concentrations did not reach these levels and consequently B.S.T. production never stopped.
- 3 The use of a different sub-clone for Expts. 11 and 12 made no difference to the fermentation since the % CO₂ plots prior to glucose limitation, and the initial rates of B.S.T. and acetate production were identical to those in Expt. 11.

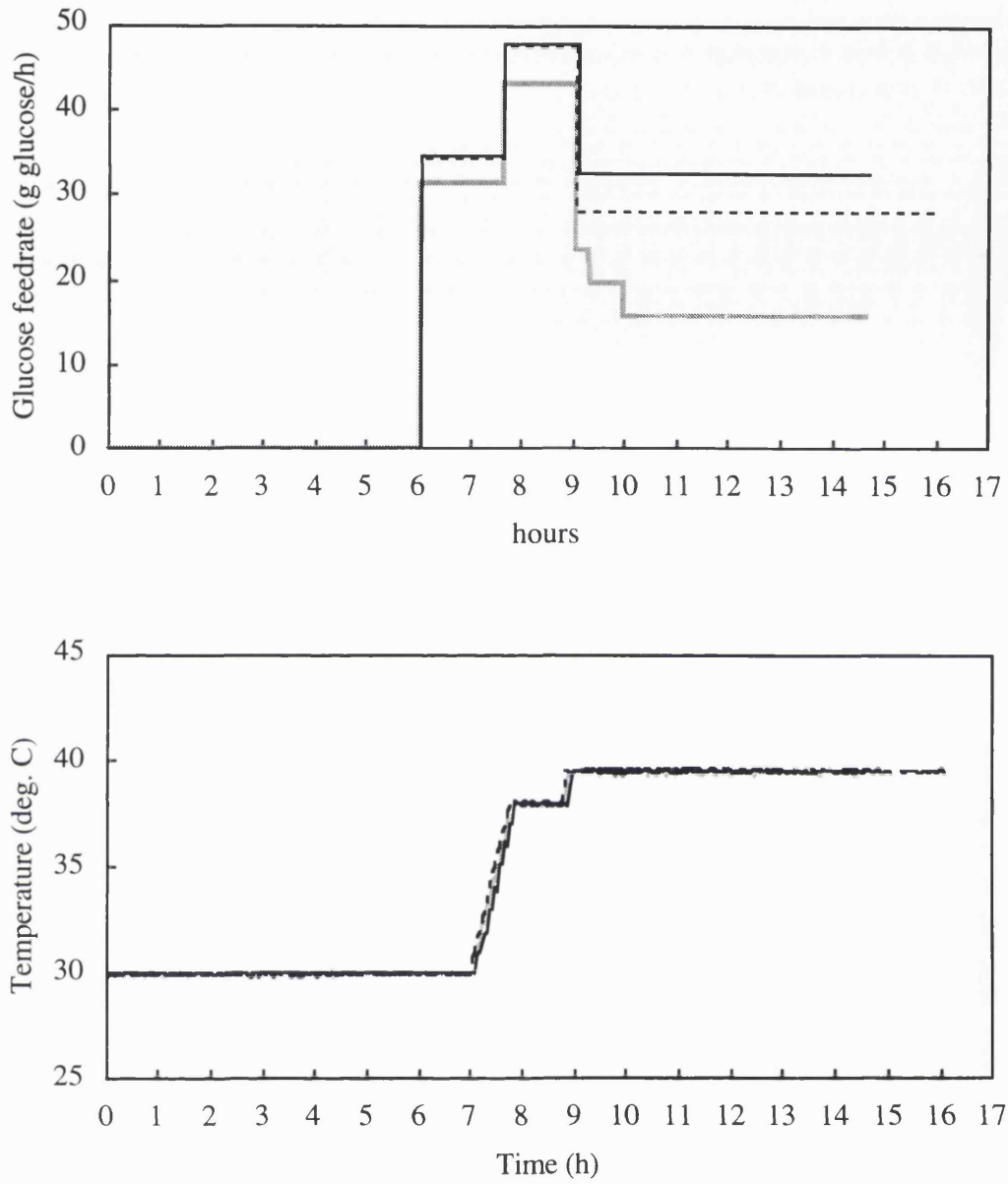


Figure 3.7a: Effect of glucose starvation on high cell density fermentations. Glucose feedrate and temperature profiles.

- Low glucose feedrate (Expt. 10).
- - - Very low glucose feedrate (Expt. 11).
- Lowest glucose feedrate (Expt. 12)

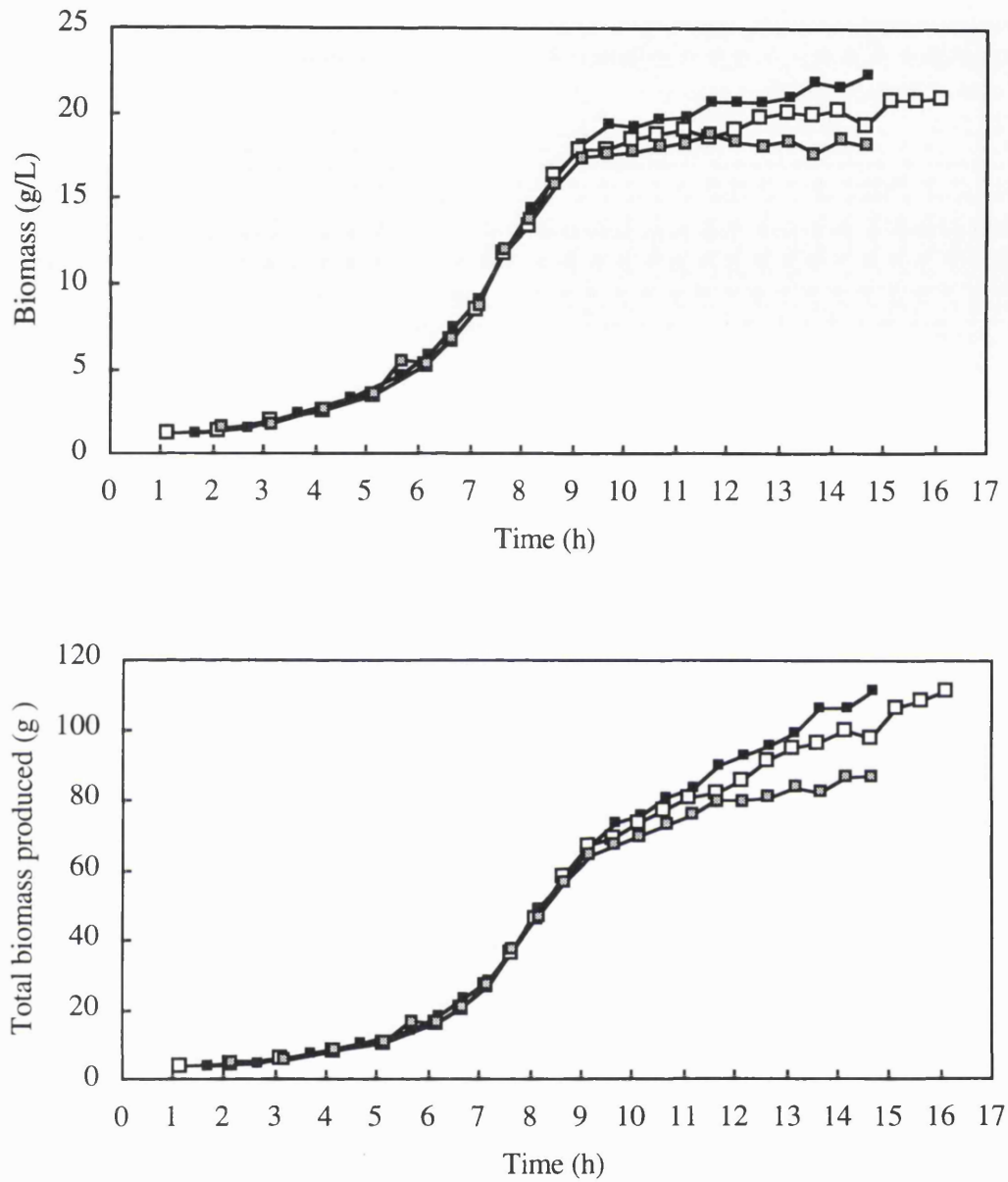


Figure 3.7b: Effect of glucose starvation on high cell density fermentations. Biomass concentration and total biomass produced.

- Low glucose feedrate (Expt. 10).
- Very low glucose feedrate (Expt. 11).
- ⊠ Lowest glucose feedrate (Expt. 12).

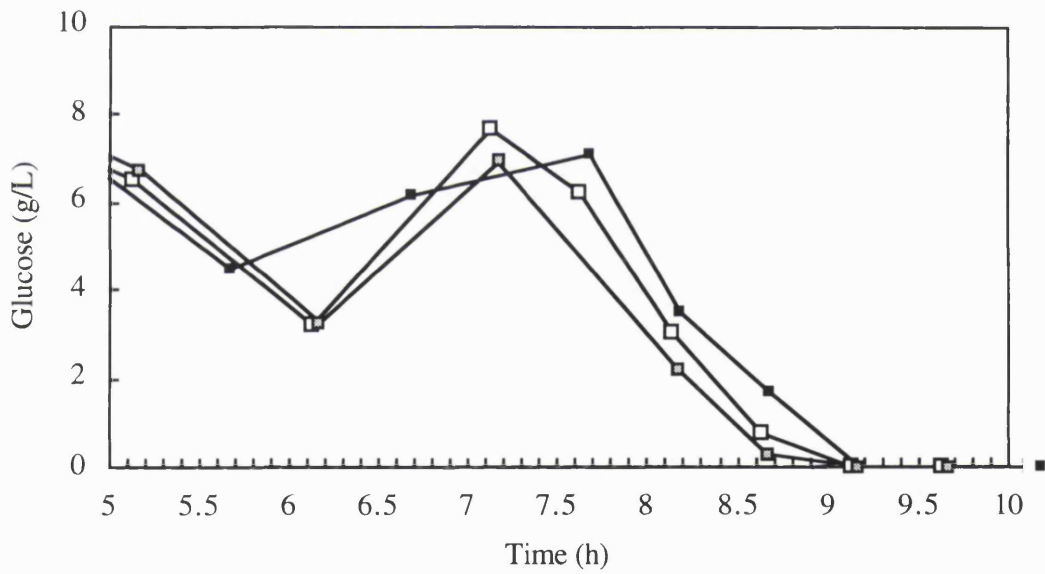
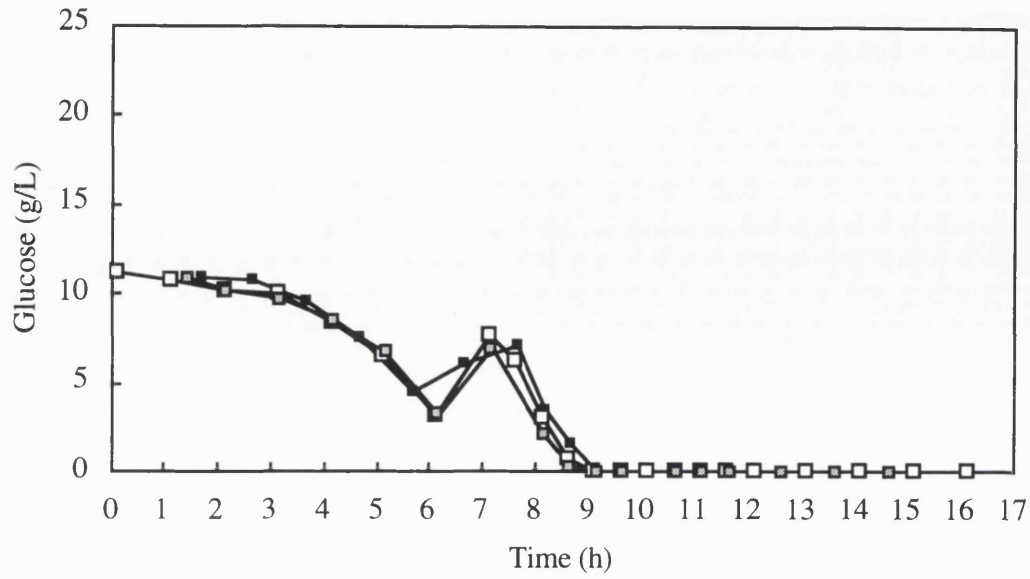


Figure 3.7c: Effect of glucose starvation on high cell density fermentations. Glucose concentrations (bottom graph has expanded scales).

- Low glucose feedrate (Expt. 10).
- Very low glucose feedrate (Expt. 11).
- ⊠ Lowest glucose feedrate (Expt. 12).

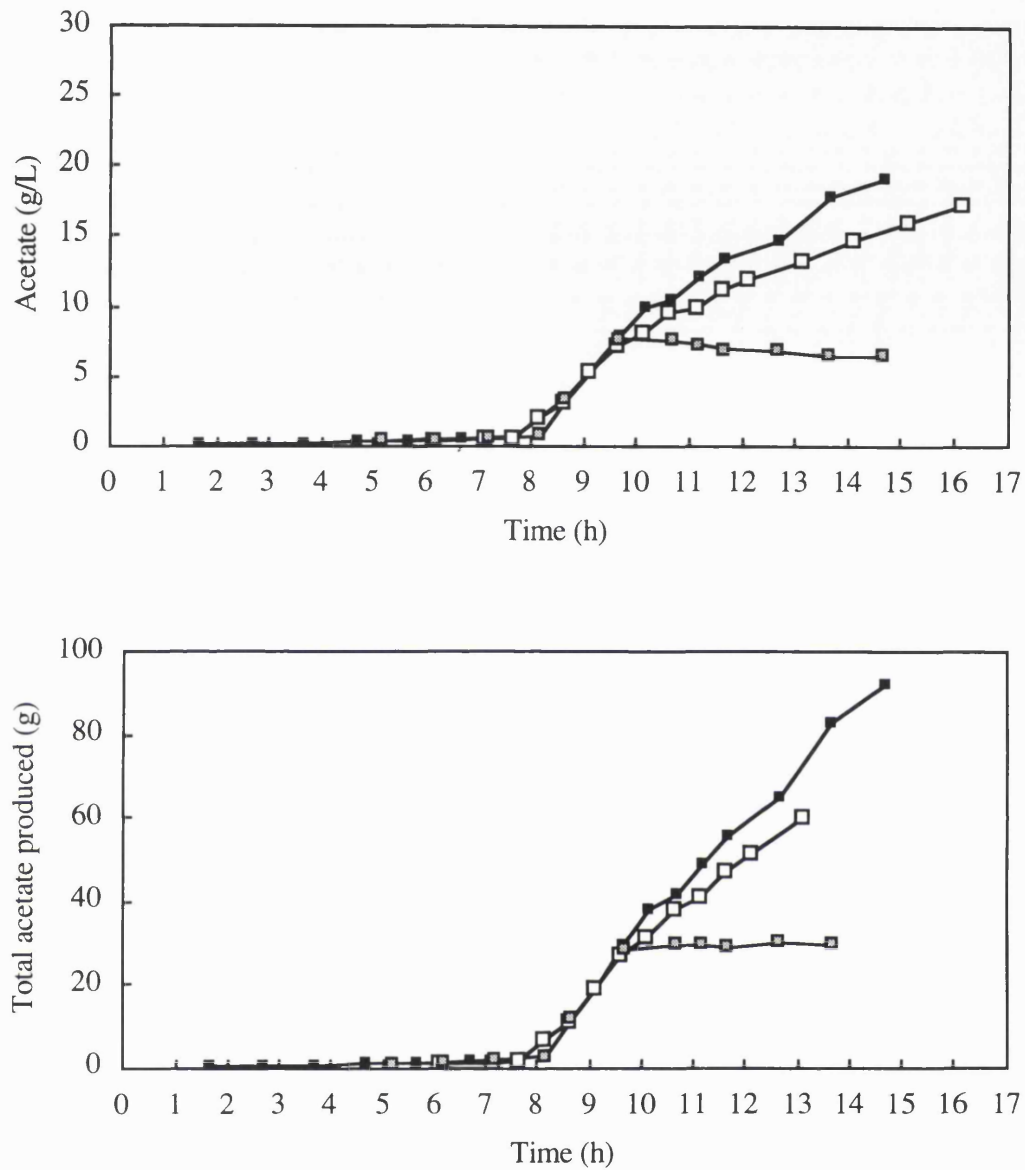


Figure 3.7d: Effect of glucose starvation on high cell density fermentations. Acetate concentration and total acetate produced.

- Low glucose feedrate (Expt. 10).
- Very low glucose feedrate (Expt. 11).
- ⊠ Lowest glucose feedrate (Expt. 12).

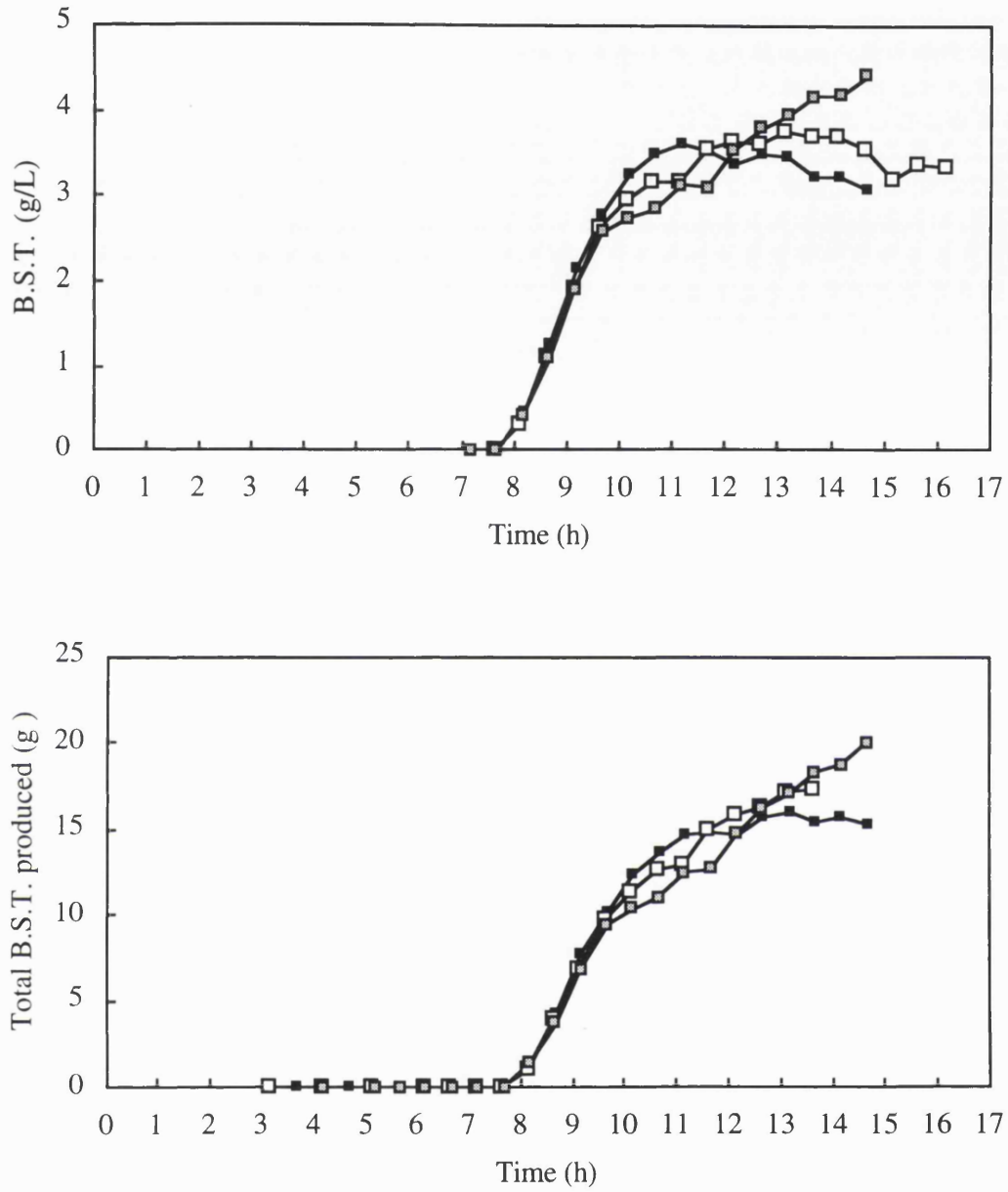


Figure 3.7e: Effect of glucose starvation on high cell density fermentations. B.S.T. concentration and total B.S.T. produced.

- Low glucose feedrate (Expt. 10).
- Very low glucose feedrate (Expt. 11).
- ⊠ Lowest glucose feedrate (Expt. 12).

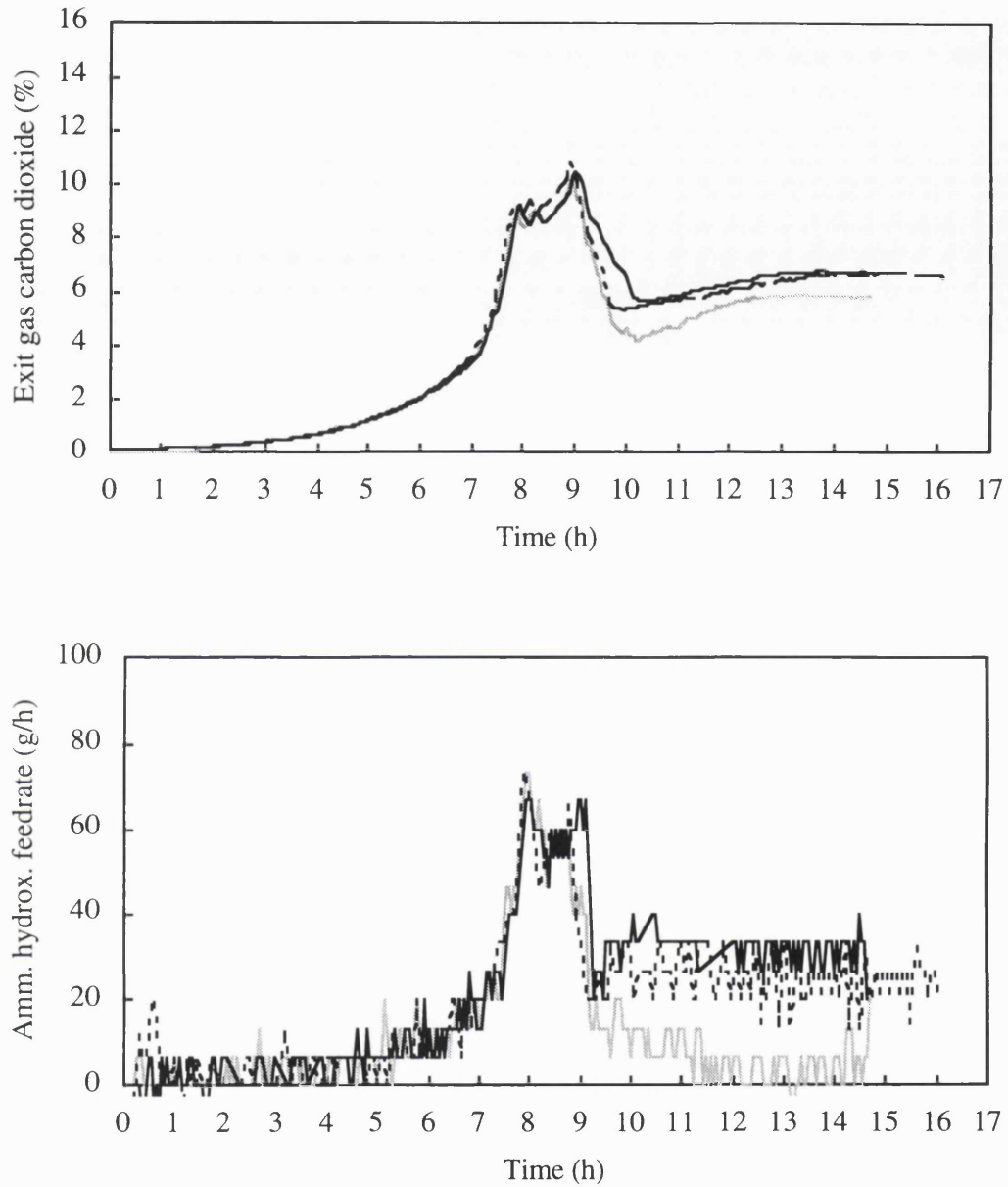


Figure 3.7f: Effect of glucose starvation on high cell density fermentations.
% CO₂ in fermenter exit gas and ammonium hydroxide feedrate.

- Low glucose feedrate (Expt. 10).
- - - Very low glucose feedrate (Expt. 11).
- Lowest glucose feedrate (Expt. 12)

3.7 Comparison of medium and high cell density fermentations (Expts. 7 and 8).

Objective:

To compare the medium and high cell density fermentation processes - especially with reference to productivity.

Method:

The two experiments compared here are Expts. 7 and 8 described previously in Secs. 3.5 and 3.6.1. Fermentation conditions were identical except that temperature induction was triggered in the medium cell density fermentation at an exit gas CO₂ concentration of 1.8% and in the high cell density fermentation at 3.6% (Figs. 3.8a and f). The glucose feeding strategy was kept the same - i.e. to limit glucose after the temperature had reached 39.5°C (Fig. 3.8c). In order to achieve this the glucose feedrate in the high cell density run was greater (Fig. 3.8a).

The dissolved oxygen was kept above 20% in both runs (Fig D3.8b). Oxygen enriched sparging was used only for the high cell density fermentation. The "high" peptone feedrate (as defined in Sec. 2.4.4) was started in both fermentations when the temperature reached 37°C. The corresponding times were 6.52 and 7.90 h for the medium and high cell density fermentations respectively.

Conclusions:

The high cell density fermentation produced B.S.T. at a faster rate because it had more cells when induction was triggered. However it also produced acetate at a faster rate and reached inhibitory levels of acetate after a shorter period of production. Therefore the final B.S.T. titre in the high cell density process was less.

Conclusions about glucose feeding:

Glucose becomes limited for the medium and high cell density fermentations at 8.0 and 9.5h respectively (Fig. 3.8c). However because of their different glucose feedrates (Fig. 3.8a) the glucose limitation in the medium cell density run is slightly more severe as indicated by the sharper drops in the exit gas % CO₂ and ammonium hydroxide feedrates (Fig. 3.8f).

As a result the biomass production is reduced after glucose limitation in the medium cell density run but not in the high cell density one (Fig. 3.8b). Similarly the acetate

production rate is reduced in both runs but the effect is much more pronounced in the medium cell density one (Fig. 3.8c). The B.S.T. production rate is not affected by glucose limitation in either fermentation (Fig. 3.8e).

Clearly therefore the comparison between the two runs is not "fair" in the sense that the high cell density fermentation has a much too high glucose feedrate. The relative productivity of the two processes is in fact partly a reflection of their respective glucose feedrates. However it has been shown that attempts to reduce the acetate production in the high cell density process led to glucose starvation. The problem is that with the manual glucose feeding available it was not possible in the high cell density process to easily determine a glucose feedrate *a priori* that would not become limiting before the temperature reached 39.5°C and at the same time lead to neither inhibitory levels of acetate concentration nor glucose starvation

Further observations:

1. The two runs are identical up to 5.75h when induction is triggered in the medium cell density fermentation causing it to have a faster growth rate at this point (Fig. 3.8b and f).
2. Biomass production was still increasing at the end of both fermentations despite acetate concentrations up to 20 g/L (Fig. 3.8d).
3. B.S.T. production starts in both runs shortly after the temperature reaches 37°C. with the initial rate of production being higher in the high cell density run (Fig. 3.8e). Production appears to decrease slightly in both runs when the acetate concentration is about 8 - 10 g/L and by the time it reaches 12-15 g/L has completely stopped.
4. Acetate production increases dramatically in both runs when the peptone feed begins (Fig 3.8d). The production rate is higher in the high cell density run.
5. Phosphate is not a limiting factor in either fermentation. This is shown by the phosphate assays for the medium cell density fermentation (Fig 3.8c) and from the experiment with extra phosphate feeding for the high cell density fermentation (see Sec. 3.6.1).

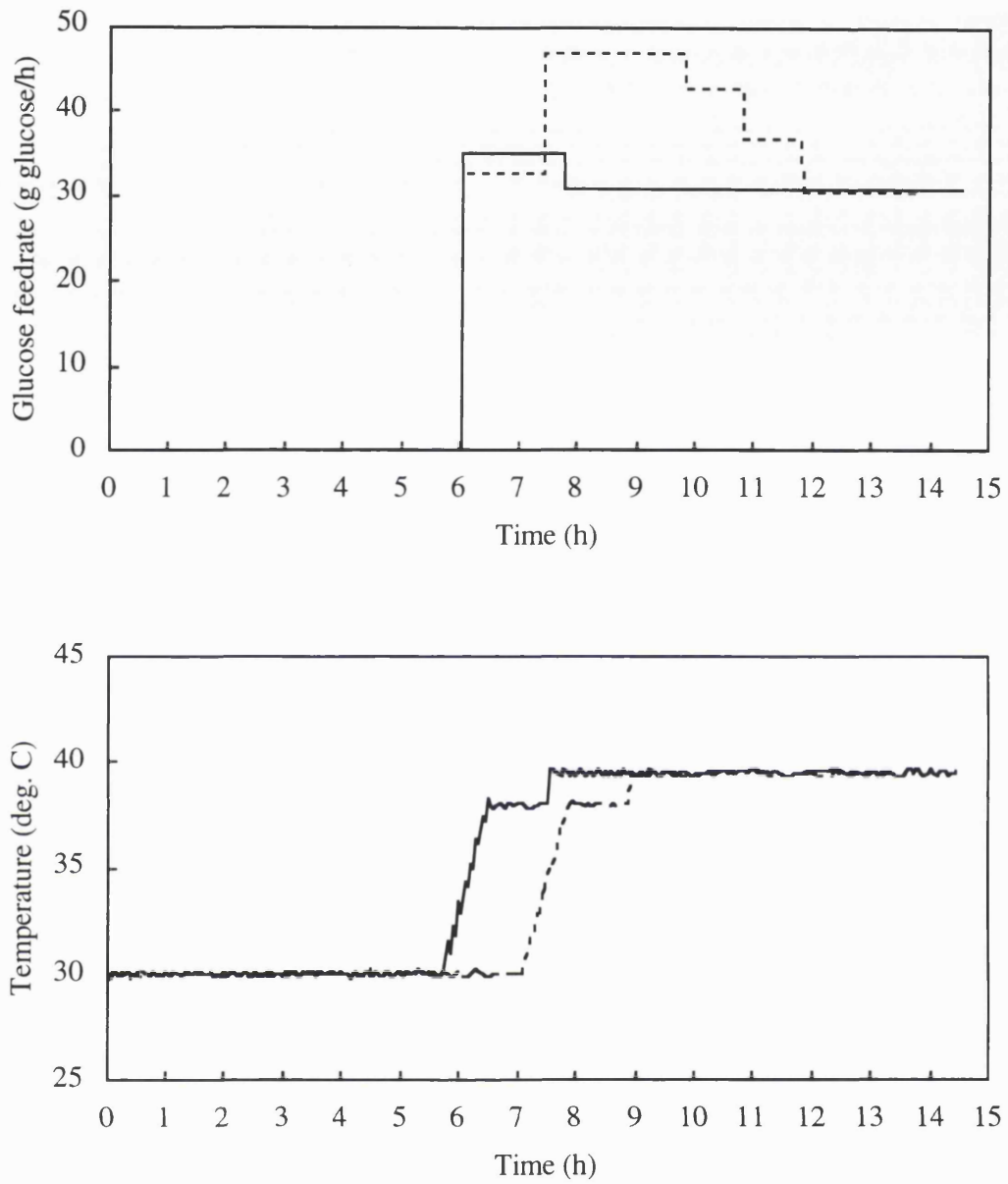


Figure 3.8a: Comparison of medium and high cell density fermentations.
Glucose feedrate and temperature profiles.

- Medium cell density (Expt. 7).
- High cell density (Expt. 8).

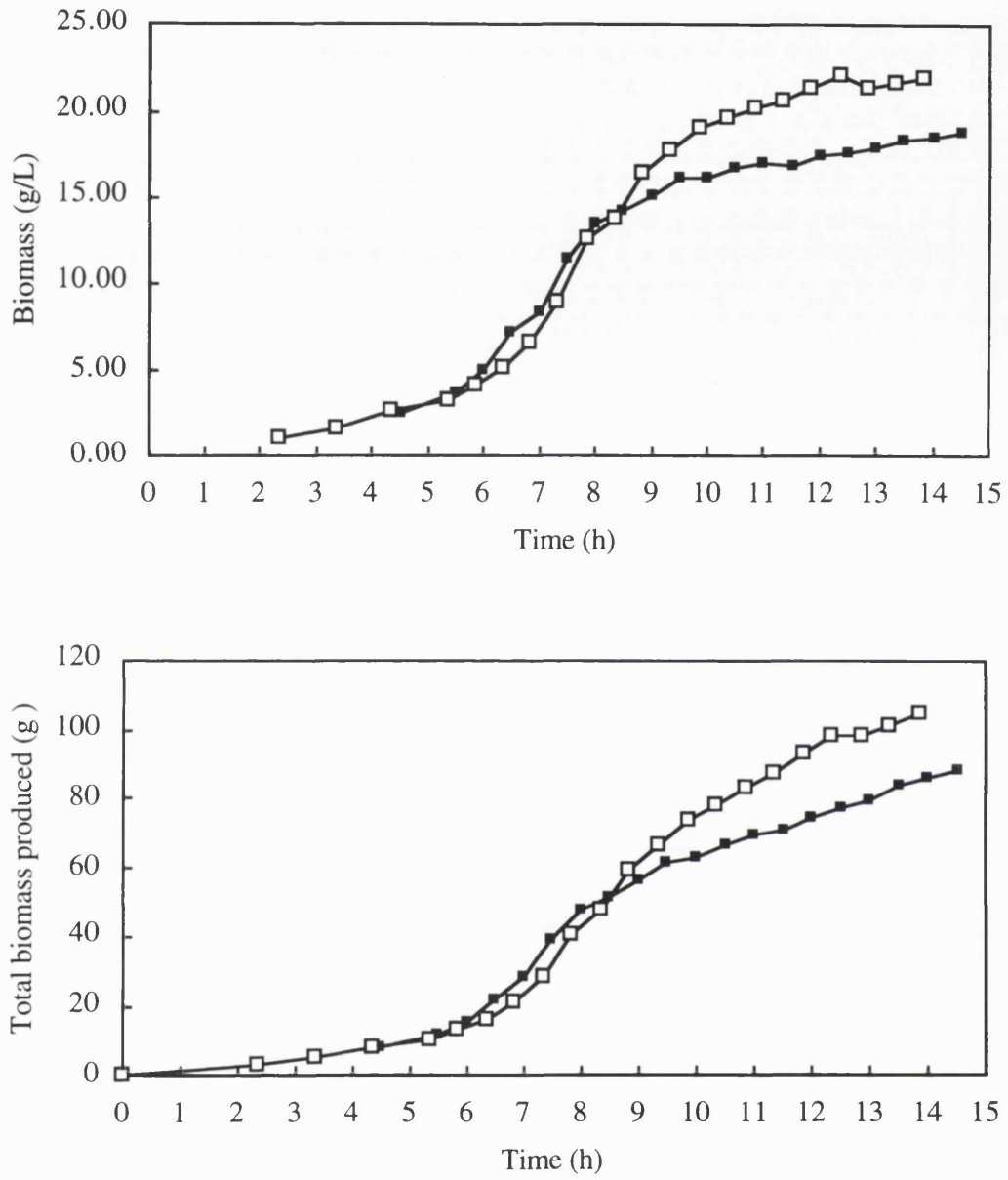


Figure 3.8b: Comparison of medium and high cell density fermentations. Biomass concentration and total biomass produced.

- Medium cell density (Expt. 7).
- High cell density (Expt. 8).

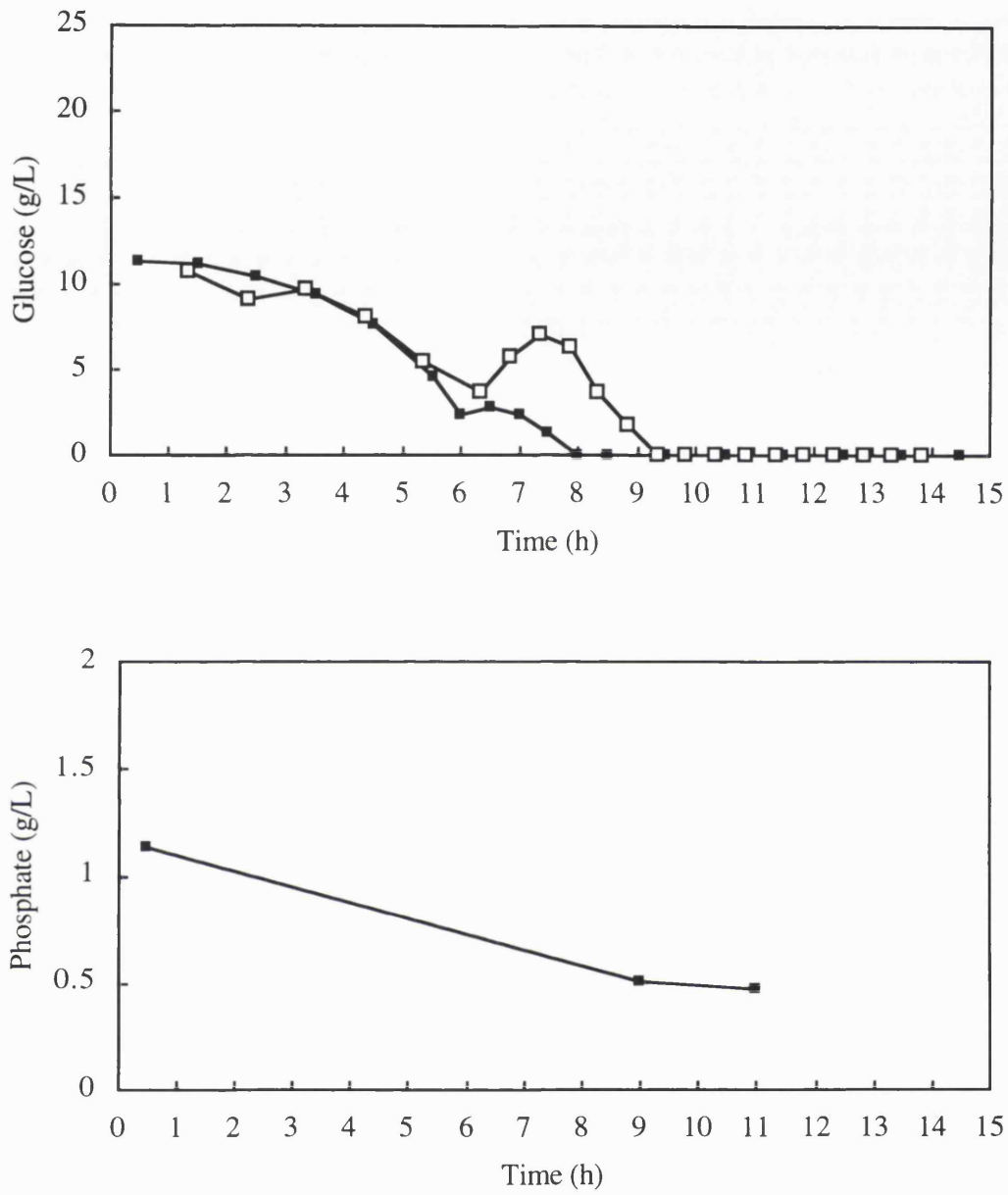


Figure 3.8c: Comparison of medium and high cell density fermentations. Glucose and phosphate concentrations.

- Medium cell density (Expt. 7).
- High cell density (Expt. 8).[no phosphate assays]

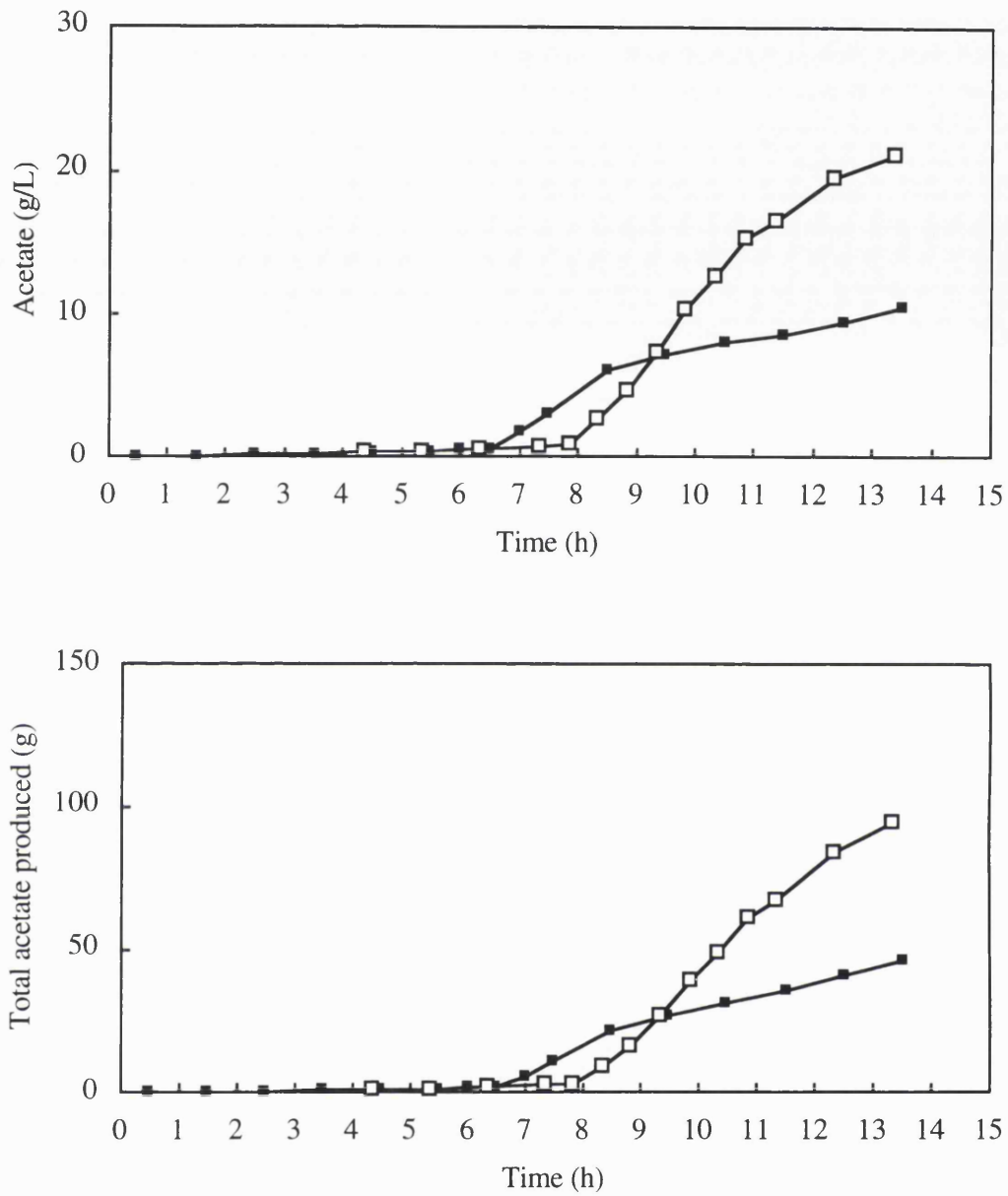


Figure 3.8d: Comparison of medium and high cell density fermentations. Acetate concentration and total acetate produced.

- Medium cell density (Expt. 7).
- High cell density (Expt. 8).

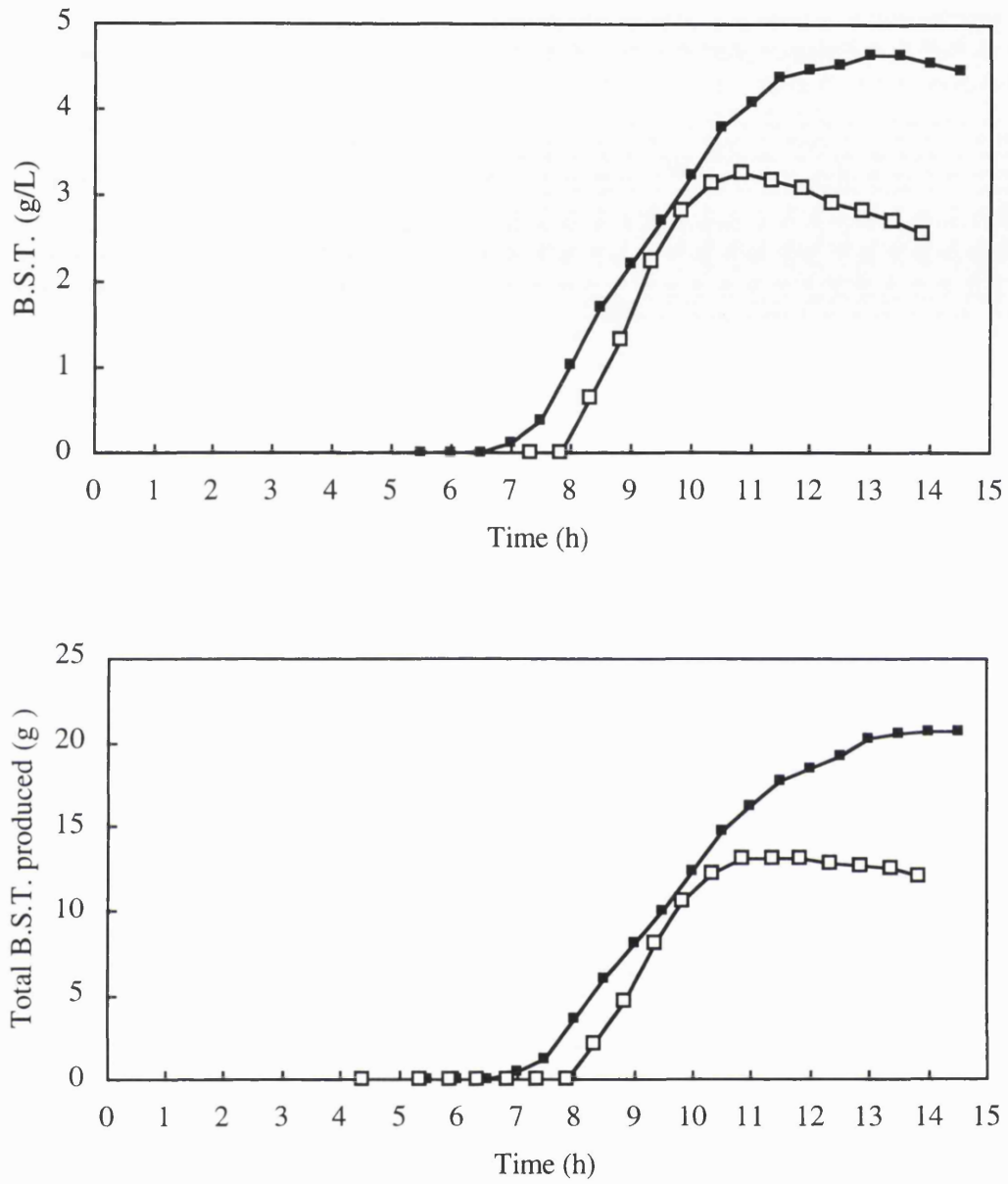


Figure 3.8e: Comparison of medium and high cell density fermentations. B.S.T. concentration and total B.S.T. produced.

- Medium cell density (Expt. 7).
- High cell density (Expt. 8).

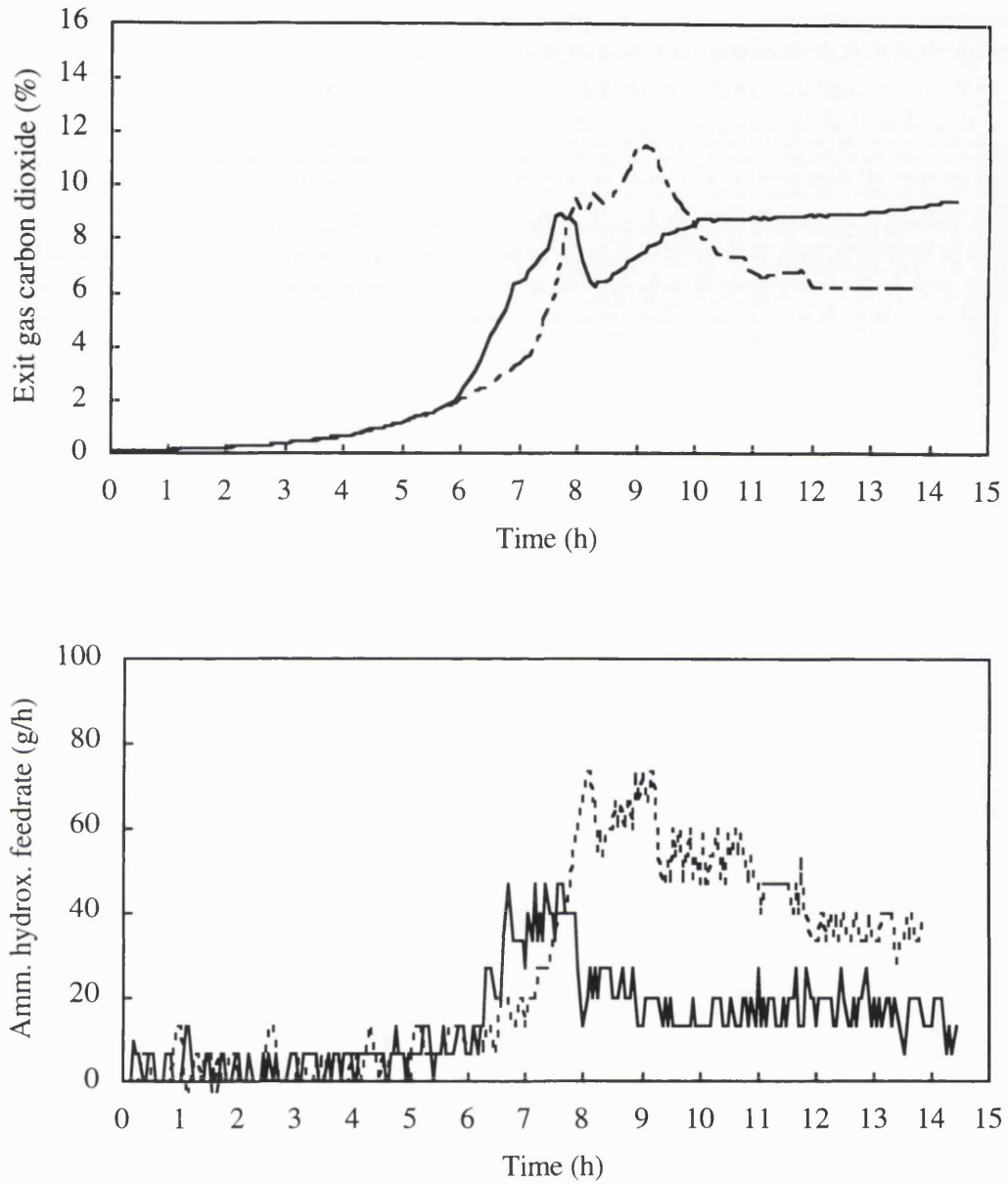


Figure 3.8f: Comparison of medium and high cell density fermentations.
% CO₂ in fermenter exit gas and ammonium hydroxide feedrate.

— Medium cell density (Expt. 7).
 ---- High cell density (Expt. 8).

3.8 Conclusions

The main conclusions from the results described in this chapter are summarised below:

Effect of Media:

Medium O was phosphate limited but medium B was not limiting in either the medium or high cell density fermentations.

Effect of glucose feeding:

- If glucose is in excess, reducing the glucose feedrate has no effect on the production of biomass, acetate or B.S.T.
- If glucose is limiting then reducing the glucose feedrate can reduce the rate of production of acetate, biomass and B.S.T. The effect of glucose limitation appears to be more pronounced on biomass production than on B.S.T. production.

Acetate production:

- Increases dramatically when peptone feeding starts.
- Can be produced at maximum rate even when glucose is limited.
- Always excreted at maximum rate when glucose in excess.

B.S.T. production:

- Starts soon after temperature reaches 37°C.
- Decreases when acetate concentration are in the range 8-10 g/L.
- Stops when acetate concentration are in the range 12-15 g/L.
- B.S.T. is not proteolytically degraded to any great extent.

Biomass production:

- Rate of biomass production decreases when B.S.T. production begins.
- Not inhibited by acetate as much as B.S.T. production is.
- The plasmid is stable (i.e. no production of plasmid free cells)

In the next chapter these results are incorporated into a mathematical model of the fermentation.

4 MODELLING

4.1 Summary

In this chapter a simple unstructured mathematical model of the process is developed. It is shown how the model equations and parameters were obtained either directly from the literature reviews (Secs. 1.4 and 1.5) and the experimental results (Sec. 3.4-3.7) or indirectly by fitting the model to one of the high cell density fermentations. The sensitivity of the model to these parameters is investigated and the most critical parameters highlighted.

Comparisons between model predictions and experimental results are then shown for two other high cell density runs and one medium cell density run. Good agreement is found between the model predictions and experiment results for both the high cell density runs but poor agreement for the medium cell density run. Reasons for this are suggested along with possible model improvements.

Finally three examples are given of how the existing model can be used: In the first case it is shown how the model can predict the effect of possible process variations; in the second case the model is used to understand the complicated ammonia consumption pattern during a fermentation and in the third case the model is used to determine the best glucose feedrate to optimise yield of B.S.T.

4.2 Introduction

The aim of this chapter is to develop the final model of the process, to validate it and to show some of its uses. The basic form of the model was outlined in Sec. 1.5.4.2. This is developed into the final model by incorporating both the observations from the literature and the results obtained with the present host/vector. The main principle used throughout this process was to keep the model as simple as possible and to minimise the number of parameters needed. This would make the model easier to understand and hence more likely to be useful in an industrial setting.

4.3 The B.S.T. model

Based on a review of the literature (Secs. 1.4 and 1.5) and the experimental results (Sec. 3.4 - 3.7) the following model was created to describe the fermentation used in this thesis:

$$\frac{dX}{dt} = \mu X - \frac{X}{V} Q \quad (4.1a)$$

$$\frac{dP}{dt} = r_P X - \frac{P}{V} Q \quad (4.1b)$$

$$\frac{dA}{dt} = r_A X - \frac{A}{V} Q \quad (4.1c)$$

$$\frac{dS}{dt} = \frac{Q_{gluc} c_{gluc}}{V} - \frac{\mu X}{Y_{SX}} - \frac{r_P X}{Y_{SP}} - \frac{r_A X}{Y_{SA}} - mX - \frac{S}{V} Q \quad (4.1d)$$

$$\frac{dV}{dt} = Q \quad (4.1e)$$

Where:

$$Q = Q_{gluc} + Q_{pept} + Q_{amm} - Q_{samp} - Q_{evap} \quad (4.2)$$

$$\mu = \mu_{\max} \left(\frac{S}{S + K_1} \right) \left(1 - \frac{A}{A_1} \right) \left(1 - \frac{r_P}{r_{P,1}} \right) \quad (4.3)$$

$$r_P = r_{P,\max} \left(\frac{S}{S + K_2} \right) \left(1 - \frac{A}{A_2} \right) \quad (4.4)$$

$$r_A = \text{Max} [r_{A,\max}, k(\mu - \mu_{crit})] \quad (4.5)$$

Note: The following are functions of temperature:

μ_{\max}	see Sec. 4.4.1.2
$r_{P,\max}$	see Sec. 4.4.2.3
m	see Sec. 4.4.4.1

The following depends on the presence of peptone:

$r_{A,\max}$	see Sec. 4.4.3.1
--------------	------------------

The model differential equations (Eqns.4.1a,b,d,e) are as previously described in the introduction (Sec. 1.4.5.2) with the following exceptions:

- An extra differential equation has been added to take account of acetate production (Eqn. 4.1c) - this also requires the addition of an additional glucose consumption term

$$\frac{r_A X}{Y_{SA}} \text{ in Eqn. 4.1d.}$$

- The kinetic equations (Eqns. 4.3 - 4.5) are new and are explained and justified below:

Specific growth rate (Eqn. 4.3):

- The standard Monod term $\left(\frac{S}{S + K_1}\right)$ is included to take account of the effect of low glucose concentration on growth. It was decided to omit a term for the effect of high glucose concentration on growth since this simplifies the model and recombinant fermentations are normally controlled so that inhibitory concentrations of glucose are avoided (as explained in Sec. 1.4.3).
- The term $\left(1 - \frac{A}{A_1}\right)$ describes the inhibitory effect of acetate on growth as reported in the literature (Sec. 1.4.3.5) and deduced from the fermentations described in Secs. 3.5 and 3.6. Since, as was explained in the literature review, there is no commonly agreed form of expression to describe this relationship the simplest linear form for the expression was chosen.
- The term $\left(1 - \frac{r_P}{r_{P,1}}\right)$ was used to describe the effect that the specific rate of B.S.T. production has on growth and again, for simplicity, a linear term was chosen. As explained in Sec. 1.4.6 this term reflects the MacDonald and Neway (1990) result that recombinant protein production has a direct effect on growth even when the glucose is not limiting. Of course if glucose is limiting then B.S.T. production will also effect growth indirectly by consuming glucose, lowering the glucose concentration and hence decreasing growth according to the Monod expression described above.
- The specific growth rate is a function of temperature as discussed in Sec. 1.4.5.1

B.S.T. production (Eqn. 4.4):

- For the reasons explained in Sec. 1.4.3.3 the Monod type expression $\left(\frac{S}{S + K_2}\right)$ was used to describe the effect of low glucose concentration on the specific rate of B.S.T. production. This effect was deduced both from the fed-batch results of Jensen and Carlsen (1990) and the experiments described in Secs 3.5 and 3.6.
- The term $\left(1 - \frac{A}{A_2}\right)$ describes the effect of acetate concentration on recombinant protein production as observed in the continuous culture experiments of Jensen and Carlsen (1989) and which agrees with the experimental results of Secs. 3.5 and 3.6. The linear form of the equation is discussed in Sec. 4.4.1.4.
- The specific B.S.T. production rate is a function of temperature as discussed in Sec. 1.4.5.2.

Acetate production (Eqn. 4.5)

- The expression used implies that acetate is produced at a maximum specific rate unless the growth rate falls below a critical value. This fits in with the previous results of Bajpai (1987) and Jensen and Carlsen (1990) and the results in Sec. 3.5 and 3.6 which showed that acetate was produced at a maximum rate unless the glucose feedrate (and hence the growth rate) was reduced below a certain value.
- The growth-only fermentations (Sec. 3.4) proved that the maximum specific production rate of acetate depends on whether peptone is present in the medium and this is also included in the model (see Sec. 4.4.3.1).

The above kinetic expressions (Eqns. 4.3 - 4.5) therefore describe the effects of glucose, temperature and peptone on the specific production rates of biomass, B.S.T. and acetate. The effects that these equations describe are supported by experimental results in the literature and in many cases corroborated by the fermentations done with the host/vector used in this project. In some cases the form of the expressions (e.g. the Monod term) are also supported experimentally whilst for others there is either no correlation available or contradictory ones and therefore simple linear terms have been assumed.

Furthermore unnecessary effects have not been included (e.g. high glucose concentrations) so that the final equations are as simple as possible yet consistent with the known experimental facts. However although each of the kinetic equations is relatively simple to understand their interaction is complex. For example the specific production rate of acetate r_A (Eqn. 4.5) can depend on the specific growth rate μ (Eqn. 4.3) which in turn is affected by the specific B.S.T. production rate r_p (Eqn. 4.4) - both of which are inhibited by acetate.

Finally, before estimating the model parameters, the assumptions made in the above model need to be stated explicitly. It is important to do this since as highlighted by Dhurati and Leopold (1990) too often assumptions are made implicitly and the resultant model is presented as being more general than is warranted. Just as often explicit assumptions are lost or ignored with the same results. In either case it is a serious problem since the assumptions define the range of conditions on which the model is claimed or demonstrated to be accurate. Use of the model outside the bounds set by these assumptions can be a risky enterprise.

Key model assumptions

- The yield constants are not functions of temperature. This is supported in the literature (Esener *et al.*, 1983).
- The Monod constants (K_1 and K_2) are not functions of temperature. This assumption was made to simplify the model - in fact there is very little published information on the effect of temperature on the Monod constants (Esener *et al.*, 1983).
- The yield constants and the growth rate are not affected by peptone feeding. The growth-only fermentations were not able to confirm this and the literature suggests that such effects are strain dependent with no effect being observed for some strains (Sec. 1.4.3).
- No medium component is limiting or inhibitory (evidence was presented in the results (Sec. 3.5) that this was probably true for medium B). This assumption has to be remembered if the model is used to predict the effect of fermentations using a different medium.

- Peptone feeding is not limiting or inhibitory. Again evidence to this effect was shown in Sec. 3.5. However if the model was used outside the peptone feedrates used in this thesis this assumption would have to be checked.
- Acetate is not consumed by the cells. This is a valid assumption for the induced runs that are modelled in this thesis since they did not show acetate consumption. However in some of the growth experiments (e.g. Expt.2 in Fig.3.2c, Sec. 3.4.1) there was evidence that the host/vector used in this project can consume acetate. The literature also indicates that some recombinant *E. coli* strains can consume acetate (Luli and Strohl, 1990). Therefore to obtain a more general mathematical model a term should be included for acetate consumption as well as production.
- Another assumption in the model that is easy to forget is that biomass is defined as the dry cell weight (g/L) minus the B.S.T. concentration (g/L). If the inclusion body only contains B.S.T. then this definition is true. However if the inclusion body also contains cell material (e.g. cell proteins, ribosomes etc.,) then really the cell biomass can be thought of in terms of two compartments: the "inactive" biomass which is trapped in the inclusion body (and which presumably can not participate in cell growth) and a normal "active" biomass part. How this affects the proposed B.S.T. model is not clear (it might just mean that some of the parameters change). In this project the composition of the inclusion bodies was not measured. Typically it may be anything from 50 - 100% (Kane and Hartley, 1988; Rinas *et al.*, 1993).
- The fermenter can be described in terms of an "average" cell (i.e. the assumption implicit in choosing an unsegregated model (Sec. 1.5.3)). This is valid if the number of cells is large (Roels and Kossen, 1978) which it is in this project.
- The cellular composition of the cell is assumed constant (i.e. the assumption implicit in choosing an unstructured model). This is unlikely to be valid when there is a sudden shift in conditions such as at induction.

4.4 Parameter estimation

In this section the model parameters are estimated. Whenever possible this was done by obtaining their values directly from experiment. If this could not be achieved values were obtained either from the literature or from a model fitting procedure. The model fitting consisted of trying different values of the parameters to obtain the best fit between the model predictions and the experimental results. Expt. 8 was chosen for this exercise since it was the most reliable data set (i.e. Expt. 9 was a repeat of Expt. 8 and gave the same results).

However it will become clear in the following sections that some of the parameters in the model are difficult to obtain from the fed-batch fermentations performed in this project. This was compounded by the fact that there were only a few fermentations which were available to use for parameter estimation since many of the earlier experiments were limited by phosphate.

Ideally many of the parameters could have been obtained more accurately from continuous culture experiments. For example the effect of acetate inhibition on production could not be determined directly from a plot of acetate concentration against the specific production rate of B.S.T because other factors such as low glucose concentration were also having an effect on the specific production rate. Furthermore in a fed-batch experiment the fermenter conditions (e.g. acetate concentration) are constantly changing. By contrast the acetate inhibition effect could have been obtained directly in a continuous culture experiment by injecting known concentrations of acetate during steady state conditions. Also continuous culture experiments would have allowed accurate determinations of parameters such as the maintenance coefficient (e.g. Fieschko and Ritch, 1986).

Nevertheless estimates for the model parameters were obtained from the fed-batch data presented here and the comparison between the model predictions and experimental results shown at the end of this chapter suggest they are sufficiently accurate to make the model a useful tool for investigating the fermentation process.

Finally the layout of the sections on parameter estimation are in the same order as shown for the model equations at the start of this chapter - i.e. biomass production parameters (eqn 4.1a) followed by B.S.T. production parameters (Eqn. 4.1b) etc.

4.4.1 Biomass production

4.4.1.1 Maximum specific growth rate at 30°C.

The observed specific growth rate was calculated from the growth experiment using medium A without peptone feeding (Expt. 1, Sec. 3.4.1). The methods used to calculate the specific growth rate are explained in detail in Appendix C. They are based on the following equation:

$$d \ln(XV) = \left[\mu - \frac{Q_{smp}}{V} \right] dt = \mu_{obs} dt \quad (4.6)$$

Fig. 4.1 shows how the observed specific growth rate was calculated from a logarithmic plot of total carbon dioxide produced *vs.* time. Curves A and B show the total carbon dioxide produced summed from the inoculation time and zero hours respectively (as explained in Sec. 2.4.4 all runs were standardised so that the time at which the exit gas %CO₂ reached 1.8% was called 5.75 hours and using this convention inoculation took place at about -13 hours). Both curves show that at low values of total carbon dioxide produced the slopes are suspect - however once the absolute value of the carbon dioxide is large enough (e.g. after six hours) the two curves converge and give the same slope. The slope was therefore taken between 6 and 8 hours and this gave an observed specific growth rate of 0.539 1/h.

Fig. 4.2 shows a logarithmic plot of total biomass in the fermenter *vs.* time for the same fermentation. The early values of total biomass are suspect because of the large errors in measuring low biomass concentrations (see Appendix B). Therefore the slope was again taken between 6 and 8 hours and this gave an observed specific growth rate of 0.529 1/h.

For reasons explained in Appendix C the two methods will not give exactly the same result and the total carbon dioxide plot gives the most accurate value of observed specific growth rate. This value (0.539 1/h) can be corrected by adding the sampling term (Eqn. 4.6), which is equal to the sample rate of 0.068 L/min during the period 6-8 hours (Sec. 2.4.4) divided by the estimated broth volume of 3.1 L (Fig. D3.2b). Thus:

$$\text{Specific growth rate} = 0.539 + (0.068 / 3.1) = 0.561 \text{ 1/h.}$$

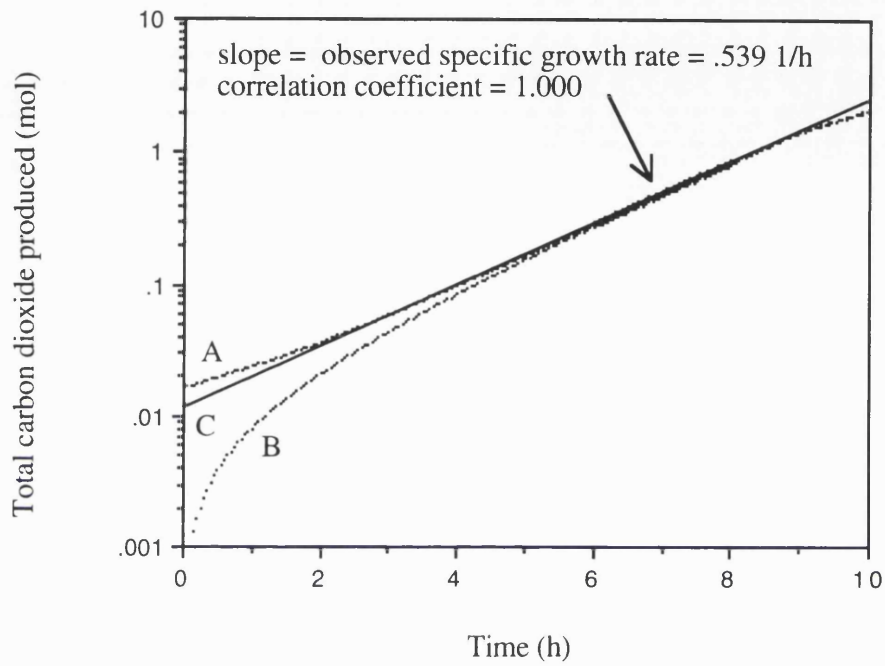


Figure 4.1: Observed specific growth rate calculated from a logarithmic plot of total carbon dioxide produced against time for Expt. 1. Curves A and B show the total carbon dioxide produced summed from the inoculation time and zero hours respectively. Curve C shows the least squares fit to curve A between 6 and 8 hours.

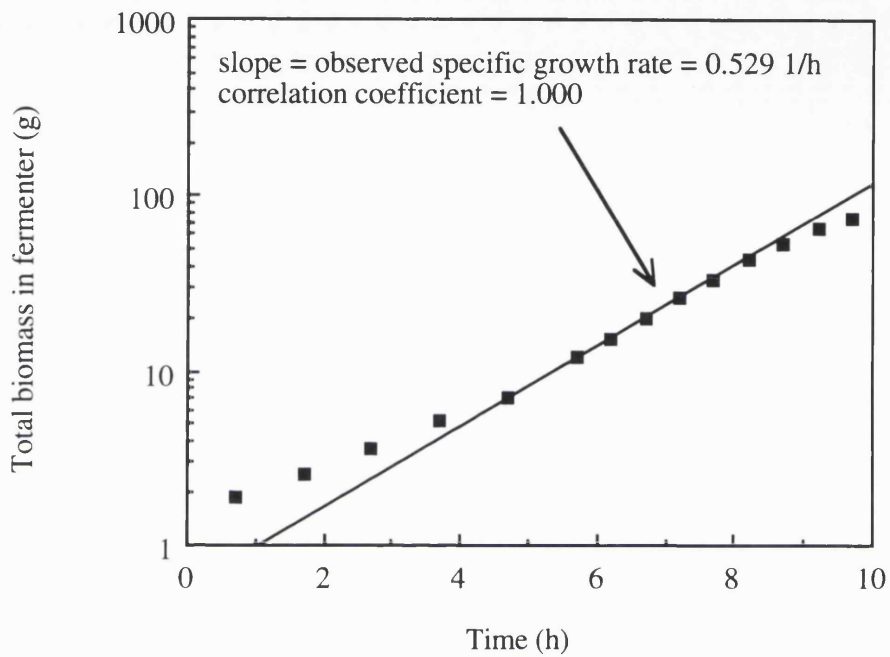


Figure 4.2: Observed specific growth rate calculated from a logarithmic plot of total biomass in fermenter against time for Expt 1. The observed specific growth rate was calculated from the least squares fit to the points between 6 and 8 hours. Note: the "total biomass in the fermenter" was calculated by multiplying the biomass by the estimated volume. It is not the same as the "total biomass produced" which includes the sampled biomass.

4.4.1.2 Effect of temperature on specific growth rate.

The above calculation gives the maximum specific growth rate at 30°C. In the model we need to know the maximum specific growth rate as a function of temperature. This could not be determined by experiment since at temperatures above 37°C B.S.T. production occurs which affects growth. One way this problem could be circumvented is to use an identical host/vector without the temperature inducible promoter. However this was not available for this project so instead the following correlation was used (Esener *et al.*, 1983):

$$\mu_{\max} = \frac{B \exp\left[-\frac{10392}{T + 273.15}\right]}{1 + 1.38 \times 10^{48} \exp\left[-\frac{34614}{T + 273.15}\right]} \quad (4.7)$$

The value of B was chosen so that this formula would give the correct specific growth rate at 30°C - i.e. 0.561 1/h. This required a value of B = 4.46 x 10¹⁴ 1/h. (The original value of B was 4.71x10¹⁴ 1/h which gave a specific growth rate of 0.593 1/h at 30°C). In other words the shape of the curve of specific growth rate vs. temperature was kept the same but the whole curve was lowered by adjusting B so that it agreed with the specific growth rate measured at 30°C for the particular host/vector used in this thesis.

4.4.1.3 Effect of low glucose concentration on growth

From the experiments performed in this project it was not possible to determine the Michaelis-Menton constant (K_1) directly so a value had to be taken from the literature. The following values have been reported for *E.coli* : 0.002 g/L (Wang *et al.*, 1979), 0.004 g/L (Monod, 1942) and 0.0068 g/L (Shehata and Marr, 1971). The value chosen for this work was 0.004 g/L which is in the mid-range of the values quoted and is the value used most often for modelling (e.g. Lee *et al.*, 1985).

4.4.1.4 Inhibition of growth by acetate.

The effects of acetate concentration on the specific growth rate is defined by the parameter A_i in Eqn. 4.3. This could not be obtained directly from the experiments described in Secs. 3.4 - 3.6 or from the literature (as discussed in Sec. 1.4.2.5). Therefore it was obtained by fitting the model to Expt. 8. (see Sec. 4.4.5). A best fit between model prediction and experimental results was obtained with:

$$A_i = 25.0 \text{ g/L}$$

It was noted in Sec. 1.4.2.5 that acetate concentrations in the range 5-10 g/L are thought to be inhibitory whilst values in the range 10-20 g/L cause growth to stop. Substituting

the value of A_i into the acetate inhibition term in Eqn. 4.3 $\left(1 - \frac{A}{A_i}\right)$ it can be calculated

that an acetate concentration of 5 - 10 g/L would reduce the specific growth rate by 20 - 40% and concentrations in the range 10 - 20 g/L would reduce it by 40 - 80%. The above equation obviously predicts growth would cease when the acetate concentration reached 25 g/L. Thus the value of A_i seems a little high but this may simply reflect that the host/vector used in this project was especially tolerant of high acetate concentrations since strain to strain variations in tolerance have been noted (Luli and Strohl, 1990).

4.4.1.5 Inhibition of growth by B.S.T. production

The reduction of growth due to B.S.T. production is defined by the parameter $r_{p,1}$ which also had to be determined from a best fit of the model predictions to Expt. 8. The value obtained was:

$$r_{p,1} = 0.22 \text{ g B.S.T/g biomass/h}$$

In the next section this value is compared with the maximum specific B.S.T. production rate to see if it is reasonable.

4.4.2 B.S.T. production

4.4.2.1 Maximum specific B.S.T. production rate

The kinetic equation for B.S.T. production in the model (Eqn. 4.4) assumes that the specific rate of B.S.T. production should be a constant at a given temperature if the cells are not starved of glucose or inhibited by acetate. Fig. 4.3a shows a plot of the specific B.S.T. production rates against time for one of the medium cell density runs (Expt. 7) and two of the high cell density runs (Expts. 8 and 9). These fermentations were discussed in detail in Secs. 3.6.1 and 3.7.

The specific B.S.T. production rate was calculated by taking the difference between the "total B.S.T. produced" at successive sample points and dividing by the time between samples and the average biomass in the tank. The first value calculated for each run after production starts is suspect since the precise time production begins is not known.

At first sight it appears from Fig 4.3_a that there is a maximum specific rate of B.S.T. production that is the same in all runs at about 0.11 g B.S.T./g biomass/h. However the situation is much more complicated than this. Firstly it has to be remembered that the temperature is increased from 38 to 39.5°C just over one hour after production starts. Secondly acetate (Fig. 4.3b) is produced at a high rate at the same time production starts (due to peptone feeding starting at this time). Finally the glucose is limiting in all these runs approximately two hours after production starts and this too will affect the specific production rate.

An attempt to separate these effects, and hence obtain a true maximum specific production rate, is made in the next section.

Finally the actual maximum specific B.S.T. production rate obtained during this project was 0.11 g B.S.T./g biomass/h which is half the value for $r_{p,1}$ (the term which defines the negative effect that recombinant production has on growth) in the previous section. Thus Eqn. 4.3 predicts a drop in the growth rate of 50% when the specific production rate is at the maximum value obtained in the fermentations studied in this project.

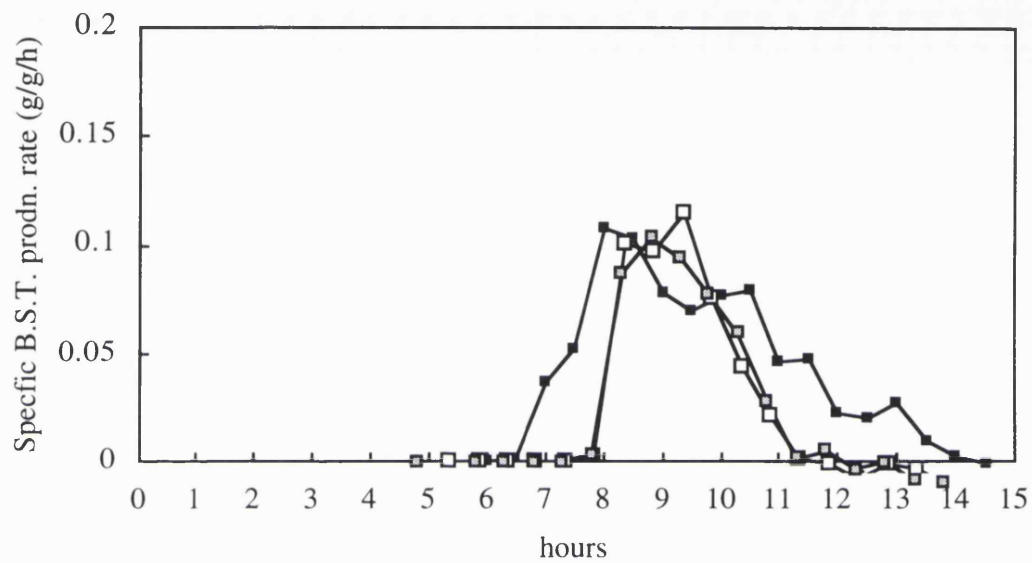


Figure 4.3a: A comparison of specific production rate of B.S.T. for one medium and two high cell density fermentations

- Expt. 7. (medium cell density)
- Expt. 8 (high cell density)
- ⊠ Expt. 9 (high cell density).

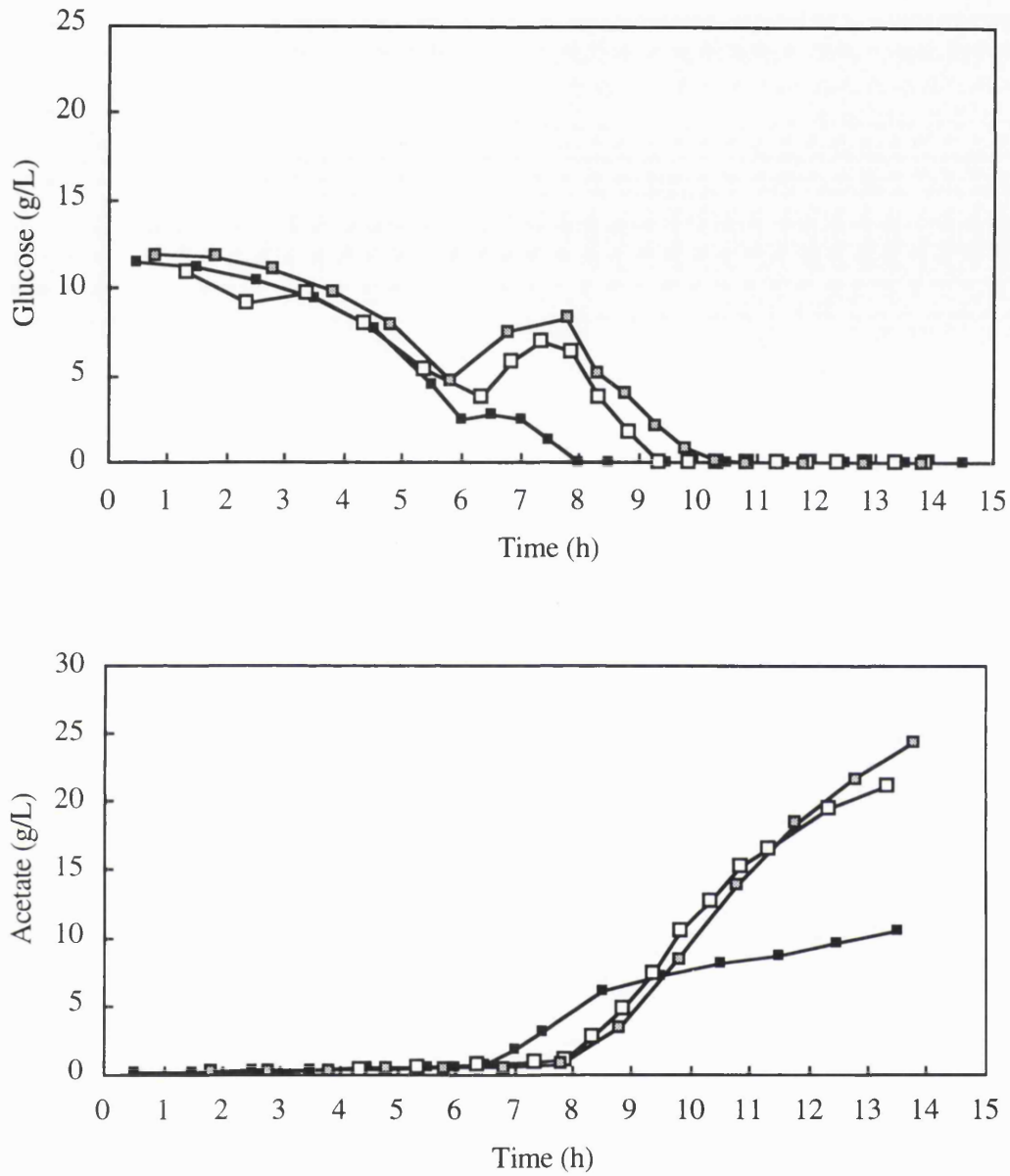


Figure 4.3b: A comparison of glucose and acetate concentrations for one medium and two high cell density fermentations

- Expt. 7. (medium cell density)
- Expt. 8 (high cell density)
- ▣ Expt. 9 (high cell density).

4.4.2.2 Inhibition of B.S.T. production by acetate

Fig. 4.4 shows a plot of specific B.S.T. production against acetate concentration for the two high cell density runs discussed in the previous section (i.e. Expts. 8 and 9). These were chosen because they had high glucose feedrates as evidenced by the fact that they produced acetate at a maximum rate for most of the production period (see Sec. 3.6.1) - therefore the effect of low glucose concentration on the specific production rate of BST would be less in these runs than for fermentations with lower glucose feedrates. To eliminate the complication of the temperature effect on production only points at 39.5°C were considered.

The correlation obtained from Fig. 4.4 gives:

$$r_p = 0.197 - 0.013A$$

which expressed in the same form as Eqn. 4.3 becomes:

$$r_p = 0.197 \left(1 - \frac{A}{15.2} \right) \quad (4.8)$$

i.e. $r_{p,\max} = 0.197$ g B.S.T./g biomass/h at 39.5°C and $A_2 = 15.2$ g acetate/L

However even though these runs had a high glucose feedrate they were still glucose limited during production and therefore the above values are only approximations. The effect of glucose limitation will be to lower the actual specific production rates shown in Fig.4.4 and hence the value of $r_{p,\max}$. To determine the true values a best fit was done (starting with the above values) between model predictions and Expt. 8 (Sec. 4.4.6). The best fit was obtained when:

$$\begin{aligned} r_{p,\max} &= 0.25 \text{ g B.S.T./g biomass/h at } 39.5^\circ\text{C} \\ A_2 &= 14.5 \text{ g acetate/L} \end{aligned}$$

These were the values used in the final model. It should be noted that $A_2 = 14.5$ g/L is less than $A_1 = 25.0$ g/L (the term for growth inhibition) and hence the model predicts a greater effect of acetate on production than growth. This agrees with the observations of Jensen and Carlsen (1990) as discussed in Sec. 3.3.6.

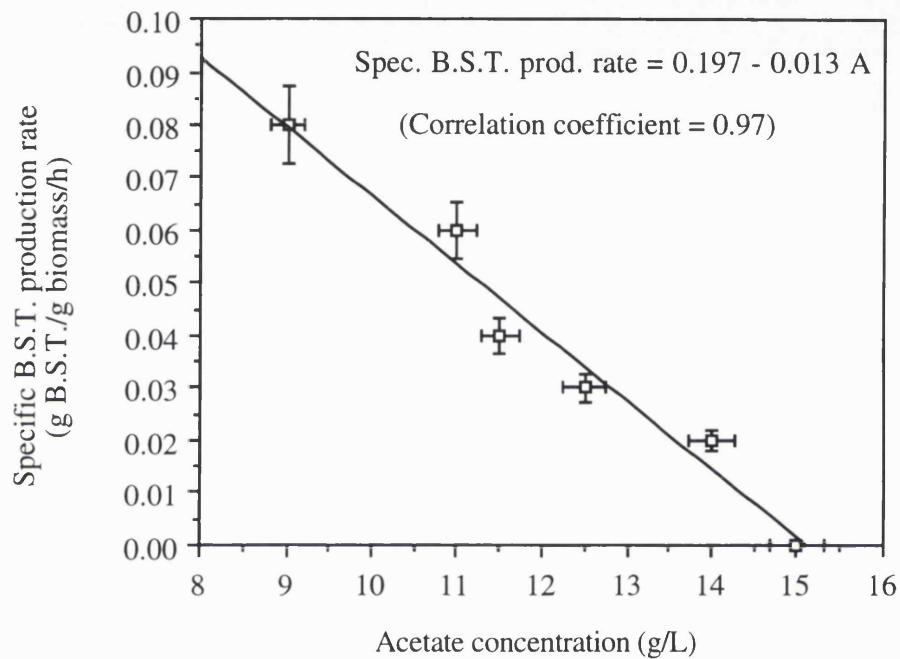


Figure 4.4: Effect of acetate concentration on specific B.S.T. production rate.

Data shown is from two high cell density fermentations (Expts. 8 and 9) at 39.5°C.. The correlation is a least squares fit to the data for both runs. The vertical error bars indicate the +/- 9% error that was calculated for the specific production rate, and the horizontal ones the +/- 2% error in the acetate assay.

4.4.2.3 Effect of temperature on B.S.T. production

In the previous section a value for the maximum specific rate of B.S.T. formation was obtained at 39.5°C. The only other temperature that was used for production in this project was 38°C. In Fig. 4.3a it can be seen that for the two high cell density runs (Expts. 8 and 9) at 8.5h (when the temperature was 38°C) the actual measured specific B.S.T. production rate was about 0.10 g B.S.T./g biomass/h. To obtain the maximum specific B.S.T. production rate from this allowance has to be made for the effect of low glucose concentration and acetate inhibition according to Eqn. 4.4:

$$r_p = r_{p,\max} \left(\frac{S}{S + K_2} \right) \left(1 - \frac{A}{A_2} \right) \quad (4.4)$$

From Fig. 4.3b in Sec. 4.4.2.1 it can be seen that the glucose and acetate concentrations at 8.5h for these high cell density runs were respectively about 4.0 and 3.0 g/L. Thus glucose was not limiting and the Monod term in Eqn. 4.4 can be eliminated. Substituting the observed specific B.S.T. production rate and the corresponding acetate concentration gives:

$$0.10 = [r_{p,\max}]_{38C} \left(1 - \frac{3.0}{14.5} \right)$$

hence:

$$[r_{p,\max}]_{38C} = 0.125 \text{ g B.S.T./g biomass/L}$$

Thus two values have been obtained for the specific production rate of B.S.T. - one at 38°C and one at 39.5°C. These are plotted in Fig. 4.5. If a linear relationship between specific production rate and temperature is assumed (as discussed in Sec. 1.4.5.2) then the straight line through these two points gives:

$$r_{p,\max} = 0.083(te - 36.5) \quad (4.9)$$

where te is the temperature in degrees Celsius. This equation was used in the model to describe the effect of temperature on the maximum specific B.S.T. production rate.

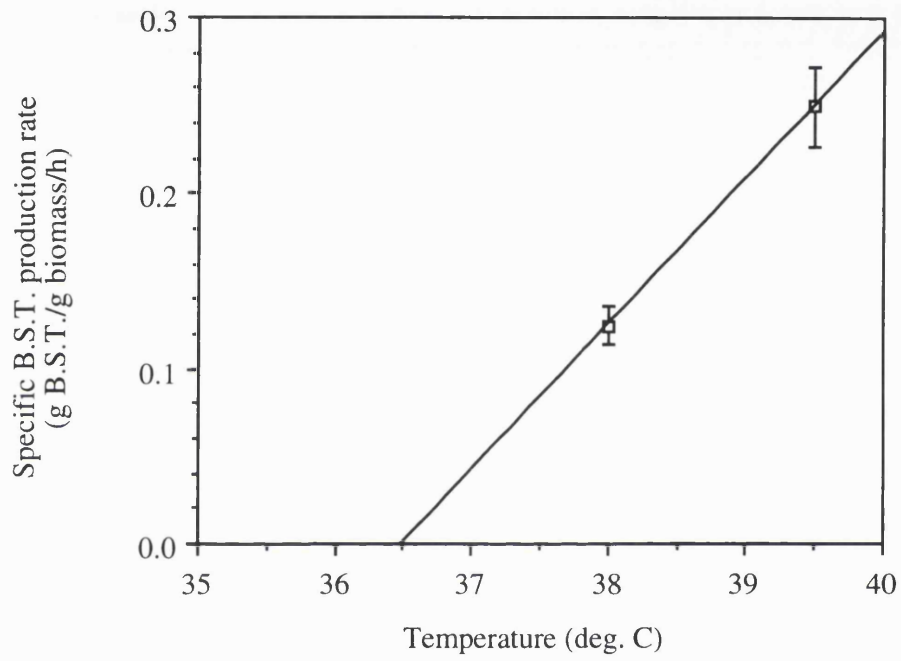


Figure 4.5: Effect of temperature on specific B.S.T. production rate for Expt.8.

4.4.2.4 Effect of low glucose concentration on B.S.T. production

It was shown in Expt 11 and 12 (Sec. 3.6.3) that if glucose feeding was reduced sufficiently when it was already limiting then B.S.T. production was decreased (i.e. "glucose starvation" was occurring). This was discussed in Sec.1.4.3.3 where the Monod expression in Eqn. 4.4 was proposed to describe this effect:

$$r_p = r_{p,\max} \left(\frac{S}{S + K_2} \right)$$

The value of K_2 could not be determined directly from the fed-batch fermentations and was therefore estimated by fitting the model predictions to the results of Expt. 8. The best fit was obtained with:

$$K_2 = 0.001 \text{ g glucose/L}$$

This value is consistent with the continuous culture results of Jensen and Carlsen (1990) and implies that the effect of low glucose concentration is more pronounced on growth than it is on recombinant protein production (Sec. 1.4.3.3).

4.4.3 Acetate production

Eqn. 4.5 of the model describes the production of acetate:

$$r_A = \text{Max}[r_{A,\max}, k(\mu - \mu_{crit})] \quad (4.5)$$

There are three parameters which need to be estimated: the maximum specific acetate production rate ($r_{A,\max}$), the critical specific growth rate (μ_{crit}) below which acetate is not excreted and the constant k .

4.4.3.1 Maximum specific acetate production rate

It was suspected from the literature (e.g. Meyer *et al.*, 1984), and discussed in Sec. 1.4.3.4, that the maximum specific production rate of acetate would be affected by the addition of peptone. This was confirmed in the growth-only fermentations (Sec.3.4.2) which showed that the specific acetate production rate increased roughly ten-fold when peptone was fed to the fermenter.

Fig. 4.6 shows the specific acetate production rate for Expt 7 (medium cell density) and Expts. 8 and 9 (high cell density). It can be seen that prior to peptone feeding (started at 6.5h in Expt. 8 and 7.9h in Expts. 8 and 9) the maximum specific acetate production rate was about 0.03 g acetate/g biomass/h for all runs and after feeding peptone the rate jumped to 0.33 g acetate/g biomass/h. Thus the following equation was incorporated into the model:

$$r_{A,\max} = \begin{cases} 0.03 & t < t_{\text{startpf}} \\ 0.33 & t \geq t_{\text{startpf}} \end{cases} \quad (4.10)$$

where t_{startpf} is the start time for peptone feeding which has to be input to the model.

4.4.3.2 Effect of growth rate on acetate production

The final parameters in Eqn. 4.5 were determined by a fitting the model predictions to the results of Expt. 8. (Sec. 4.4.6). The best fit was obtained when:

$$\begin{aligned} \mu_{\text{crit}} &= 0.045 \text{ 1/h} \\ k &= 3.0 \text{ g acetate/g biomass} \end{aligned}$$

Values in the literature for these parameters (Sec. 1.4.3.4) range from 0.65 to 1.6 g acetate/g biomass for k and from 0.145 to 0.51 1/h for μ_{crit} which suggests that the host/vector used in this project produces more acetate than normal.

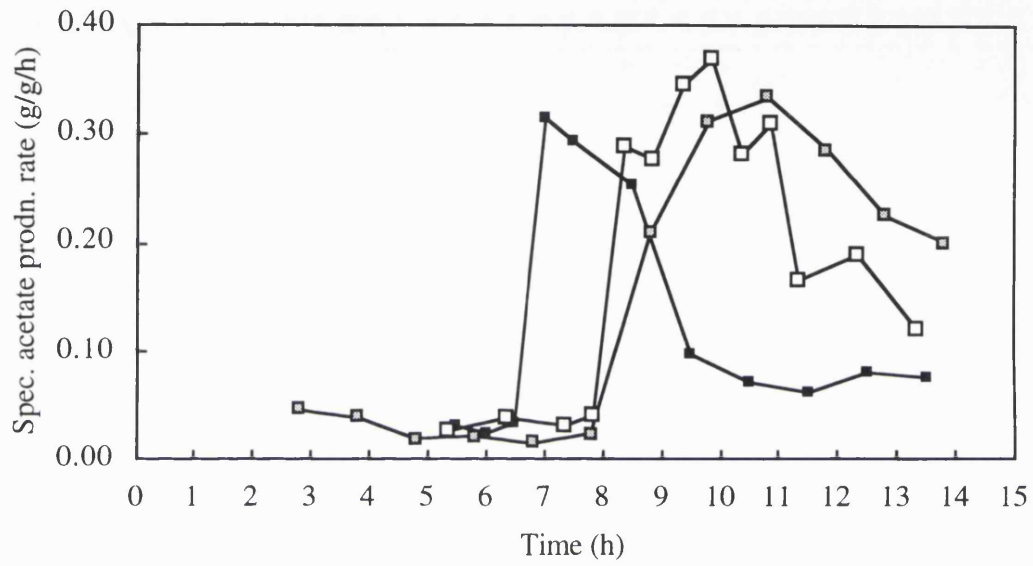


Figure 4.6: A comparison of specific acetate production rate for one medium and two high cell density fermentations

- Expt. 7. (medium cell density)
- Expt. 8 (high cell density)
- ▣ Expt. 9 (high cell density).

4.4.4 Glucose Consumption

Thus far estimates have been obtained for the parameters used in the kinetic equations (4.3 - 4.5). The only remaining parameters left to determine are for the glucose consumption equation (Eqn. 4.1d):

$$\frac{dS}{dt} = \frac{Q_{gluc}c_{gluc}}{V} - \frac{\mu X}{Y_{SX}} - \frac{r_P X}{Y_{SP}} - \frac{r_A X}{Y_{SA}} - mX - \frac{S}{V}Q \quad (4.1d)$$

There are four parameters: the yield coefficients (Y_{SX} , Y_{SP} , and Y_{SA}) and the maintenance coefficient (m).

4.4.4.1 Maintenance coefficient

The following expression from Esener *et al.*, (1983) was used to define the maintenance coefficient as a function of temperature:

$$m_T = C \exp\left(-\frac{\Delta H}{RT}\right) \quad (4.11)$$

where $\Delta H = 83700$ J/mol as discussed in Sec. 1.4.5.3 (and the gas constant $R = 8.314$ J/mol/K).

Cutayar and Poillon (1989) found $m = 0.04$ g glucose/g biomass/h at a temperature of 37°C which using Eqn. 4.11 gives $m = 0.02$ g glucose/g biomass/h at 30°C. Other values measured directly at 30°C were 0.04 g glucose/g biomass/h (Heijnen and Roels, 1981) and 0.046 g glucose/g biomass/h (Marr *et al.*, 1962). A mid-range value of 0.03 g glucose/g biomass/h was taken which allows the constant C to be calculated:

$$C = 7.93 \times 10^{12} \text{ g glucose/g biomass/h}$$

Using this value and substituting for C and R in Eqn. 4.11 gives:

$$m_T = 7.93 \times 10^{12} \exp\left(-\frac{10067}{T}\right) \quad (4.12)$$

As stated this equation gives a maintenance coefficient of 0.03 g glucose/g biomass/h at 30°C which agrees with the literature values. At 39.5°C (i.e. during B.S.T. production) Eqn. 4.12 gives $m = 0.0083$ g glucose/g biomass/h. This value is not unreasonably high since, for example, Cutayar and Poillon (1989) found that in a recombinant *E. coli* fermentation which reached 110 g DCW/L the final maintenance values were in the range 0.2 to 0.25 g glucose/g biomass/h.

4.4.4.2 Yield of biomass on glucose

In order to calculate the yield coefficient Y_{SX} one of the growth-only fermentations without peptone feeding was used. The advantage of using a growth-only fermentation is that the production term $\frac{r_P X}{Y_{SP}}$ in Eqn. 4.1d can be neglected. Also since growth was at 30°C the maintenance term mX will be quite small. Finally using a run that did not have peptone feeding means that the acetate term $\frac{r_A X}{Y_{SA}}$ will also be small.

Fig. 4.7 shows a plot of total biomass produced against the total glucose consumed. The latter included a subtraction, as per Eqn 4.1d, for glucose consumed for maintenance and acetate production. A value of $m = 0.03$ was used for the maintenance term and a yield coefficient of 1.0 g acetate/g glucose was assumed for acetate. This gave $Y_{SX} = 0.517$ g biomass/g glucose. This value was then used in a model fitting procedure (see below) to get a better estimate of $Y_{SA} = 1.5$ g acetate/g glucose and using this value a new value of $Y_{SX} = 0.515$ g biomass/g glucose was obtained. Clearly the precise value of Y_{SA} does not have a big effect on Y_{SX} since as noted above only a small amount of acetate was produced in Expt. 1. Similar values of Y_{SX} have been found for other recombinant *E. coli* host/vectors - e.g. Riesenber *et al.*, 1991 (0.52 g biomass/g glucose) and Yang *et al.*, 1992 (0.55 g biomass/g glucose).

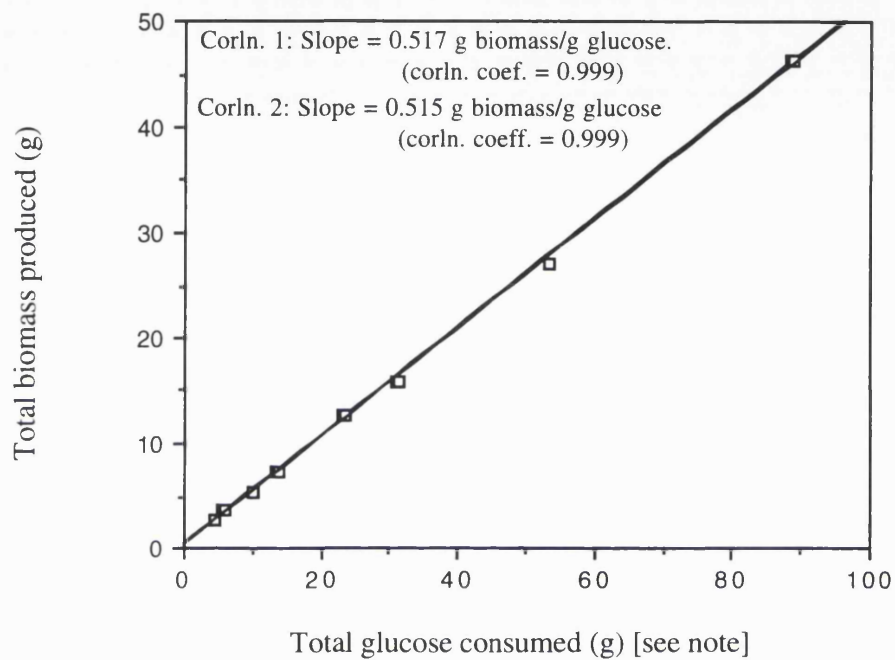


Figure 4.7: Calculation of yield coefficient for biomass (Y_{SX}).

Two correlations were obtained depending on the value of the yield coefficient for acetate (Y_{SA}):

- $Y_{SA} = 1.0$ g acetate/g glucose
- $Y_{SA} = 1.5$ g acetate/g glucose

Note: The total glucose consumed was calculated from Eqn.4.1d - i.e. an allowance was made for glucose being used for maintenance and acetate production.

4.4.4.3 Yield of acetate and B.S.T. on glucose

The values of Y_{SA} and Y_{SP} were obtained by fitting the model to Expt. 8. A best fit was obtained with the following values: $Y_{SA} = 0.70$ g glucose/g acetate and $Y_{SP} = 1.50$ g glucose/g B.S.T.

4.4.5 Volume balance equation

The final equation that needs to be considered before using the model is the volume balance equation (Eqn. 4.1e):

$$\frac{dV}{dt} = Q_{gluc} + Q_{pept} + Q_{amm} - Q_{samp} - Q_{evap}$$

The values of the glucose feedrate, peptone feedrate and sampling rate are all model inputs specified by the user. However the evaporation rate and the ammonium hydroxide feedrate have to be calculated by the model.

Evaporation Rate

This value was determined experimentally by taking the difference between the initial broth volume plus feeds (measured with load cells) and the final broth volume and dividing by the total fermentation time. (All volumes were measured when the broth was unagitated and degassed). An average value over six fermentations was $Q_{evap} = 0.005 \pm 0.002$ L/h was obtained which was used in the model. Calculated in this way the "evaporation rate" also takes account of the change in volume due to RQ variation.

The model assumed that Q_{evap} was constant which was justified given that it is small compared with the glucose and peptone feedrates (typically 0.1 L/h). However to make the model more general the term could be made a function of temperature and airflow.

Ammonium hydroxide feedrate

Finally in order to calculate the broth volume the model has to be able to predict the ammonium hydroxide feedrate which is added to the fermenter to keep the pH constant. The amount of ammonium hydroxide fed depends on the amount of biomass and acetate produced (see Fig. 4.8).

For the growth-only fermentation and for the high cell density prior to peptone feeding there is the same correlation between total biomass produced and total ammonium hydroxide fed to the fermenter. However after peptone addition in the high cell density run there is much more acetate production and hence more ammonium hydroxide fed per amount of biomass produced.

The total ammonium hydroxide fed can therefore be expressed by:

$$\text{tot. amm. hydrox. fed} = a (\text{tot. acetate produced}) + b (\text{tot biomass produced})$$

where a and b are constants. These were determined by minimising the function (f):

$$f = \text{tot. amm. hydrox. fed} - a (\text{tot. acetate produced}) - b (\text{tot biomass produced}) = 0$$

This gave the following values:

$$\begin{aligned} \text{and} \quad a &= 1.55 \text{ g 8M ammonium hydroxide/g acetate} \\ b &= 1.88 \text{ g 8M ammonium hydroxide/g biomass} \end{aligned}$$

In practice the prediction of ammonium hydroxide feedrate was incorporated into the model by using the specific rates of biomass and acetate production (μ and r_A) and multiplying this by the total biomass produced (XV) and a term (n) to convert from g to L of 8M ammonium hydroxide. The final equation used in the model was as follows:

$$Q_{amm} = (1.88\mu + 1.55r_A)XVn$$

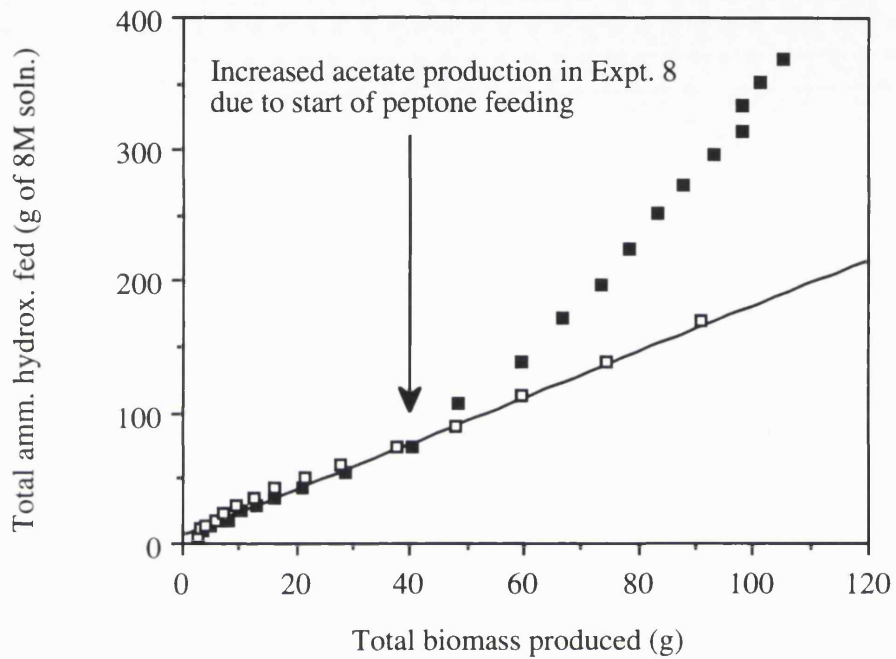


Figure 4.8: Correlation between total biomass produced and total ammonium hydroxide fed in Expt. 2 (growth-only with no peptone feed) and Expt. 8 (high cell density with peptone feeding).

- Expt. 2 (growth-only fermentation)
- Expt. 8 (high cell density fermentation)

4.4.6 Fitting the model to a high cell density fermentation

As explained in the above sections many of the parameters had to be obtained by determining what values gave the best fit between model predictions and experimental results. This model fitting was done using Expt. 8 since this had the most reliable data in that Expt. 9 was virtually a repeat of Expt. 8 (the only difference being an extra medium feed) and had given the same results (Sec. 3.6.1). The actual procedure used was a trial and error method: varying each parameter in turn until a good fit was obtained between the model predictions and the experimental results as shown in Fig. 4.9. This plot shows that the final fit between the model "predictions" and experimental results was good. Fig. 4.10 also shows that the model accurately predicts the ammonium hydroxide feedrate profile.

However it has to be remembered that the real test of the model is whether it can accurately predict the results for fermentations other than the ones for which the parameters were estimated. This will be discussed in the remainder of this chapter after first giving a summary of parameter estimation and a sensitivity analysis.

4.4.7 Summary of parameter estimation and sensitivity analysis

Table 4.1 shows a summary of all the model parameters and Table 4.2 shows the sensitivity of the model prediction of final B.S.T. titre (in Expt. 11) to errors in these parameters. The most sensitive term (A_2) defines the effect of acetate on the specific B.S.T. production rate. Other sensitive parameters are the yield coefficient (Y_{SX}) and those parameters which define the effect of temperature on the specific B.S.T. production rate ($r_{p,2}$) and the specific biomass production rate (B).

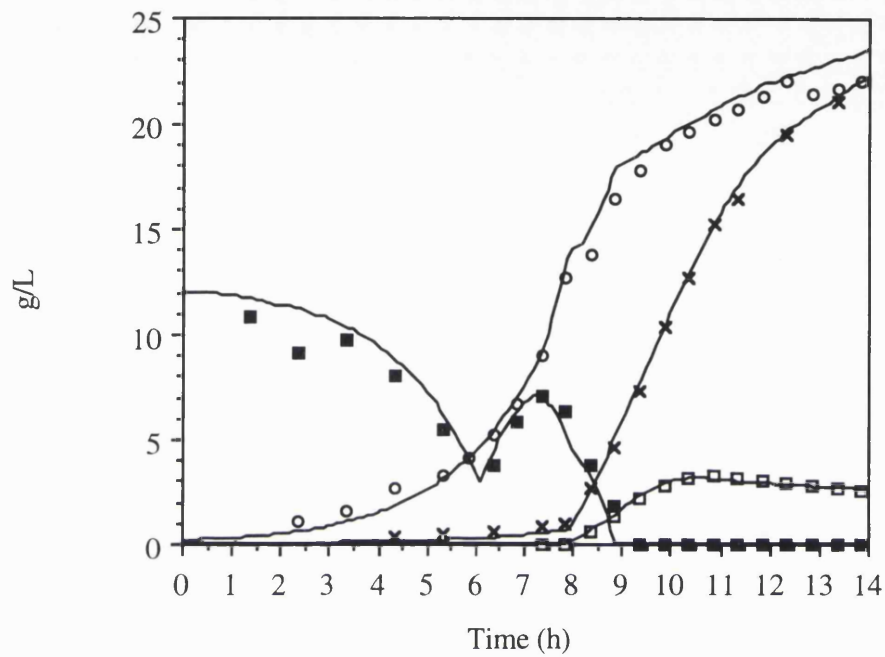


Figure 4.9: Comparison between model "predictions" and Expt. 8.(high glucose feedrate)
(Note: this run was used for model fitting).

The solid lines indicate the model predictions and the following symbols show the experimental results:

- Glucose
- B.S.T.
- × Acetate
- Biomass

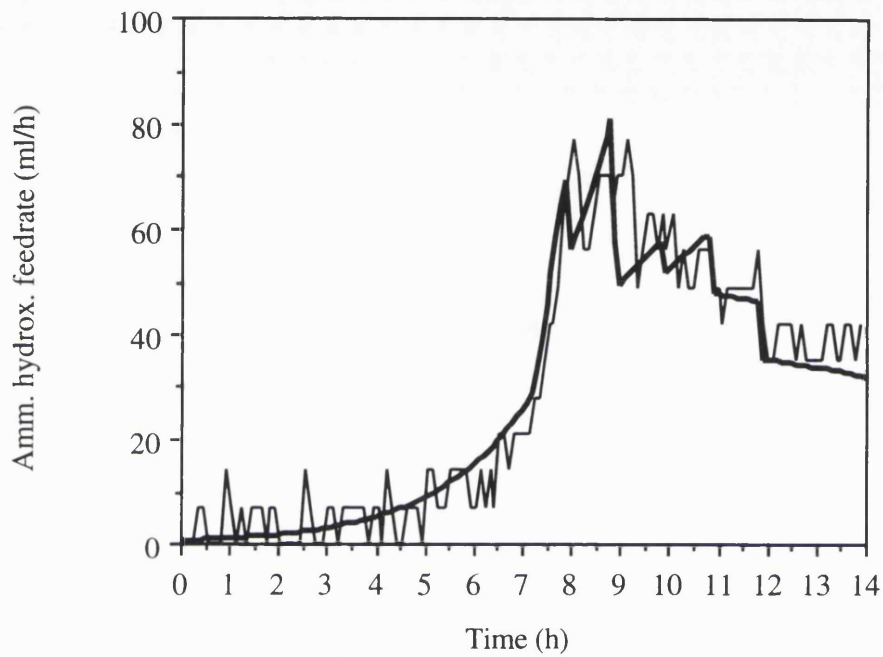


Figure 4.10: Comparison between model "predictions" and Expt. 8.(high glucose feedrate).

Ammonium hydroxide feedrate.

(Note: this run was used for model fitting).

The heavy lines indicate the model predictions and the lighter lines indicate the actual experimental rate determined from load cell readings.

Table 4.1
Summary of parameter estimation

Sec.	Parameter	Value	Obtained from
4.4.1.2	B	4.46×10^{14} 1/h	Expt. 1. a
4.4.1.3	K_1	0.004 g glucose/L	(Monod, 1942)
4.4.1.4	A_1	25.0 g acetate/L	Expt. 8.
4.4.1.5	$r_{p,1}$	0.22 g B.S.T./L	Expt. 8.
4.4.2.2	A_2	14.2 g acetate/L	Expt. 8
4.4.2.3	$r_{p,2}$	0.083 g B.S.T./g biomass/L	Expt. 8 b
4.4.2.4	K_2	0.001 g glucose/L	Expt. 8
4.4.3.1	$r_{A,max}$	0.03 or 0.33 g acetate/g bio/h	Expt. 8
4.4.3.2	k	3.0 g acetate/g biomass	Expt. 8
4.4.3.2	μ_{crit}	0.045 1/h	Expt. 8
4.4.4.1	C	7.93×10^{12} g glucose/g bio/h	(Esener <i>et al.</i> , 1983) c
4.4.4.2	Y_{SX}	0.52 g biomass/g glucose	Expt. 1
4.4.4.3	Y_{SA}	1.50 g acetate/g glucose	Expt. 8
4.4.4.3	Y_{SP}	0.70 g B.S.T./g glucose	Expt. 8

Notes:

- a. B was determined so that the specific growth rate at 30°C = 0.561 1/h.
- b. Max. spec. B.S.T. production rate is a function of temperature as explained in Sec. 4.4.2.3.
- c. C was determined so that the maintenance coefficient at 30°C = 0.03 g glucose/g biomass/h.

Table 4.2

Summary of sensitivity analysis:

Effect on predicted final B.S.T. titre (for Expt. 11) of plus and minus 10% changes to each model parameter.

Parameter	Value	Percentage change to predicted B.S.T. titre at 14h due to change in parameter of	
		-10%	+10%
B	4.46×10^{14} 1/h	-3.6%	-23.7%
K_1	0.004 g glucose/L	-5.3%	+5.0%
A_1	25.0 g acetate/L	+1.8%	-3.9%
$r_{P,1}$	0.22 g B.S.T./L	-8.8%	-4.3%
A_2	14.2 g acetate/L	-27.5%	+23.7%
$r_{P,2}$	0.083 g B.S.T./g biomass/L	-16.3%	+4.8%
K_2	0.001 g glucose/L	+5.7%	-5.0%
$r_{A,max}$	0.03 or 0.33 g acetate/g bio/h	+11.9%	-13.7%
k	3.0 g acetate/g biomass	+8.1%	-7.2%
μ_{crit}	0.045 1/h	-7.9%	+8.6%
C	7.93×10^{12} g glucose/g bio/h	-4.3%	+3.3%
Y_{SX}	0.52 g biomass/g glucose	-3.6%	-16.6%
Y_{SA}	1.50 g acetate/g glucose	+3.1%	-5.1%
Y_{SP}	0.70 g B.S.T./g glucose	+2.8%	-3.6%

4.5 How to run the model

In order to run the model the following information has to be supplied by the user:

- The initial degassed and unagitated broth volume (L) and the concentrations (g/L) of biomass, acetate and glucose at the start of the fermentation.
- The temperature ($^{\circ}\text{C}$) profile throughout the fermentation.
- The feedrate profile of glucose (g glucose/h) and the concentration of glucose feed used (g glucose/L feed solution)
- The feed profiles (L/h) for peptone and any additional medium feeds.
- The sampling rate (L/h) throughout the fermentation.
- The time (h) at which the fermentation ends.

The model outputs the volume and concentration of biomass, acetate, glucose and B.S.T. throughout the fermentation. Any combination of these variables can also be plotted (e.g. total g of product = B.S.T. concentration x volume). Alternatively values which the model uses in its calculations can also be plotted (e.g. ammonium hydroxide feedrate, specific acetate production rate etc.).

The model equations were coded in a high level language *Mathematica* which makes it easier to understand and change the model. The price paid for this is relatively long computational times (e.g. 15 minutes to simulate a 14h run using a SPARC 4 workstation).

4.6 Comparison of model predictions and experimental results

4.6.1 Effect of glucose feeding on high cell density fermentations

The model was used to predict the effect of glucose feeding on two high cell density fermentations (Expt. 11 and 12) which had lower glucose feedrates than Expt. 8 for which the model was fitted. Fig. 4.11 shows the glucose feed profiles for all three runs. (Note: the temperature profiles were identical in all runs).

Fig. 4.12. shows the model predictions compared with the experimental results for Expt. 11 which had the medium glucose feedrate. It can be seen that the model predictions agree very well with the experimental results and in particular predicts the events which occur at the following times:

- 6.05h Start of glucose feeding causes an increase in glucose concentration
- 7.90h Start of peptone feeding causes an increase in acetate production and (due to a dilution effect) a kink in the biomass curve.
- 9.20h Onset of glucose limitation causes a decrease in growth rate and acetate production.
- 13h B.S.T. production stops due to high inhibitory concentrations of acetate.

Fig. 4.13 shows a comparison between model predictions and experimental results for ammonium hydroxide feedrate. This is quite a severe test of the model since the ammonium hydroxide feedrate is measured accurately every three minutes by means of a load cell and hence allows the model predictions to be checked on a shorter timescale than the assay values (obtained every thirty minutes). Clearly there is again good agreement between model and experiment. In particular the model predicts the characteristic double peak in the ammonium hydroxide feedrate that was common to most of the fermentations performed during this project. It also accurately predicts the drop in feedrate when

glucose becomes limiting and the final feedrate during glucose limitation. A more detailed analysis of the ammonium hydroxide feed profile will be given in Sec. 4.7.2 to show how the model can be used to increase understanding of the process.

Fig. 4.14 shows a comparison between the predicted and calculated broth volumes and again a good agreement is found.

Fig. 4.15 shows a comparison between model predictions and experimental results for Expt. 12 which had a lower glucose feedrate. The model accurately predicts the events occurring at the following times:

- 6.05h Start of glucose feeding causes increase in glucose concentration
- 7.90h Start of peptone feeding causes an increase in acetate production and (due to a dilution of first rapidly fed peptone) a kink in the biomass curve.
- 8.70h Onset of glucose limitation causes a decrease in growth rate and acetate production. (Note this occurs at a different time from Expt.11 due to the decreased glucose feedrate).
- 10.0h Further reduction in glucose feedrate causes acetate production to stop and the acetate concentration to decline (since broth volume is increasing due to glucose and peptone feeding).
- 14h B.S.T. production still continuing due to lower levels of acetate concentration than in Expt. 11.

It should be noted that the biomass prediction is not so good for this fermentation but that the general trend is correct (i.e. final biomass concentration decreases with glucose feeding Expt 8>Expt.11>Expt.12).

Fig. 4.16 shows the ammonium hydroxide feedrate prediction for Expt. 12 and as before it agrees well with the experimental results.

Finally Fig 4.4 shows a comparison between the model predictions of B.S.T. concentration for Expt. 8, 11 and 12 on the same plot. As expected (since this run was used to estimated many of the model parameters) there is good agreement between model

predictions and experimental results for Expt. 8. For the other two fermentations the agreement is reasonable and the model predicts the correct trends for B.S.T. concentration as explained below:

Expt.11: The model predicts the higher final titre that was achieved because of the reduced glucose feedrate which caused a reduction in acetate concentration and hence less inhibition of product formation.

Expt. 12: The model predicts that the B.S.T. production rate between 9 and 10h will be lower in this run due to glucose starvation but that production will continue for longer since acetate concentrations are much less than Expt. 11.

In conclusion the model accurately predicts the effects of glucose feeding on high cell density fermentations. In the next section it will be seen if the model is capable of going one step further and predicting the results of a medium cell density run. This is a more stringent test of the model since in this case the temperature profile as well as the glucose feed profile is varied.

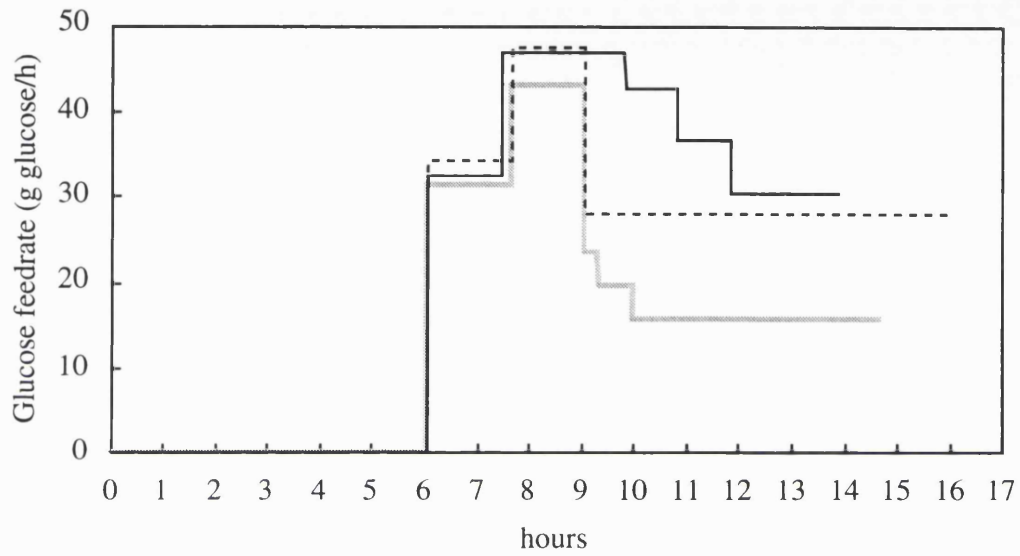


Figure 4.11: Glucose feedrates for the three high cell density fermentations used for modelling. (Note: only Expt. 8 was used for parameter estimation).

- Expt. 8 (high glucose feedrate)
- - - Expt. 11 (medium glucose feedrate)
- Expt. 12 (low glucose feedrate).

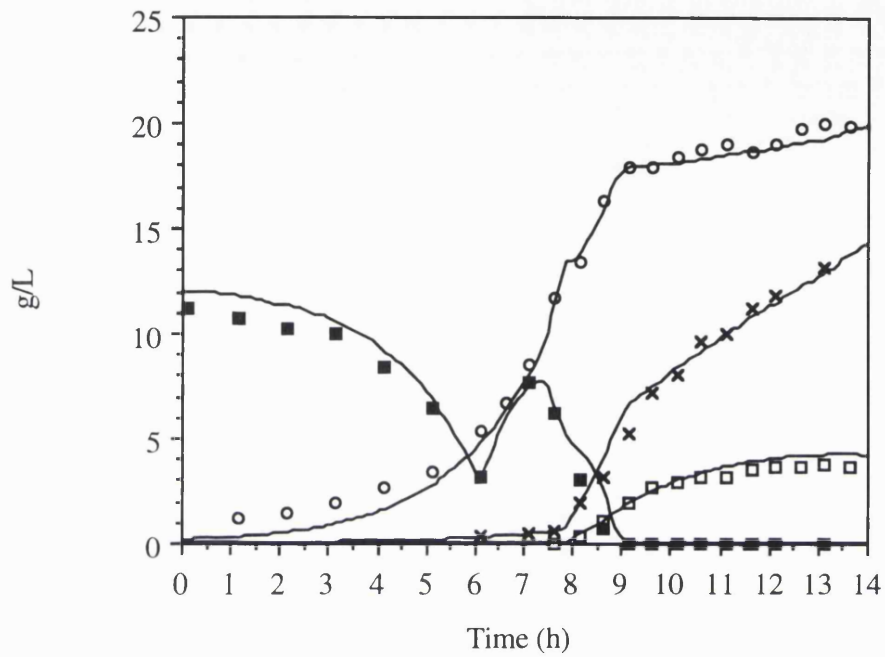


Figure 4.12: Comparison between model predictions and Expt. 11. (medium glucose feedrate)

The solid lines indicate the model predictions and the following symbols show the experimental results:

- Glucose
- B.S.T.
- × Acetate
- Biomass

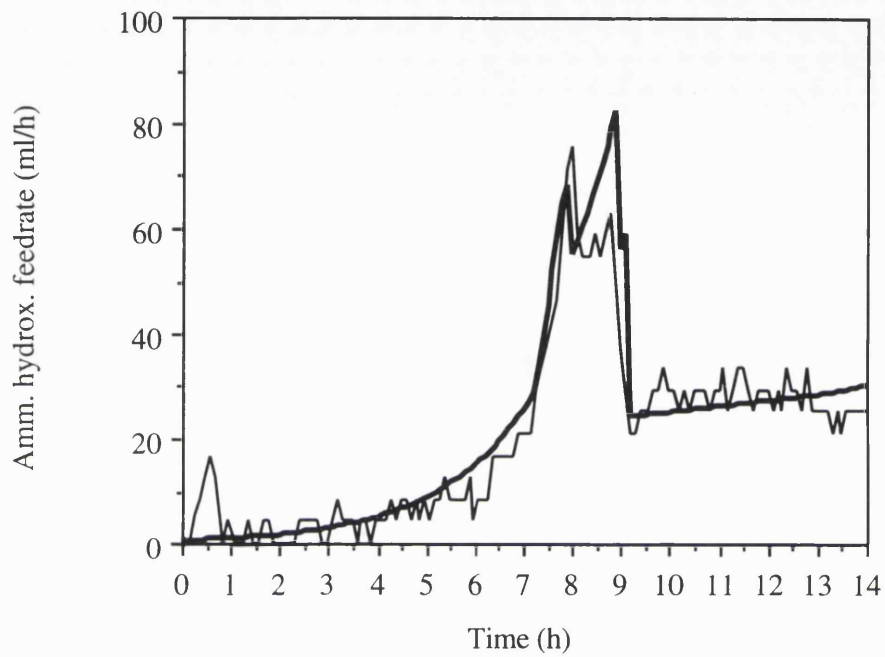


Figure 4.13: Comparison between model predictions and Expt. 11.(medium glucose feedrate)
Ammonium hydroxide feedrate.

The heavy lines indicate the model predictions and the lighter lines indicate the actual experimental rate determined from load cell readings.

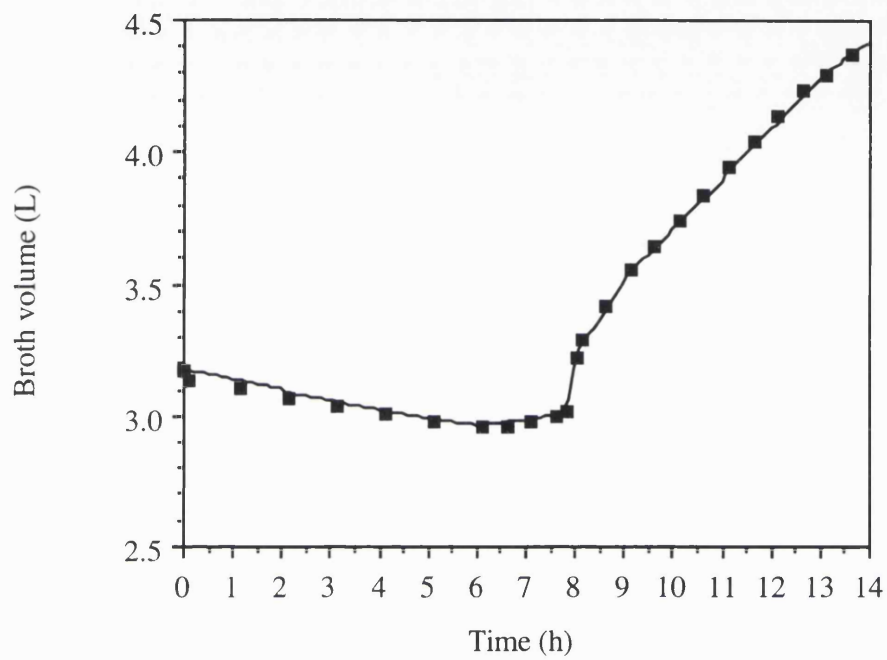


Figure 4.14: Comparison between model predictions and Expt. 11.(medium glucose feedrate) for broth volume.

The solid lines indicate the model predictions and the symbols show the calculated broth volume derived as explained in Sec. 3.2.2.

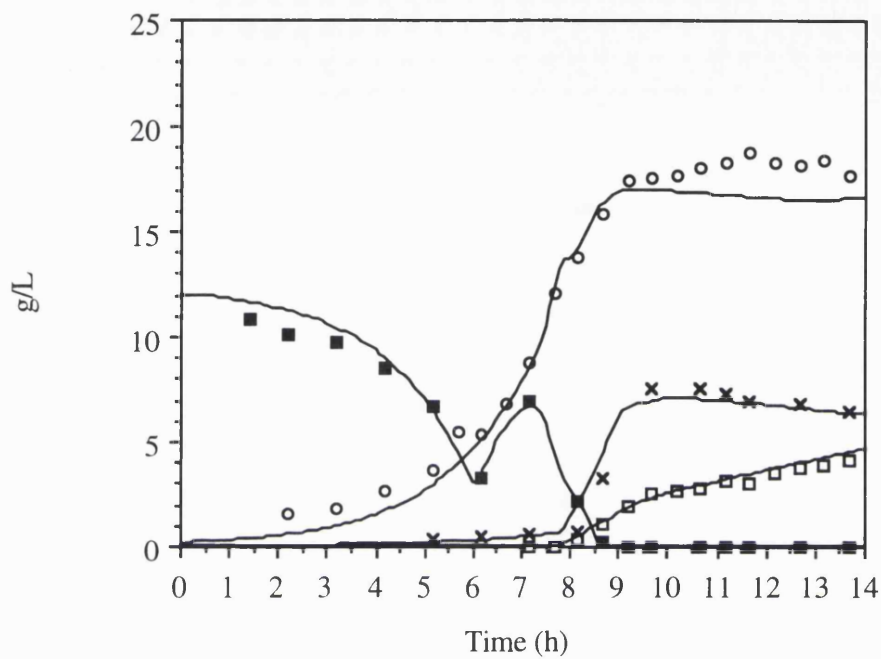


Figure 4.15: Comparison between model predictions and Expt. 12. (low glucose feedrate)

The solid lines indicate the model predictions and the following symbols show the experimental results:

- Glucose
- B.S.T.
- × Acetate
- Biomass

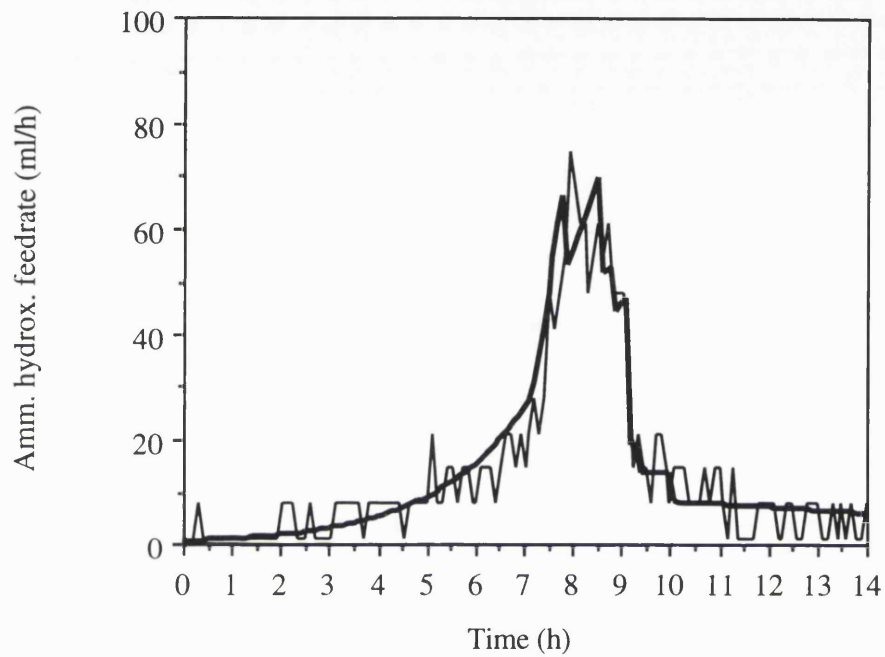


Figure 4.16: Comparison between model predictions and Expt. 12.(low glucose feedrate)
Ammonium hydroxide feedrate.

The heavy lines indicate the model predictions and the lighter lines indicate the actual experimental rate determined from load cell readings.

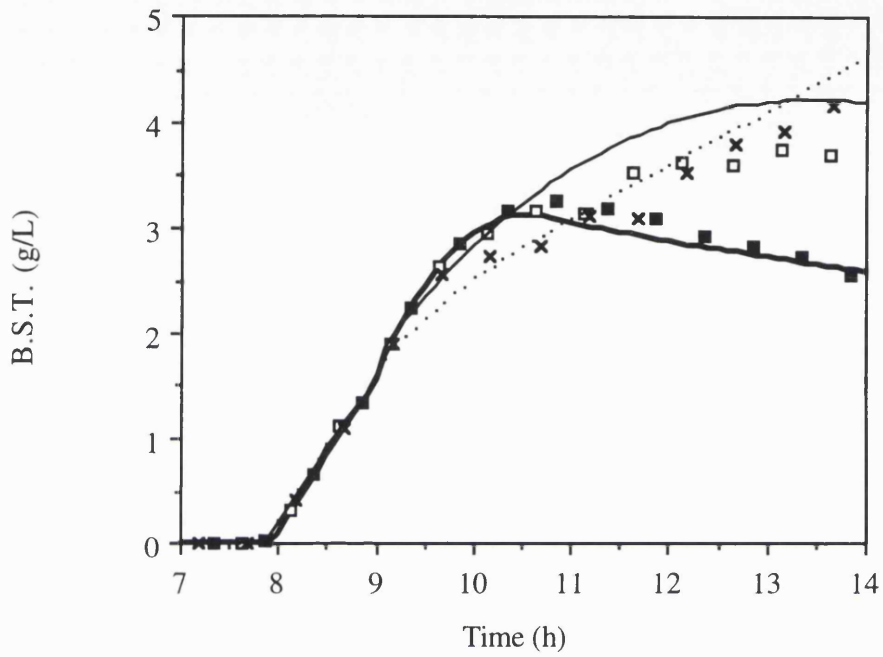


Figure 4.17: Effect of glucose feeding on B.S.T. production. Comparison between model predictions (lines) and experimental results (symbols) for Expt 8 (for which the model was fitted) and Expts. 11 and 12.

■	and	—	Expt. 8 (high glucose feedrate)
□	and	—	Expt. 11 (medium glucose feedrate)
×	and	Expt. 12 (low glucose feedrate)

4.6.2 Comparison between model predictions and experimental results for medium cell density fermentation

Fig. 4.18 shows there is poor agreement between model predictions and experimental results for the medium cell density fermentation (Expt. 7) after about 6.5h. The model overestimates the rate of B.S.T. production at this time and hence also predicts a much reduced biomass due to growth being inhibited by the high production rate. As discussed in Sec. 4.4.2.1 Expt. 7 had a lower initial specific B.S.T. production rate compared with the high cell density fermentations or the other medium cell density fermentation (unfortunately this run, Expt. 6, became phosphate limited later in the run and so could not be used for checking the model). Thus it is unclear if this is simply an anomalous experimental result or whether the model is failing to predict the correct B.S.T. production rate.

Fig. 4.19 shows the result of reducing the specific B.S.T. production rate term in the model so that it agrees with the experiment. This causes all the biomass, acetate and glucose curves to agree with the experimental results up to 8.5h. However after 8.5h the model still fails because it does not predict the decrease in acetate production. After 8.5h it therefore overpredicts acetate concentration and hence overpredicts the inhibitory effect of acetate on B.S.T. production.

In conclusion it is clear that the model does not accurately predict the result of the medium cell density fermentation. The most likely reasons for this failure are that the model parameters may not have been determined with enough precision or that the equations which were taken from the literature for the dependence of growth and maintenance on temperature may have been inappropriate. Of course it is also possible that, as suggested by Nielsen and Villadsen (1993), an unstructured model is inherently unable to cope with the changes that are occurring during induction. Ultimately it is not possible in this work to determine which of the above factors is the most important cause of the model's inability to predict the results of the medium cell density fermentation.

However it should be stressed that the ability to predict the results of a fermentation with a different temperature profile is a severe test of the model. Furthermore even if the model is restricted to a given temperature profile it is still a useful tool for process development as will be discussed in the next section.

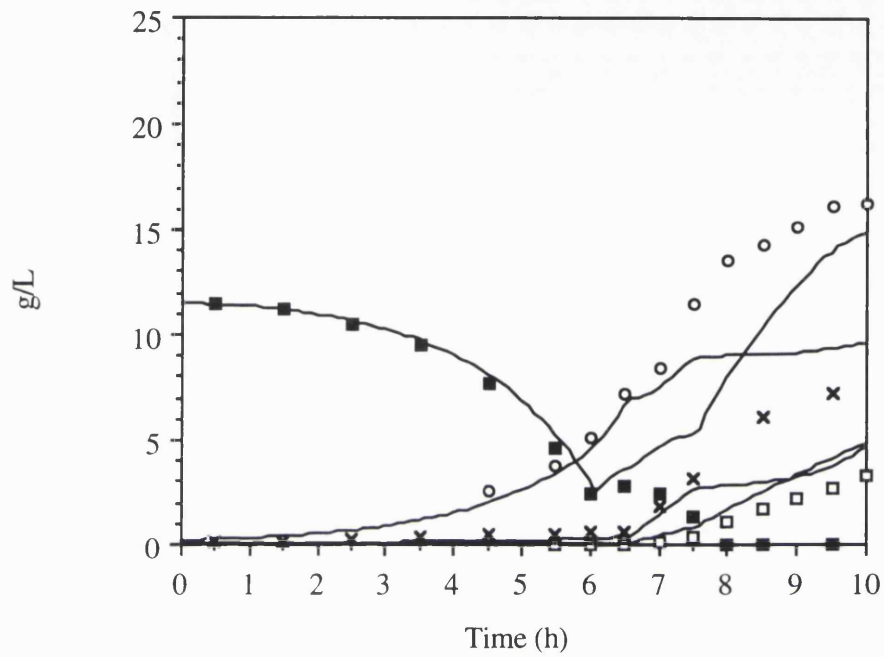


Figure 4.18: Comparison between model predictions and Expt. 7.(medium cell density).

The solid lines indicate the model predictions and the following symbols show the experimental results:

- Glucose
- B.S.T.
- × Acetate
- Biomass

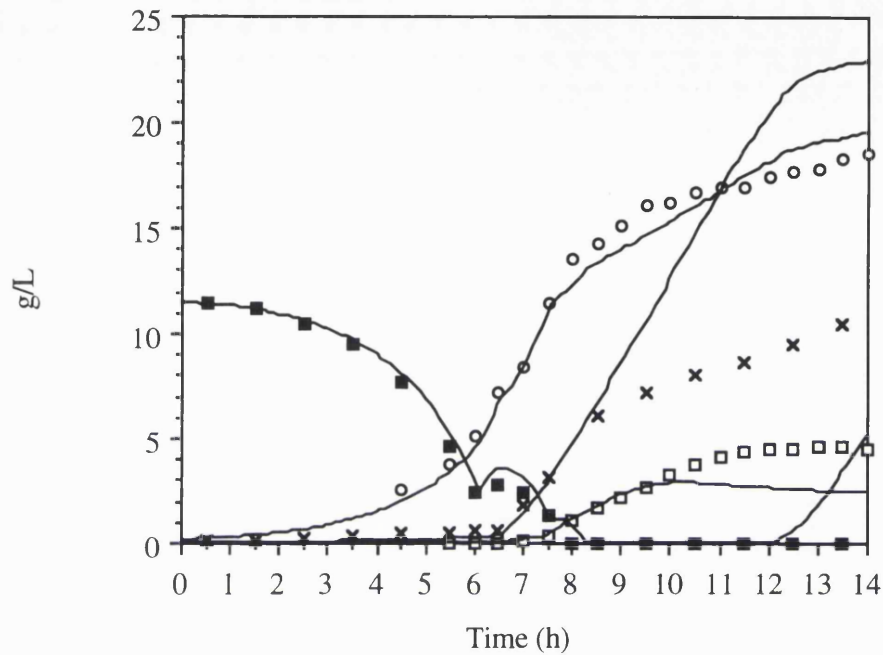


Figure 4.19: Comparison between "corrected" model predictions and Expt. 7. (medium cell density)

The maximum specific B.S.T. production rate was altered in the model so that the predicted and experimental B.S.T. concentrations would agree up to 8.5h.

The solid lines indicate the model predictions and the following symbols show the experimental results:

- Glucose
- B.S.T.
- × Acetate
- Biomass

4.7 Examples of using the model.

In the following sections three examples will be given of how the model can be used to increase understanding of the process or improve yield. All the examples are restricted to the high cell density B.S.T. fermentation process.

4.7.1 Predicting the effects of process variations

One simple but useful way that the model can be used is to run it with possible variations in the process variables (e.g. different glucose feed concentrations) and see how these might affect the process and in particular the final product yield. Table 4.3 shows the results of such an investigation. (Expt. 11 was used as the standard process).

Table 4.3

Predictions of the effects of process variations on the final B.S.T. yield and titre.

Process Variable	Variation (%)	Change in final B.S.T. yield (%)	Change in final product titre (%)
Glucose Flowrate	+5%	-11.7%	-22.3%
	-5%	+1.6%	+2.6%
Exit gas CO ₂ concentration	+5%	-15.1%	-14.5%
	-5%	+1.1%	+1.2%

These results are discussed below:

Glucose feedrate (+/- 5%).

In this case the model is predicting the effect of a process variation in the glucose feedrate which might, for example, be caused by an error in the glucose flowmeter. The first point

to make is that the effect of overfeeding glucose by 5% is much more dramatic than the effect of underfeeding by 5%. The reason for this is that the fermentation being considered is Expt. 11 which had a reasonably high acetate production rate. If the glucose feedrate is increased by 5% this causes the acetate production to increase and consequently B.S.T. is inhibited that much sooner. The net result is a large (-11.7%) drop in the product yield.

The effect on final titre is even greater (-22.3%) because once the fermentation stops producing B.S.T. the concentration falls due to the dilution effect of the glucose and peptone feeds. Thus the titre is very dependent on the harvest time which in this case has been arbitrarily set at 14h. The result is interesting since it shows that for this fermentation a small error in the glucose feeding can cause a much larger change in the final titre.

Exit gas CO₂ concentration:

In this simulation it has been assumed that there is a fault in the mass spectrometer such that carbon dioxide concentration is in error by 5%. Since induction and all the feed profiles are triggered by the %CO₂ value this means that they will occur at the wrong time. The net effect is the same as inducing the fermentation either 0.09 hours too early or too late (an overestimate of the carbon dioxide concentration by 5% being equivalent to an induction that is 0.09 hours early and vice-versa).

This was simulated in the model by changing all the feed start times as well as the time of induction. The resultant predictions are shown in Table 4.3. Once again there is a rather asymmetric effect: an underestimate of the %CO₂ causes little change to the process whereas an overestimate decreases the yield and titre by about 15%. The latter case is equivalent to inducing early (i.e. at too low a cell density) - this means there is less biomass in the tank and hence there is a longer period before glucose becomes limiting which in turn causes higher levels of acetate production. Thus B.S.T. production is more inhibited and the final yield and titre are reduced. As before it is interesting to note that for this fermentation a 5% error in the mass spectrometer can cause a much larger (15%) reduction in the yield and final titre.

Clearly other process variations could be simulated but the two examples give above are sufficient to illustrate the possible use of the model.

4.7.2 Interpreting ammonia consumption profiles.

It has already been shown how the model can accurately predict the ammonium hydroxide feedrate profile for a high cell density fermentation. In this section it is shown how the model can be used to interpret this profile and aid understanding of the process.

It was shown in Sec. 4.4.5 that the model predicts the ammonium hydroxide feedrate by taking into account the two factors which contribute to it: namely biomass and acetate production. Fig 4.20 plots these two contributions to the ammonium hydroxide as predicted by the model for Expt. 11. (the ammonium hydroxide flowrate profile is the sum of these two contributions). The profile can be explained as follows:

- 0-7.9h Prior to the start of peptone feeding biomass production is the main cause of ammonia feeding.

- 7.90h Peptone feeding starts causing an increase in acetate production and hence ammonia consumption but B.S.T. production also starts and this causes the growth rate to fall with a consequent decrease in ammonia consumption. The net effect is a slight decrease in ammonium hydroxide feedrate.

- 7.9-9.0h An increase in total biomass during this period causes an increase in both contributions to ammonium hydroxide feeding.

- 9.0h Glucose limitation causes a decrease in the growth rate and acetate production rate and hence a large drop in the ammonium hydroxide feedrate.

- 14.0h At the end of the fermentation acetate and biomass production have about equal contributions to ammonium hydroxide feedrate.

It should be recalled throughout this discussion that the predicted and experimental ammonium hydroxide feedrate profiles were very similar (see Fig. 4.20) so the above analysis explains not only the predicted but the actual feedrate profile.

The usefulness of such an analysis is that it provides insight into how to interpret the ammonium hydroxide feed profile which can be measured accurately and monitored on-line.

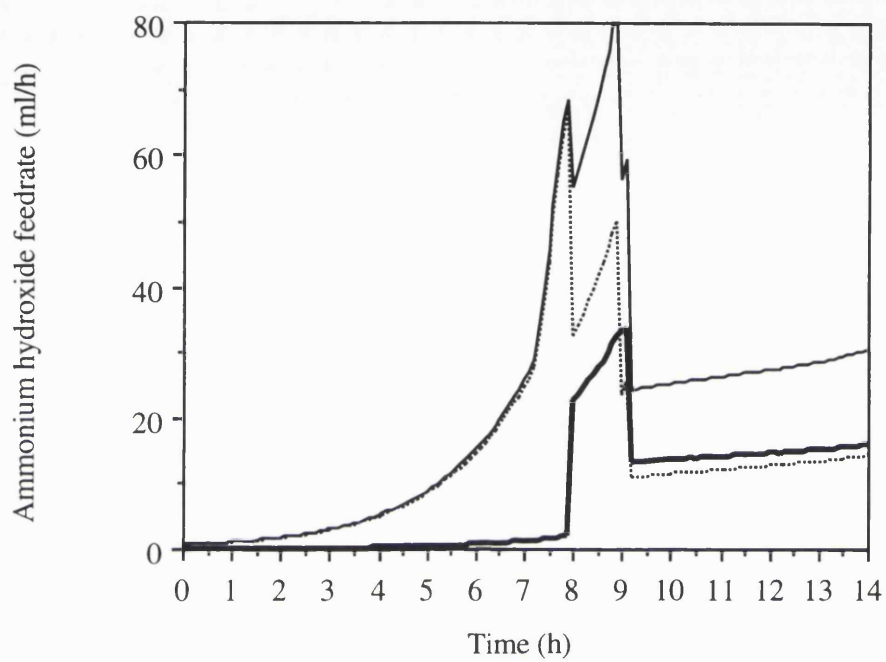


Figure 4.20: Plot of model predictions for Expt. 11 of ammonium hydroxide feedrate and the amount of that feedrate due to biomass and acetate production

- Ammonium hydroxide feedrate
- Ammonium hydroxide feedrate due to biomass production
- Ammonium hydroxide feedrate due to acetate production

4.7.3 Determining the constant glucose feedrate to optimise specific yield.

The third and final example of using the model is the prediction of the effect of constant glucose feeding on specific yield.

At the start of this thesis (Fig. 1.1, Sec. 1.4.2) the results of Jensen and Carlsen (1990) were reported which showed the effect of different glucose feedrates on specific yield of MAE-hGH in a fed batch *E. coli* fermentation. Fig. 4.21 shows the same results but also included is the equivalent plot for B.S.T. using the model. Each point indicates the predicted specific yield of B.S.T. at 14 h with a different glucose feedrate. (The glucose feedrates were converted to the units Jensen and Carlsen use by dividing by a nominal broth volume of 4.0L).

The main point to note about the two curves in Fig. 4.21 is that they follow the same trend - that is at low glucose feedrates starvation causes low specific yields whilst at high rates overproduction of acetate inhibits production. (The two curves are not expected to overlay since each host/vector will be different quantitatively in their response to these effects).

The specific yield is a somewhat confusing parameter to interpret since it is affected by both production and growth. Therefore the effects have been separated out in Fig. 4.22 (unfortunately there is no data to do this for the Jensen and Carlsen fermentations). This plot shows that the biomass concentration increases linearly with glucose feedrate whereas the B.S.T. titre curve goes through a maximum (but shifted to a higher flowrate than the maximum for the specific yield plot).

Clearly Figs. 4.4. and 4.5 can be used to choose the constant glucose feedrate to optimise specific yield of B.S.T. or B.S.T. concentration (the respective glucose feedrates being 3.5 and 5.0 g glucose/L/h).

This simple example of using the model to predict the effect of constant glucose feedrates was chosen because the result could be compared with the data of Jensen and Carlsen (1990). However the model could also be used to predict the effects of linear or exponential glucose feeding.

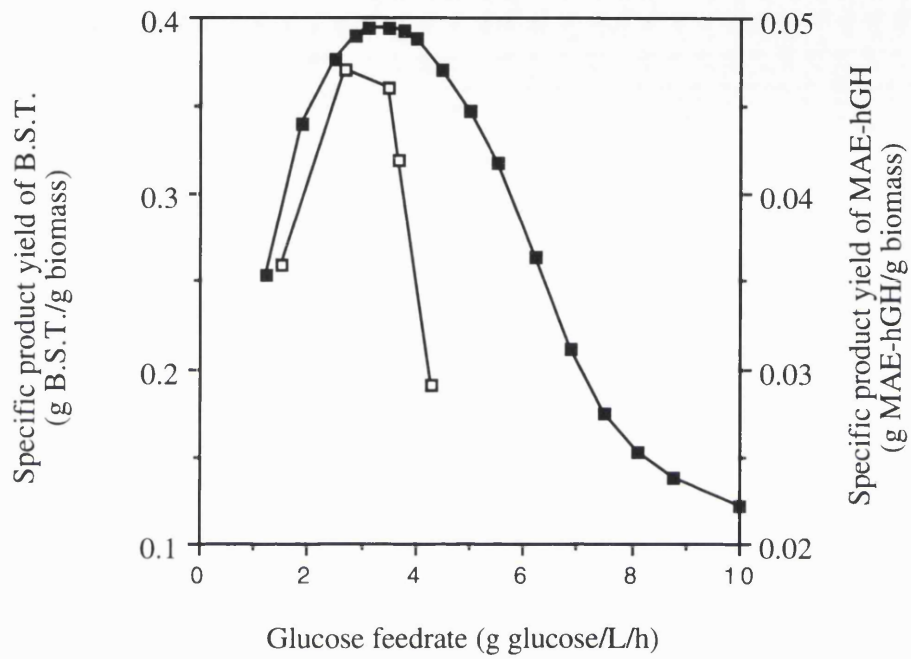


Figure 4.21: Effect of constant glucose feedrate on specific product yield.

The open symbols show the experimental results of Jensen and Carlsen (1990) with a recombinant *E. coli* producing MAE-hGH. The solid symbols show the B.S.T. model predictions.

- Predictions from B.S.T. model.
- Experimental results from Jensen and Carlsen (1990)

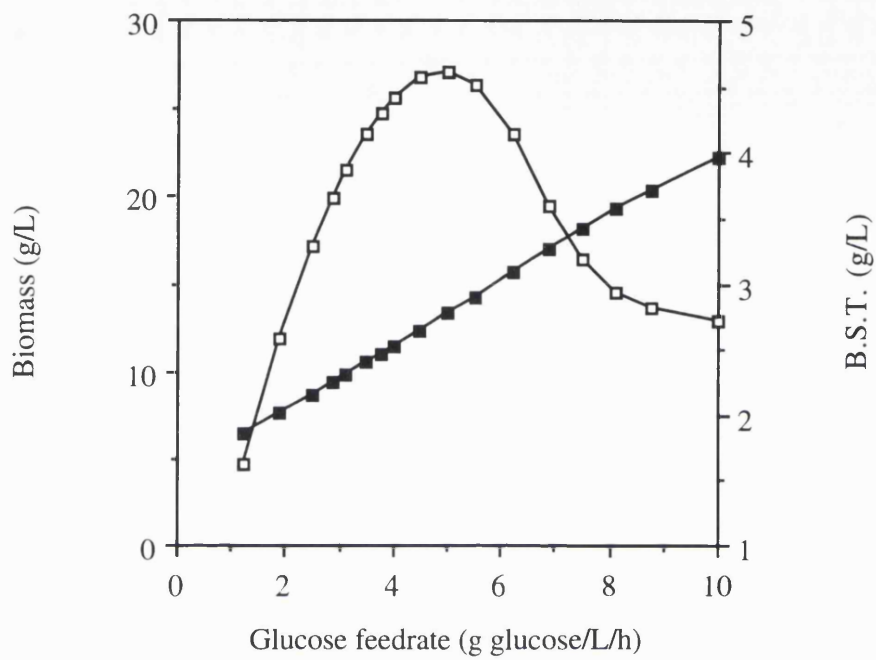


Figure 4.22: Effect of constant glucose feedrate on biomass and B.S.T. concentrations

The symbols show the model predictions of final (14h) biomass and B.S.T. concentrations at different constant glucose feedrates. This data was used to obtain the specific yield plot shown in Fig. 4.21

- Biomass
- B.S.T.

4.8 Discussion and conclusions

In this chapter a simple 15 parameter unstructured model has been developed that predicts the broth volume and concentrations of glucose, biomass, B.S.T. and acetate throughout the fermentation studied in this thesis given the initial concentrations, the temperature profile and the profiles for glucose, peptone, and media feeds as well as the sampling rate.

It was shown how the model was developed, and parameters estimated, using results from the literature and the current host/vector. It was noted that the lack of available data for parameter estimation may mean that some of the model parameters are not adequately determined.

However it was concluded that the model could accurately predict the effects of different glucose feedrates on high cell density fermentations. It was shown how the model could be used to interpret the ammonium hydroxide feedrate profiles and how it could be used to predict the effect of process variations. Finally an example was given of how the model could be used to predict the constant glucose feedrate required to optimise specific B.S.T. yield or B.S.T. titre.

It was concluded that the model in its present form was unable to predict the results of a medium cell density fermentation (i.e. induced at a 4.5 g DCW/L instead of 9.0 g DCW/L). The main reasons for this were the model's overprediction of the initial specific B.S.T. production rate and the model's inability to predict the decrease in acetate production due to glucose limitation.

It was suggested that the following may improve the model's performance:

- Better estimates for the model parameters especially by using continuous culture experiments to determine unequivocal cause and effect relationships - for instance the effect of acetate on growth rate.
- Better correlations for the effect of temperature on the specific rates of biomass and B.S.T. production. More experiments are needed using different temperature profiles. In particular the use of another host/vector, identical to RV308/pHKY531 but lacking

a functional B.S.T. gene, would allow the effect of temperature on growth to be studied above 37°C without the complication of B.S.T. production.

- A better equation for predicting the effect of acetate production - in particular the more mechanistic approach of considering glucose fluxes within the cell and limited respiration capacity (e.g. analogous to the Sonnleiter and Kappeli (1986) yeast model). However as discussed in the introduction, developing such a model would be difficult due to a lack of understanding of these mechanisms and also the complications due to temperature changes and peptone feeding.
- Ultimately accurate predictions of the complicated events occurring during induction may only be possible by using a more complex structured model.

The overall conclusion is, however, that the model developed here is an improvement over many in the literature because it is simpler and easier to understand yet uniquely is able to take account of the production and inhibitory effect of acetate in a fermentation producing high yields of heterologous protein and using a complex peptone feed.

5 CONCLUSIONS

This thesis has studied what is currently the most common industrial recombinant fermentation process (i.e. temperature induced *E. coli* producing high yields of heterologous protein and using a complex feed) for which there is a scarcity of information in the literature.

The effect of glucose feeding and time of induction were both investigated and the following conclusions drawn:

Glucose feeding.

It was concluded that there is an optimal glucose feedrate to maximise product yield or titre. Higher glucose feedrates caused inhibitory acetate concentrations whilst lower feedrates led to glucose starvation. The same effects have been reported and explained qualitatively by Jensen and Carlsen (1990).

It was concluded that the mathematical model of the fermentation developed in this thesis was able to quantitatively describe the above effects of glucose feeding. The model was developed using existing knowledge of *E. coli* and results with the current host/vector. It was shown how the model, given inoculation conditions and feed and temperature profiles, was able to predict the concentrations of biomass, B.S.T., glucose and acetate throughout the fermentation. Uniquely the model predicts the production and inhibitory effect of acetate including the increased acetate production that occurs due to peptone feeding.

Timing of induction

It was concluded that the time of induction did not affect the specific rate of acetate production and that the specific rate of B.S.T. production was the same or higher when the fermentation was induced at twice the cell density. Thus the high cell density fermentation had a faster rate of B.S.T. production (since it had more cells) but also reached inhibitory concentrations of acetate sooner. As a result the final B.S.T. titre was lower in the high cell density process. It was not possible

with the glucose feeding strategy employed here to run the fermentations at non-inhibitory acetate concentrations.

It was concluded that the model developed in this thesis was not able to accurately predict the effect of the time of induction on product titre and yield. Possible reasons for this were suggested.

However it was concluded that the model described here could be a useful industrial tool for process development. Examples were given of how the existing model could be used: to interpret process information (e.g. ammonium hydroxide profiles); to predict the effects of process variations (e.g. errors in the mass spectrometer); and to choose the optimum glucose feedrate to maximise product yield or titre. It could also be used as the basis for a model which more accurately predicts the effects of temperature. Most significantly the model presented here is simpler than most existing mathematical models for recombinant *E. coli* fermentations in the literature and is therefore more likely to be useful in an industrial context.

A APPENDIX A: Measurement of dry cell weight

A1.1 Summary

In this appendix the reason for choosing direct dry cell weight measurement rather than optical density is given. It is then shown how the rinsed dry cell weight was determined.

A1.2 Optical Density and Dry Cell Weight

Dry cell weight is one of the most important parameters in an *E. coli* fermentation, yet surprisingly, there is no standard method for measuring it. The most common method used is to measure the optical density (O.D.) of a sample (either directly or after dilution). Even here there is a wide range of wavelengths chosen (see Table A1.1). More importantly all the O.D. methods rely on performing at least one calibration curve against directly measured dry cell weights (in an oven). Often research papers will explain how the O.D. measurements are taken but rarely do they describe the method used for measuring dry cell weight directly to get the calibration curve. In particular they often fail to state if the cells are rinsed prior to drying and what they are rinsed with.

Some authors (e.g. Ataai and Shuler, 1985) do not use O.D. at all but rely on direct dry cell weight measurement. This is the method used in this thesis for three reasons:

1. The main advantage of O.D. is that it gives an rapid estimate of biomass which can be used for control or to trigger various fermentation events. O.D. was therefore not needed in this work since the only event triggered by an estimate of biomass was the start of induction and this was done using the more accurate and frequent mass spectrometer measurement of exit gas carbon dioxide concentration.
2. It was more convenient to use direct dry cell weight measurement since samples had to be spun down in Eppendorf tubes anyway to obtain cell free broth for chemical analysis.

3. Inclusion bodies may affect the correlation between dry cell weight and O.D. For example two samples with the same dry cell weight might give different O.D.s depending on the size of the inclusion bodies they contained.

Table A1.1

Wavelengths chosen for measurement of optical density in *E. coli* fermentations

Wavelength (nm)	Reference
470	Riesenberg <i>et al.</i> (1990)
525	Jensen and Carlsen (1989)
540	Bauer and Shiloach (1974)
550	Yang <i>et al.</i> (1992)
570	Cutayar and Poillon (1989)
580	Forberg <i>et al.</i> (1983)
595	Allen and Luli (1987)
600	Ramirez and Bentley (1993)
610	Strandberg and Enfors (1991c)
660	Yee and Blanch (1993)
680	MacDonald and Neway (1990)

A1.3 Rinsed Dry Cell Weight

Normally a direct measurement of dry cell weight is done by centrifuging a known volume of fermenter broth in a pre-weighed container which is then dried to constant weight. The cell pellet is often re-suspended, rinsed, and re-centrifuged to remove media (this may be repeated twice) and the rinsing is done with either D.I. water or some solution which prevents possible lysis of cells (see Table A1.2).

Table A1.2

Cell pellet rinsing methods used for direct determination of dry cell weight by centrifugation for *E. coli* fermentations.

No. of rinses	Rinsing medium	Reference
0	None	Fieschko and Ritch (1986)
1	D.I. water	Cutayar and Poillon (1989) Reiling <i>et al.</i> (1985) Yang (1992)
1	MgCl ₂ and Tris buffer	Bauer and Shiloach (1974)
2	D.I. water	Forberg <i>et al.</i> (1983) Kim and Shuler (1990)
2	Buffered saline then D.I. water	Allen. and Luli (1987)

In this work early tests showed that rinsing the cells with D.I. water prior to drying did indeed reduce the measured dry cell weight - presumably due to removal of medium from the cell pellet (see below). Ideally therefore the rinsed dry cell weight should have been obtained for every sample. However there was not enough time to do this since samples were taken every half hour and the fermentation also had to be monitored and feeds started etc. Therefore it was decided to measure dry weight (non-rinsed) for each sample and to convert this to a rinsed dry weight value by means of a correlation. The correlation was obtained by performing both rinsed and non-rinsed dry cell weight measurements in tandem for a few selected samples in each run.

A1.4 Rinsed Dry Cell Weight Correlation

The correlations between the non-rinsed and rinsed dry cell weights for the different fermentation media are shown in Fig. A1.1. Theoretically the correlations can be explained as follows:

Rinsing removes medium that would otherwise stay in the Eppendorf in two ways:

- a) Stuck as a meniscus above the cell pellet
- b) Trapped within the cell pellet.

We can estimate both effects. For example medium O or A has a concentration of about 15 g/L (actually 13 and 16 g/L respectively). If we add on the zero hour glucose concentration (12 g/L) then each sample taken will contain medium with a concentration of about 27 g/L. The two rinsing effects can now be quantified:

- a) If 0.01 ml of medium is stuck as a meniscus in the 1 ml Eppendorf (i.e. 1% of the total volume) then rinsing will reduce the dry cell weight by:

$$0.01 \times 27 = 0.27 \text{ g/L.}$$

In fact for medium O and A the correlation gives a value of 0.20 g/L suggesting that that the meniscus contains slightly less than 1% of the total volume which seems reasonable.

- b) It can be assumed that the cell pellet when it is first spun down contains 75% medium by weight (p.16 Pirt 1975). Therefore if it contains c mg of cells it will contain $3c$ mg of medium. The true rinsed dry cell weight would be c g/L. The non-rinsed dry cell weight would be $c + (3c \times 0.027)$ g/L. Thus a plot of rinsed vs non-rinsed dry cell weight should have a slope of:

$$1 / (1 + 0.081) = 0.925$$

This compares reasonably well with the actual slope of 0.914 in Fig A1.1.

For medium C (initial medium concn. = 37 g/L medium + 12 g/L glucose = 49 g/L) similar calculations predict an intercept of 0.49 g/L and a slope of 0.87 compared with the actual values of (Fig. A1.1) 0.56 g/L and 0.86. Again this is a reasonable agreement given the assumptions that had to be made.

In practice there is a complication to the above analysis - namely that the medium concentration varies throughout the fermentation because certain medium components are being consumed and others either fed or produced by the cells. Nevertheless the fact that the correlation coefficients are so good suggests that for a given medium a single rinsing correlation is sufficient throughout the fermentation.

This may not be true however for the runs which used media B or B+. Unlike the media O&A and medium C correlations which have just been discussed these runs had high peptone feedrates and (in the case of medium B+ runs) extra medium feed. Correlation #1 in Fig. A1.1 shows the result of taking a single correlation for the medium B&B+ rinsing data. The slope of this correlation (0.85) is less than we would expect from the initial medium B&B+ density of 38 g/L which from the above theory should give a slope of $1 / (1 + 3 \times 0.038) = 0.90$. In Fig. A1.2 an alternative correlation (#2) is shown which is a best fit to the data prior to feeding peptone. This gives a slope of 0.917 which is closer to the predicted value. It was therefore decided to use rinsing correlation #2 for medium B&B+ runs prior to peptone feeding and correlation #1 after feeding starts.

To test if this approach was reasonable data from growth-only non-peptone fed fermentations using medium A and B were compared (Expts. 1 and 2). Fig. A1.3 shows that during exponential growth the plots of exit gas %CO₂ and total glucose used were identical. This strongly suggests that the total biomass plots should also be identical. Fig. A1.4 shows these plots with the biomass data for the medium B run calculated using both correlations described above. Clearly correlation #2 gives a better fit.

In conclusion the correlations shown in Fig. A1.1 were used for experiments using media O&A and C. For experiments which used media B&B+ two correlations were used: Correlation #2 (Fig A1.2) was used to correct the non-rinsed dry cell weight prior to feeding peptone and correlation #1 (Fig. A1.1) was used after feeding starts. The uncertainty in correcting for rinsing means that there is an inaccuracy in the final biomass measurement. This is indicated in some of the biomass plots for media B&B+ runs by showing biomass values calculated using both correlations.

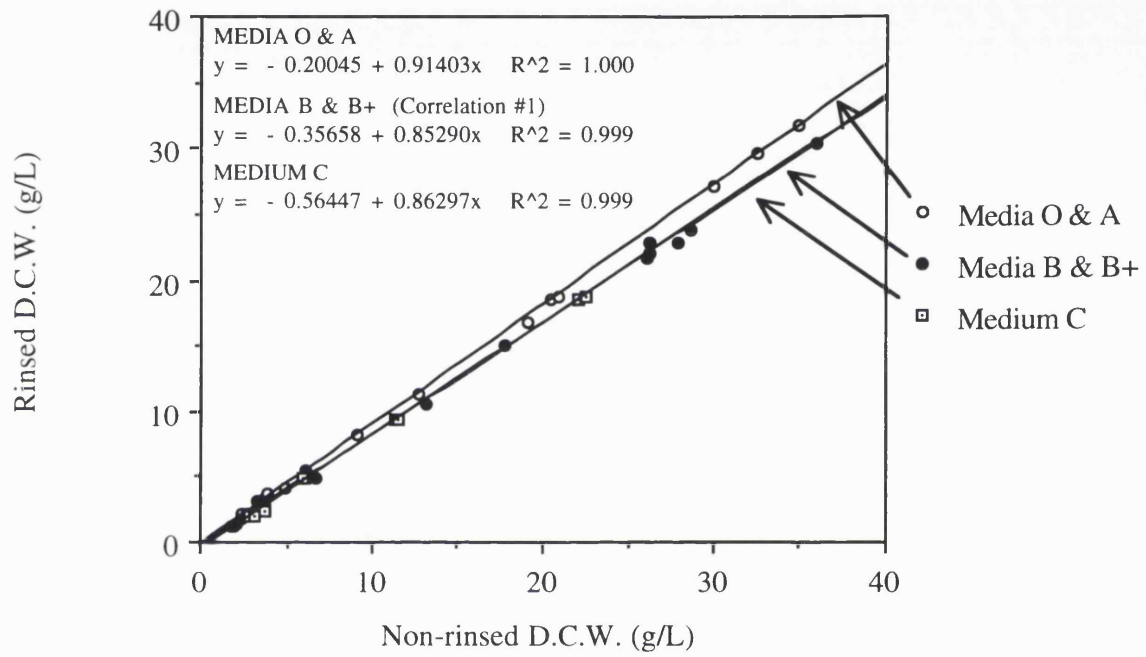


Figure A1.1: Correlation between rinsed and non-rinsed dry cell weight (D.C.W.) for the different media used in this thesis.

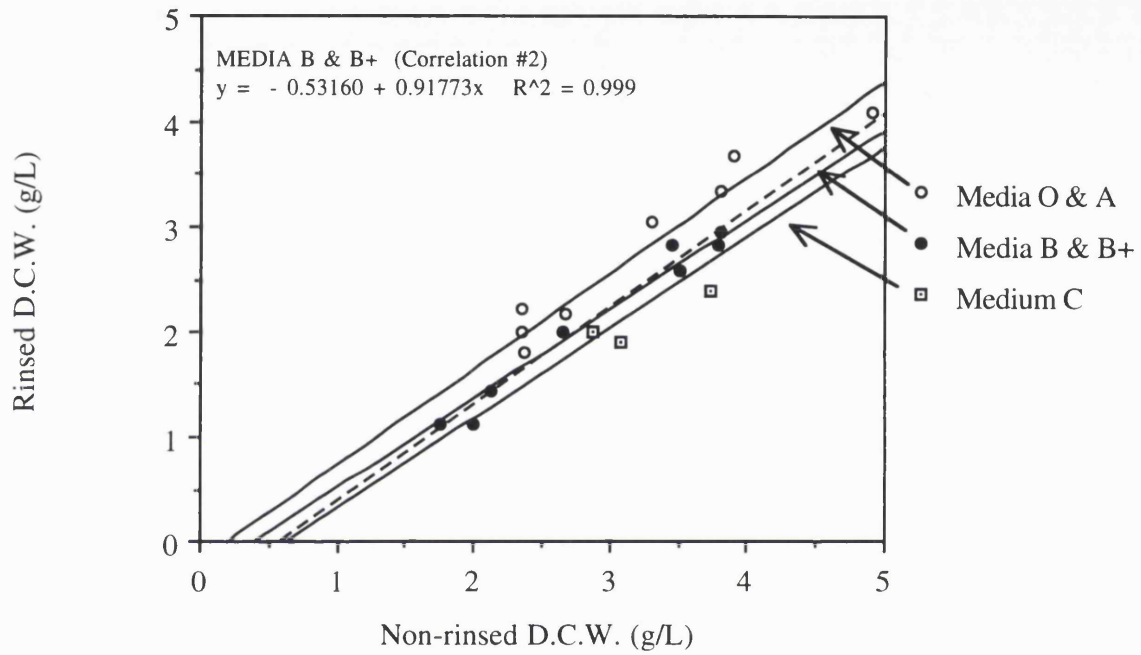


Figure A1.2: Expanded portion of Fig.A1.1 showing only samples taken before peptone feeding started (i.e. < 5 g D.C.W./L).The solid lines show the same correlations as determined in Fig.A1.1. The dotted line shows an alternative correlation for media B&B+ based only on samples taken prior to peptone feeding.

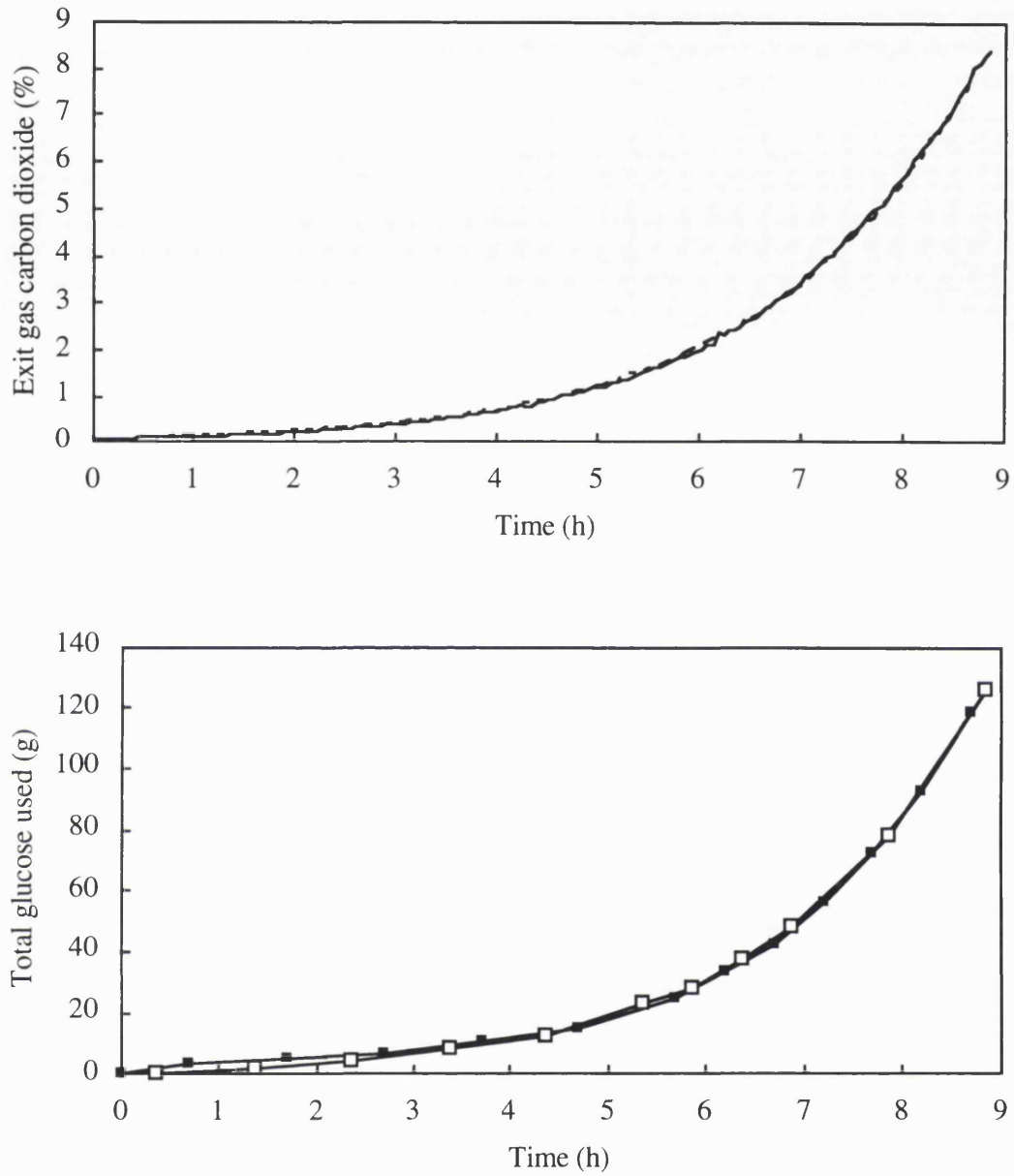


Figure A1.3: Comparison between exponential growth on media A and B.
% CO₂ in fermenter exit gas and total glucose used.

— and ■ Medium A (Expt. 1)
- - - and □ Medium B (Expt. 2)

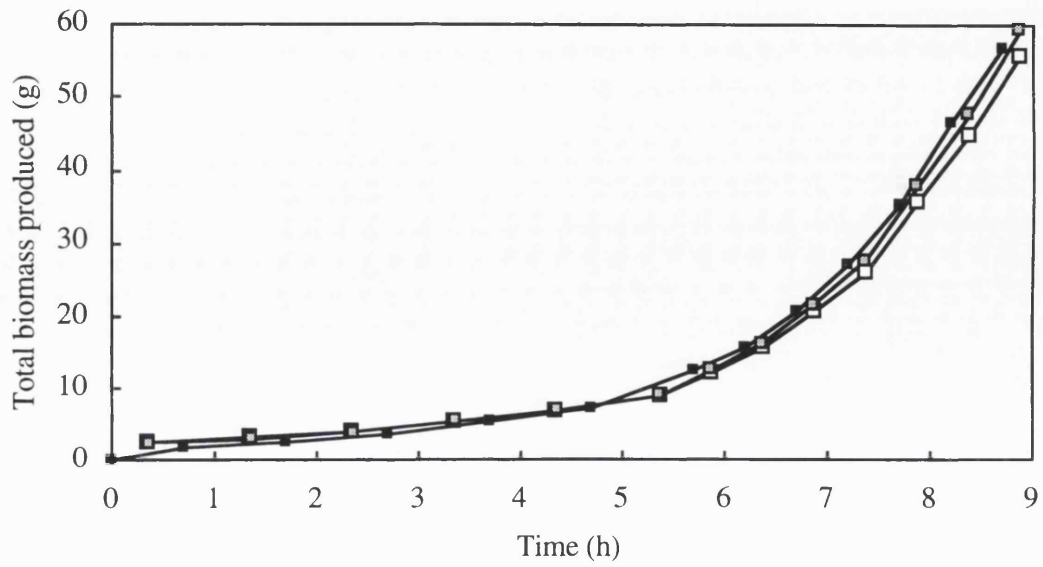


Figure A1.4: Comparison between exponential growth on media A and B.
Total biomass produced.

- Medium A (Expt. 1)
- Medium B (Expt. 2) [Rinsing correlation #1]
- ▣ Medium B (Expt. 2) [Rinsing correlation #2]

B APPENDIX B: Biomass error analysis

Figs. B1.1 shows the absolute and relative biomass errors plotted against the biomass for sixty samples. The absolute biomass error was calculated by taking the difference between the maximum and minimum of the four biomass values obtained for each sample and dividing by two. The relative biomass error was calculated by dividing this absolute biomass error value by the biomass and multiplying by one hundred.

The relative biomass error plot shows that when the biomass is greater than about 5 g/L the relative error is constant at about $\pm 3\%$. Below a biomass value of 5 g/L however a better measure of the biomass error is obtained by using the absolute biomass value which averages at about 0.5 g/L. These values are used in the Sec. 3.3 in the discussion about reproducibility and accuracy.

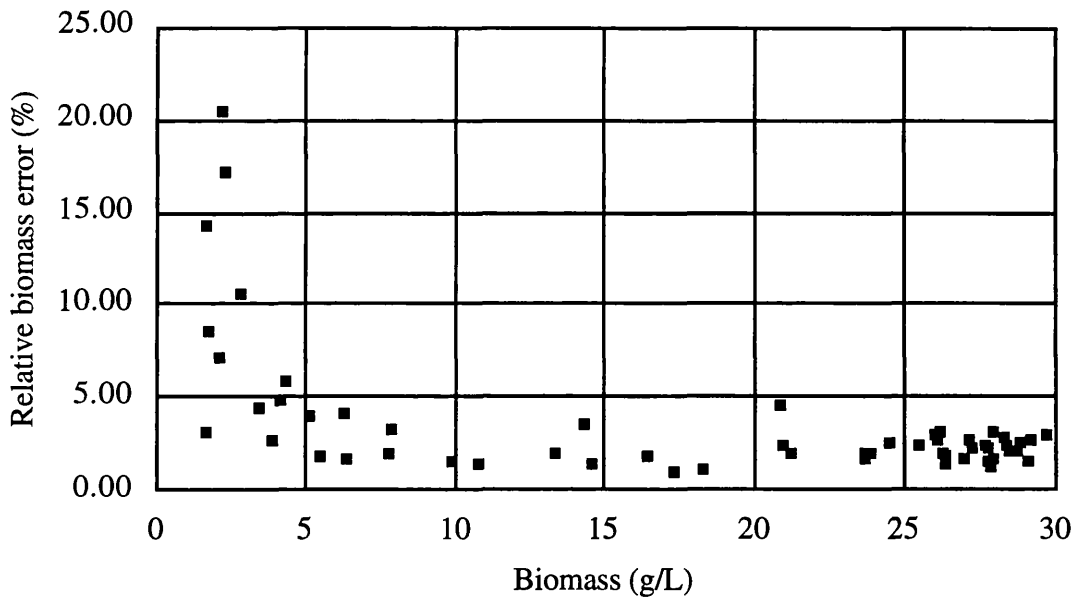
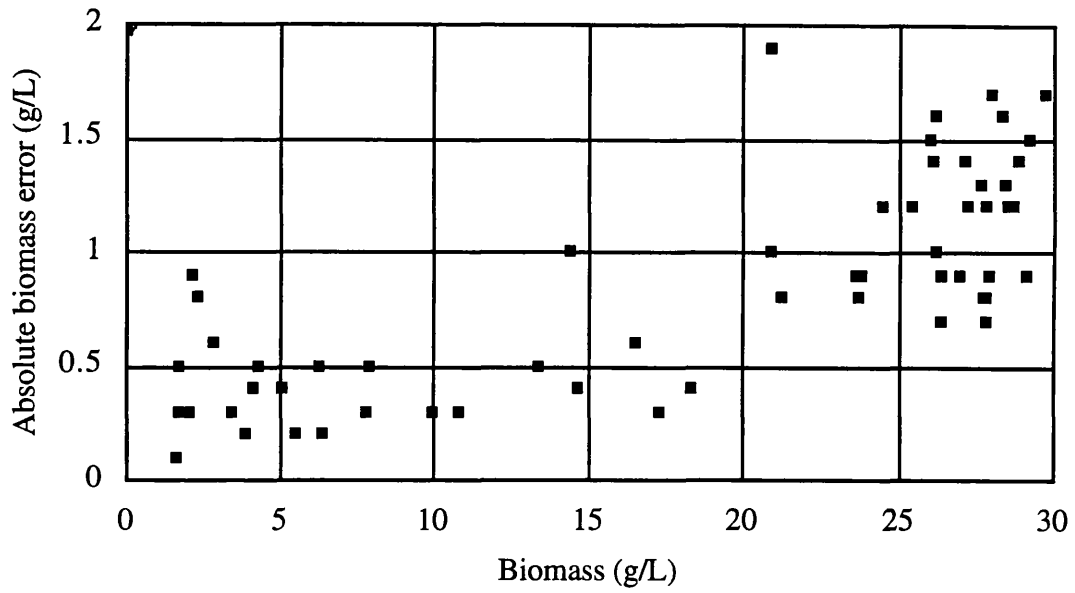


Figure B1.1: Absolute and relative biomass error vs. biomass.

C APPENDIX C: Calculating specific growth rate

The specific growth rate is defined by the following equation:

$$\frac{d(XV)}{dt} = \mu(XV) - Q_{smp}X \quad (C1.1a)$$

This can be re-arranged to give:

$$d \ln(XV) = \left[\mu - \frac{Q_{smp}}{V} \right] dt = \mu_{obs} dt \quad (C1.1b)$$

Thus the slope of a logarithmic plot of total biomass vs. time will be equal to the observed specific growth rate. The true specific growth rate can be obtained from this by subtracting the sampling rate divided by the broth volume.

To illustrate this the solid symbols in Fig. C1.1 show a computer simulation of total biomass assuming a starting value of 1.0 g at 1.0 h, a specific growth rate of 0.693 1/h (a doubling every hour) and a sampling rate of 20% of the broth volume every hour. The small solid squares show the total biomass in the tank calculated at 0.1 hourly intervals. The larger solid triangles show the values at the time the hourly samples are taken.

The open symbols show the "total biomass produced" calculated in the same way as was used in the results (Secs. 3.4 - 3.7) - i.e. adding the total biomass sampled to the total biomass in the tank for each assay point.

The four solid lines show different ways of calculating the specific growth rate:

Line A: This is an exponential fit to the data points from just after the sample is taken to just before the next one is removed (in this case between 3 and 4 hours). This is the only method that gives the correct specific growth rate of 0.693 1/h.

Line B: A best fit through the sample points (indicated by the solid triangles) gives an observed specific growth rate of 0.485. This method had to be used in Fig. 4.2 (Sec. 4.3.1) for calculating specific growth rate from total biomass since biomass values were only available at the sample points. It can be corrected approximately by adding on a term

for the sampling rate divided by the volume (Eqn. C1.1b) which in this case is 0.2 1/h. This gives $0.485 + 0.2 = 0.685$ 1/h which is close to the correct value of 0.693 1/h.

Line C: This is a best fit through all the data points. The above correction then gives: $0.493 + 0.2 = 0.693$ 1/h. This better method could be used for the total carbon dioxide plot (Fig. 4.1, Sec. 4.3.1) since in this case the mass spectrometer data points were available between biomass sample times.

Line D: This is a best fit through the total biomass produced points. At first it seems that this method should give the correct specific growth rate since it does add back the total sample biomass at each assay point. However it actually gives an underestimate of specific growth rate since the sampled biomass does not take part in growth. Thus although total biomass produced was used in the results section it is not used in calculation of specific growth rate (Sec. 3.4.1).

Finally the specific growth rate could be calculated from another version of Eqn. C1.1a:

$$V \frac{dX}{dt} + X \frac{dV}{dt} = \mu(XV) - Q_{smp} X \quad (C1.1c)$$

But from a volume balance:

$$\frac{dV}{dt} = Q_{feed} - Q_{smp} - Q_{evap} \quad (C1.2)$$

therefore re-arranging Eqn. C1.1c and substituting for $\frac{dV}{dt}$ from Eqn. C1.2 gives:

$$d \ln X = \left[\mu - \frac{Q_{feed} - Q_{evap}}{V} \right] dt = \mu_{obs} dt \quad (C1.1e)$$

Thus a logarithmic plot of biomass concentration vs time gives the observed specific growth rate and this can be corrected to give the true specific growth if the total feedrate and evaporation rate are known.

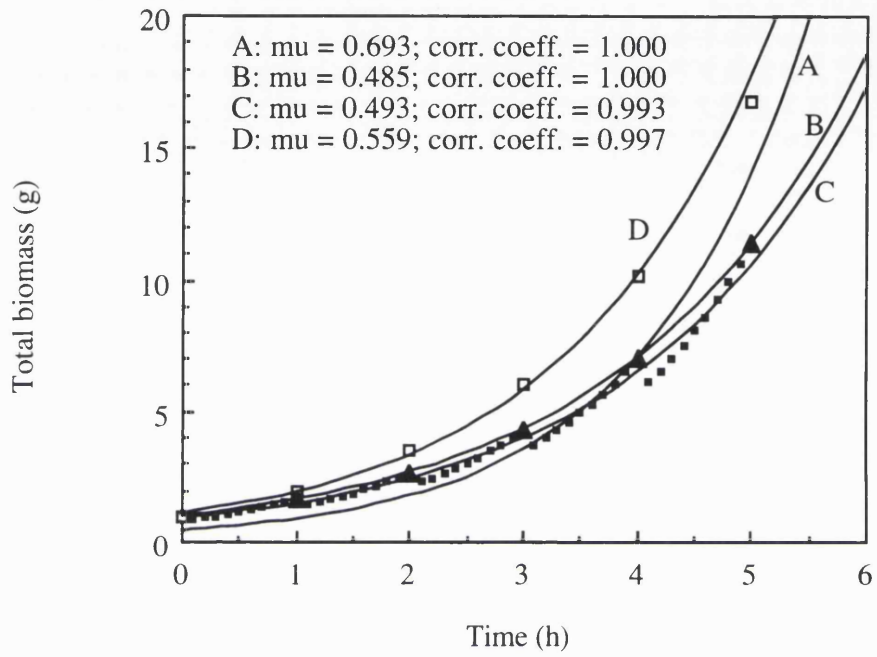


Figure C1.1: Example of different ways of calculating specific growth rate.
(see text for explanation).

D APPENDIX D: Supplementary process plots

3.1 Layout of plots

For each set of experiments described in Chapter 3 the following supplementary plots are shown:

- a) Estimated broth volume.
- b) pH
- c) Oxygen feedrate.
- d) Dissolved oxygen concentration.
- e) Respiratory quotient.

The labelling of these plots follows similar conventions to that used in the main text - e.g. the supplementary plots to Figs. 3.8a-f are labelled D3.8a-d.

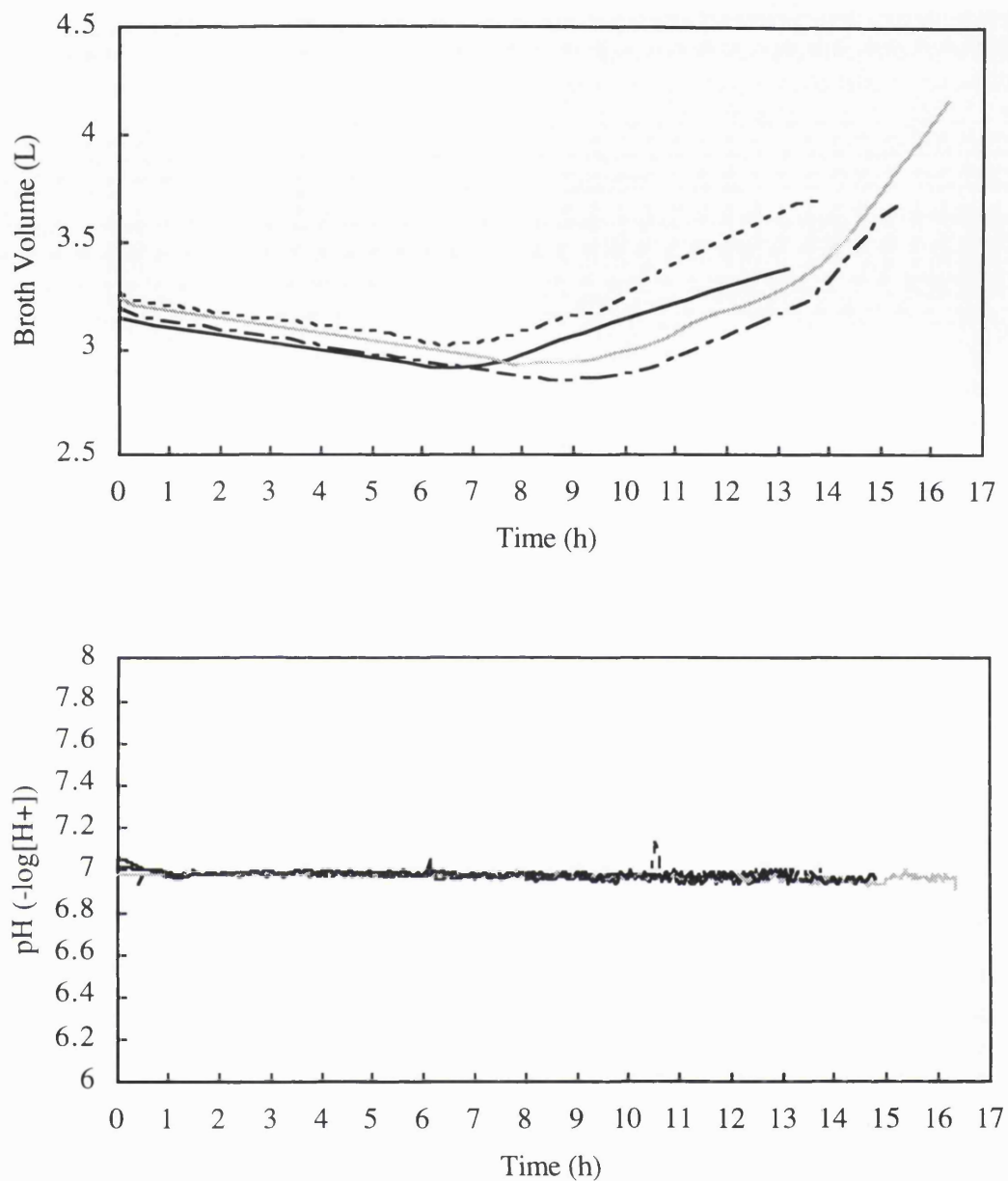


Figure D3.2a: Effect of different media on growth.
Estimated broth volume and pH.

- Medium A (Expt. 1)
- - - Medium B (Expt. 2)
- Medium C (Expt. 3)
- - - Medium C (Expt. 4)

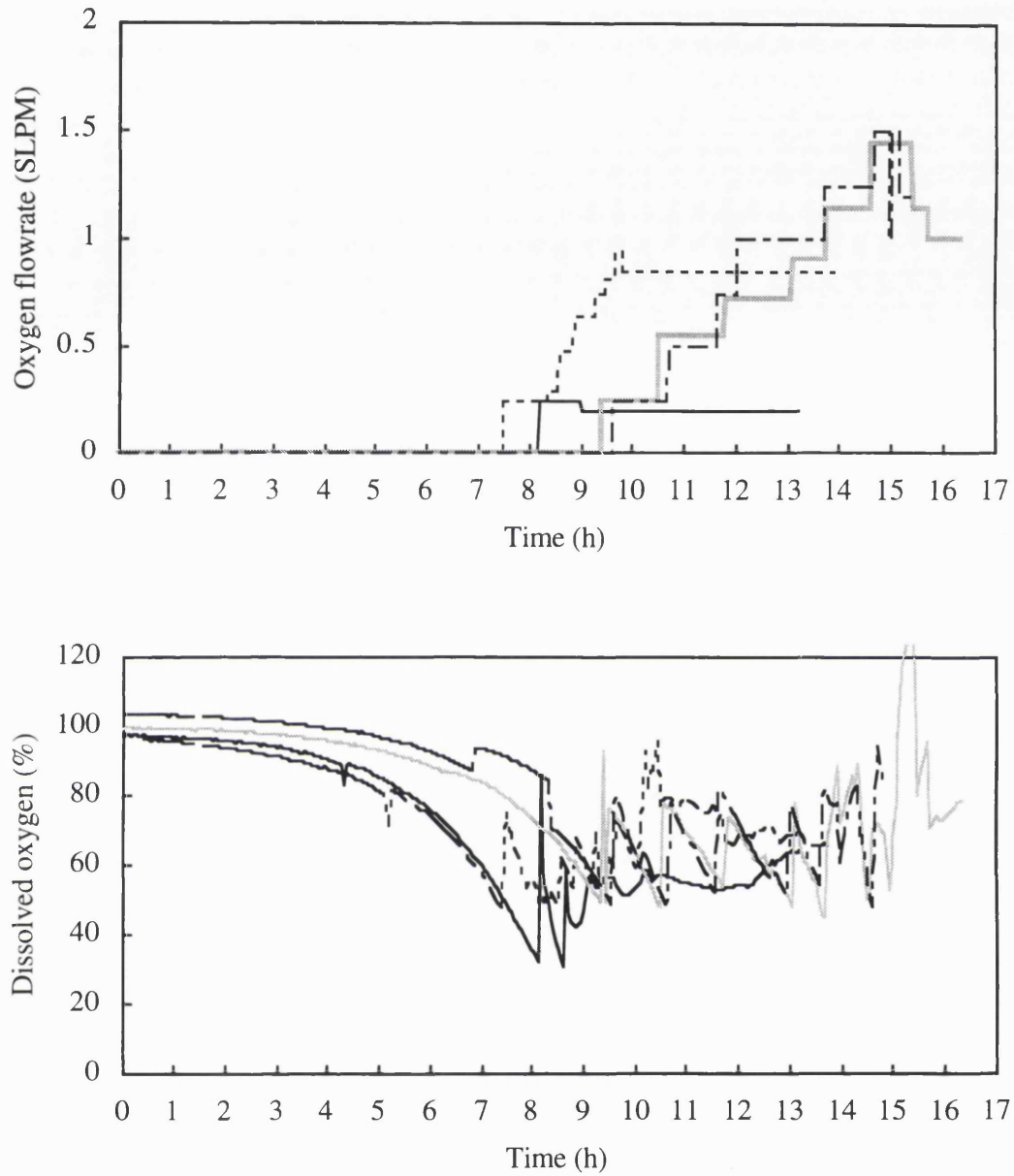


Figure D3.2b: Effect of different media on growth.
Oxygen flowrate and dissolved oxygen concentration.

- Medium A (Expt. 1)
- - - Medium B (Expt. 2)
- Medium C (Expt. 3)
- - - Medium C (Expt. 4)

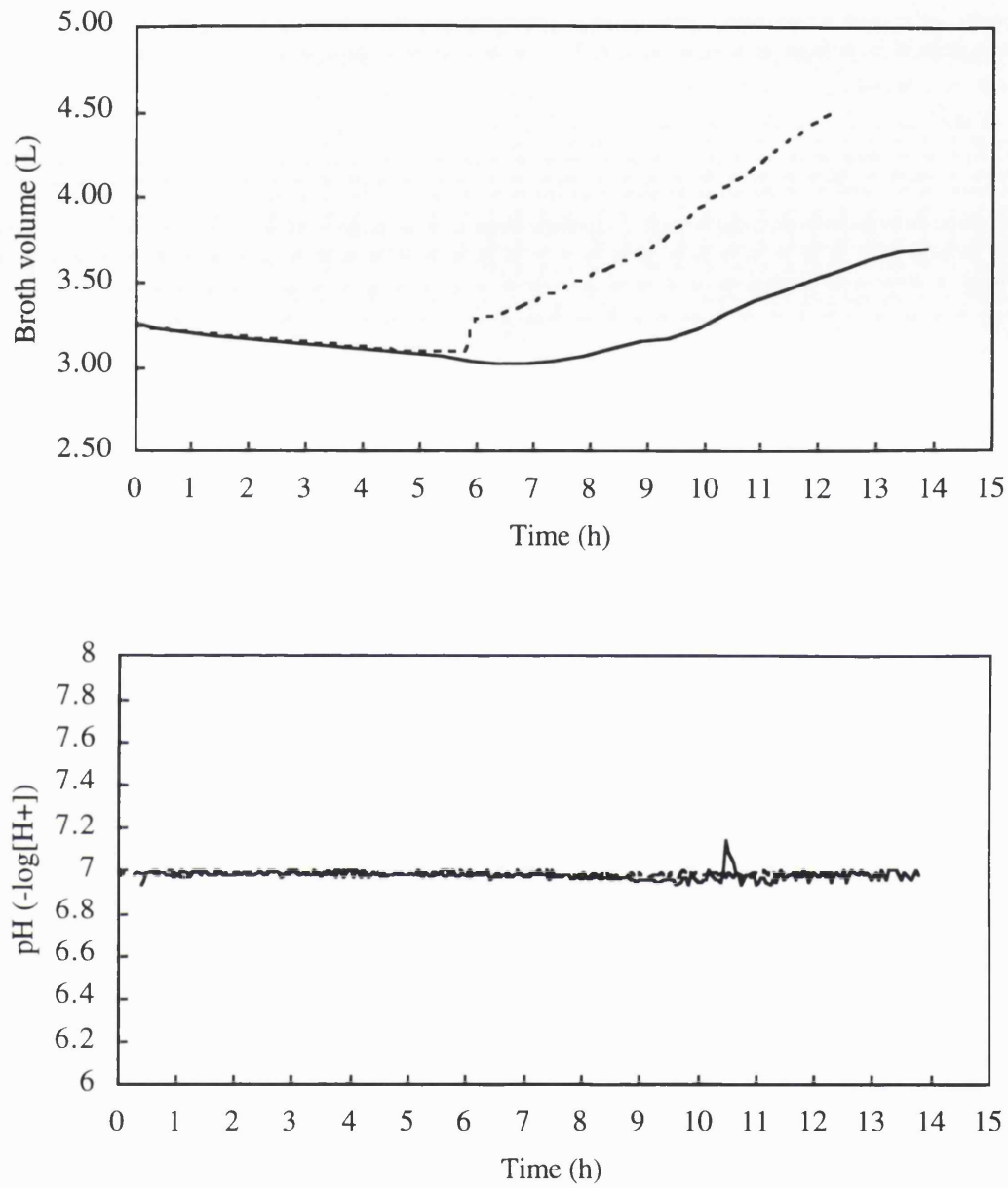


Figure D3.3a: Effect of peptone feeding on growth.
Estimated broth volume and pH.

- No peptone feed (Expt. 2)
- Peptone feed started at 5.77 h (Expt. 5).

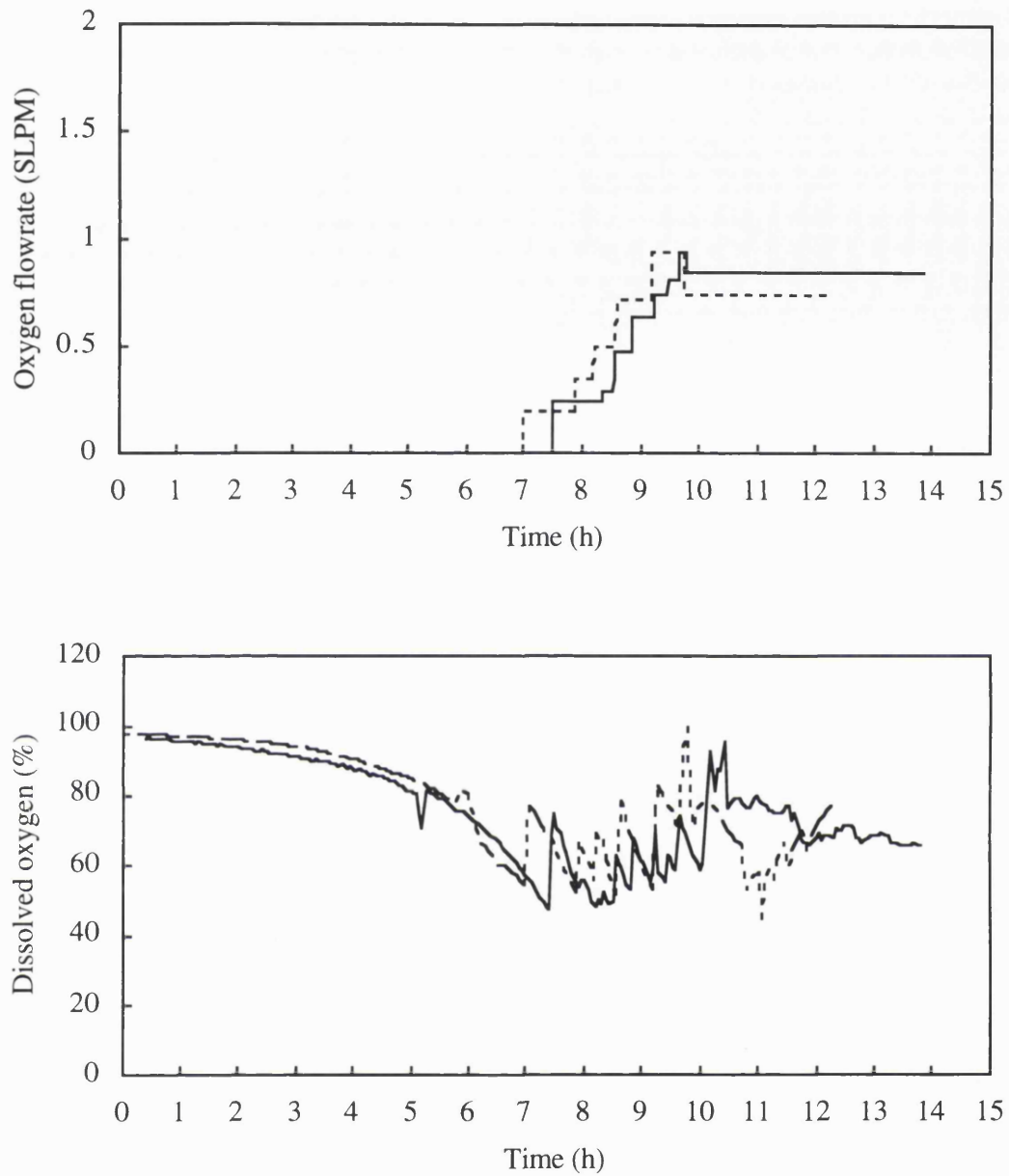


Figure D3.3b: Effect of peptone feeding on growth.
Oxygen flowrate and dissolved oxygen concentration.

— No peptone feed (Expt. 2)
---- Peptone feed started at 5.77 h (Expt. 5).

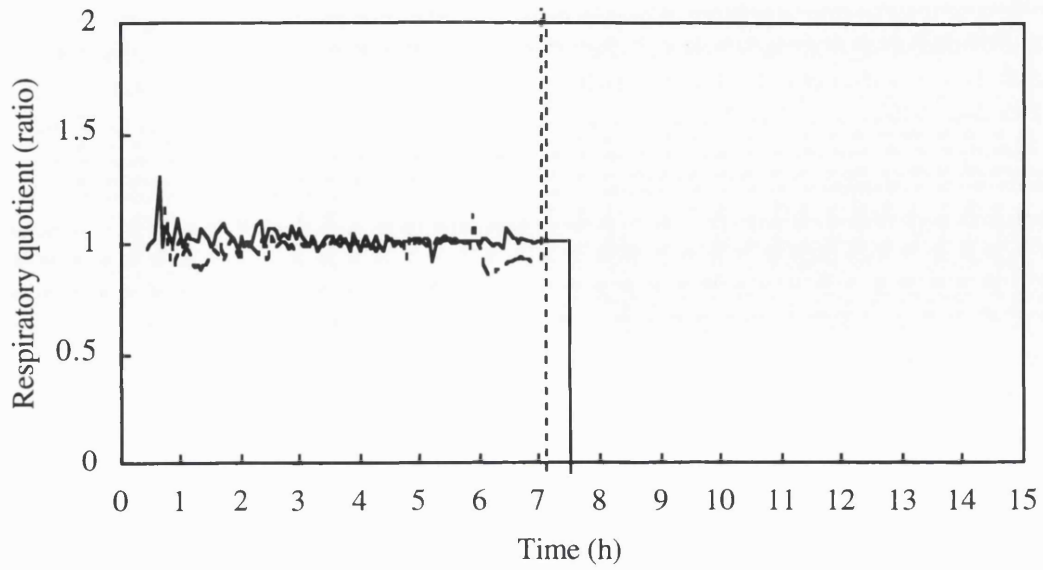


Figure D3.3c: Effect of peptone feeding on growth.
Respiratory quotient.

- No peptone feed (Expt. 2)
- Peptone feed started at 5.77 h (Expt. 5).

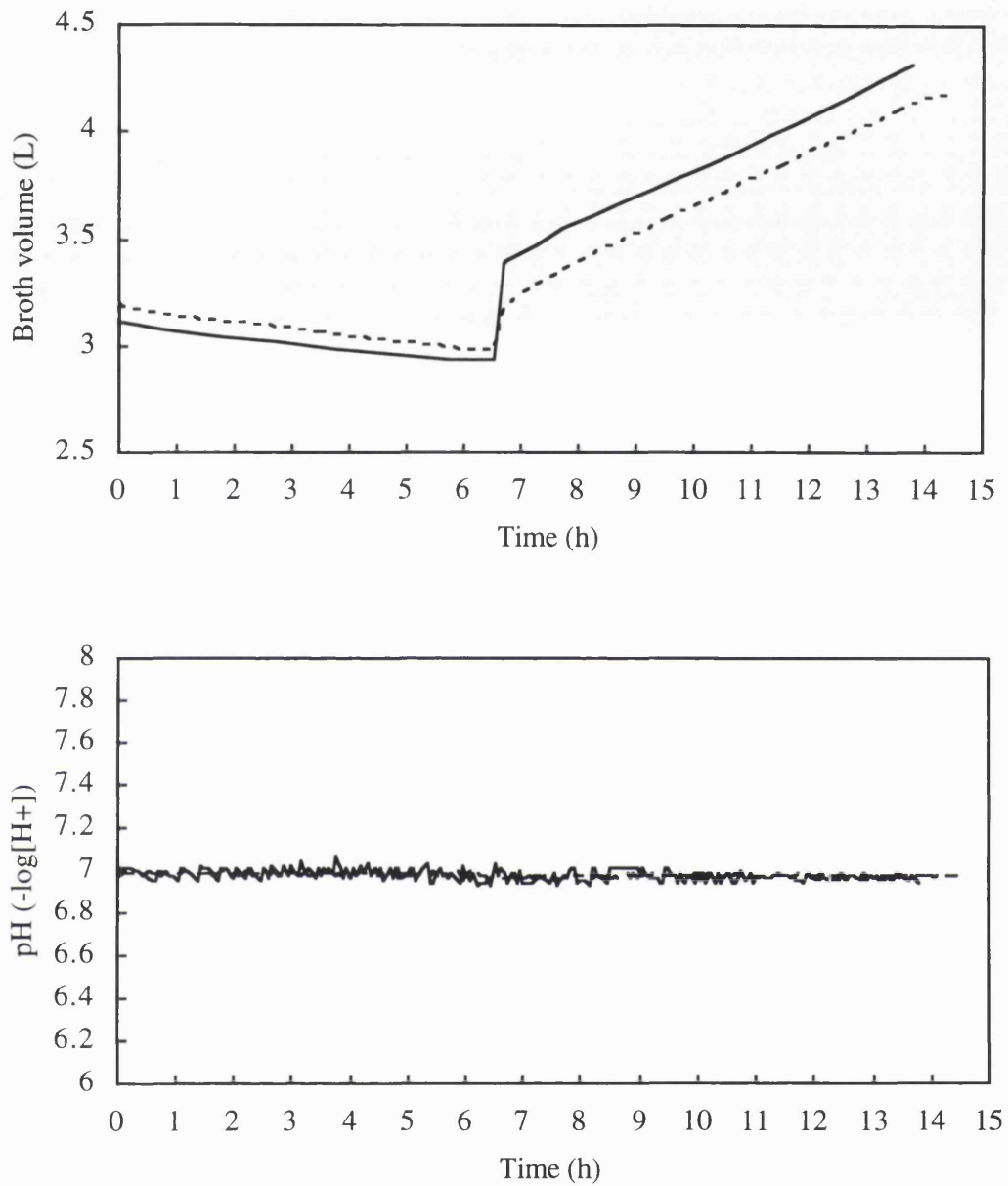


Figure D3.4a: Effect of different media on medium cell density fermentations.
Estimated broth volume and pH.

— Medium O (Expt. 6).
- - - Medium B (Expt. 7)

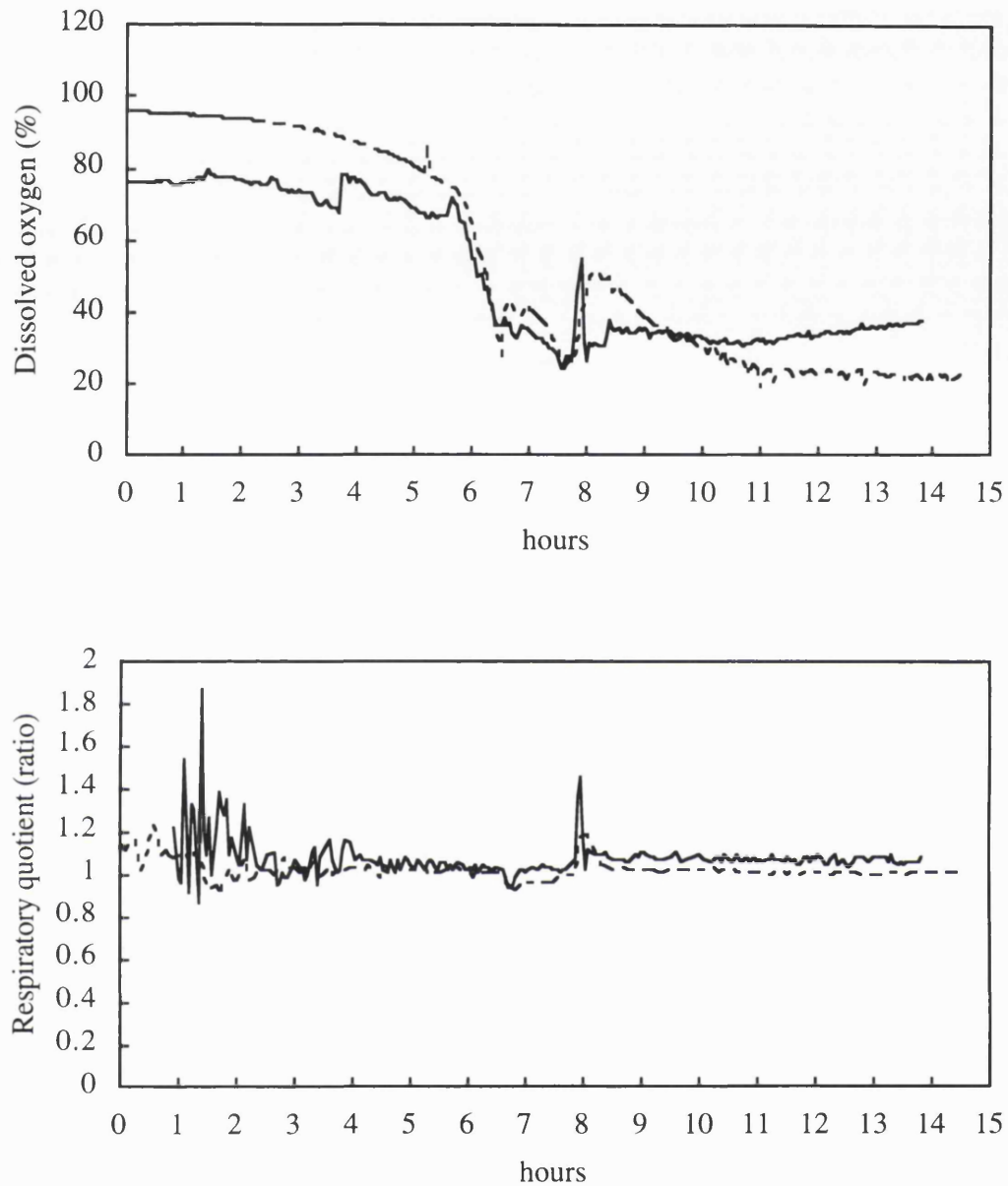


Figure D3.4b: Effect of different media on medium cell density fermentations.

Dissolved oxygen concentration and respiratory quotient.

(Note: neither run used oxygen enriched sparging).

- Medium O (Expt. 6). [DO2 probe faulty].
- Medium B (Expt. 7).

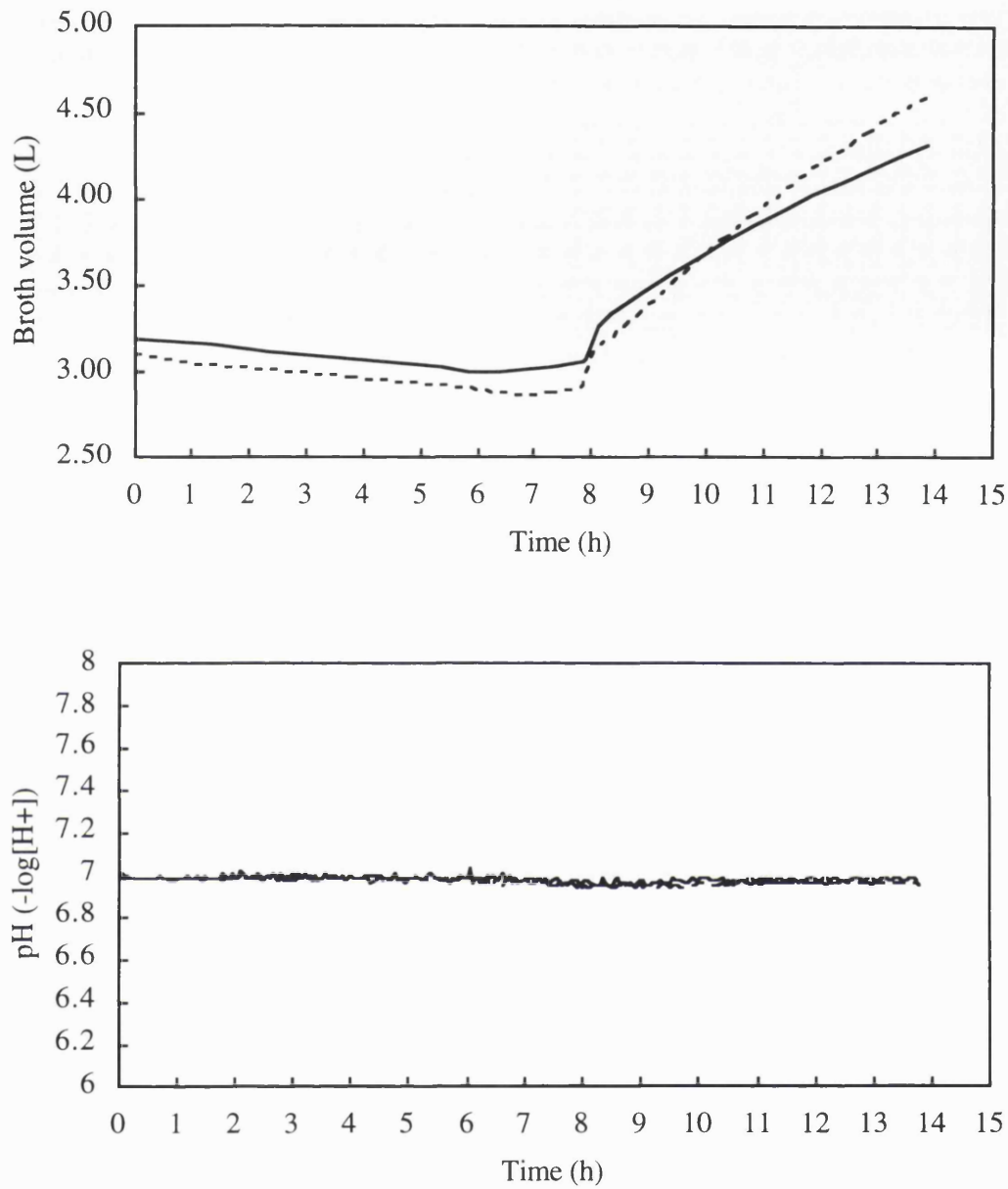


Figure D3.5a: Effect of different media on high cell density fermentations.
Estimated broth volume and pH.

— Medium B (Expt. 8).
- - - Medium B+ (Expt. 9).

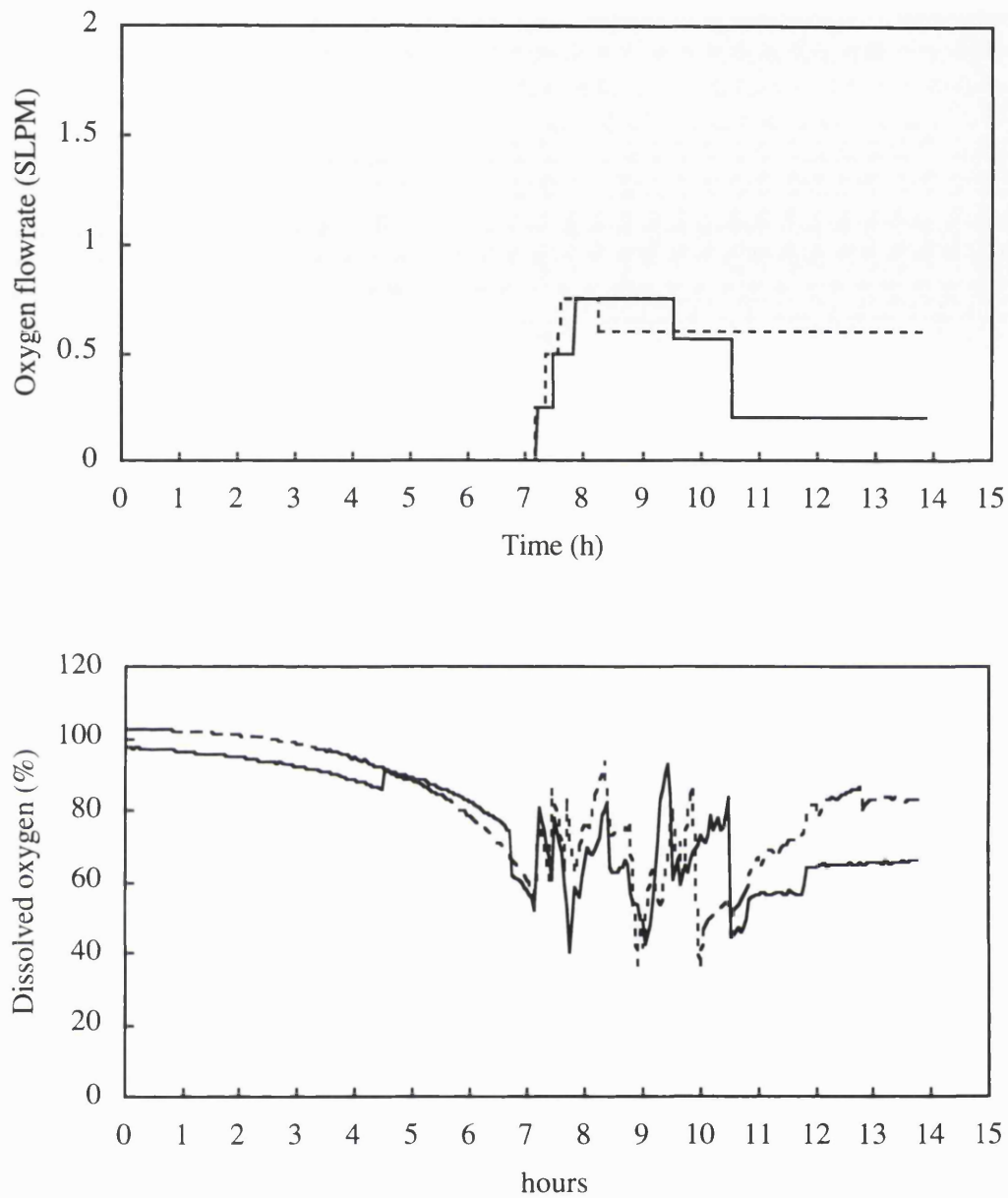


Figure D3.5b: Effect of different media on high cell density fermentations.
Oxygen flowrate and dissolved oxygen concentration.

— Medium B (Expt. 8).
---- Medium B+ (Expt. 9).

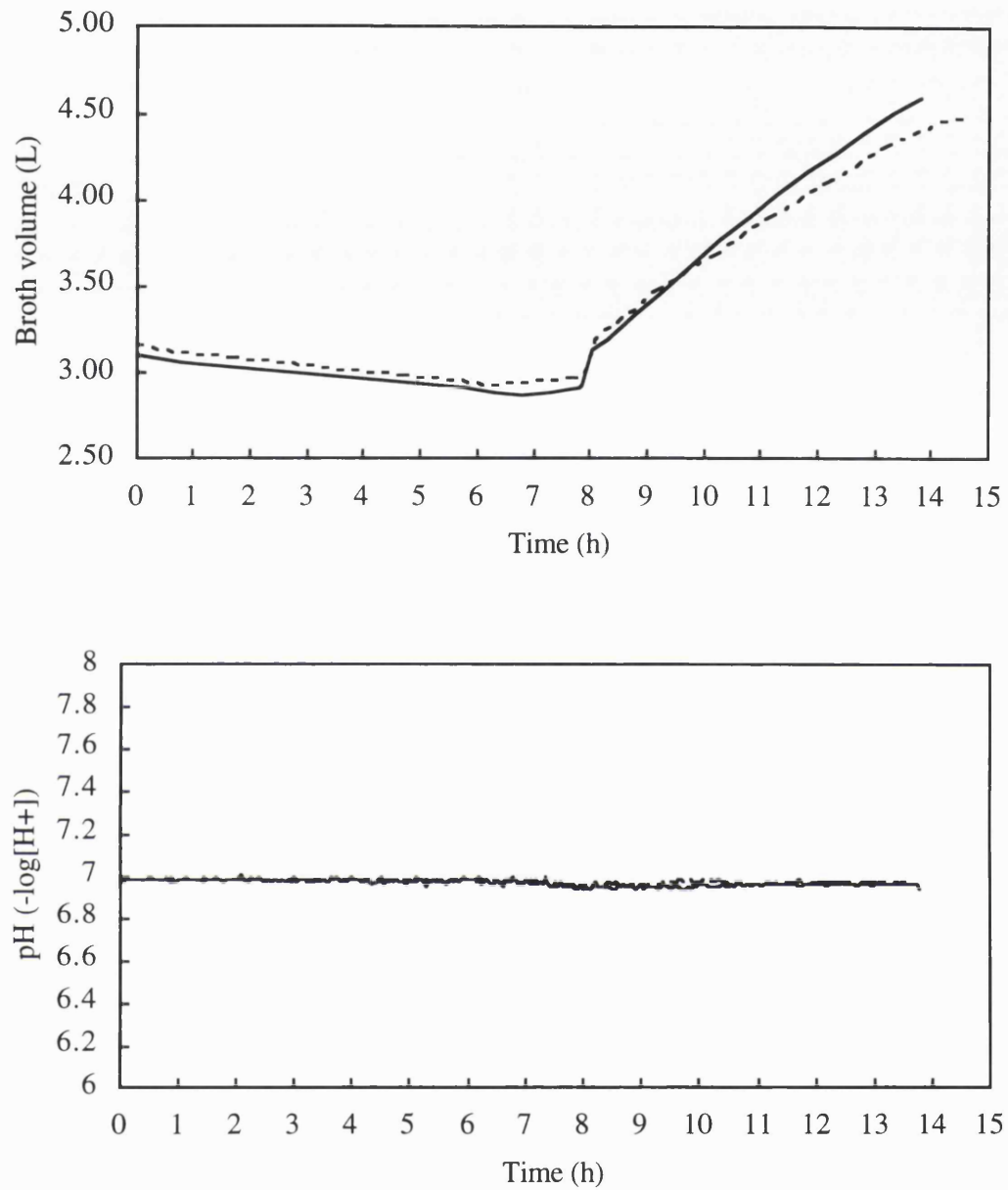


Figure D3.6a: Effect of glucose feedrate on high cell density fermentations.
Estimated broth volume and pH.

— Control (Expt. 9).
---- Low glucose feedrate (Expt. 10).

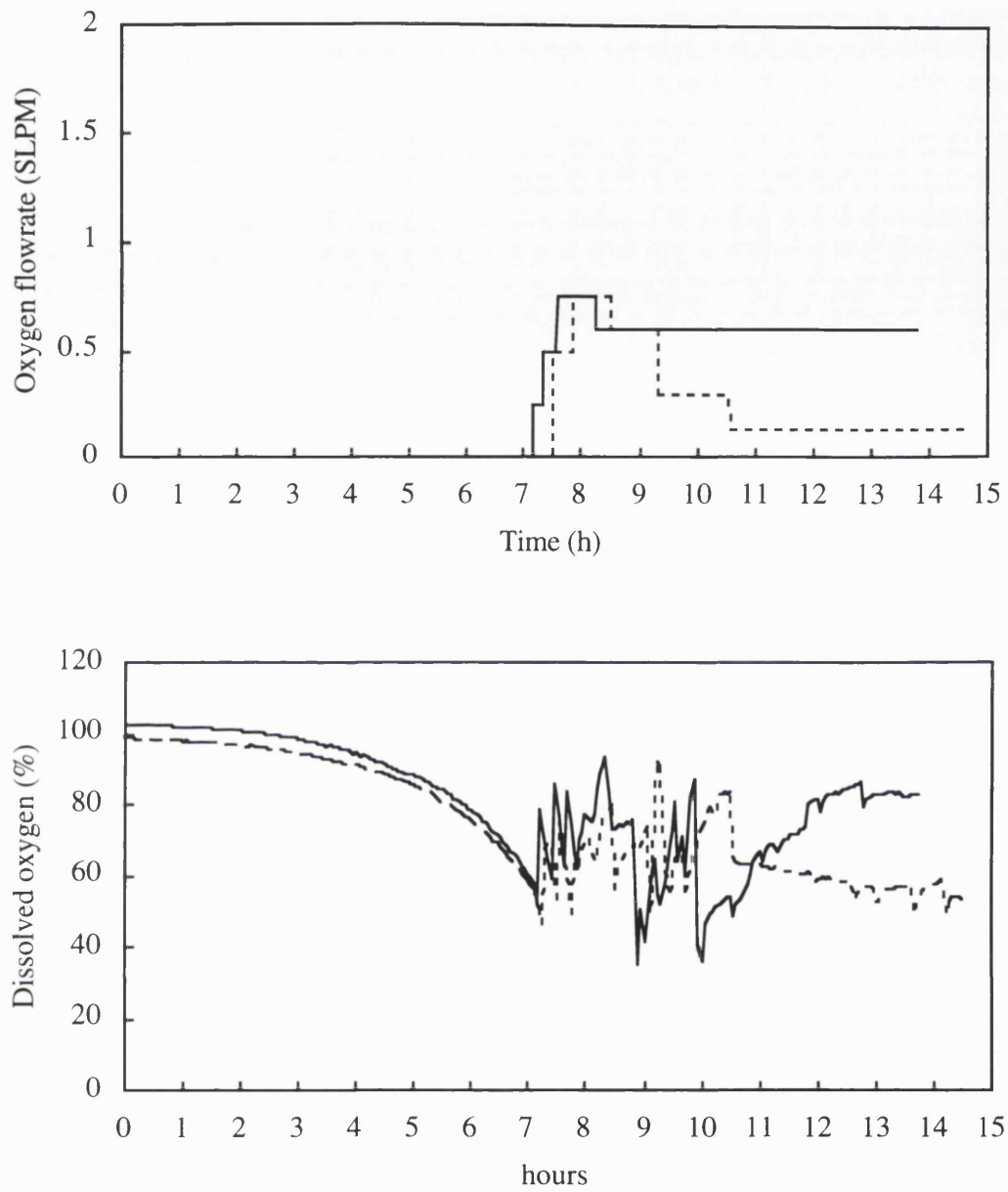


Figure D3.6b: Effect of glucose feedrate on high cell density fermentations.
Oxygen flowrate and dissolved oxygen concentration.

— Control (Expt. 9).
---- Low glucose feedrate (Expt. 10).

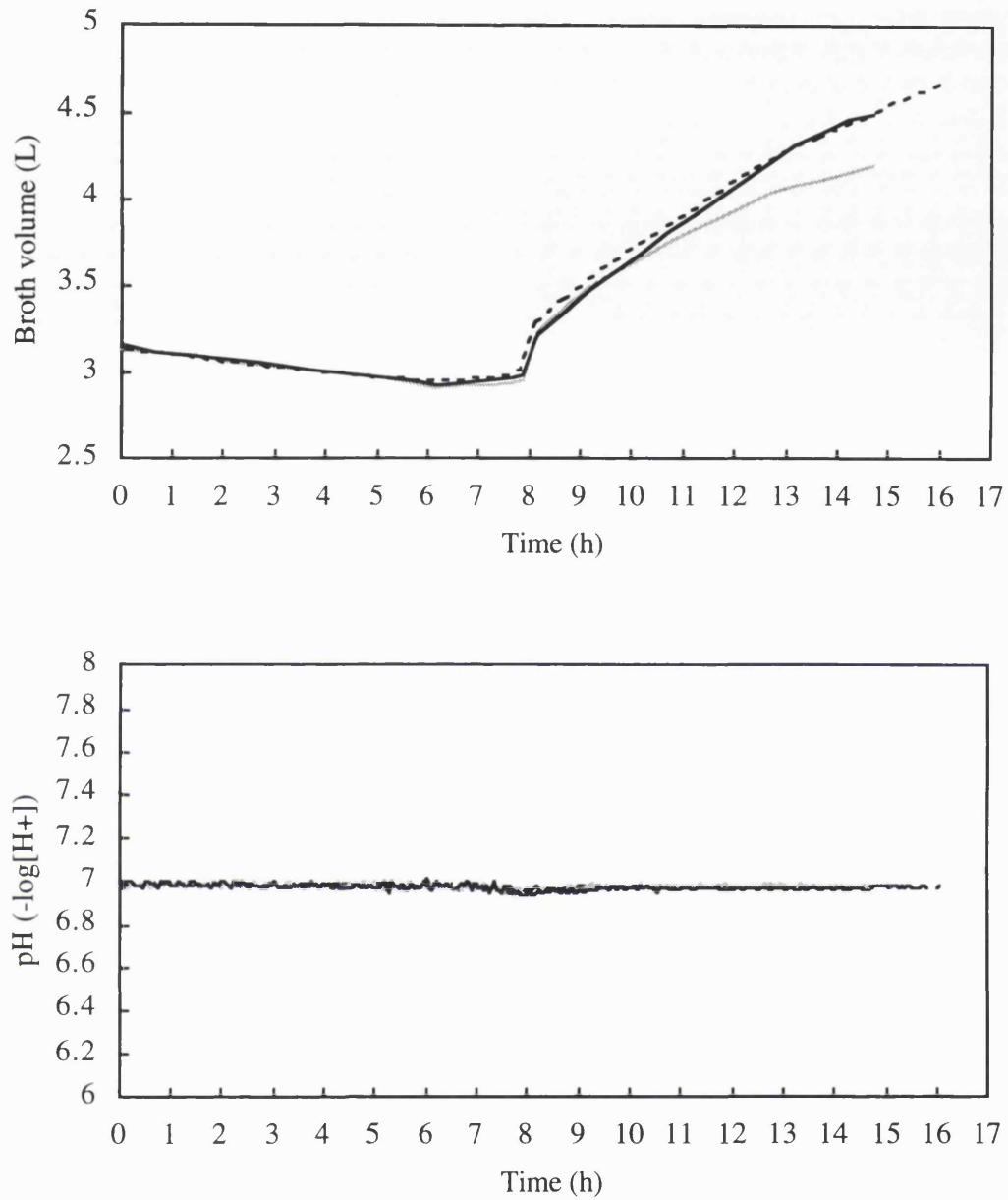


Figure D3.7a: Effect of glucose starvation on high cell density fermentations.
Estimated broth volume and pH.

- Low glucose feedrate (Expt. 10).
- - - Very low glucose feedrate (Expt. 11).
- Lowest glucose feedrate (Expt. 12)

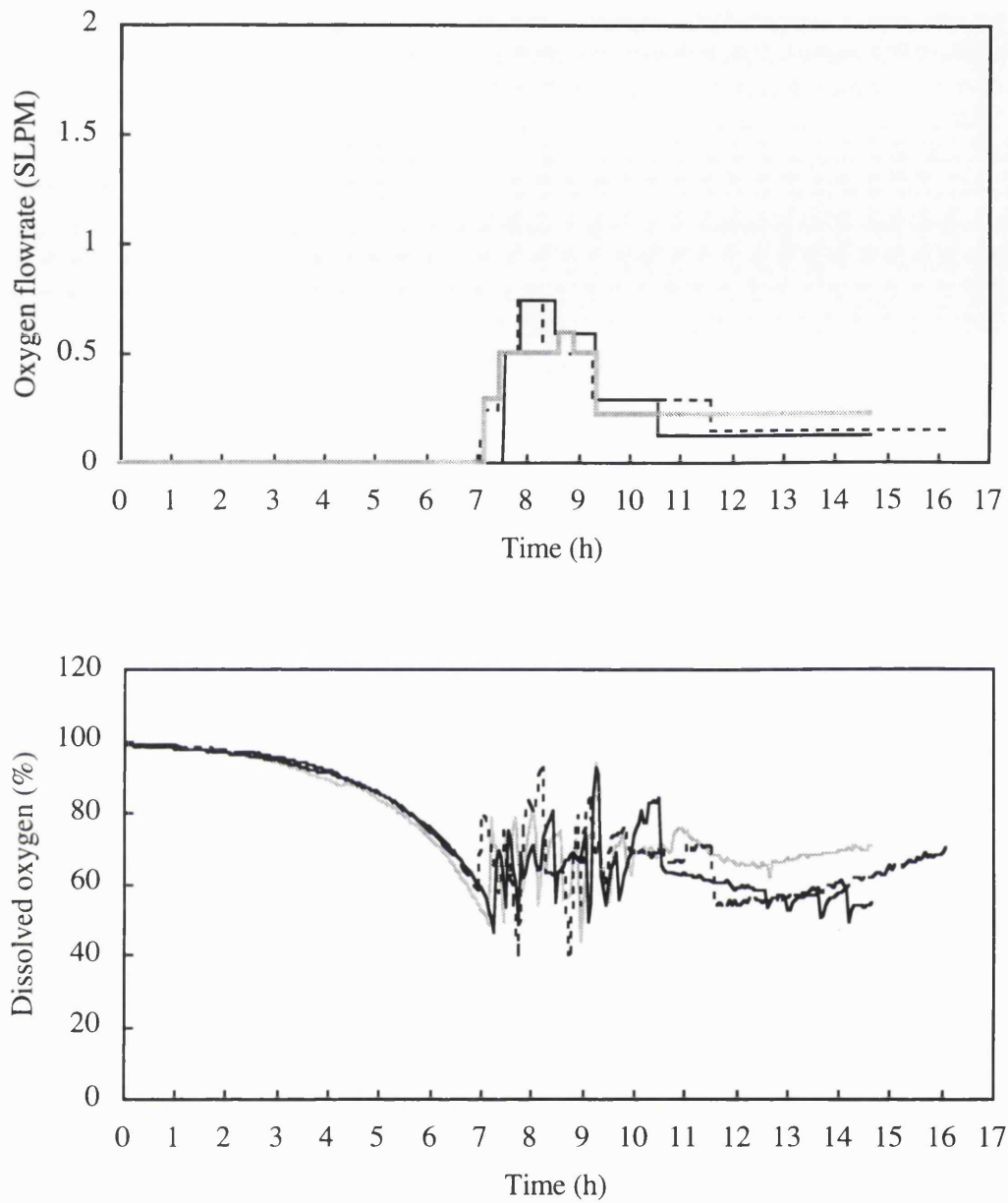


Figure D3.7b: Effect of glucose starvation on high cell density fermentations.
Oxygen flowrate and dissolved oxygen concentration.

- Low glucose feedrate (Expt. 10).
- Very low glucose feedrate (Expt. 11).
- Lowest glucose feedrate (Expt 12)

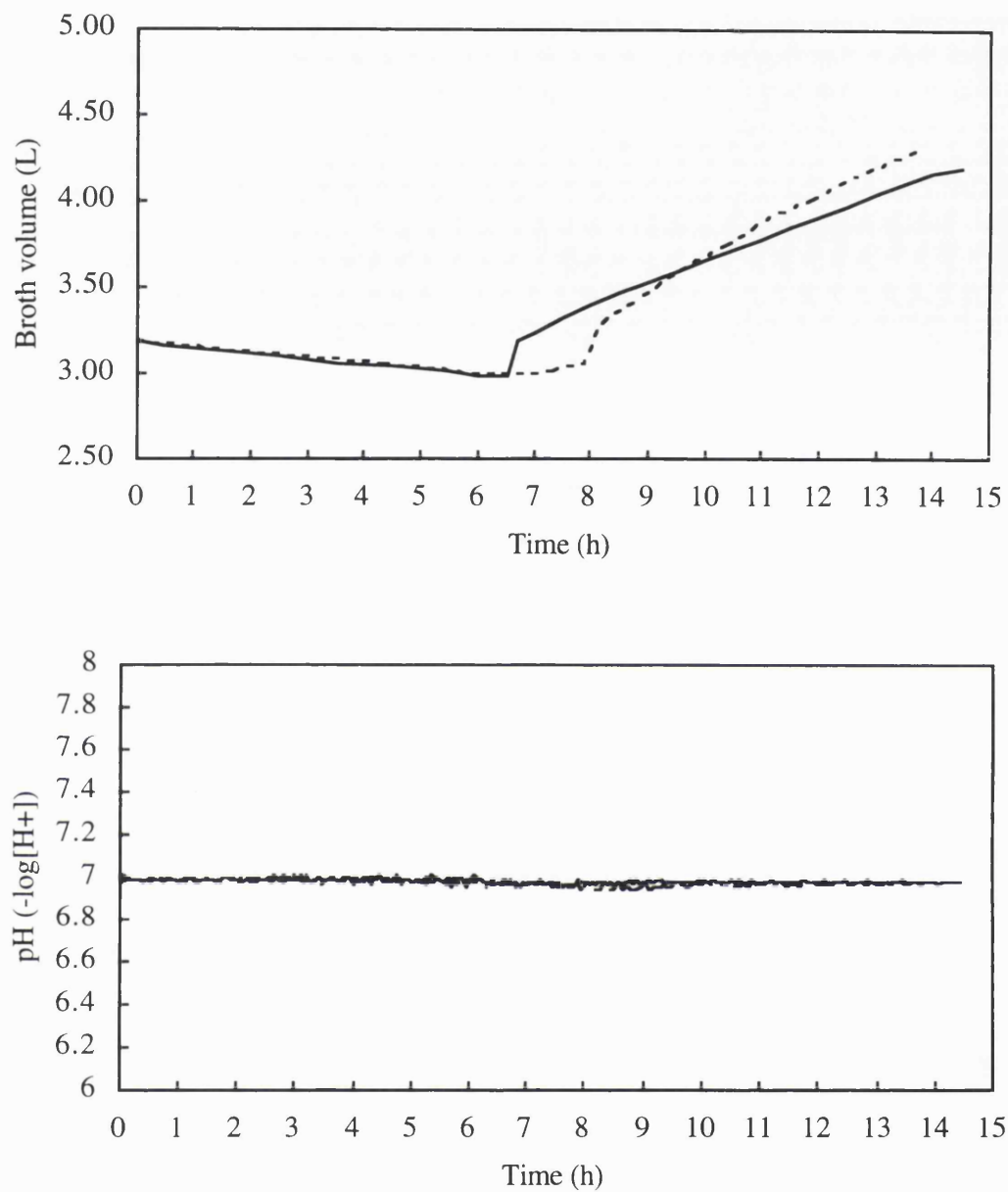


Figure D3.8a: Comparison of medium and high cell density fermentations.
Estimated broth volume and pH.

- Medium cell density (Expt. 7).
- - - High cell density (Expt. 8).

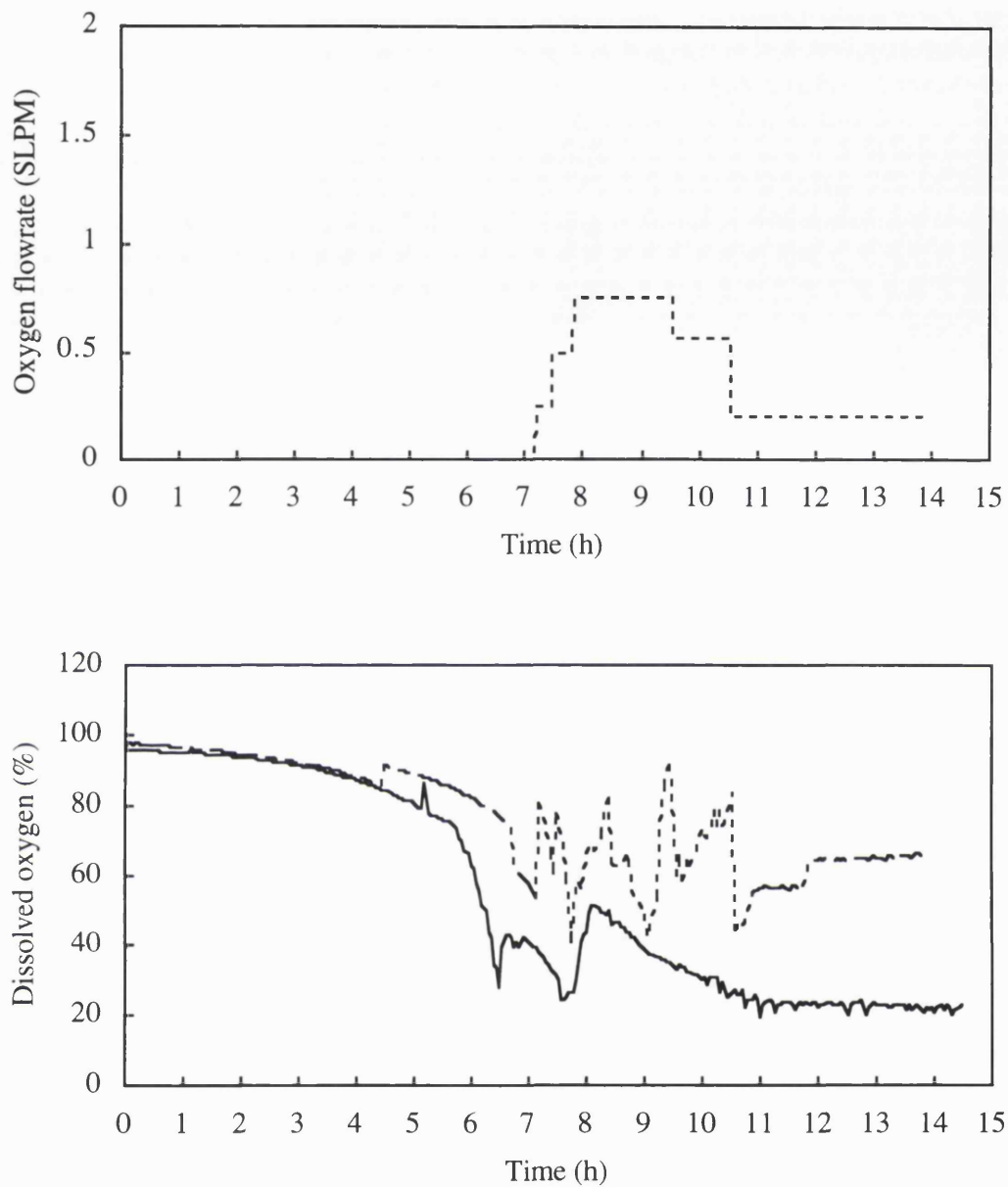


Figure D3.8b: Comparison of medium and high cell density fermentations.

Oxygen flowrate and dissolved oxygen concentration.

(Note: No oxygen enriched sparging used for Expt. 7).

— Medium cell density (Expt. 7).

---- High cell density (Expt. 8).

NOMENCLATURE

Abbreviations

Amm.	Ammonium
ANN	Artificial Neural Network
ATP	Adenosine tri-phosphate
B.S.T.	Methionine-aspartic-bovine somatotropin.
CO ₂	Carbon dioxide
DCW	Dry cell weight
DI	De-ionised
DO ₂	Dissolved oxygen
<i>E. coli</i>	<i>Escherichia coli</i>
FSD	Full scale deflection.
HCD	High cell density
hGH	Human growth hormone
HPLC	High performance liquid chromatography.
hydrox.	Hydroxide
IL	Interleukin
IPTG	Isopropyl-β-D-thiogalactopyranoside
lac	lactose
M9	A minimal medium for growing cells
MAE-hGH	met-ala-glu-human growth hormone
MCD	Medium cell density
met-asp	Methionine-aspartic
NADPH ₂	Reduced nicotinamide adenine dinucleotide phosphate
OD	Optical density
pHKY531	Plasmid used in this project.
pL, pR	Promoter (left), Promoter (right)
RQ	Respiratory Quotient
RV308	Host organism used in this project
Strep.	Streptomycin
TCA	Tri-carboxylic acid cycle (Krebs cycle)
Tet.	Tetracycline
TGF	Tissue growth factor.
U	Assay unit for concentration of TGF.

Symbols

a	Conversion factor (g 8M amm. hydrox./g acetate)
A	Acetate concentration (g acetate/L broth)
A_1	Acetate concn. for maximum inhibition of biomass production (g acetate/h)
A_2	Acetate concn. for maximum inhibition of B.S.T. production (g acetate/h)
b	Conversion factor (g 8M amm. hydrox./g biomass)
b	Constant in Blackmann equation for growth.(g glucose.L/h)
B	Constant in expression for temperature dependence of μ (1/h).
B'	Constant in Blackmann equation for growth (g glucose.h/L)
c_{gluc}	Glucose feed concentration (g glucose/L feed solution)
C	Constant which in expression for maintenance as a function of temperature (g glucose/g biomass/h).
d	Constant in Moser equation for growth
k	Constant in expression for acetate production rate (g acetate/g DCW)
k'	Constant in expression for acetate inhibition of growth (L/g acetate)
k_A	Constant in expression for acetate inhibition of growth (L/g acetate)
K	Constant in growth expressions (g glucose/h)
K_1	Michaelis-Menton coefficient for biomass production (g glucose/L)
K_2	Michaelis-Menton coefficient for B.S.T. production (g glucose/L)
m	Maintenance coefficient (g glucose/g biomass/h)
n	Conversion factor (g/L 8M ammonium hydroxide solution)
Q	Total feedrate minus evaporation rate (L/h)
Q_{amm}	Ammonium hydroxide feedrate (L/h)
Q_{evap}	Evaporation rate (L/h)
Q_{feed}	Total feedrate (L/h)
Q_{gluc}	Glucose feedrate (L/h)
Q_{pept}	Peptone feedrate (L/h)
Q_{samp}	Sampling rate (L/h)
r_A	Specific rate of acetate. production (g acetate/g biomass/h)
$r_{A,max}$	Maximum specific rate of acetate production (g acetate/g biomass/h)
$r_{G,crit}$	Critical specific glucose uptake rate (g glucose/g biomass/h)
r_P	Specific rate of B.S.T. production (g B.S.T./g biomass/h)
$r_{P,2}$	Term in equation for temperature dependence of r_P (g B.S.T./g biomass/h)
$r_{P,max}$	Maximum specific rate of B.S.T. production (g B.S.T./g biomass/h)

$r_{P,1}$	Term for product inhibition of growth (g B.S.T./g biomass/h)
R	Gas Constant (8.314 J/mol/K)
S	Glucose concentration (g glucose/L broth)
t	Time (h)
$t_{startpf}$	Start time for peptone feeding (h)
t_e	Temperature ($^{\circ}\text{C}$)
T	Temperature (K)
V	Broth volume (L)
X	Biomass concentration (g biomass/L broth)
Y_{SA}	Yield coefficient for acetate (g acetate/g glucose)
Y_{SP}	Yield coefficient for peptone (g peptone/g glucose)
Y_{SX}	Yield coefficient for biomass (g biomass/g glucose)

Greek symbols

ΔH	Activation energy in expression for the dependence of maintenance on temperature (kJ/mol)
μ	Specific growth rate (1/h)
μ_{crit}	Critical specific growth rate for acetate production (1/h)
μ_{max}	Maximum specific growth rate (1/h)
μ_{obs}	Observed specific growth rate (1/h)

BIBLIOGRAPHY

- Allen, B., Luli, G.W., 1987
A gradient-feed process for *E. coli* fermentations.
BioPharm. **1** 38-41
- Asenjo, J. A., Spencer, J. L., Phuvan, V., 1986
Optimization of the simultaneous saccharification and fermentation of an insoluble substrate into microbial metabolites.
Ann. N.Y. Acad. Sci. **469** 404-420
- Ataai, M.M., Shuler, M.L., 1985
Simulation of the growth pattern of *Escherichia coli* under anaerobic conditions.
Biotechnol. Bioeng. **27** 1027-1035
- Bailey, J.E., Ollis, D.F., 1986a
Biochemical Engineering Fundamentals.
McGraw-Hill 2nd Ed. 393
- Bailey, J.E., Ollis, D.F., 1986b
Biochemical Engineering Fundamentals.
McGraw-Hill 2nd Ed. 270
- Bajpai, R., 1987
Control of bacterial fermentations.
Ann. N.Y. Acad. Sci. **506** 446-458
- Bauer, S., Shiloach, J., 1974
Maximal exponential growth rate and yield of *E. coli* obtainable in a bench-scale fermenter.
Biotechnol. Bioeng. **16** 933-941
- Bentley, W.E., Kompala, D.S., 1989
A novel structured kinetic approach for the analysis of plasmid instability in recombinant bacterial cultures.
Biotechnol. Bioeng. **33** 49-61
- Bentley, W.E., Mirjalili, N., Andersen, D.C., Davis, R.H., 1990
Plasmid-encoded protein: The principal factor in the "metabolic burden" associated with recombinant bacteria.
Biotechnol. Bioeng. **35** 668-681
- Bogle, I.D.L., Hounslow, M.J., Middleburg, A.P.J., 1991
Modelling of inclusion body formation for optimisation of recovery in biochemical processes. Presented at PSE 91, 4th International Congress on Process Systems Engineering, Montebello, Canada.

- Calcott, P.H., Kane, J.F., Krivi, G.G., Bogosian, G., 1988
Parameters affecting the production of bovine somatotropin in *Escherichia coli* fermentations.
J. Ind. Microbiol. **29** 257-266
- Chen, H-C., Hwang, C-F., Mou, D-G., 1992
High-density *Escherichia coli* cultivation process for hyperexpression of recombinant porcine growth hormone.
Enzyme Microb. Technol. **14** 321-326
- Cheng, Y-S. E., Kwoh, D.Y., Kwoh, T.J., Zipser, D., 1981
Stabilization of degradable protein by its overexpression in *Escherichia coli*.
Gene **14** 121
- Cheruy, A., Durand, A., 1979
Optimisation of erythromycin biosynthesis by controlling pH and temperature: Theoretical aspects and practical application.
Biotechnol. Bioeng. Symp. **9** 303-320
- Cutayar, J.M., Poillon, D., 1989
High cell density culture of *E. coli* in a fed-batch system with dissolved oxygen as substrate feed indicator.
Biotechnol. Lett. **11** 155-160
- Da Silva, N.A., Bailey, J.E., 1986
Theoretical growth yield estimates for recombinant cells.
Biotechnol. Bioeng. **28** 741-746
- De Boer, H.A., Shepard, H.M., 1983
Strategies for optimizing foreign gene expression in *Escherichia coli*. In *Genes: Structure and expression*. A.M. Kroon (ed.).
John Wiley and Sons Ltd. 205-250
- Dhurjati, P.S., Leipold, R.J., 1990
Biological modeling. Chapter 8 of *Computer Control of Fermentation*. Omstead, D.R. (ed.).
C.R.C. Press, Florida. 207-221
- Di Massimo-Peel, C., Montague, G.A., Willis, M.J., Morris, A.J., 1992
Enhancing industrial bioprocess monitoring through artificial neural networks. In *Modelling and Control of Biotechnical Processes*. Karim, M.N. and Stephanopoulos, G. (eds.). IFAC Symposia Series, 1992. No.10.
Pergammon Press 395-399
- Doelle, H.W., Ewings, K.N., Hollywood, N.W., 1982
Regulation of glucose metabolism in bacterial systems.
Adv. Biochem. Eng. **23** 1-35
- Esener, A.A., Roels, J.A., Kossen, N.W.F., 1983
Theory and application of unstructured growth models: Kinetic and energetic aspects.
Biotechnol. Bioeng. **25** 2803-2841

- Fieschko, J., Ritch, T., 1986
Production of human alpha consensus interferon in recombinant *Escherichia coli*.
Chem. Eng. Commun. **45** 229-240
- Forberg, C., Enfors, S-O., Haggstrom, L., 1983
Control of immobilized, non-growing cells for production of metabolites.
Eur. J. Appl. Microbiol. Biotechnol. **17** 143-147
- Galindo, E., Bolivar, F., Quintero, R., 1990
Maximizing the expression of recombinant proteins in *Escherichia coli* by manipulation of culture conditions; optimization of culture medium for improved plasmid stability.
J. Ferm. and Bioeng. **69** 159-65
- George, H.A., Powell, A.L., Dahlgren, M.E., Herber, W.K., 1992
Physiological effects of TGF alpha-PE40 expression in recombinant *Escherichia coli* JM109.
Biotechnol. Bioeng. **40** 437-445
- Georgiou, G., 1988
Optimizing the production of recombinant proteins in microorganisms.
AIChE Journal **34** 1233-1248
- Glasse, J., Kara, B., Ward, A.C., Montague, G.A., 1992
Enhancing fermentation development procedures via artificial neural networks. In *Modelling and Control of Biotechnical Processes*. Karim, M.N. and Stephanopoulos, G. (eds.). IFAC Symposia Series, 1992. No.10.
Pergamon Press 147-153
- Han, H., Lim, H.C., Hong, J., 1992
Acetic acid formation in *Escherichia coli* fermentation.
Biotechnol. Bioeng. **39** 663-671
- Heijnen, J.J., Roels, J.A., 1981
A macroscopic model describing yield and maintenance relationships in aerobic fermentation processes.
Biotechnol. Bioeng. **23** 739-763
- Jensen, E.B., Carlsen, S., 1990
Production of recombinant human growth hormone in *Escherichia coli*: Expression of different precursors and physiological effects of glucose, acetate and salts.
Biotechnol. Bioeng. **36** 1-11
- Kane, J.F., Hartley, D.L., 1988
Formation of recombinant inclusion bodies in *Escherichia coli*.
Tibtech **6** 95-101
- Kim, B.G., Shuler, M.L., 1990
Analysis of pBR322 replication kinetics and its dependency on growth rate.
Biotechnol. Bioeng. **36** 233-242

- Knorre, W.A., Deckwer, W.D., Korz, D., Pohl, H-D., 1990
High-cell-density fermentation of *Escherichia coli* for rDNA-products. In *DECHEMA Biotechnology Conferences 4*.
VCH Verlagsgesellschaft 787-790
- Koh, B.T., Nakashimada, U., Pfeiffer, M., Yap, M.G.S., 1992
Comparison of acetate inhibition on growth of host and recombinant *E. coli* K12 strains.
Biotechnol. Lett. **14** 1115-1118
- Konstantinov, K.B., Nishio, N., Yoshida, T., 1990
Glucose feeding strategy accounting for the decreasing oxidative capacity of recombinant *Escherichia coli* in fed-batch cultivation for phenylalanine production.
J. Ferm. and Bioeng. **70** 253-260
- Landwall, P., Holme, T., 1977
Removal of inhibitors of bacterial growth by dialysis culture.
J. Gen. Microbiol. **103** 345-352
- Lee, C-W., Gu, M-B., Chang, H-N., 1989
High-density culture of *Escherichia coli* carrying recombinant plasmid in a membrane cell recycle fermenter.
Enzyme Microb. Technol. **11** 49-54
- Lee, S.B., Bailey, J.E., 1984
Genetically structured models for *lac* promoter-operator function in the chromosome and in multicopy plasmids: *lac* promoter function.
Biotechnol. Bioeng. **26** 1383-1389
- Lee, S.B., Seressiotis, A., Bailey, J.E., 1985
A kinetic model for product formation in unstable recombinant populations.
Biotechnol. Bioeng. **27** 1699-1709
- Luli, G.W., Stohl, W.R., 1990
Comparison of growth, acetate production and acetate inhibition of *Escherichia coli* strains in batch and fed-batch fermentations.
Appl. Environ. Microbiol. **56** 1004-1011
- MacDonald, H.L., Neway, J.O., 1990
Effects of medium quality on the expression of human interleukin-2 at high cell density in fermentor cultures of *Escherichia coli* K-12.
Appl. Environ. Microbiol. **56** 640-645
- Majewski, R.A., Domach, M.M., 1990
Simple constrained-optimization view of acetate overflow in *E. coli*.
Biotechnol. Bioeng. **35** 732-738
- Markl, H., Zenneck, C., Dubach, A.CH., Ogbonna, J.C., 1993
Cultivation of *Escherichia coli* to high cell densities in a dialysis reactor.
Appl. Microbiol. Biotechnol. **39** 48-52

- Marr, A.G., Nilson, E.H., Clark, D.J., 1962
The maintenance requirement of *Escherichia coli*.
Ann. N.Y. Acad. Sci. **102** 536
- Matsui, T., Yokota, H., Sato, S., Mukataka, S., 1989
Pressurized culture of *Escherichia coli* for a high concentration.
Agric. Biol. Chem. **53** 2115-20
- Meyer, H., Leist, C., Fiechter, A., 1984
Acetate formation in continuous culture of *Escherichia coli* K12D1 on defined and complex media.
J. Biotechnol. **1** 355-358
- Mizutani, S., Mori, H., Shimizu, S., Sakaguchi, K., 1986
Effect of amino acid supplement on cell yield and gene product in *Escherichia coli* harboring plasmid.
Biotechnol. Bioeng. **28** 204-209
- Mizutani, S., Iijima, S., Shimizu, K., Matsubara, M., 1987
Mathematical modelling and response characteristics of runaway replication for temperature shift-up.
Biotechnol. Prog. **3** 101-108
- Monod, J., 1942
Recherches sur la croissance des cultures bacteriennes.
Hermann et cie., Paris. **2nd. Ed.**
- Mori, H., Yano, T., Kobayashi, T., Shimizu, S., 1979
High density cultivation of biomass in fed-batch system with DO-stat.
J. Chem. Eng. Japan **12** 313-319
- Nancib, N., Branlant, C., Boudrant, J., 1991
Metabolic roles of peptone and yeast extract for the culture of a recombinant strain of *Escherichia coli*.
J. Ind. Microbiol. **8** 165-170
- Niedhart, F.C., VanBogelen, R.A., 1987
Heat shock response. In *Escherichia coli and Salmonella trphimurium: cellular and molecular biology*. Neidhart F.C., Ingraham, J.L., Low, K.B., Mgasanik, K.B., Schaechter, M., and Umberger, H.E. (eds.).
Am. Soc. Microbiol. **Vol. 2** 1334-1345
- Nielsen, J., Emborg, C., Halberg, K., Villadsen, J., 1989
Compartment model concept used in the design of fermentation with recombinant microorganisms.
Biotechnol. Bioeng. **34** 478-486
- Nielsen, J., Villadsen, J., 1992
Modelling of microbial kinetics.
Chem. Eng. Science **47** 4225-4270

Pan, J.G., Rhee, J.S., Lebeault, J.M., 1987

Physiological constraints in increasing biomass concentration of *Escherichia coli* B in fed-batch culture.

Biotechnol. Lett. **9** 89-94

Park, S., Ryu, D.D.Y., 1990

Effect of operating parameters on specific production rate of a cloned-gene product and performance of recombinant fermentation process.

Biotechnol. Bioeng. **35** 287-295

Pirt, S.J., 1975

Principles of microbe and cell cultivation.

Blackwell Scientific Publications **1st Ed.**

Ramirez, D.M., Bentley, W.E., 1993

Enhancement of recombinant protein synthesis and stability via coordinated amino acid addition.

Biotechnol. Bioeng. **41** 557-565

Reiling, H.E., Laurila, H., Fiechter, A., 1985

Mass culture of *Escherichia coli*: Medium development for low and high density cultivation of *Escherichia coli* B/r in minimal and complex media.

J. Biotechnol. **2** 191-206

Riesenber, D., Menzel, K., Schultz, V., Knorre, W.A., 1990

High cell density fermentation of recombinant *Escherichia coli* expressing human interferon alpha 1.

Appl. Microbiol. Biotechnol. **34** 77-82

Riesenber, D., Schultz, V., Knorre, W.A., Pohl, H.D., 1991

High cell density fermentation of *Escherichia coli* at controlled specific growth rate.

J. Biotechnol. **20** 17-28

Riggin, R.M., Dorulla, G.K., Miner, D.J., 1987

A reversed-phase high-performance liquid chromatographic method for characterization of biosynthetic human growth hormone.

Anal. Biochem. **167** 199-209

Rinas, U., Kracke-Helm, H.A., Schugerl, K., 1989

Glucose as a substrate in recombinant strain fermentation technology.

Appl. Microbiol. Biotechnol. **31** 163-167

Rinas, U., Boone, T.C., Bailey, J.E., 1993

Characterization of inclusion bodies in recombinant *Escherichia coli* producing high levels of porcine somatotropin.

J. Biotechnol. **28** 313-320

Rivera, S.L., Karim, M.N., 1992

On-line estimation of bioreactors using recurrent neural networks. In *Modelling and Control of Biotechnical Processes*. Karim, M.N. and Stephanopoulos, G. (eds.). IFAC Symposia Series, 1992. No.10. Pergamon Press 159-162

Robbins Jr., J.W., Taylor, K.B., 1989

Optimization of *E. coli* growth by controlled addition of glucose. *Biotechnol. Bioeng.* **34** 1289-1294

Roels, J.A., Kossen, N.W.F., 1978

On the modelling of microbial metabolism. *Prog. Ind. Microbiol.* **14** 95-204

Royce, P.N., 1993

A discussion of recent developments in fermentation monitoring and control from a practical perspective. *CRC Crit. Rev. in Biotechnol.* **13** 117-151

Schoner, B.E., Hsiung, H.M., Belagaje, R.M., Schoner, R.G., 1984

Role of mRNA translational efficiency in bovine growth hormone expression in *E. coli*. *Proc. Natl. Acad. Sci. USA* **81** 5403-5407

Seo, J-H., Bailey, J.E., 1985

A segregated model for plasmid content and production synthesis in unstable binary fission recombinant organisms. *Biotechnol. Bioeng.* **27** 156-165

Shehata, T.E., Marr, A.G., 1971

Effect of nutrient concentration on the growth of *Escherichia coli*. *J. Bacteriol.* **107** 210

Shiloach, J., Van de Walle, M., Kaufman, J.B., Fass, R., 1991

High density growth of microorganisms for protein production. Presented at 34th OHOLO conference Eilat, Israel: "*Biologicals from recombinant microorganisms and animal cells*".

Balaban Publishers, Rekovot, Israel. 34-45

Shimuzu, N., Fukuzono, S., Fujimori, K., Nishimura, N., 1988

Fed-batch cultures of recombinant *Escherichia coli* with inhibitory substance concentration monitoring. *J. Ferm. Technol.* **66** 187-191

Sonnleitner, B., Kappeli, O., 1986

Growth of *Saccharomyces cerevisiae* is controlled by its limited respiratory capacity: formulation and verification of a hypothesis. *Biotechnol. Bioeng.* **28** 927-937

- Strandberg, L., Enfors, S-O., 1991a
Batch and fed batch cultivations for the temperature induced production of a recombinant protein in *E. coli*.
Biotechnol. Lett. **13** 609-614
- Strandberg, L., Enfors, S-O., 1991b
Factors influencing inclusion body formation in the production of a fused protein in *Escherichia coli*.
Appl. Environ. Microbiol. **57** 1669-1674
- Strandberg, L., Kohler, K., Enfors, S-O. 1991c
Large-scale fermentation and purification of a recombinant protein from *Escherichia coli*.
Proc. Biochem. **26** 225-234
- Strudsholm, K., Nielson, J., Emborg, C., 1992
Product formation during batch fermentation with recombinant *Escherichia coli* containing a runaway plasmid.
Bioprocess Eng. **8** 173-181
- Stryer, L., 1981
Biochemistry.
W. H. Freeman and Company **2nd Ed.**
- Thompson, B.G., Kole, M., Gerson, D.F., 1985
Control of ammonium concentration in *Escherichia coli* fermentations
Biotechnol. Bioeng. **27** 818-824
- Tonga, A.P., Fu, J., Shuler, M.L., 1993
Use of a simple mathematical model to predict the behaviour of *Escherichia coli* producing beta-lactamase within continuous single- and two- stage reactor systems.
Biotechnol. Bioeng. **42** 557-570
- Tsai, L.B., Mann, M., Rotgers, C., Fenton, D., 1987
The effect of organic nitrogen and glucose on the production of recombinant insulin-like growth factor in high cell density *Escherichia coli* fermentations.
J. Ind. Microbiol. **2** 181-186
- Wang, I.C., Cooney, C.L., Demain, A.L., Dunnill, P., Humphrey, A.E., and Lilly, M.D., 1979
Fermentation and Enzyme Technology
John Wiley and Sons **1st Ed.** 74
- Whitney, G.K., Glick, B.R., Robinson, C.W., 1989
Induction of T4 DNA ligase in a recombinant strain of *E. coli*.
Biotechnol. Bioeng. **33** 991-998
- Wilhelm, O.G., Jaskunas, S.R., Vlahos, C.J., Bang, N.U., 1990
Functional properties of the recombinant kringle-2 domain of tissue plasminogen activator produced in *Escherichia coli*.
J. Biol. Chem. **265** 14606-14611

Williams, F.M., 1967

A model of cell growth dynamics.

J. Theor. Biol. **15** 190

Yang, X-M., 1992

Optimization of a cultivation process for recombinant protein production by *Escherichia coli*.

J. Biotechnol. **23** 271-289

Yang, X-M., Xu, L., Eppstein, L., 1992

Production of recombinant human interferon-alpha 1 by *Escherichia coli* using a computer-controlled cultivation process.

J. Biotechnol. **23** 291-301

Yee, L., Blanch, H.W., 1992

Recombinant protein expression in high cell density fed-batch cultures of *Escherichia coli*.

Bio/Technol. **10** 1550-1556

Yee, L., Blanch, H.W., 1993

Recombinant trypsin production in high cell density fed-batch cultures in *Escherichia coli*.

Biotechnol. Bioeng. **41** 781-790

Zabriskie, D.W., Arcuri, E.J., 1986

Factors influencing productivity of fermentations employing recombinant microorganisms.

Enzyme Microb. Technol. **8** 706-717